AD

USAAVLABS TECHNICAL REPORT 65-75

A STUDY OF THE KAMAN DYNAMIC ANTIRESONANT VIBRATION ISOLATOR

By

Roland C. Anderson
Michael F. Smith

January 1966

U. S. ARMY AVIATION MATERIEL LABORATORIES
FORT EUSTIS, VIRGINIA

CONTRACT DA 44-177-AMC-196(T)

KAMAN AIRCRAFT CORPORATION
BLOOMFIELD, CONNECTICUT

Disclaimers

The findings in this report are not to be construed as an official Department of the Army position unless so designated by other authorized documents.

When Government drawings, specifications, or other data are used for any purpose other than in connection with a definitely related Government procurement operation, the United States Government thereby incurs no responsibility nor any obligation whatsoever; and the fact that the Government may have formulated, furnished, or in any way supplied the said drawings, specifications, or other data is not to be regarded by implication or otherwise as in any manner licensing the holder or any other person or corporation, or conveying any rights or permission, to manufacture, use, or sell any patented invention that may in any way be related thereto.

Trade names cited in this report do not constitute an official endorsement or approval of the use of such commercial hardware or software.

Disposition Instructions

Destroy this report when no longer needed. Do not return it to originator.

DEPARTMENT OF THE ARMY
U. S. ARMY AVIATION MATERIEL LABORATORIES
FORT EUSTIS, VIRGINIA 23604

This report has been reviewed by the U. S. Army Aviation Materiel Laboratories. The analyses and conclusions are considered to be technically sound. This report is published for the dissemination and application of the information contained herein.

Task 1P125901A14229
Contract DA 44-177-AMC-196(T)
USAAVLABS Technical Report 65-75
January 1966

A STUDY OF THE

KAMAN DYNAMIC ANTIRESONANT VIBRATION ISOLATOR

Kaman Report No. R-574

By

Roland C. Anderson
Michael F. Smith

Prepared By

Kaman Aircraft Corporation
Bloomfield, Connecticut

For

U. S. ARMY AVIATION MATERIEL LABORATORIES
Fort Eustis, Virginia

ABSTRACT

This report contains the analysis and experimental model testing of the Dynamic Antiresonant Vibration Isolator (DAVI) conducted under a research contract DA 44-177-AMC-196(T) at Kaman Aircraft Corporation, Bloomfield, Connecticut, sponsored by U. S. Army Aviation Materiel Laboratories, Fort Eustis, Virginia.

Theoretical analysis was conducted on the basic DAVI configuration (DAVI α) to determine the vibration isolation performance with damping and to determine the shock transmissibility equations of the DAVI α with and without damping. Theoretical analysis was also done on the Series-Damped DAVI (DAVI γ) to determine optimum damping.

Experimental model testing was then done by investigating various means of achieving damping in the configuration to determine its effect on the isolation and to determine the best possible pivot arrangements. From these results, an optimum experimental DAVI design was obtained.

An experimental platform was constructed utilizing four optimum DAVI models for isolation. This configuration utilizing the DAVI α was capable of testing up to 200 pounds, and the frequency was varied from 5 c.p.s. to 100 c.p.s. to obtain the transmissibility curves. Drop tests of the DAVI platform were done and compared to drop tests of conventional spring-mass systems with the same spring rate.

Results of the analysis and model testing show the DAVI to be capable of over 98-percent isolation at very low frequencies with low static deflections. The isolation provided by the DAVI α configuration, at a tuned frequency, is independent of the mass of the isolated item. Analysis and drop tests show that the DAVI α gives better shock transmissibility for its fundamental mode than a conventional isolation system with the same spring rate.

FOREWORD

This research program for the study of the Kaman Dynamic Antiresonant Vibration Isolator (DAVI) was performed by Kaman Aircraft Corporation under Contract DA 44-177-AMC-196(T) for the U.S. Army Aviation Materiel Laboratories (USAAVLABS), Fort Eustis, Virginia.

The program was conducted under the technical direction of Mr. J. E. Yeates, Aeromechanics Group Leader, and Mr. J. H. McGarvey, Contracting Officer's Representative.

Principal Kaman personnel in this program were Messrs. R. C. Anderson, Project Engineer; M. F. Smith, Research Engineer; H. A. Cooke, Research Technician; and J. C. Wilson, Research Specialist. The work was done under the direction of Mr. R. Jones, Chief of Vibrations Research and Mr. W. G. Flannelly, Assistant Chief of Vibrations Research.

Appreciation is due Dr. Howard Butler, Rensselaer Polytechnic Institute Hartford Graduate Center, for his assistance while serving as consultant for Kaman Aircraft Corporation.

TABLE OF CONTENTS

LIST OF ILLUSTRATIONS

LIST OF TABLES

LIST OF SYMBOLS

A	Distance of C.G. from edge of top-plate in Y^+ direction, 6 DOF
a	Distance of C.G. from edge of DAVI-plate in Y^+ direction, 6 DOF
B	Distance of C.G. from edge of top-plate in Y^- direction, 6 DOF
b	Distance of C.G. from edge of DAVI-plate in Y^- direction, 6 DOF
C	Damping coefficient
C_c	Critical damping
C_D	Damping coefficient between M_D and shaker table
C.G.	Center of gravity
C_T	Damping coefficient between mass M_T and mass M_D or between M_T and shaker table (if M_D = o) 1 and 2 DOF
C_{ZD}	Damping coefficient between top-plate and DAVI-plate, 6 DOF
C_{ZT}	Damping coefficient between DAVI-plate and shaker table, 6 DOF
$C_{\theta D}$	Damping coefficient in pitching of DAVI-plate, 6 DOF
$C_{\theta T}$	Damping coefficient in pitching of top-plate, 6 DOF
$C_{\phi D}$	Damping coefficient in roll of DAVI-plate, 6 DOF
$C_{\phi T}$	Damping coefficient in roll of top-plate, 6 DOF
C_θ	Damping coefficient of DAVI bar angular motion, 6 DOF

D	Dissipation function
DOF	Degree of freedom
f	$\frac{\omega_A}{\Lambda}$ - ratio of antiresonant frequency to system natural frequency, 2 DOF
h	$\frac{\omega}{\omega_A}$ - ratio of input frequency to antiresonant frequency, 2 DOF
I	DAVI bar inertia
I_T	Inertia of top-plate
I_D	Inertia of DAVI-plate
K_T	Spring constant between M_D and M_T
K_D	Spring constant between M_D and shaker table
M	C.G. distance from top-plate edge in X^+ direction, 6 DOF
M_D	Isolated mass attached to DAVI
M_T	Mass isolated by conventional isolators
m	C.G. distance from DAVI-plate edge in X^+ direction, 6 DOF
m_o	DAVI inertia bar mass
N	C.G. distance from top-plate edge in X^- direction, 6 DOF
n	C.G. distance from DAVI-plate edge in X^- direction, 6 DOF
P	$\left[M_D + m_o (1 - \frac{R}{r})^2 + \frac{I}{r2}\right]$, i.e., effective mass of DAVI plate in dynamical system
R	C.G. distance of DAVI bar from mass pivot
r	Distance between pivots on DAVI bar
T	Kinetic energy

T_D	Transmissibility of DAVI
T_{DVHF}	Transmissibility of DAVI at very high frequency
T_{DIP}	Transmissibility at the invariant point
V	Potential energy
Z_D	Vertical displacement of DAVI-plate
Z_T	Vertical displacement of top-plate
Z_S	Vertical displacement of shaker table
α	$\frac{P-\mu}{P}$, a convenient mass ratio
β	$\frac{\mu}{P}$, a convenient mass ratio
γ	2ζ , a damping ratio
θ_D	Pitching angle of DAVI-plate
θ_T	Pitching angle of top-plate
θ	Angular deflection of DAVI bar
ζ	$\frac{C}{C_C}$, damping ratio
λ	$\frac{\omega}{\omega_R}$, nondimensionalized input frequency
λ_A	$\frac{\omega_A}{\omega_R}$, antiresonant to resonant frequency ratio
μ	$M_D + (1 - \frac{B}{r})m_O$, a convenient mass ratio
μ_o	$\frac{P-\mu}{M_T}$, a convenient mass ratio

ρ	$1 - \lambda^2$, a convenient nondimensionalised term
σ	$2\zeta \frac{\omega}{\omega_n}$, a convenient nondimensionalised term
ϕ_D	Roll of DAVI-plate
ϕ_T	Roll of top-plate
ω	Forcing frequency
ω_A	Antiresonant frequency
ω_{IP}	Frequency at the invariant point
ω_R.	Natural frequency of DAVI, 1 DOF
Ω	Natural frequency of DAVI, 2 DOF

INTRODUCTION

VIBRATION AND SHOCK ISOLATION - THE STATE OF THE ART

Shock or vibration isolators are resilient mounts placed between a piece of machinery or equipment and its supporting structure to attenuate the transmissibility of time dependent loadings from the machinery to the structure, as in the case of reciprocating engines, or from the structure to the equipment, as in the mounting of delicate instruments in vehicles. When the loadings are applied suddenly, producing a transient response in the isolated item, the condition is referred to as shock. When the loadings are periodic and sustained for periods of time which are long in comparison to their period, the disturbance is classified as vibration.

All present shock and vibration isolators are basically only springs. Whether they incorporate damping or not, whether they are linear or nonlinear, metallic, or nonmetallic, their primary function is to act as purely resilient elements.

All present vibration isolators operate on the same principle: the transmissibility (that is, the ratio of the displacement of the isolated item to the displacement of the opposite end of the isolator) is less than one only if the natural frequency of the isolated mass on the isolator is less than the excitation frequency divided by the square root of two. It is impossible, for example, to obtain 90-percent isolation (0.1 transmissibility) with a conventional isolator unless the natural frequency of the isolated mass on the isolator is less than one-third the forcing frequency. Incorporation of viscous damping requires a still lower ratio of natural frequency to forcing frequency to achieve the same amount of isolation.

THE PROBLEM WITH CONVENTIONAL ISOLATORS

The natural frequency of a single-degree-of-freedom body mounted on a spring is a function of its static deflection only. The static deflection is defined as the amount the spring deflects under the weight of the body it supports. The greater the isolation desired, the larger the static

deflection becomes, allowing larger excursions of the isolated body under a periodic excitation, such as maneuvers of a vehicle. Because the most severe shock loads occur in bottoming of the isolator, the "soft" mounting desirable from a vibration standpoint may be dangerous from a shock standpoint unless the body is permitted an extremely large space in which it can move under purely elastic restraint.

For many reasons, the amount an isolated item can be allowed to deflect under load is necessarily limited, especially in vehicles. The isolated equipment must ultimately be connected to structure through pipes, wires, linkages, or similar connectors which will be affected by large deflections. Solder joints, for example, often fail in fatigue, resulting from continual deflection of wires. Space is generally limited to some degree. The most serious prohibition on large deflections is caused, however, by considerations of stress and elastic stability in the mounts themselves.

In the isolation of items from small deflections at very high frequencies, these problems are not conspicuous, but they are so obviously serious in the lower frequency range that they have most often rendered isolators entirely useless for vibration attenuation. Crede (Reference 5) notes, for example, that "The steady-state vibration of a Naval vessel occurs at a frequency that is generally too low to permit effective vibration isolation". He continues to explain that "The general philosophy in the design of isolators for Naval shipboard service is to design for protection against severe shock and, at the same time, to avoid excessive amplification of the steady-state vibrations". Plunkett, in Reference 9, concluded that vibration and shock isolation are incompatible requirements in the case of submarines. Most of the isolators used in helicopters are incorporated for shock loading only; insofar as vibration is concerned, they act as magnifiers.

It is a rule of thumb that isolation of frequencies below about 15 c.p.s., through the use of isolator mounts, is entirely impractical in vehicles. Unfortunately, most of those frequencies of vibration most distressful to the human body are below this figure (Reference 10) as are some of the problematical structural vibrations in missile work, such as those due to buffeting at maximum dynamic pressure and the "Pogo Effect" in the Titan II.

The solution to these problems is to provide a device which will give a very high percentage of isolation with a very small static deflection.

ISOLATOR APPLICATIONS BEYOND THE STATE OF THE ART

The isolation of decks, cargo pallets, passenger seats, and other devices in which the supported mass undergoes large changes is not practical with present isolators. Because the natural frequency is a function of the isolated mass, a passenger seat, for example, would magnify the vibrations when lightly loaded or empty. A partially loaded isolated cargo pallet would make the vibrations substantially worse than the vibrations it is supposed to attenuate.

To implement the vibration isolation of such devices, an isolator is required which will provide substantially the same degree of isolation irrespective of the load carried. The effective application of such an isolator to surface ships, helicopters, ground vehicles, pneumatic tools, etc., could be of great practical significance.

THE DAVI

The DAVI is a passive vibration isolation device which can provide a high degree of isolation at low frequency with very low static deflection. At a predetermined antiresonant frequency, the nearly zero transmissibility across a DAVI is independent of the mass of the isolated item. Analysis and test show that the DAVI gives significantly better shock isolation for its fundamental mode than a standard isolator.

This report discloses the results of an analytical and experimental research contract on the DAVI. It was conducted at Kaman Aircraft Corporation and was sponsored by USAAVLABS under Contract DA-44-177-AMC-196(T). The theoretical phases of this program successfully established the parameters of consequence to vibration and shock isolation obtainable from a DAVI, and the experimental work on a DAVI working model corroborated analytical predictions of the DAVI concept in vibration isolation.

THEORETICAL ANALYSIS

DAVI α

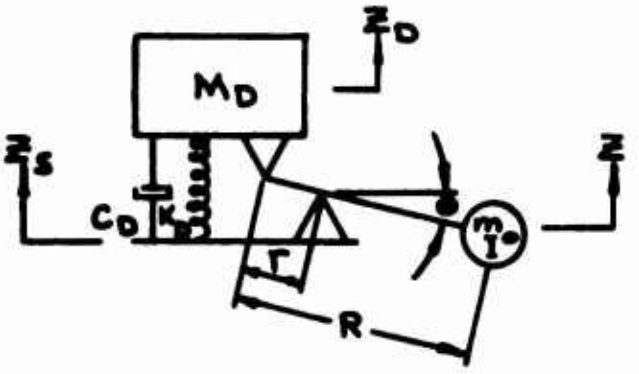

Figure 1. DAVI α

The energies of this system are written as follows:

Kinetic Energy:

$$T = \frac{1}{2} M_D \dot{z}_D^2 + \frac{1}{2} I \dot{\theta}^2 + \frac{1}{2} m_o \dot{z}^2 \qquad (1)$$

Potential Energy:

$$V = \frac{1}{2} K_D (z_D - z_S)^2 \qquad (2)$$

Dissipation Function:

$$D = \frac{1}{2} C_D (\dot{z}_D - \dot{z}_S)^2 \qquad (3)$$

The equation of motion, applying Lagrange's equation, is:

$$\left[M_D + \frac{I}{r^2} + m_o\left(1 - \frac{R}{r}\right)^2\right] \ddot{z}_D + C_D \dot{z}_D + K_D z_D = \left[\frac{I}{r^2} - m_o \frac{R}{r}\left(1 - \frac{R}{r}\right)\right] \ddot{z}_S + C_D \dot{z}_S + K_D z_S \qquad (4)$$

Assuming a steady-state sinusoidal solution, the transmissibility equation is:

$$T_D = \frac{Z_D}{Z_S} = \frac{-\left[\frac{1}{r^2} - m_o \frac{R}{r}\left(1 - \frac{R}{r}\right)\right]\omega^2 + i\omega C_D + K_D}{-\left[M_D + \frac{1}{r^2} + m_o\left(1 - \frac{R}{r}\right)^2\right]\omega^2 + i\omega C_D + K_D} \quad (5)$$

Let: $$P = M_D + m_o\left(1 - \frac{R}{r}\right)^2 + \frac{I}{r^2}$$

$$\mu = M_D + m_o\left(1 - \frac{R}{r}\right)$$

Substituting P and μ into equation (5)

$$T_D = \frac{-(P-\mu)\omega^2 + i\omega C_D + K_D}{-P\omega^2 + i\omega C_D + K_D}$$

where ω is the forcing frequency.

Zero transmissibility is obtained when:

$$\omega^2 = \omega_A^2 = \frac{K_D}{P-\mu} \quad (6)$$

It should be noted that the above antiresonant frequency is independent of the isolated mass (M_D). The resonant frequency with zero damping is obtained when the transmissibility equals ∞, or

$$\omega^2 = \omega_R^2 = \frac{K_D}{P}$$

The resonant frequency with damping is derived from:

$$-P\omega^2 + i\omega C_D + K_D = 0 \quad (7)$$

which can be nondimensionalized to.

$$-\left(\frac{\omega}{\omega_R}\right)^2 + 2\zeta i\left(\frac{\omega}{\omega_R}\right) + 1 = 0 \tag{8}$$

where

$$2\zeta = \frac{C_D}{\sqrt{K_D P}}$$

The antiresonant frequency with damping is:

$$-(P-\mu)\,\omega^2 + i\omega C_D + K_D = 0 \tag{9}$$

which is nondimensionalized to

$$-\left(1-\frac{\mu}{P}\right)\left(\frac{\omega}{\omega_R}\right)^2 + 2\zeta i\left(\frac{\omega}{\omega_R}\right) + 1 = 0 \tag{10}$$

from which

$$\left(\frac{\omega}{\omega_R}\right)^2 = \frac{1}{1-\frac{\mu}{P}}\left\{1 - \frac{2\zeta^2}{1-\frac{\mu}{P}}\left[1 \pm \sqrt{1-\frac{1}{\zeta^2}\left(1-\frac{\mu}{P}\right)}\right]\right\} \tag{11}$$

Transmissibility is given by:

$$T_D^2 = \left\{1 + \frac{\frac{\mu}{P}\left(\frac{\omega}{\omega_R}\right)^2\left[1-\left(\frac{\omega}{\omega_R}\right)^2\right]}{\left[1-\left(\frac{\omega}{\omega_R}\right)^2\right]^2 + \left[2\zeta\left(\frac{\omega}{\omega_R}\right)\right]^2}\right\}^2 + \left\{\frac{2\frac{\mu}{P}\zeta\left(\frac{\omega}{\omega_R}\right)^3}{\left[1-\left(\frac{\omega}{\omega_R}\right)^2\right]^2 + \left[2\zeta\left(\frac{\omega}{\omega_R}\right)\right]^2}\right\} \tag{12}$$

Figures 2, 3, and 4 show how transmissibility varies for different values of α/P and ζ.

It is seen from these figures that with increased damping the amplification at resonance is decreased as in conventional isolation systems. The amount of isolation obtained at the antiresonance is also decreased, and the high frequency isolation is decreased similar to results of a conventional isolation system.

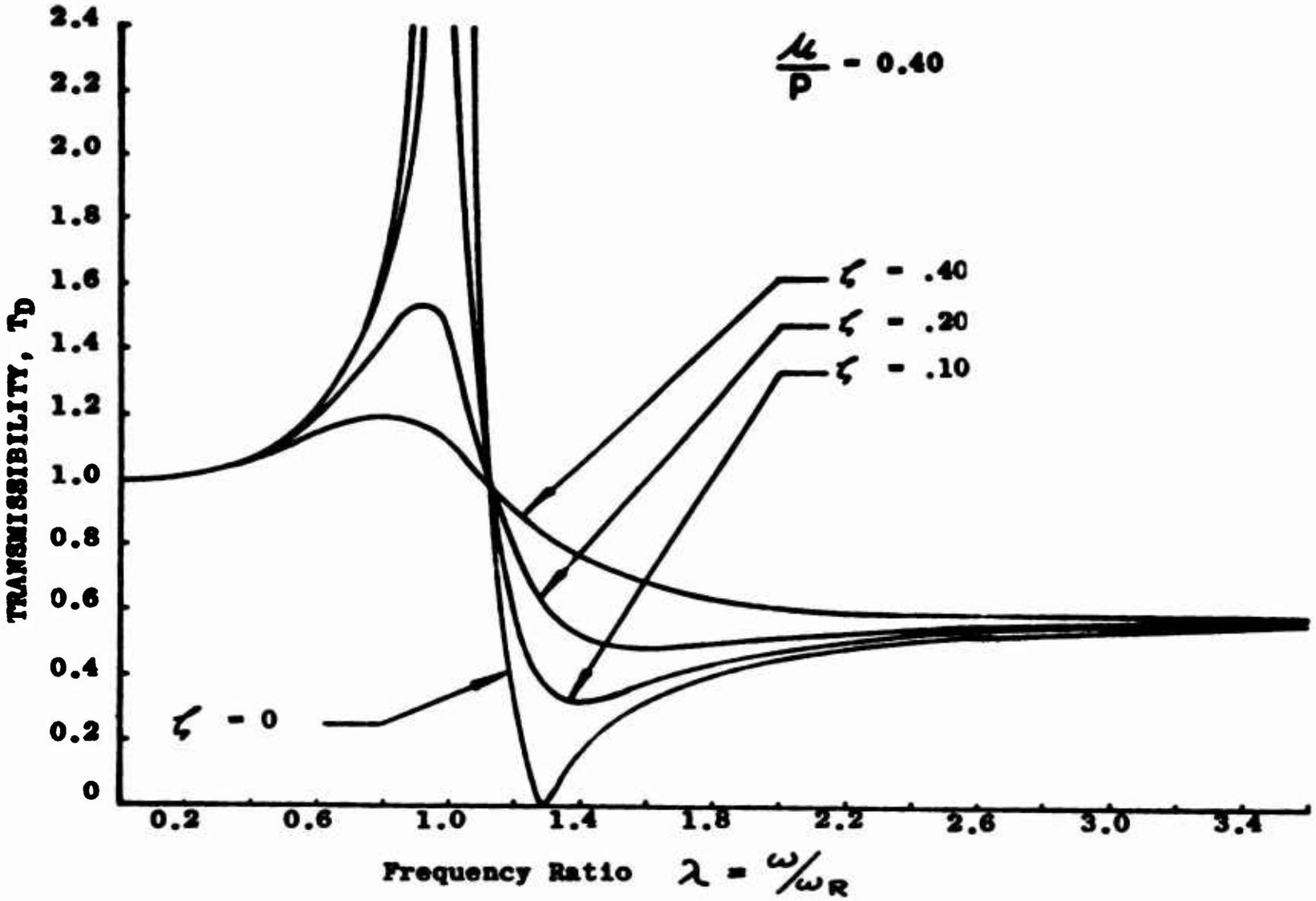

Figure 2. Theoretical Response Curve for DAVI α

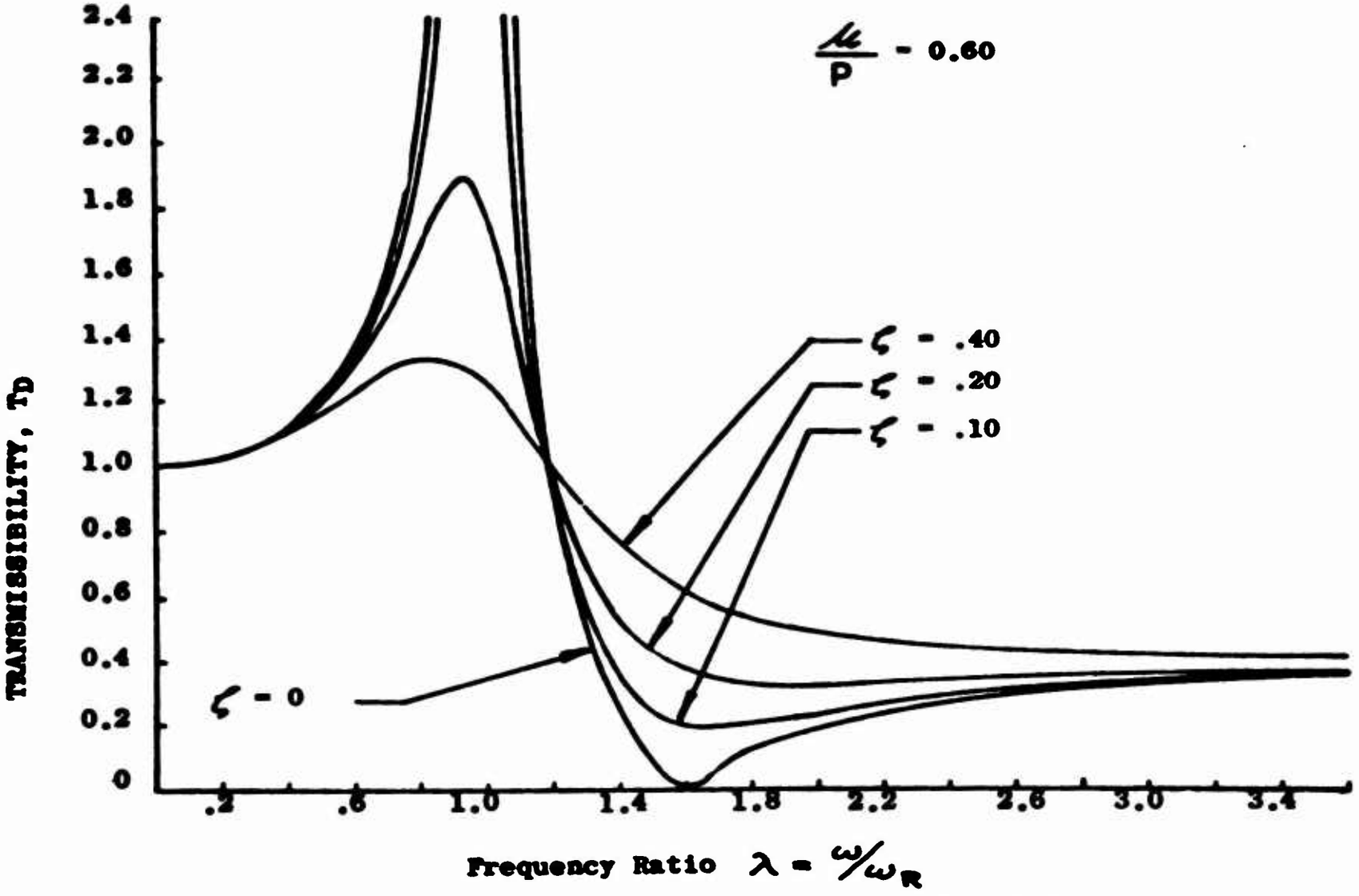

Figure 3. Theoretical Response Curve for DAVI ∝

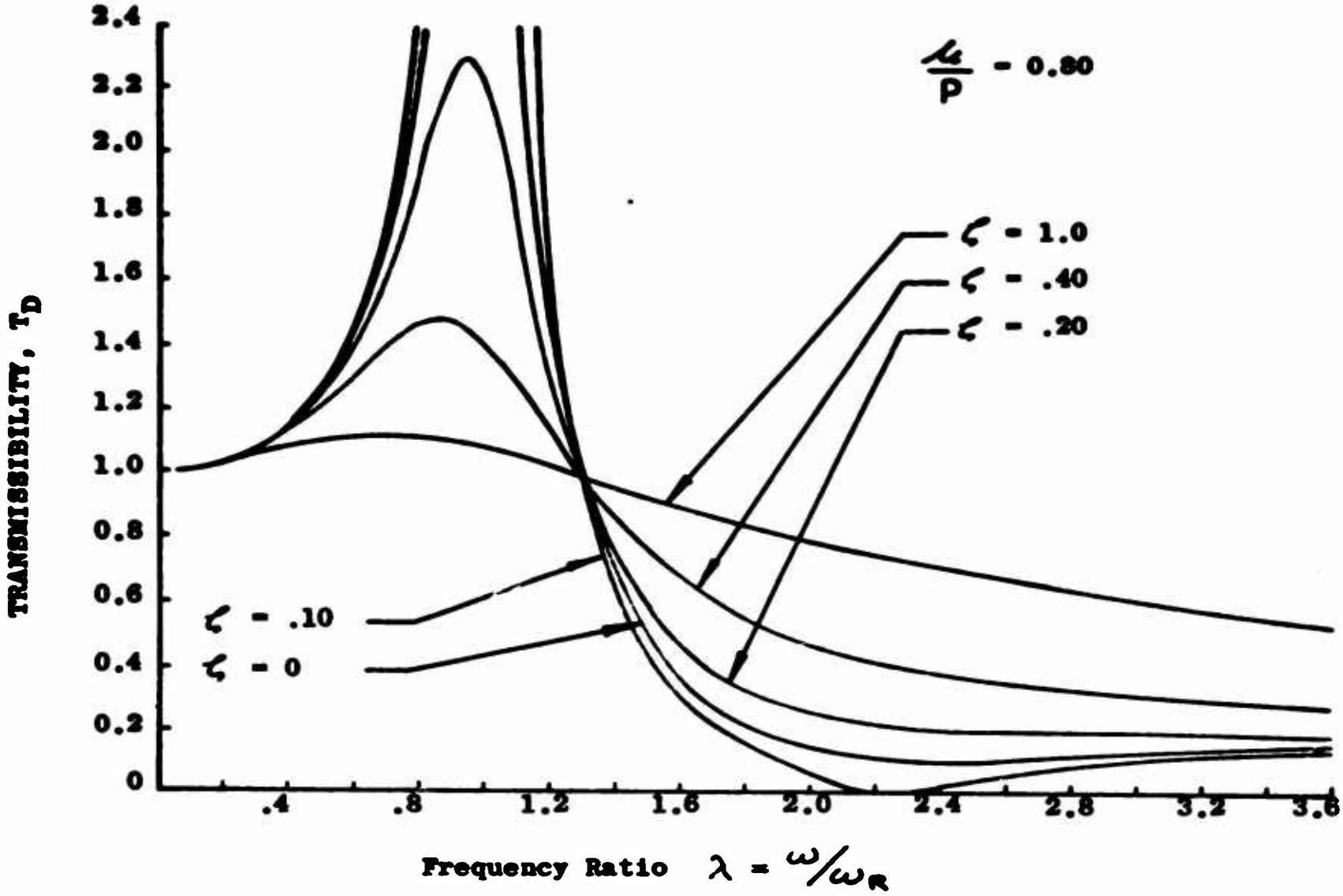

Figure 4. Theoretical Response Curve for DAVI α

Locus of Maxim and Minima of Transmissibility

Making the following substitution in equation (12), let

$$\rho = 1-\left(\frac{\omega}{\omega_R}\right)^2 = 1-\lambda^2$$

$$\sigma = 2\zeta\frac{\omega}{\omega_R}$$

$$\gamma = 2\zeta$$

$$\lambda = \frac{\omega}{\omega_R} \; ; \; \lambda_A = \frac{\omega_A}{\omega_R}$$

$$\beta = \frac{\mu}{\rho}$$

$$\alpha = 1-\frac{\mu}{\rho} = 1-\beta = \frac{\omega_R^2}{\omega_A^2}$$

Then:
$$T_D^2 = \left[1+\frac{\beta\lambda^2\rho}{\rho^2+\sigma^2}\right]^2+\left[\frac{\sigma\beta\lambda^2}{\rho^2+\sigma^2}\right]^2$$

$$T_D^2 = \frac{\rho^2+\sigma^2+2\beta\lambda^2\rho+(\beta\lambda^2)^2}{\rho^2+\sigma^2}$$

$$T_D^2 = \frac{(1-\lambda^2+\beta\lambda^2)^2+(\gamma\lambda)^2}{(1-\lambda^2)^2+(\gamma\lambda)^2}$$

$$T_D^2 = \frac{(1-\alpha\lambda^2)^2+(\gamma\lambda)^2}{(1-\lambda^2)^2+(\gamma\lambda)^2} \qquad (13)$$

To find the maxima and minima, set the first derivative of the transmissibility with respect to frequency ratio ($\lambda = \omega/\omega_R$) equal to zero. Rewriting equation (13) as follows:

$$T_D^2 = \frac{\left(\frac{1}{\lambda} - \alpha\lambda\right)^2 + \gamma^2}{\left(\frac{1}{\lambda} - \lambda\right)^2 + \gamma^2} \tag{14}$$

Let

$$T_D^2 = \frac{N}{D}$$

Then

$$\frac{\partial T_D}{\partial \lambda} = 2T_D \frac{\partial T_D}{\partial \lambda} = \frac{D\frac{\partial N}{\partial \lambda} - N\frac{\partial D}{\partial \lambda}}{D^2} = 0 \tag{15}$$

Therefore, the condition for maxima or minima transmissibility is:

$$T_D = \frac{\frac{\partial N}{\partial \lambda}}{\frac{\partial D}{\partial \lambda}}$$

$$T_D = \frac{\left(\frac{1}{\lambda} - \alpha\lambda\right)\left(\frac{1}{\lambda^2} + \alpha\right)}{\left(\frac{1}{\lambda} - \lambda\right)\left(\frac{1}{\lambda^2} + 1\right)} \tag{16}$$

$$T_D = \frac{1 - \alpha^2\lambda^4}{1 - \lambda^4}$$

Since

$$\omega_A^2 = \frac{1}{1-\beta}\,\omega_R^2$$

$$\omega_A^2 = \frac{1}{\alpha}\,\omega_R^2$$

$$\frac{\omega_A}{\omega_R} = \frac{1}{\sqrt{\alpha}} = \lambda_A^2,$$

we have

$$T_D^2 = \frac{\lambda_A^4 - \lambda^4}{\lambda_A^4(1-\lambda^4)} \tag{17}$$

If: $\lambda = 0$, then $T_D^2 = 1$

$\lambda_A > 1$ and $0 < \lambda < 1$, then T_D^2 is positive

$\lambda_A > 1$ and $\lambda = 1$, then $T_D^2 = \infty$ (0 damping)

$\lambda_A > 1$ and $\lambda = \lambda_A$, then $T_D^2 = 0$

$\lambda_A = 1$ and $\lambda >> \lambda_A$, then $T_D^2 \rightarrow 1 - \alpha^2$

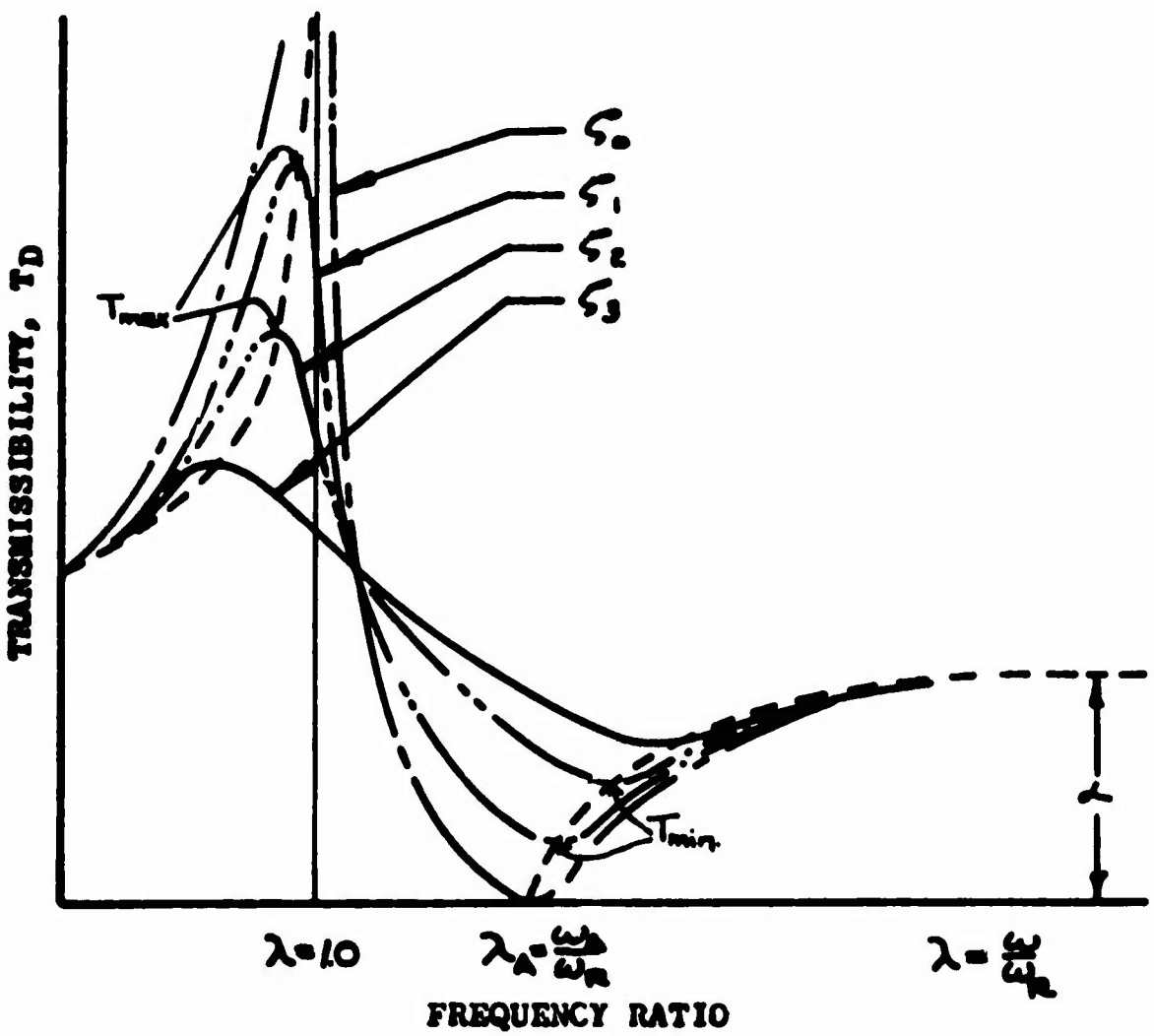

Figure 5. Response Curve Showing T_{max} and T_{min} for Varied ζ

Figure 5 shows, in general, how the maximum and minimum values of transmissibility plot relative to the damping dependent frequency response curves. As can be seen, at frequencies lower than the resonant frequency, the maximum transmissibility, $T_{D_{max}}$, varies inversely, frequency-wise, with the damping ratio ζ ; that is, frequency of $T_{D_{max}}$ for a specific value of damping (e.g., ζ = 1.0) occurs at a lower frequency than the frequency of T_{max} for a lower value of damping (e.g., ζ = 0). Above the anti-resonant frequency, the minimum values of transmissibility, $T_{D_{min}}$, vary directly frequency-wise with ζ ; that is, the frequency of $T_{D_{min}}$ for a specific value of damping (say, ζ = 1.0) occurs at a higher frequency than the frequency of T_{min} for a lower value of damping.

Furthermore, it can be seen that for all values of ζ the transmissibility approaches the value $\alpha = \frac{p-\mu}{p}$ at large values of λ , the frequency ratio.

Invariant Point

From equation (5), the transmissibility is:

$$|T_D|^2 = \frac{\left(1 - \frac{\omega^2}{\omega_R^2} + \frac{\mu}{p}\frac{\omega^2}{\omega_R^2}\right)^2 + \left(2\zeta\frac{\omega}{\omega_R}\right)^2}{\left(1 - \frac{\omega^2}{\omega_R^2}\right)^2 + \left(2\zeta\frac{\omega}{\omega_R}\right)^2} \qquad (18)$$

which is of the form

$$|T_D|^2 = \frac{A\zeta^2 + B}{C\zeta^2 + D} \qquad (19)$$

If $\frac{A}{C} = \frac{B}{D}$, then T_D is independent of damping (Reference 6, Den Hartog). In equation (18), T_D is independent of damping when

$$\pm 1 = \frac{1 - \frac{\omega^2}{\omega_R^2} + \frac{\mu}{p}\frac{\omega^2}{\omega_R^2}}{1 - \frac{\omega^2}{\omega_R^2}} = 1 + \frac{\mu}{p}\frac{\frac{\omega^2}{\omega_R^2}}{1 - \frac{\omega^2}{\omega_R^2}}$$

The positive solution is obviously trivial. Taking the negative solution gives

$$-2 = \frac{\mu}{p} \frac{\left(\frac{\omega}{\omega_R}\right)^2}{1-\left(\frac{\omega}{\omega_R}\right)^2}$$

or

$$\left(\frac{\omega_{IP}}{\omega_R}\right)^2 = \frac{2}{2-\frac{\mu}{p}}$$

where ω_{IP} is the frequency at the invariant point.

Noting that $1-\frac{\mu}{p} = \left(\frac{\omega_R}{\omega_A}\right)^2 = T_{DVHF}$, that is, the transmissibility of the DAVI at very high frequency, the above expression becomes:

$$\left(\frac{\omega_{IP}}{\omega_R}\right)^2 = \frac{2}{1-T_{DVHF}} \qquad (20)$$

which, of course, reduces to $\frac{\omega_{IP}}{\omega_R} = \sqrt{2}$ when $T_{DVHF} = 0$, that is, a convertional isolator

It should be noted from equation (20) that the invariant point of a DAVI is always further above resonance than is the invariant point of a conventional isolator.

The transmissibility at the invariant point is given by:

$$T_{DIP} = \frac{1-\left(\frac{\omega}{\omega_R}\right)^2 + \frac{\mu}{p}\left(\frac{\omega}{\omega_R}\right)^2}{1-\left(\frac{\omega}{\omega_R}\right)^2} \qquad (21)$$

or

$$T_{DIP} = \frac{T_{DVHF}-1}{T_{DVHF}+1} \qquad (22)$$

When $T_{DVHF} = 0$, $T_{DIP} = -1.0$, that is, a conventional isolator. Because $0 < T_{DVHF} < 1$ in the DAVI, the invariant point always lies between resonance and anti-resonance and the invariant transmissibility is always less than one.

THE SERIES-DAMPED TWO-DEGREE-OF-FREEDOM DAVI 2

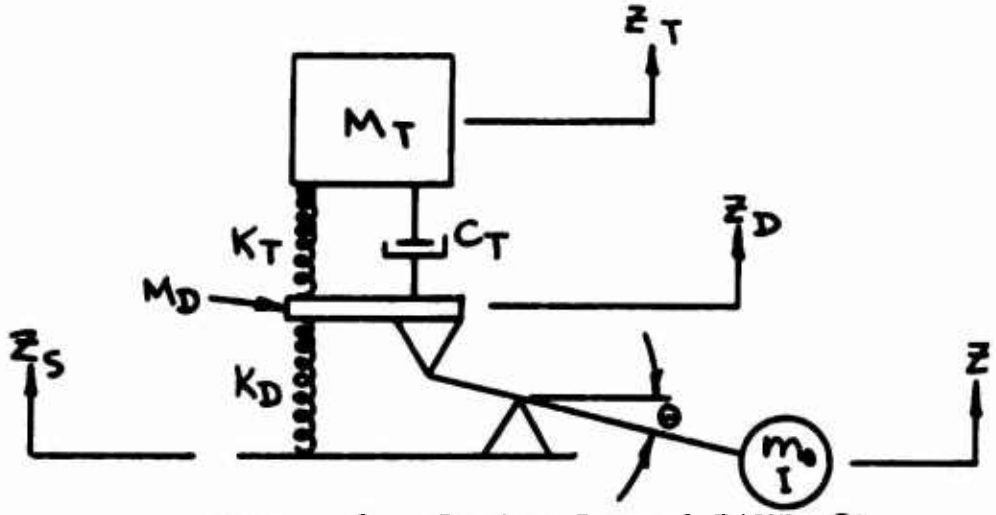

Figure 6. Series-Damped DAVI 2

Description of System

The Series-Damped Two-Degree-Of-Freedom DAVI is shown diagrammatically in Figure 6 above. It consists of the isolated mass, M_T, supported on an intermediate platform of mass, M_D, by a spring-damper system defined parametrically by spring constant, K_T, and damping coefficient, C_T. The intermediate platform is supported by the DAVI system whose parameters are spring constant, K_D, mass, m, and inertia, I. The DAVI system is assumed to be frictionless.

Derivation of Equations

The energies of the system are written as follows:

Kinetic Energy:

$$T = \frac{1}{2} M_T \dot{z}_T^2 + \frac{1}{2} M_D \dot{z}_D + \frac{1}{2} m \dot{z}^2 + \frac{1}{2} I \dot{\theta}^2 \qquad (23)$$

Potential Energy:

$$V = \frac{1}{2} K_T (z_T - z_D)^2 + \frac{1}{2} K_D (z_D - z_S)^2 \qquad (24)$$

Dissipation Function:

$$D = \frac{1}{2} C_T (\dot{z}_T - \dot{z}_D)^2 \qquad (25)$$

Substituting the relations for θ and S into the energy expressions, we get:

$$T = \frac{1}{2} M_T \dot{z}_T^2 + \frac{1}{2} M_D \dot{z}_D^2 + \frac{1}{2} m_o \left[\left(1 - \frac{R}{r}\right) \dot{z}_D + \frac{R}{r} \dot{z}_S \right]^2 + \frac{1}{2} \frac{1}{r^2} \left(\dot{z}_D - \dot{z}_S\right)^2 \tag{26}$$

$$V = \frac{1}{2} K_T \left(z_T - z_D\right)^2 + \frac{1}{2} K_D \left(z_D - z_S\right)^2 \tag{27}$$

$$D = \frac{1}{2} C_T \left(\dot{z}_T - \dot{z}_D\right)^2 \tag{28}$$

From these energy equations the following equations of motion are derived by Lagrangian techniques.

z_T Equation:

$$M_T \ddot{z}_T + C_T \dot{z}_T + K_T z_T - C_T \dot{z}_D - K_T z_D = 0 \tag{29}$$

z_D Equation:

$$\left[M_D + \left(1 - \frac{R}{r}\right)^2 m_o + \frac{1}{r^2}\right] \ddot{z}_D + C_T \dot{z}_D + \left(K_T + K_D\right) z_D - C_T \dot{z}_T - K_T z_T + m_o \frac{R}{r} \left(1 - \frac{R}{r}\right) \ddot{z}_S - \frac{1}{r^2} \ddot{z}_S - K_D z_S = 0 \tag{30}$$

Assuming a steady-state sinusoidal solution and writing in matrix form, this becomes:

$$\begin{vmatrix} \left[-M_T \omega^2 + i\omega C_T + K_T\right] & \left[-C_T i\omega - K_T\right] \\ \left[-C_T i\omega - K_T\right] & \left[-\left[M_D + \left(1 - \frac{R}{r}\right)^2 m_o + \frac{1}{r^2}\right] \omega^2 + i\omega C_T + K_T + K_D\right] \end{vmatrix} \begin{vmatrix} z_T \\ z_D \end{vmatrix}$$

$$= \left\{ \left[m_o \frac{R}{r} \left(1 - \frac{R}{r}\right) - \frac{1}{r^2} \right] \omega^2 + K_D \right\} z_S \begin{vmatrix} 0 \\ 1 \end{vmatrix} \tag{31}$$

Using Cramer's rule, the transmissibility equation for the motion of the mass, M_T, can be written:

$$\frac{Z_T}{Z_S} = \frac{\left\{\left[m_o \frac{R}{r}\left(1-\frac{R}{r}\right)-\frac{I}{r^2}\right]\omega^2+K_D\right\}\begin{vmatrix} 0 & -C_T i\omega - K_T \\ 1 & -\left[M_D+\left(1-\frac{R}{r}\right)^2 m_o+\frac{I}{r^2}\right]\omega^2 + i\omega C_T + K_T + K_D \end{vmatrix}}{\Delta}$$

$$\frac{Z_T}{Z_S} = \frac{\left\{\left[m_o \frac{R}{r}\left(1-\frac{R}{r}\right)-\frac{I}{r^2}\right]\omega^2+K_D\right\}(C_T i\omega + K_T)}{\Delta} \qquad (32)$$

where $\Delta = 0$ is the characteristic equation of the system.

Let:

$$P = M_D + \left(1-\frac{R}{r}\right)^2 m_o + \frac{I}{r^2}$$

$$\mu = M_D + \left(1-\frac{R}{r}\right) m_o$$

$$\mu - P = M_o \frac{R}{r}\left(1-\frac{R}{r}\right) - \frac{I}{r^2}$$

Then, the following expression for the absolute value of the transmissibility squared can be written:

$$T_D^2 = \frac{\left[-(P-\mu)\omega^2+K_D\right]^2 (K_T + C_T^2\omega^2)}{\left[(m_T\omega^2-K_T)(P\omega^2-K_D)-M_T K_T \omega^2\right]^2 + C_T^2\omega^2\left[(P+M_T)\omega^2-K_D\right]^2} \qquad (33)$$

Further let:

$$\Omega^2 = \frac{K_T}{M_T} \qquad h = \frac{\omega}{\omega_A}$$

$$C_c = 2\sqrt{M_T K_T} = 2 M_T \Omega \qquad \mu_o = \frac{P-\mu}{M_T}$$

$$\zeta = \frac{C}{C_c} \qquad \alpha\omega_A^2 = \frac{K_D}{P}$$

$$f = \frac{\omega_A}{\Omega} \qquad \frac{\alpha}{\mu_o} = \frac{M_T}{P}$$

By substitution we get, in nondimensional form:

$$T_D^2 = \frac{\alpha^2(1-h^2)^2\left[1+(2\zeta)^2 f^2 h^2\right]}{\left[(h^2f^2-1)(h^2-\alpha)-\frac{\alpha}{\mu_o}h^2\right]^2+(2\zeta)^2h^2f^2\left[(1-\frac{\alpha}{\mu_o})h^2-\alpha\right]^2} \quad (34)$$

The Invariant Points

T_D^2 is of the form $\frac{A+B(2\zeta)^2}{C+D(2\zeta)^2}$

and will be independent of ζ if:

$$\frac{A}{C} = \frac{B}{D}$$

that is, if:

$$\frac{1}{(h^2f^2-1)(h^2-\alpha)-\frac{\alpha}{\mu_o}h^2} = \pm\frac{1}{(1+\frac{\alpha}{\mu_o})h^2-\alpha} \quad (35)$$

Taking the positive sign we have:

$$(h^2f^2-1)(h^2-\alpha)-\frac{\alpha}{\mu_o}h^2 = (1+\frac{\alpha}{\mu_o})h^2-\alpha$$

i.e.,

$$h^4f^2-\alpha h^2f^2-h^2-\alpha-\frac{\alpha}{\mu_o}h^2 = h^2+\frac{\alpha}{\mu_o}h^2-\alpha$$

To solve for h, the forcing function frequency ratio, write in quadratic form, and solve, for h^2:

$$f^2h^4-(\alpha f^2+2+\frac{2\alpha}{\mu_o})h^2+2\alpha = 0$$

$$\therefore h^2 = \frac{1}{2f^2}\left\{\alpha f^2+2(1+\frac{\alpha}{\mu_o})\pm\sqrt{\left[\alpha f^2+2(1+\frac{\alpha}{\mu_o})\right]^2-8\alpha f^2}\right\} \quad (36)$$

Taking the negative sign of equation (35):

$$(h^2f^2-1)(h^2-\alpha)-\frac{\alpha}{\mu_o}h^2=-(1-\frac{\alpha}{\mu_o})h^2+\alpha$$

i.e.,

$$h^4f^2-\alpha h^2f^2-h^2+\alpha-\frac{\alpha}{\mu_o}h^2=-h^2-\frac{\alpha}{\mu_o}h^2+\alpha \qquad (37)$$

From equations (36) and (37), it is seen that three invariant points are obtained other than the trivial case of h = 0 and h = 1, two from equation (36) and $h^2 = \alpha$ from equation (37).

The transmissibility at the $h^2 = \alpha$ point is found by substitution in equation (33) to be:

$$T_D=\frac{\mu}{\alpha}(1-\alpha)$$

Making the substitutions found on Page 19, the transmissibility becomes:

$$T_D=\frac{\mu}{M_T}$$

and will be above or below the antiresonant frequency, depending on whether

$$\mu=M_D+(1-\frac{R}{r})m$$

is greater or less than 2P.

Figures 7, 8, and 9 show typical frequency response curves for the Series-Damped DAVI for various values of the peak-to-null frequency ratio, f, for various values of mass ratio, μ_o, and for different values of damping ratio, ζ. Numerical values of the curves were obtained by programming the transmissibility equation onto a digital computer. The curves plotted are a representative sample of a comprehensive parameter study with $M_D = 0$ and $\alpha = 1$. In Figures 7 and 9, the invariant points occur as predicted in equation (36). In Figure 8, the invariant point is at h = 1.03 and being close to h = 1 does not show in the results.

It is seen from these figures that although the Series-Damped DAVI 7 is a two-degree-of-freedom system, 100-percent isolation can be obtained at its tuned or anti-resonant frequency. This tuned frequency is not affected by the amount of isolated mass. This parametric study also shows that an optimum amount of damping can be obtained which will attenuate the low frequency resonance condition and give transmissibility less than .5 for the higher mode. High frequency isolation approaches zero as in a conventional isolator.

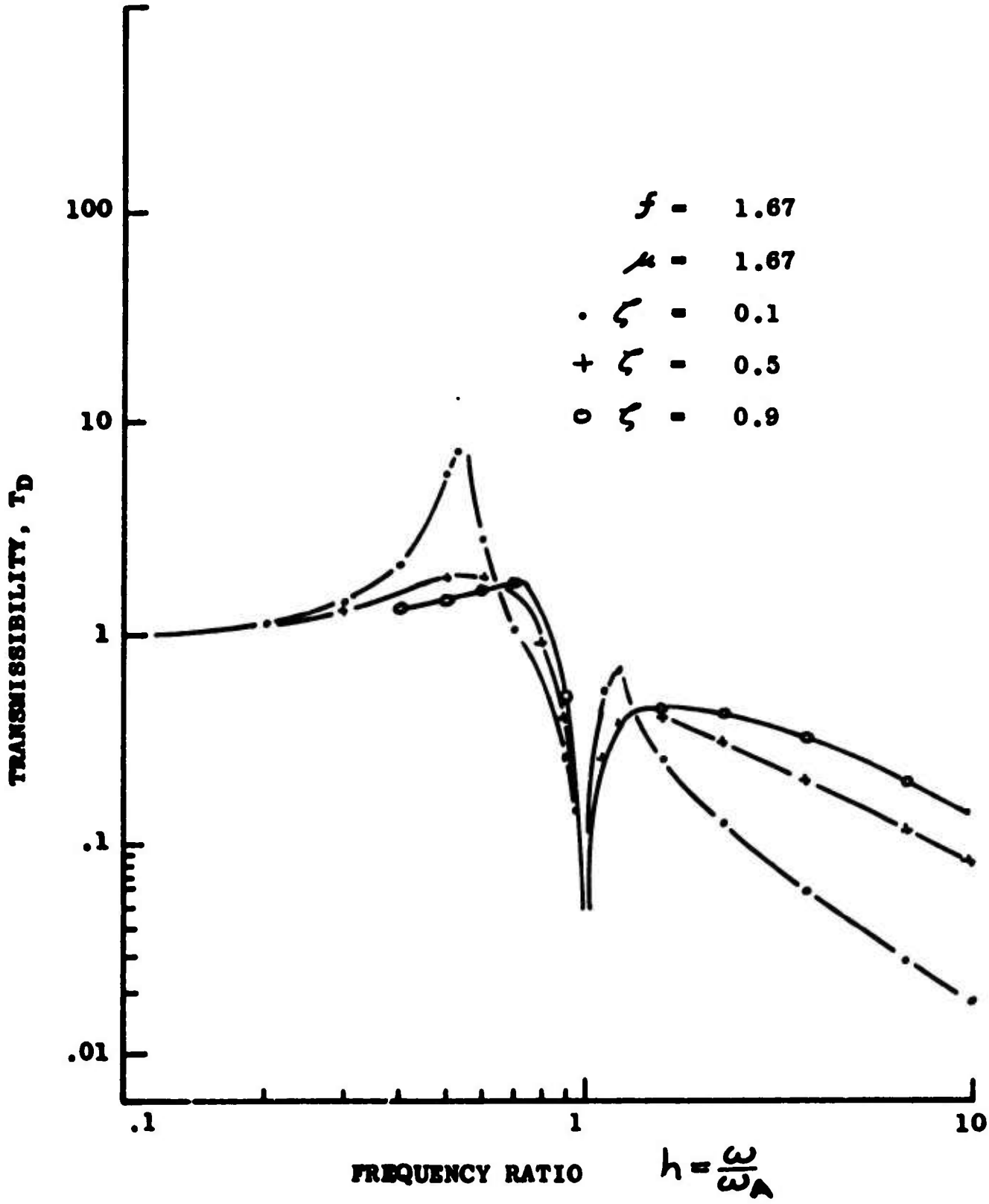

Figure 7 . Theoretical Response Curve for Series DAVI γ

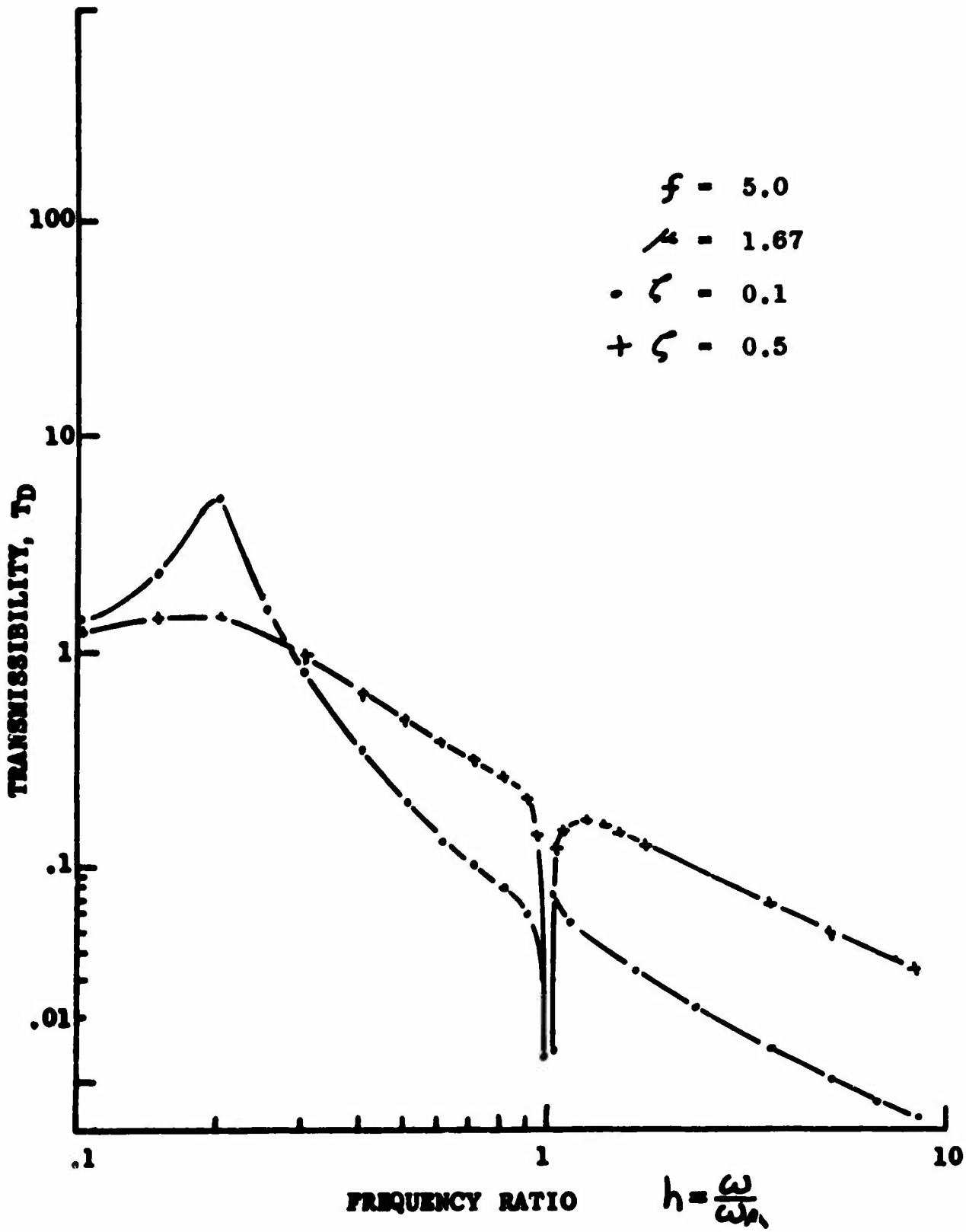

Figure 8 . Theoretical Response Curve for Series DAVI 7

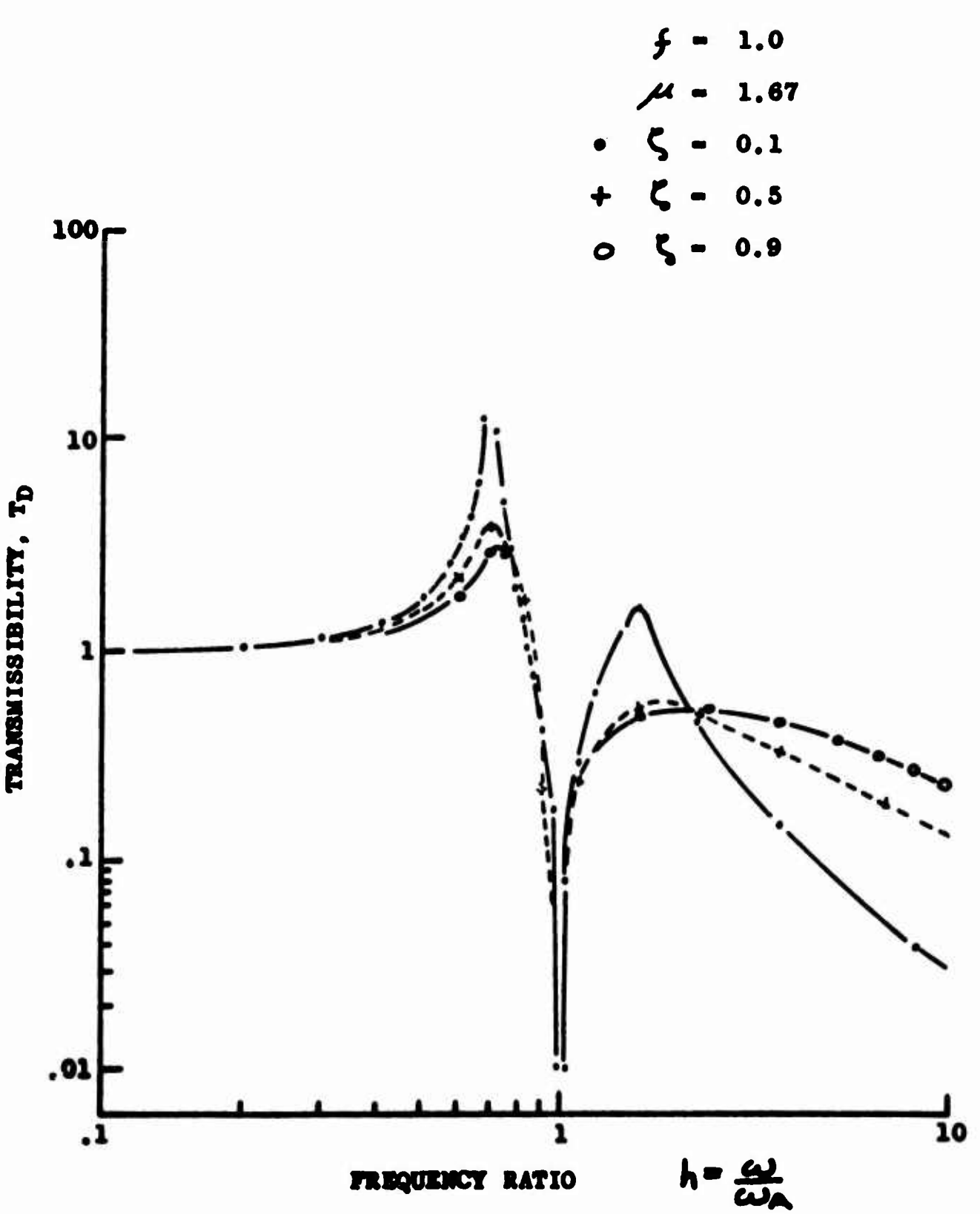

Figure 9. Theoretical Response Curve for Series DAVI

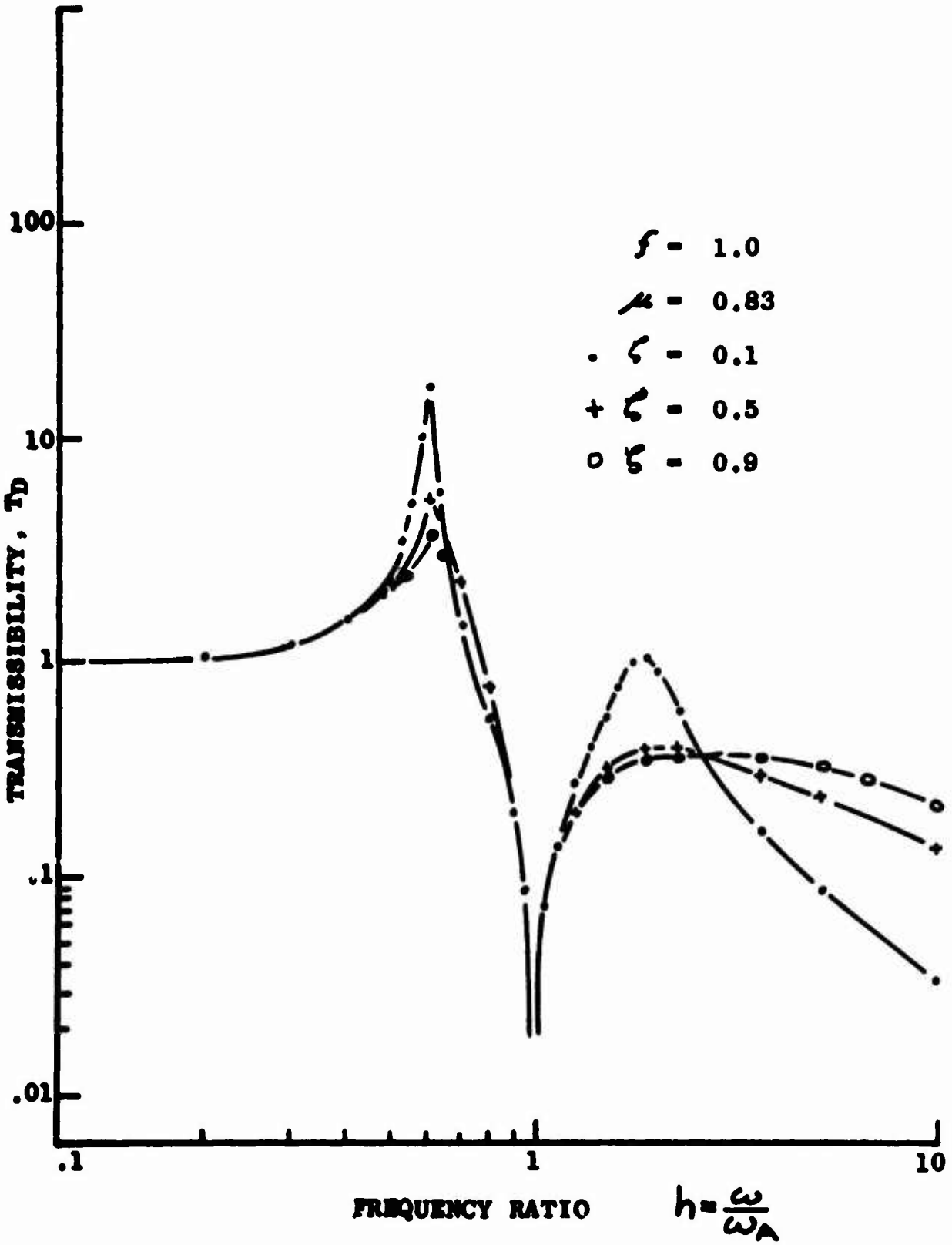

Figure 10 . Theoretical Response Curve for Series DAVI

SHOCK TRANSMISSIBILITY

Conventional Isolator

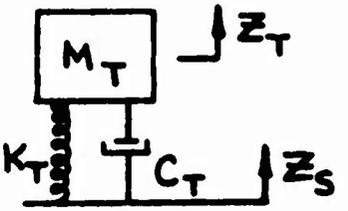

Figure 11. Conventional Isolator

The equation of motion for this system is:

$$M_T \ddot{z}_T + C_T (\dot{z}_T - \dot{z}_S) + K_T (z_T - z_S) = 0 \qquad (38)$$

If

$$z_S = a \cdot t, \quad \dot{z}_S = a, \text{ and } \ddot{z}_S = 0,$$

the above equation can be written:

$$M_T \ddot{z} + C_T \dot{z} + K_T z = 0 \qquad (39)$$

where $z = z_T - z_S$

This equation has the standard solution

$$z = e^{-\zeta \omega_R t} \left[A \cos \sqrt{1-\zeta^2}\omega_R t + B \sin \sqrt{1-\zeta^2}\omega_R t \right] \qquad (40)$$

where

$$\omega_R = \sqrt{\frac{K_T}{M_T}} \quad \text{and} \quad 2\zeta = \frac{C_T}{\sqrt{M_T K_T}}$$

The initial conditions are assumed to be:

$$z = 0 \text{ and } \dot{z}_T = 0 \text{ at } t = 0$$

From the first initial condition, it follows immediately that $A = 0$.

The second initial condition is applied as follows:

$$z = z_T - z_S = B e^{-\zeta\omega_R t} \sin\sqrt{1-\zeta^2}\,\omega_R t \tag{41}$$

$$\dot{z} = \dot{z}_T - \dot{z}_S = B\left[\sqrt{1-\zeta^2}\,\omega_R e^{-\zeta\omega_R t}\cos\sqrt{1-\zeta^2}\,\omega_R t - \zeta\omega_R e^{-\zeta\omega_R t}\sin\sqrt{1-\zeta^2}\,\omega_R t\right] \tag{42}$$

Thus, since $\dot{z}_s = a$ and $\dot{z}_T = 0$ at $t = 0$,

$$B = \frac{-a}{\sqrt{1-\zeta^2}\,\omega_R}$$

and the displacement of M_T is described by

$$z_T = a\left[t - \frac{e^{-\zeta\omega_R t}}{\sqrt{1-\zeta^2}\,\omega_R}\sin\sqrt{1-\zeta^2}\;\omega_R t\right] \tag{43}$$

and the velocity by

$$\dot{z}_T = a\left\{1 - e^{-\zeta\omega_R t}\left[\cos\sqrt{1-\zeta^2}\,\omega_R t - \frac{\zeta}{\sqrt{1-\zeta^2}}\sin\sqrt{1-\zeta^2}\,\omega_R t\right]\right\} \tag{44}$$

and the acceleration by

$$\ddot{z}_T = a\omega_R e^{-\zeta\omega_R t}\left[\frac{1-2\zeta^2}{\sqrt{1-\zeta^2}}\sin\sqrt{1-\zeta^2}\,\omega_R t + 2\zeta\cos\sqrt{1-\zeta^2}\,\omega_R t\right] \tag{45}$$

This will be a maximum when $\dddot{z}_T = 0$

That is, when $\tan\ \omega_\alpha t = \dfrac{(1-4\zeta^2)\sqrt{1-\zeta^2}}{(3-4\zeta^2)\zeta}$ (46)

$$\omega_\alpha t = \frac{1}{3\zeta} \text{ when } \zeta = << 1$$

where

ω_α = ω damped

Thus, the maximum acceleration is:

$$\ddot{z}_{T_{MAX}} = a\omega_R e^{-\zeta\omega_R t}\left\{\frac{1+2\zeta-6\zeta^2-8\zeta^3+8\zeta^4}{3-4\zeta^2}\right\}\cos\sqrt{1-\zeta^2}\omega_R t \qquad (47)$$

which for small damping

$$\ddot{z}_{T_{MAX}} = a\omega_R e^{-\zeta\omega_R t}\left(\frac{1+2\zeta}{3}\right)\cos\omega_d t$$

DAVI α

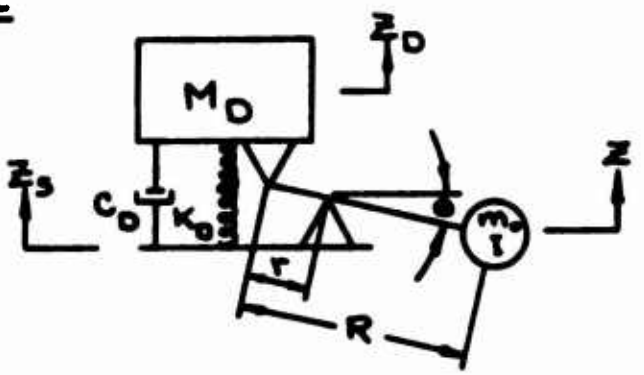

Figure 12. DAVI α

The equation of motion for this system is:

$$\left[M_D + \frac{I}{r^2} + m_o\left(1-\frac{R}{r}\right)^2\right]\ddot{z}_D + C_D\dot{z}_D + K_D z_D$$
$$= \left[\frac{I}{r^2} - m_o\frac{R}{r}\left(1-\frac{R}{r}\right)\right]\ddot{z}_s + C_D\dot{z}_s + K_D z_s \qquad (48)$$

If $z_s = a\cdot t$, $\dot{z}_s = a$ and $\ddot{z}_s = o$

and this can be written in the form:

$$P\ddot{z} + C_D\dot{z} + K_D z = 0 \qquad (49)$$

Then, the analysis from this point is the same as for the conventional isolator.

Thus, as derived for the Conventional Damped System:

$$z_D = a\left[t - \frac{e^{-\zeta\omega_R t}\,\mathrm{SIN}\sqrt{1-\zeta^2}\,\omega_R t}{\sqrt{1-\zeta^2}\,\omega_R}\right] \tag{50}$$

$$\dot{z}_D = a\left[1 - e^{-\zeta\omega_R t}\left(\cos\sqrt{1-\zeta^2}\,\omega_R t - \frac{\zeta}{\sqrt{1-\zeta^2}}\,\mathrm{SIN}\sqrt{1-\zeta^2}\,\omega_R t\right)\right] \tag{51}$$

$$\ddot{z}_D = a\omega_R e^{-\zeta\omega_R t}\left[\frac{1-2\zeta^2}{\sqrt{1-\zeta^2}}\,\mathrm{SIN}\sqrt{1-\zeta^2}\,\omega_R t + 2\cos\sqrt{1-\zeta^2}\,\omega_R t\right] \tag{52}$$

with the difference that the resonant frequency for the DAVI is given by:

$$\omega_R = \sqrt{\frac{K_D}{P}}, \qquad P = M_D + \frac{I}{r^2} + m_o\left(1 - \frac{R}{r}\right)^2,$$

and

$$2\zeta = \frac{C_D}{\sqrt{PK_D}}.$$

If the damping for the two systems being compared (the Conventional Damped System and the Damped DAVI α) is adjusted to be numerically the same, a comparison can be made between the forces transmitted to the isolated masses.

$$\frac{\ddot{z}_D}{\ddot{z}_T} = \frac{\omega_R\ \text{(DAVI)}}{\omega_R\ \text{(CONVENTIONAL SYSTEM)}}$$

$$\frac{z_D}{z_T} = \sqrt{\frac{\frac{K_D}{P}}{\frac{K_T}{M_T}}}$$

If $K_T = K_D$,

$$\frac{z_D}{z_T} = \sqrt{\frac{M_T}{M_D + \frac{I}{r^2} + m_o\left(1 - \frac{R}{r}\right)^2}} \tag{53}$$

Since M_T, the isolated mass of the conventional system, and M_D, the isolated mass of the DAVI, are equal, it is seen from the above equation that the DAVI will always have better shock transmissibility for a step velocity shock than a conventional isolator with the same spring rate.

DAMPING CONSIDERATIONS

From the preceding theoretical analysis, it is noted that damping in the basic DAVI has the conventional effect of lowering the resonant peak; however, it also has the additional characteristic of reducing the degree of isolation at antiresonance or within the antiresonant "bucket". To corroborate this analysis, several methods of damping were considered for testing on laboratory models.

FRICTION DAMPING

The use of steel wool or a friction plate interconnection between the excitation source and the isolated mass was considered not suitable because of the difficulty of controlling the effective damping rate and because of the small relative displacements involved for this general size DAVI model.

Because damping cannot always be tested separately from the pivotal motion, incorporation of damping within the pivot appeared to have merit. It was decided that this should be investigated by using sliding friction in the form of spherical-Teflon bearing rod ends, and rolling friction in the form of ball-bearing rod-end pivots. Laboratory models utilizing these two configurations were tested; the results appear in another section of this report.

HYSTERESIS DAMPING

Visco-elastic materials, fiberglass reinforced plastics, damping tapes, and lead wool were considered in this area but did not have sufficient merit to pursue their usage for the desired model.

The inherent hysteresis characteristic of rubber was apparent both as an individual damper and as a combined pivot-damper. This will again be discussed under the Pivot Configurations.

The low internal damping of steel (considered as a flexural pivot, helical spring, or cantilever spring) suggests the need for an additional source if damping is required. Such configurations were constructed and tested in determining the optimum DAVI design.

HYDRAULIC DAMPING

Hydraulic damping, as considered here, connotates damping proportional to the square of velocity such as the axial strut. The basic size, weight, cost, and predictability eliminated the practicality of such a configuration on the size of the DAVI being considered under the contract.

VISCOUS DAMPING

Viscous damping here refers to damping which is proportional to the first power of velocity. Although these units are found in "miniature" sizes, the weight and cost factors are not attractive. To correlate the analytical results, a small rotary viscous damper (rate - 0.5 to 25 in.lb./rad./sec.) was installed on a laboratory DAVI model and tested.

AIR (PNEUMATIC) DAMPING

The air dashpot was most ideally suited to the small DAVI models because of its size, weight, and relatively low cost. Excellent experimental test correlation was obtained with this configuration; however, because of the thin piston connecting rod, buckling of the rod occurred near the maximum damping rate (2.5 lb./in./sec.), necessitating a "beefing-up" modification of the rod.

PIVOT CONFIGURATIONS

As noted in the analytical study, one of the parameters affecting the antiresonant frequency is r, or the distance separating the source pivot from the isolated pivot. The smaller r, the less bar inertia (I) is required for given conditions; thus, the weight of the DAVI system can be kept minimal. To physically make r small, the method or design of pivotal action becomes most important, keeping in mind the ever present effects of damping. According to the Work Plan of the contract, three areas of pivotal configurations were investigated.

ELASTIC PIVOTS

To derive a characteristic, virtually undamped response, low hysteresis elastic pivots were considered. Figure 36 shows a model which was more than 99-percent effective in obtaining such a response. Note in this figure the arrangement of the supporting flexural brass straps, alternating from inertia bar to source plate and inertia bar to isolated plate. The intersections of the crossed straps, in effect, become the pivotal axes, and the distance between them represents r. Analysis of this system will show only minute shifting of the pivotal axes during the cantilever mode bending of the flexural straps.

A commercially manufactured product known as the "Free-Flex" pivot, available in various diametral sizes, is based upon the above flexural principle. DAVI laboratory models were designed utilizing these pivots, which resulted ultimately in the final model configuration for this contract. This type of pivot appears to be ideally suited to the DAVI concept within given loading conditions, as the response and fatigue parameters will show.

SLIDING PIVOTS

Sliding and/or rolling pivots, as mentioned previously in the considerations for friction damping, in the form of spherical and/or ball bearings, respectively, would seem to offer a very practical and relatively inexpensive approach to pivot design. Loading conditions should be generously increased with this type of pivot, provided the coulomb damping effect is not harmful. The translatory

motion of the cosine effect, due to the oscillatory inertia bar, should not be of consequence provided the bar position under the static load is neutral. Excessive cosine effects would, of course, necessitate design study.

RUBBER PIVOTS

As mentioned previously, the hysteresis characteristics of rubber suggest an area of pivot configuration whereby very compact and inexpensive DAVI units can be designed. Several commercial rubber bushings were considered to adapt to DAVI pivot configurations. Wall thickness, length, and diameter variations could afford means of obtaining desired spring rates from natural rubber and synthetic compounds. Analyses based upon the methods of Crede (Reference 5) support the feasibility of a rubber pivoted DAVI.

OPTIMIZATION OF DAVI DESIGN

ORIGINAL DAVI

Reference 8 is the Kaman report describing the original concept of the DAVI and is the basis under which this contract was generated. As an interesting introduction to the evolution towards the optimum DAVI design, a photograph of the original DAVI model is shown in Figure 13.

SLIDING PIVOTS

From the analytical schematic of the basic DAVI, a logical model construction was to use standard bearing rod ends. The first configuration utilized two spherical Teflon-lined rod ends for the base supports and a single one for the upper or isolated mass support. Care was taken to assure very loose bearings so as to minimize damping friction.

A 10-pound-per-inch spring was installed across the DAVI plates, and the unit was mounted on a shaker for vertical excitation. Because of the instability of a single support (upper) on a single DAVI model, a stabilizing support was used for the mass to be isolated.

With a 5-pound mass on the unit, a very erratic response was obtained. After many adjustments and tests, a 20-pound-per-inch spring was substituted, and the mass was increased to 10 pounds. Table 1 and Figure 14 show the response to these conditions, indicating a heavily damped system.

To reduce this heavy damping, ball-bearing rod ends were substituted for the base supports. Figure 15 shows a laboratory model of this configuration with the spring removed. Tables 2 and 3 and Figure 16 show typical results of tests to determine the inertia effects for this arrangement; again, highly damped tendencies were evident. Tables 4, 5, 6, and 7 and Figures 17, 18, 19, and 20 show some of the results of varying mass, the removing of bearing seals, and the substituting of bearings. Some of the bearings were also degreased and lubricated with lighter oils, but no improvement was evidenced, as seen in Tables 8 and 9 and in Figures 21 and 22. Heavy damping characteristics still persist.

To investigate the effects of a loose pivot shaft clamp-up (pivoting on shaft rather than in bearing), the support

bolts were loosened. A comparative test result is shown in Tables 10 and 11 and Figure 23.

Although many tests were conducted, each with the basic results as presented, it is still felt that further investigations of this general configuration may be more rewarding, perhaps in the areas of heavy masses where the bearings would be working nearer to their load capabilities, than such light loadings as tested here.

RUBBER PIVOTS

As pointed out previously, rubber pivots should afford simplicity and compactness of construction at reasonable cost. Several commercial rubber bushings were obtained and adapted to DAVI models; however, they proved much too stiff in torsional deflection for the desired small size model. Using the methods of Crede (Reference 5), calculations suggested a 40-durometer rubber should satisfy the desired dimensions. Through the facilities of the Kaman Materials Laboratory, a 1/4-inch shaft was centered in a 5/8-inch inside diameter aluminum bushing and molded in place with a 40-durometer neoprene compound. Two identical bushings were then bonded into an aluminum block which also served as the inertia bar housing. Figure 24 shows how the pivots were attached to the base and mass supports.

The first exposure was to a horizontal excitation, that is with the DAVI pushing horizontally against the supported mass; the DAVI was not itself supporting the mass. This, in effect, is a zero static load on the isolator. The interesting response is shown in Table 12 and Figure 25. As can be seen, the characteristic basic DAVI curve is apparent, but some scatter is present. Of particular note is the 80-percent isolation factor at the 12-cycle antiresonance. Some of the scatter was attributed to the nonrigid laboratory table upon which the shaker was clamped.

Orienting the shaker vertically and stabilizing the mass to be isolated produced much better results. Tables 13 and 14 and Figures 26 and 27 show the performance for isolated weights of 5 pounds and 7 pounds respectively. Note that degree of isolation is increased to better than 90 percent with the heavy mass. Also apparent is a tendency for a second resonance at the higher frequencies. This is believed to be a second mode caused by radial deformations within the rubber pivot and is an area which should be investigated by more detailed research.

To eliminate the operation of bonding the pivots into the pivot bar housing and to increase the shaft diameter for better retention with the base and mass supports, 3/8-inch shafts were centered in the two 3/4-inch bores in the bar housing and were molded in place with 40-durometer neoprene. Although the volume of rubber then torsionally deformed was slightly greater than for the previous configuration, approximately the same degree of isolation was attained for the 5-pound and 7-pound weights, as noted in Tables 15 and 16 and Figures 28 and 29.

In the same manner as the preceding, a 40-durometer natural rubber pivot was constructed and tested. Table 17 and Figure 30 illustrate the performance. The highly damped curve suggests that the natural rubber has inherently higher hysteresis, and the antiresonance has shifted to a lower frequency, thus indicating a lower spring rate for this material.

Tables 18 and 19 and Figures 31 and 32 show similar test results using 65-durometer neoprene as the pivot material, where a comparison of the respective curves for the 5-pound weight configuration reveals higher resonant and antiresonant frequencies for the 65-durometer material but the same degree of isolation. This again shows the independence of spring rate (durometer) and internal shear (hysteresis) for the same basic materials.

Table 20 and Figures 33a and 33b are clear verifications of the independence of antiresonant frequency from isolated mass (although greater isolation is attained with the larger mass as stated before) and of the lowering of the resonant frequency with increased mass (wider bandwidth).

The collective effect of the parameters of inertia, isolated weight, resonant frequency, antiresonant frequency, transmissibility, and isolation are shown in Tables 21 and 22 and Figures 34 and 35 which are carpet plots for the 40- and 65-durometer neoprene, respectively.

The research conducted on these rubber pivot configurations is extremely encouraging and leaves little doubt but that in this field of generous compounding abilities a material should be available, or made available, which would develop outstanding DAVI performance.

ELASTIC PIVOTS

It was believed that the very low hysteresis effect in metallic cantilever springs should be able to give virtually 100-percent isolation when arranged as a flexural pivot in the DAVI principle. Theoretical investigation supported this belief, and a flexural laboratory model was constructed using phenolic plates, brass strips, and a threaded inertia bar. Figure 36 shows this model mounted on a 50-pound shaker. The isolation ability of the model is seen in Figure 37 where the unit is being excited at 10 c.p.s. Although not instrumented, measurements under magnification indicated approximately 99-percent isolation in this case.

Knowledge of commercially manufactured units based upon the flexural pivot theory offered the means for what appeared to be a practical design wherein the pivot itself incorporated the system spring rate. The manufacturer concerned offered these pivots in various diametral sizes, with three angular ratings ($7\text{-}1/2^{\circ}$, 15°, and 30°) for each size depending upon the thickness (stiffness) of the flexural member. Several 15° pivots, 5/8-inch diameter, were acquired for evaluation, and a unidirectional laboratory model was made and tested with excellent results.

TWO-DIMENSIONAL MODEL

It was then desired to investigate the possibility of a model capable of isolating in two directions, say the vertical and lateral motions. The two-dimensional model was constructed using these pivots in a Hooke's Joint arrangement as seen in Figure 38. The model was mounted on a vertically oriented shaker and loaded with a 5-pound weight as seen in Figure 39. Two wide, flat pieces of brass were used to stabilize the mass in the vertical direction, while imposing a negligible effect upon the system spring rate. Tables 23, 24, and 25 and Figures 40, 41, and 42 show typical test results for different inertia bar values.

A lateral excitation was then imposed upon the model, and, as noted in Figure 43, the isolator is pushing against virtually zero mass. Greater than 99-percent isolation is obtained as evidenced by Table 26 and Figure 44.

An oblique response was then performed to test the characteristics of simultaneous vertical and lateral inputs. Figures 45 and 46 show the test setup and the isolating model, while Table 27 and Figure 47 offer the measured response. The increased isolation, over the vertical and lateral excitations, is believed to be due to the increase in "effective" mass caused by the direction of applied force to the model. The second peak at 25 c.p.s. is believed to be due to the internal elasticity of the wooden model when strained in this direction.

Table 28 and Figures 48 through 52 show the effects of varying the isolated mass, again indicating the relative independence upon the antiresonant frequency, and the shifting of the resonant frequency.

PARAMETRIC DAMPING

After it was determined that the virtually undamped flexural pivot characteristics were satisfactory, the experimental correlation of damping the system was considered. A small air dashpot was commercially available which had variable damping rates up to 2.5 pound-second per inch. The damper was easily installed on angle brackets mounted to the base and mass support legs, as seen in Figure 53.

Table 29 is a record of the response parameters, and Figures 54 through 58 show the plotted curves. The damping notations c = 0, 1, 2, 3, and 4 are not actual rates but indicate the increased step inputs to the maximum rate of the damper. Excellent correlation was obtained up to Figure 58 when, as the plot shows, a decreased damping rate is indicated for the fully damped unit. This phenomenon repeated itself in several tests until, when viewed under a stroboscopic light, it was seen that the small piston rod was bucking under the heavy damping load, thereby effectually reducing the damping rate. The decision was made to stiffen the piston rod by soldering a sleeve around it. While this was being done, the viscous damper tests were begun.

VISCOUS DAMPING

The above model was modified by removing the angle brackets and installing a base and top plates to accommodate the more bulky and heavier rotary viscous damper which had variable rates from 0.5 to 25.0 inch-pound per radians per second.

Table 30 records the parameters for one of the series of tests, and Figures 59 through 68 show the respective response curves. As in the previous tests, the damping notation merely refers to an arbitrary setting on the damper. The curve for C = 0 was obtained with the damper connecting link removed. With the link installed and the rate adjustment screw backed out (C = 1), Figure 60 was obtained showing the characteristic reduced peak and raised trough. Figure 61 resulted from a minute increase in rate (C = 2). A large adjustment resulted in the curve in Figure 62 where it appeared that the damping was decreased. With a much heavier connecting link than the air dashpot, buckling was improbable; however, it was believed that the connecting plates or the model itself was perhaps straining. As a check, another minute increase in damping rate was made (C = 4), which yielded an almost identical response as seen in Figure 63. An appreciable reduction in rate was then made (C = 5), which brought back a reasonable response, Figure 64.

The bar inertia was then decreased to determine its effect and responded, as predicted by the theoretical analysis, with an increase in both resonant and antiresonant frequencies (Figure 65, C = 6). With the inertia remaining the same, an attempt was made to induce the "buckling" phenomenon again. The damper setting was increased to C = 7, with a resulting response as seen in Figure 66. Another slight increased damping adjustment was made (C = 8) and responded as shown in Figure 67. The bar inertia was increased to its original configuration, and the damper minutely increased to C = 9. Figure 68 shows the tendency to decrease the resonant and antiresonant frequencies. The next increase in damping rate produced a failure across the pivot housing in the wooden support leg. The "buckling" phenomenon may very well have been the result of some internal failing under the resistive forces of the high damping setting.

Results of these damping tests conclude that damping in the DAVI can be optimized, as the theory has derived.

SINGLE-DEGREE-OF-FREEDOM DAVI (UNIDIRECTIONAL)

From the excellent results obtained with the quality of the laboratory models used thus far, an aluminum model was constructed preparatory to manufacturing the subsequent platform units. Calculations and consultations with the pivot manufacturer showed that the 15° pivot was insufficient to carry the desired load of 50 pounds per DAVI unit; therefore, the stiffer 7-1/2° pivots were ordered. Even though the 7-1/2° pivots were able to support the static load, the predicted fatigue life was much reduced; however, it was felt that these pivots would afford valuable data in the anticipation of possibly manufacturing them with special materials.

Excellent isolation was attained at 99 percent for the 15° pivot, and 98 percent for the 7-1/2° pivot when tuned to approximately 10.4 c.p.s. Tables 31 and 32 and Figures 69 and 70 reflect these results.

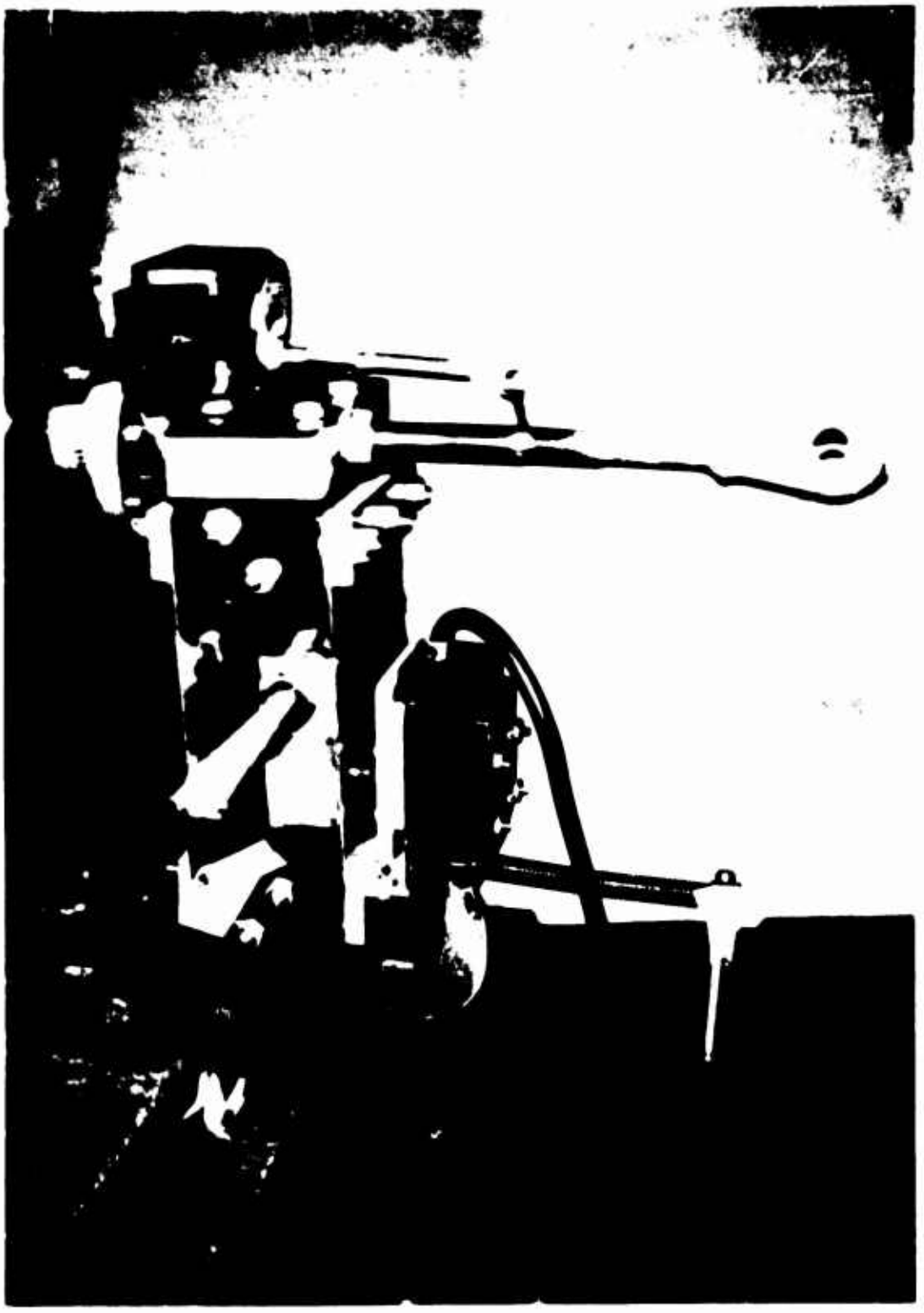

Figure 13. Original DAVI Model

TABLE I

DAVI TRANSMISSIBILITY TEST DATA
SLIDING PIVOT CONFIGURATION
SPHERICAL-BEARING BASE SUPPORT
SPRING CONSTANT, 20 POUNDS PER INCH
ISOLATED WEIGHT, 10 POUNDS
BAR INERTIA, BASIC

Frequency (c.p.s.)	Input	Output	Output / Input
5.0	59.00	61.00	1.04
5.5	61.00	65.00	1.07
6.0	61.00	70.00	1.15
6.5	60.00	77.00	1.28
7.0	55.00	84.00	1.53
7.5	48.00	84.00	1.75
8.0	40.00	76.00	1.90
8.5	34.00	65.00	1.92
9.0	32.00	54.00	1.59
9.5	31.00	44.00	1.41
10.0	31.00	35.00	1.13
10.5	31.00	30.00	.97
11.0	31.00	25.00	.81
11.5	34.00	25.00	.73
12.0	34.00	22.00	.65
12.5	33.00	19.00	.58
13.0	32.00	17.00	.53
13.5	31.00	16.00	.52
14.0	30.00	15.00	.50
14.5	29.00	14.00	.48
15.0	28.00	13.00	.47
15.5	27.50	12.00	.44
16.0	26.50	11.50	.44
16.5	25.50	11.00	.43
17.0	24.50	10.50	.43
17.5	23.50	10.00	.43
18.0	22.50	10.00	.45
19.0	21.00	9.50	.45
20.0	19.00	9.00	.48
25.0	13.50	7.50	.56
30.0	9.60	6.00	.63
35.0	7.50	4.90	.65
40.0	6.50	4.00	.62

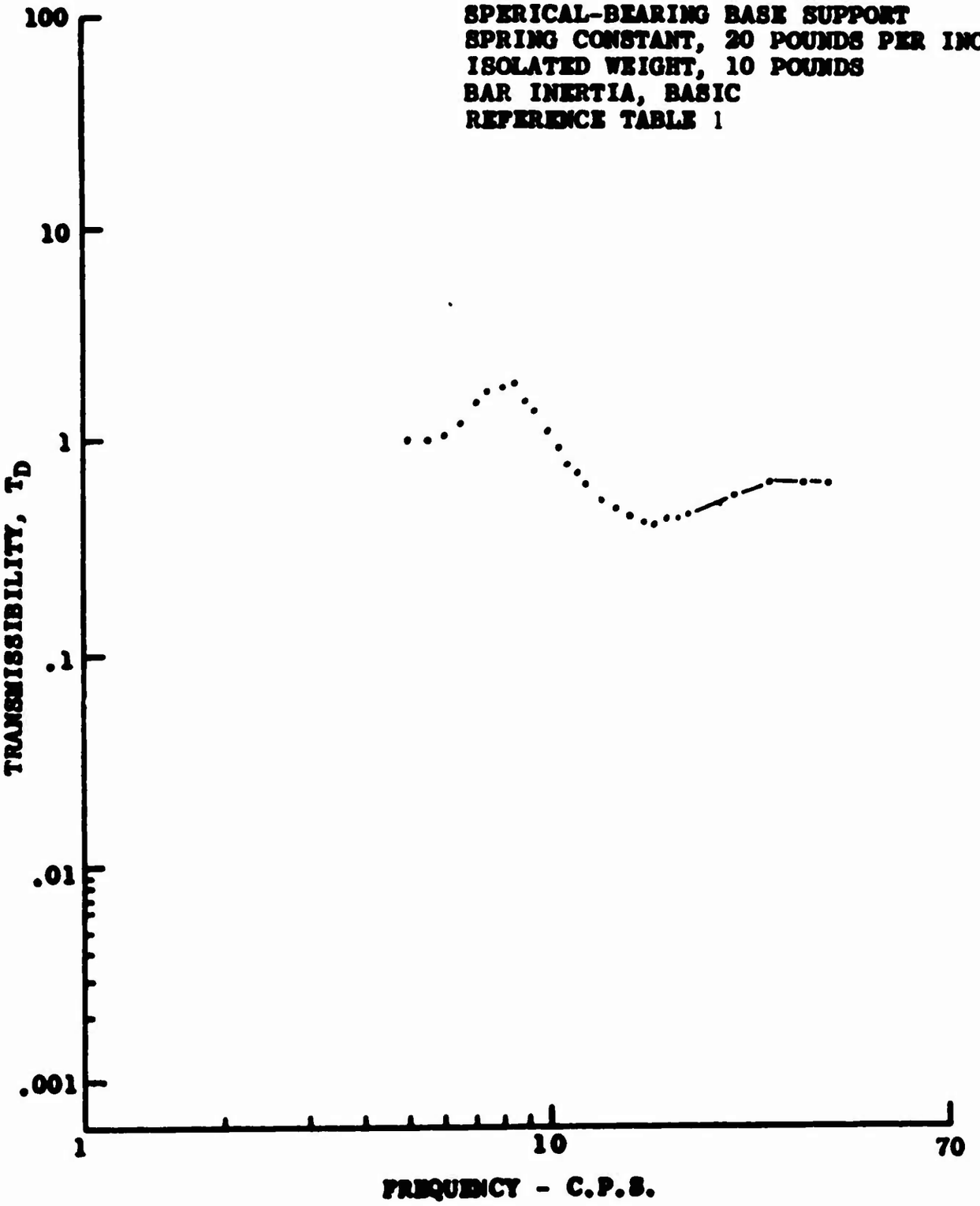

Figure 14. Sliding Pivot Configuration Response Curve

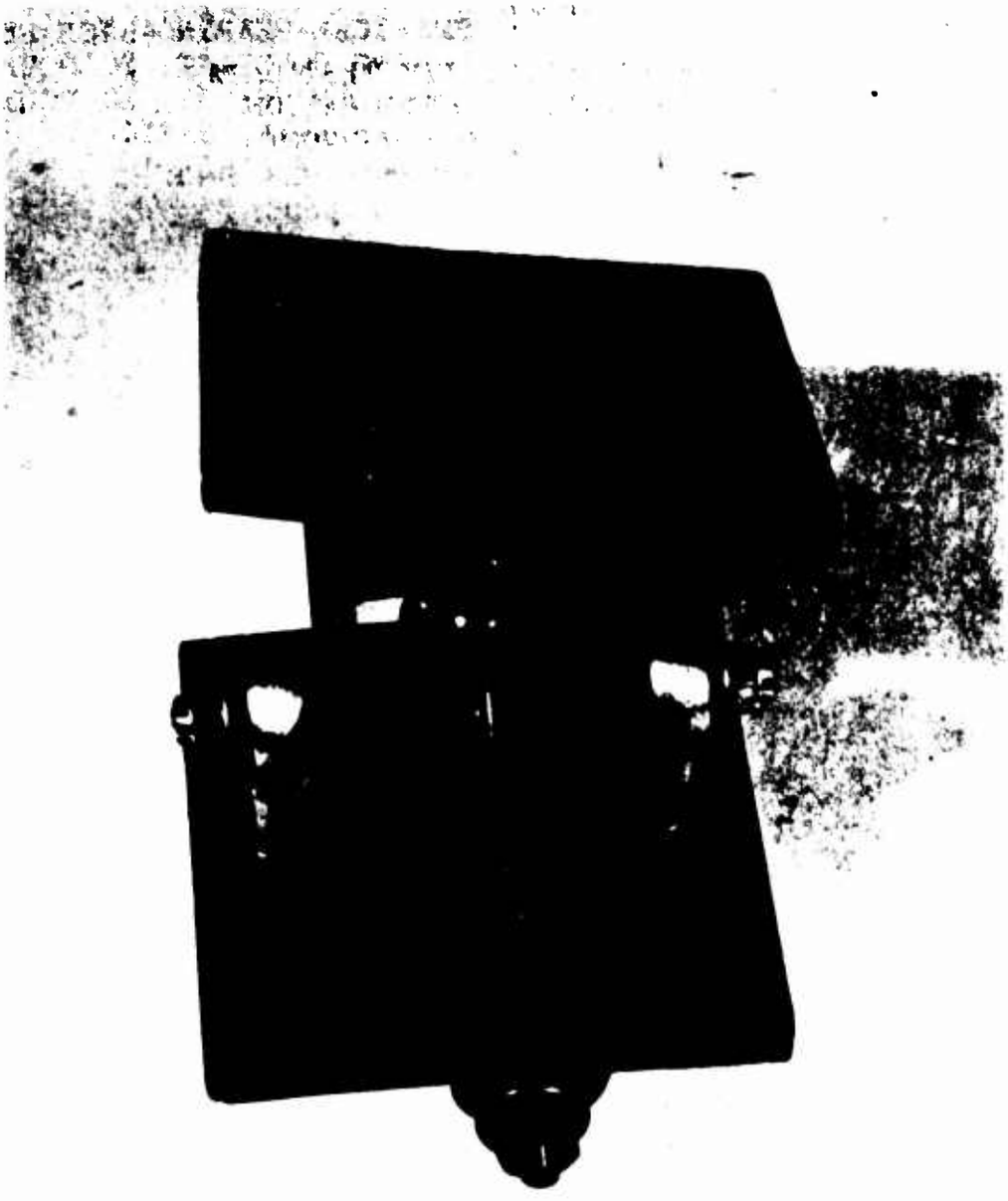

Figure 15. Sliding Pivot DAVI Model

TABLE 2

DAVI TRANSMISSIBILITY TEST DATA
SLIDING PIVOT CONFIGURATION
BALL-BEARING BASE SUPPORT
SPRING CONSTANT, 10 POUNDS PER INCH
ISOLATED WEIGHT, 5 POUNDS
BAR INERTIA, BASIC

Frequency (c.p.s.)	Input	Output	$\frac{\text{Output}}{\text{Input}}$
5.0	71.00	97.00	1.37
5.5	46.00	87.00	1.90
6.0	49.00	40.00	.82
6.5	51.00	22.00	.43
7.0	54.00	19.00	.35
7.5	54.00	18.00	.33
8.0	50.00	19.00	.38
8.5	49.00	19.70	.40
9.0	48.00	20.00	.42
9.5	46.50	20.00	.43
10.0	44.50	20.00	.45
10.5	43.00	19.80	.46
11.0	41.00	19.50	.48
11.5	39.50	19.00	.48
12.0	37.50	18.50	.50
12.5	35.50	18.00	.51
13.0	34.00	17.50	.52
13.5	32.00	16.50	.52
14.0	30.50	16.00	.53
14.5	29.00	16.00	.55
15.0	28.00	15.50	.56
16.0	25.00	15.00	.60
17.0	23.00	14.00	.61
18.0	21.00	13.20	.63
19.0	19.50	13.10	.67
20.0	17.00	12.90	.76
22.0	13.50	12.00	.89
24.0	11.80	10.60	.90
26.0	11.60	9.60	.83
28.0	10.50	9.00	.86
29.0	11.40	7.60	.67
30.0	11.40	7.10	.62
31.0	12.10	5.40	.45
32.0	12.10	4.80	.40
34.0	13.80	3.00	.22
35.0	12.10	5.50	.46
36.0	11.60	4.00	.35
37.0	10.70	2.00	.19
40.0	9.40	1.30	.14

TABLE 3

DAVI TRANSMISSIBILITY TEST DATA
SLIDING PIVOT CONFIGURATION
BALL-BEARING BASE SUPPORT
SPRING CONSTANT, 10 POUNDS PER INCH
ISOLATED WEIGHT, 5 POUNDS
BAR INERTIA, INCREASED

Frequency (c.p.s.)	Input	Output	$\frac{\text{Output}}{\text{Input}}$
5.0	68.00	71.00	1.04
5.5	69.00	69.00	1.00
6.0	69.00	61.00	.88
6.5	69.00	61.00	.88
7.0	66.00	60.00	.91
7.5	65.00	59.00	.91
8.0	61.00	56.00	.92
8.5	59.00	54.00	.92
9.0	55.00	51.00	.93
9.5	52.00	49.00	.94
10.0	50.00	45.00	.90
10.5	47.00	44.00	.94
11.0	44.00	43.00	.98
11.5	40.00	40.00	1.00
12.0	49.00	49.00	1.00
13.0	43.00	43.00	1.00
14.0	31.00	33.00	1.06
15.0	28.00	31.00	1.11
16.0	24.00	28.00	1.17
18.0	18.50	24.00	1.30
20.0	14.50	20.00	1.38
22.0	13.00	16.00	1.23
23.5	11.40	16.00	1.40
24.0	12.10	13.50	1.12
26.0	12.00	11.50	.96
30.0	10.30	10.30	1.00
35.0	11.50	7.00	.61
40.0	11.00	5.00	.46

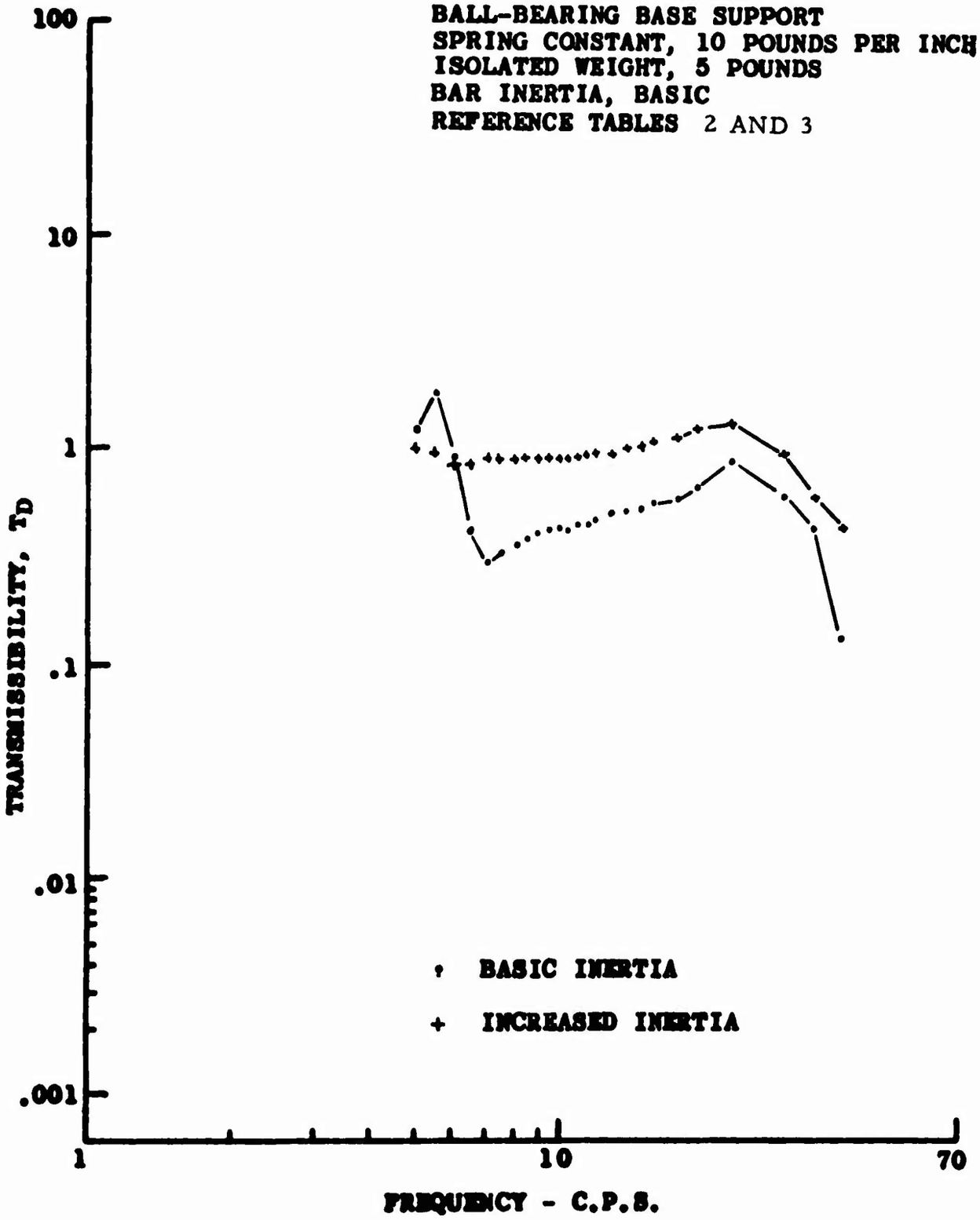

Figure 16. Sliding Pivot Configuration Response Curve

TABLE 4

DAVI TRANSMISSIBILITY TEST DATA
SLIDING PIVOT CONFIGURATION
BALL-BEARING BASE SUPPORT
SPRING CONSTANT, 20 POUNDS PER INCH
ISOLATED WEIGHT, 5 POUNDS
BAR INERTIA, BASIC

Frequency (c.p.s.)	Input	Output	$\frac{\text{Output}}{\text{Input}}$
5.0	53.00	73.00	1.37
5.5	55.00	85.00	1.55
6.0	55.00	100.00	1.82
6.2	52.00	115.00	2.21
6.4	38.00	130.00	3.43
6.6	31.00	120.00	3.90
6.8	30.00	111.00	3.69
7.0	29.50	98.00	3.28
7.5	32.20	82.00	2.56
8.0	35.00	60.00	1.72
8.5	37.50	44.00	1.18
9.0	39.00	31.50	.81
10.0	39.80	16.00	.40
10.5	39.00	14.50	.37
11.0	38.50	12.60	.33
11.2	38.00	12.30	.32
11.4	37.50	11.80	.32
11.6	37.00	11.50	.31
11.8	36.50	11.70	.32
12.0	35.00	11.50	.33
12.5	34.50	11.00	.32
13.0	33.50	11.10	.33
13.5	32.00	11.50	.36
14.0	30.00	11.10	.37
15.0	27.50	10.70	.39
16.0	25.00	10.80	.43
18.0	20.00	10.10	.51
20.0	16.00	9.80	.61
25.0	10.40	8.70	.84
30.0	8.10	7.00	.87
35.0	10.00	4.50	.45
40.0	8.30	1.80	.22
45.0	6.80	1.00	.15
50.0	5.10	.40	.08
55.0	4.10	.60	.15
60.0	3.33	.40	.12

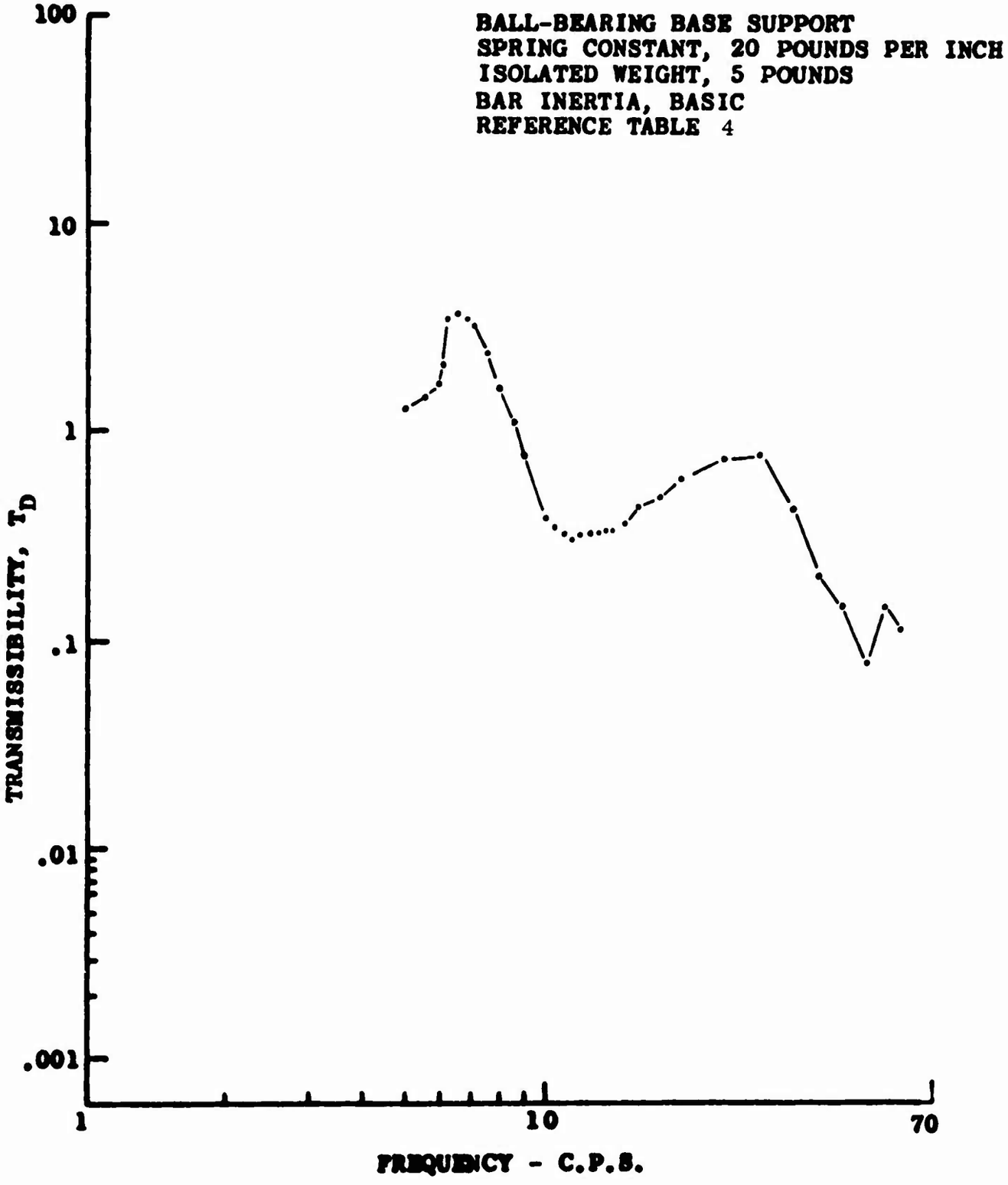

Figure 17. Sliding Pivot Configuration
Response Curve

TABLE 5

DAVI TRANSMISSIBILITY TEST DATA
SLIDING PIVOT CONFIGURATION
BALL-BEARING BASE SUPPORT
SPRING CONSTANT, 20 POUNDS PER INCH
ISOLATED WEIGHT, 10 POUNDS
BAR INERTIA, BASIC

Frequency (c.p.s.)	Input	Output	$\frac{\text{Output}}{\text{Input}}$
5.0	64.00	67.00	1.05
5.5	66.00	74.00	1.12
6.0	59.00	89.00	1.51
6.5	49.00	102.00	2.08
7.0	40.00	100.00	2.50
7.5	30.00	81.00	2.70
8.0	29.00	66.00	2.28
8.5	31.00	51.00	1.65
9.0	36.00	42.00	1.16
9.5	37.00	36.00	.98
10.0	36.00	33.00	.92
10.5	35.00	30.00	.86
11.0	34.00	26.00	.77
11.5	33.00	23.00	.70
12.0	32.00	21.00	.66
12.5	32.00	19.00	.60
13.0	30.00	18.00	.60
14.0	29.00	15.00	.52
15.0	27.50	13.00	.47
16.0	26.00	11.00	.42
17.0	25.00	8.00	.32
18.5	22.00	8.00	.36
20.0	19.00	8.00	.42
25.0	13.40	6.50	.48
30.0	10.10	5.00	.50
35.0	8.60	4.30	.50
40.0	11.00	3.50	.32

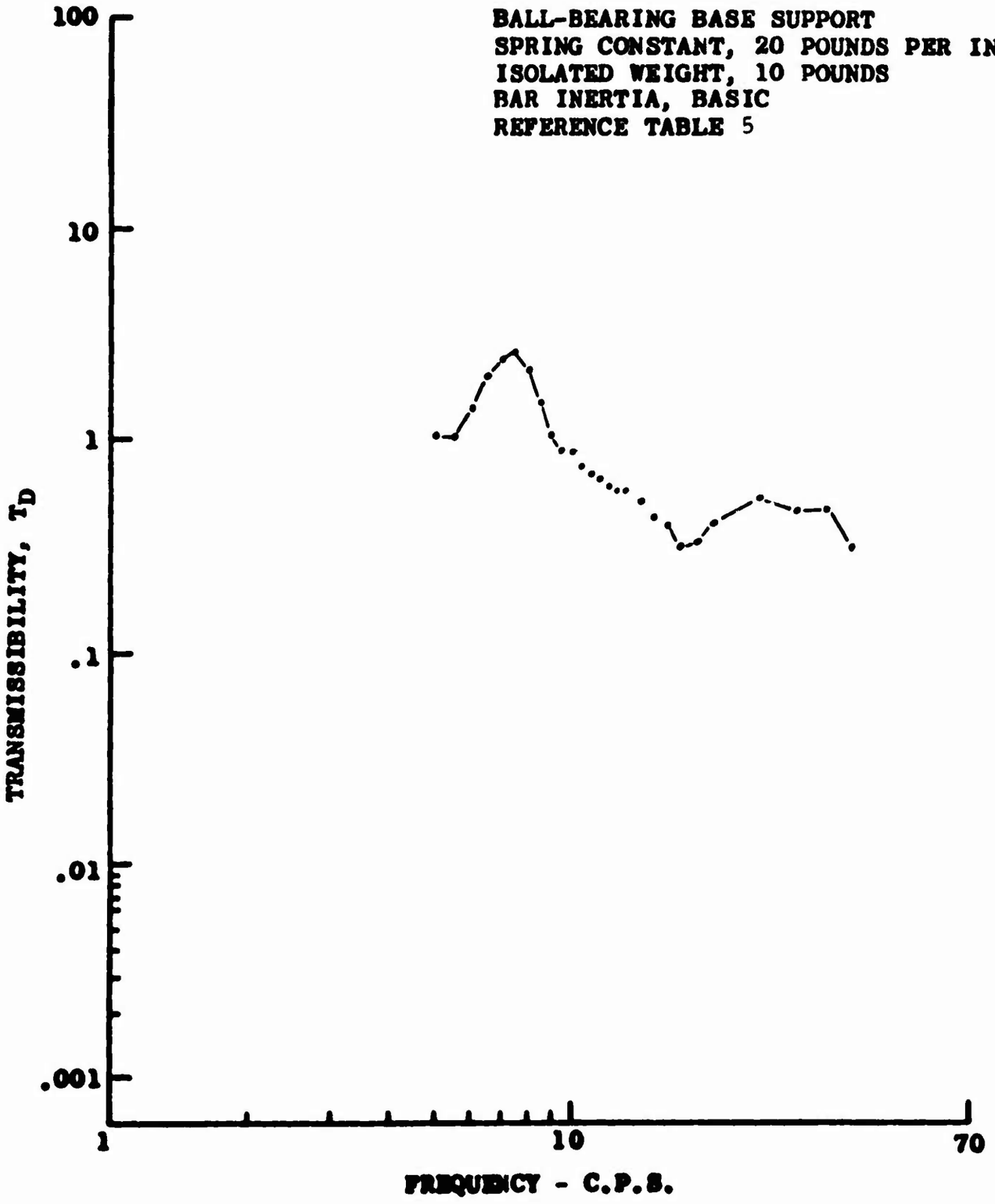

Figure 18. Sliding Pivot Configuration
Response Curve

TABLE 6

DAVI TRANSMISSIBILITY TEST DATA
SLIDING PIVOT CONFIGURATION
BALL-BEARING BASE SUPPORT
SPRING CONSTANT, 20 POUNDS PER INCH
ISOLATED WEIGHT, 10 POUNDS
BAR INERTIA, BASIC

Frequency (c.p.s.)	Input	Output	Output / Input
5.0	56.00	64.00	1.14
5.5	60.00	76.00	1.26
6.0	59.00	91.00	1.54
6.5	51.00	111.00	2.17
7.0	37.00	109.00	2.95
7.5	31.00	87.00	2.81
8.0	33.00	63.00	1.91
8.5	34.00	46.00	1.35
9.0	35.00	35.00	1.00
9.5	38.00	32.00	.85
10.0	39.00	24.00	.62
10.5	39.00	20.00	.51
11.0	38.00	17.00	.45
11.5	38.00	14.00	.37
12.0	37.00	13.00	.35
12.5	36.00	12.00	.33
13.0	34.00	11.00	.32
13.5	33.00	11.00	.33
14.0	32.00	10.50	.33
15.0	30.00	9.00	.30
16.0	28.00	8.50	.30
18.0	23.00	8.00	.35
20.0	20.00	7.00	.35
22.0	16.50	6.00	.36
25.0	14.50	6.00	.41
30.0	9.00	5.10	.56
35.0	20.00	17.00	.49
40.0	5.00	4.00	.80

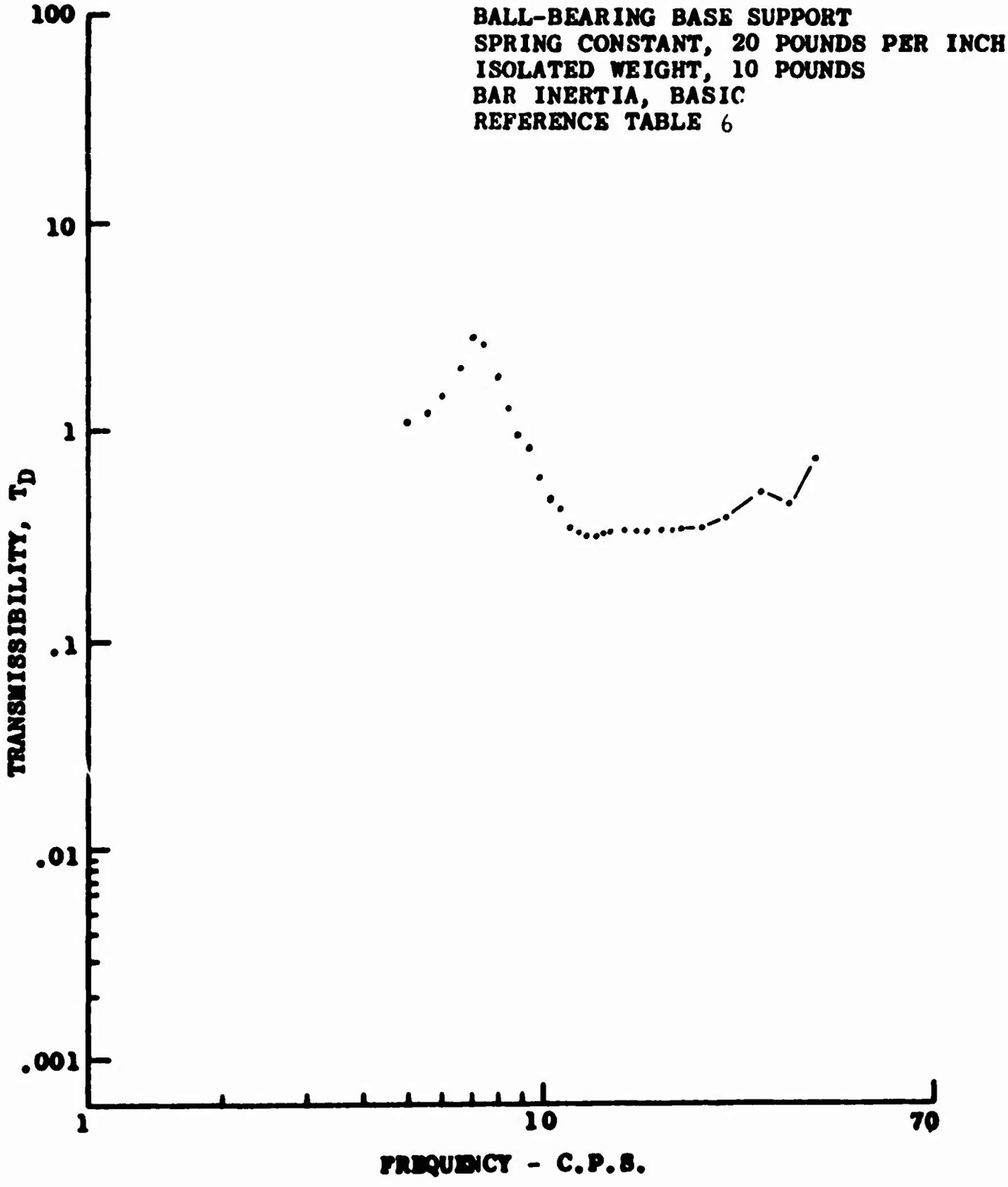

Figure 19. Sliding Pivot Configuration
Response Curve

TABLE 7

DAVI TRANSMISSIBILITY TEST DATA
SLIDING PIVOT CONFIGURATION
BALL-BEARING BASE SUPPORT
SPRING CONSTANT, 20 POUNDS PER INCH
ISOLATED WEIGHT, 10 POUNDS
BAR INERTIA, BASIC

Frequency (c.p.s.)	Input	Output	$\frac{\text{Output}}{\text{Input}}$
5.0	62.00	75.00	1.21
5.5	65.00	83.00	1.28
6.0	65.00	95.00	1.47
6.5	60.00	111.00	1.85
7.0	60.00	127.00	2.11
7.5	32.00	130.00	4.07
8.0	31.00	99.00	3.20
8.5	30.00	84.00	2.80
9.0	30.00	66.00	2.20
9.5	35.00	51.00	1.45
10.0	37.00	42.00	1.14
10.5	38.00	34.00	.90
11.0	38.00	28.00	.74
11.5	38.00	23.00	.61
12.0	38.00	20.00	.53
12.5	37.00	18.00	.49
13.0	36.00	16.00	.45
14.0	33.50	13.00	.37
15.0	31.00	11.00	.36
16.0	29.00	10.00	.35
17.0	26.00	9.80	.38
18.5	24.00	8.60	.36
20.0	21.00	8.10	.39
22.0	18.00	7.30	.90
25.0	14.00	7.00	.50
30.0	10.00	6.00	.60
35.0	8.30	5.20	.63
40.0	10.00	2.40	.24

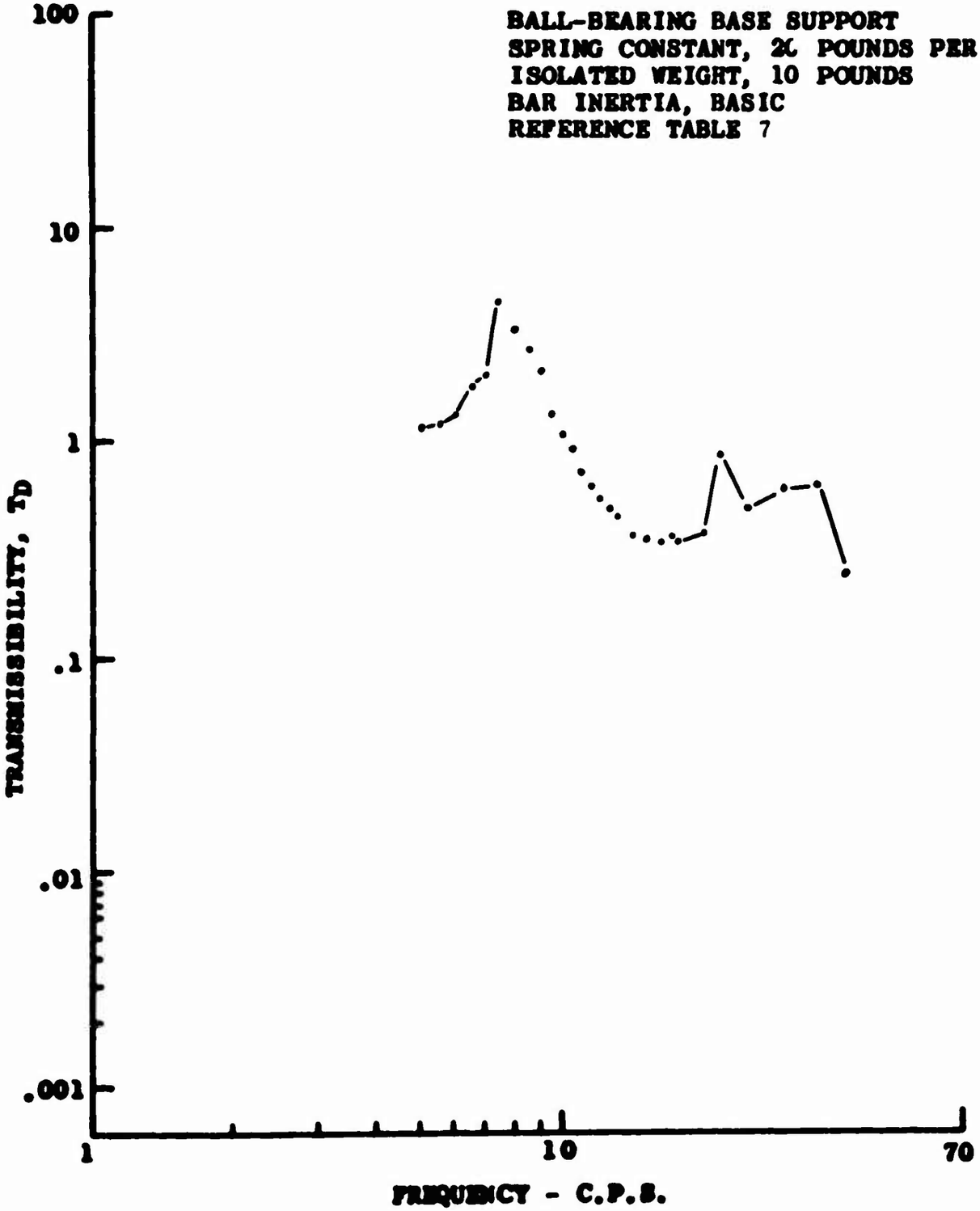

Figure 20. Sliding Pivot Configuration
Response Curve

TABLE 8

DAVI TRANSMISSIBILITY TEST DATA
SLIDING PIVOT CONFIGURATION
LIGHT-LUBE BALL-BEARING BASE SUPPORT
SPRING CONSTANT, 10 POUNDS PER INCH
ISOLATED WEIGHT, 10 POUNDS
BAR INERTIA, BASIC

Frequency (c.p.s.)	Input	Output	Output / Input
5.0	60.00	111.00	1.85
5.5	60.00	126.00	2.27
6.0	52.00	128.00	2.46
6.5	48.00	116.00	2.42
7.0	41.00	86.00	2.10
7.5	55.00	27.00	.49
8.0	55.00	20.00	.37
8.5	54.00	16.00	.30
9.0	53.00	14.00	.26
9.5	51.00	12.00	.24
10.0	52.00	11.00	.21
10.5	51.00	11.00	.22
11.0	50.00	11.50	.23
11.5	48.50	11.00	.23
12.0	47.00	11.00	.24
12.5	46.00	11.00	.24
13.0	44.00	10.50	.24
13.5	43.00	10.50	.25
14.0	41.00	10.00	.25
14.5	40.00	10.00	.25
15.0	38.20	10.00	.26
16.0	36.00	9.70	.27
17.0	33.00	9.50	.29
18.0	31.00	9.00	.29
19.0	29.00	8.20	.28
20.0	27.00	8.00	.30
21.0	25.00	7.80	.31
22.0	23.00	7.00	.31
25.0	19.00	6.00	.32
30.0	13.40	5.10	.38
35.0	10.00	3.50	.35
40.0	7.00	3.30	.47

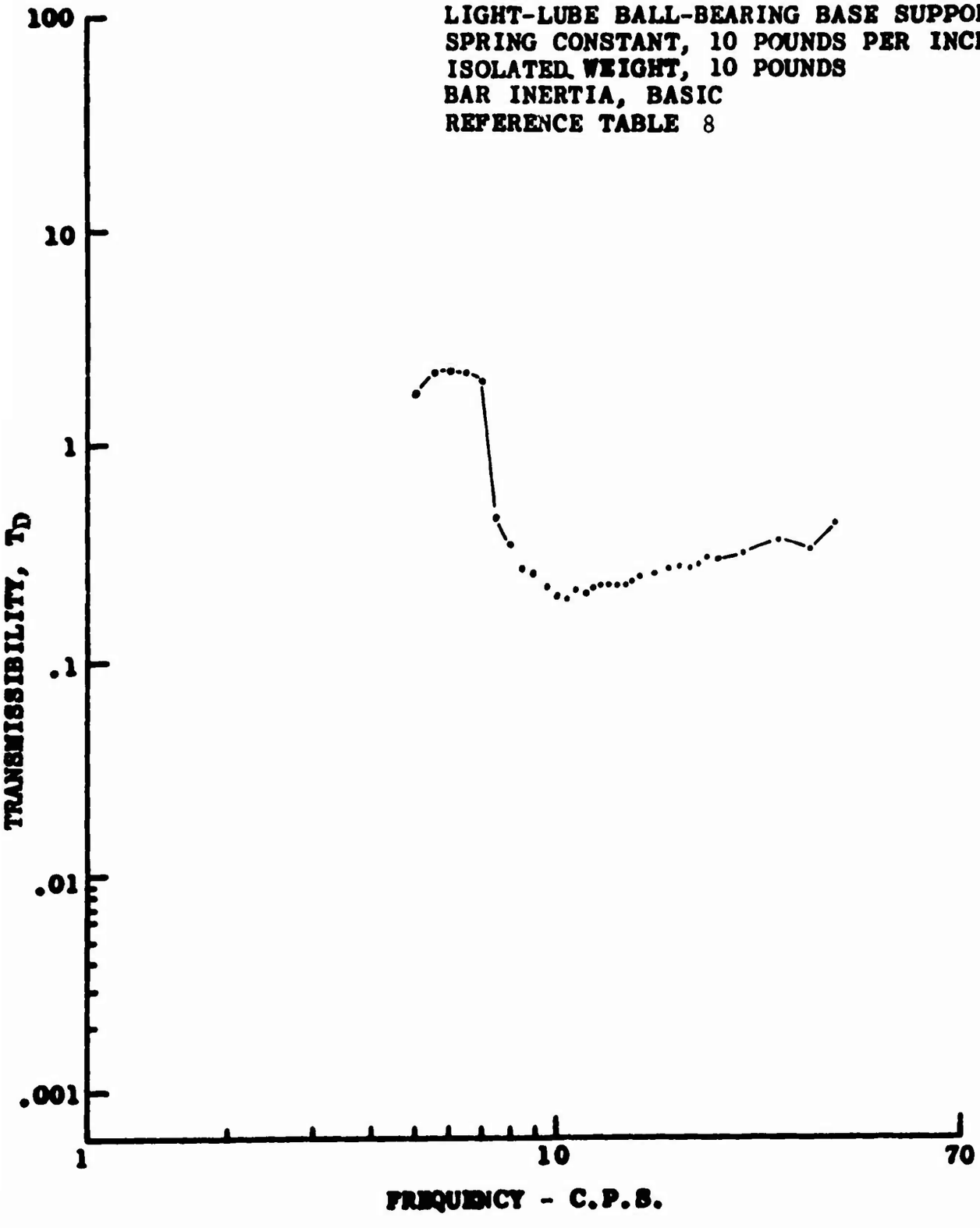

Figure 21. Sliding Pivot Configuration Response Curve

TABLE 9

DAVI TRANSMISSIBILITY TEST DATA
SLIDING PIVOT CONFIGURATION
LIGHT-LUBE BALL-BEARING BASE SUPPORT
SPRING CONSTANT, 20 POUNDS PER INCH
ISOLATED WEIGHT, 10 POUNDS
BAR INERTIA, BASIC

Frequency (c.p.s.)	Input	Output	$\frac{\text{Output}}{\text{Input}}$
5.0	59.00	61.00	1.03
5.5	61.00	66.00	1.08
6.0	61.00	69.00	1.13
6.5	60.00	71.00	1.18
7.0	59.00	73.00	1.24
7.5	55.00	77.00	1.40
8.0	49.00	81.00	1.65
8.5	40.00	82.00	2.05
9.0	33.00	76.00	2.30
9.5	29.00	66.00	2.28
10.0	27.00	59.00	2.19
10.5	28.00	49.00	1.75
11.0	29.50	41.50	1.41
11.5	30.00	35.00	1.17
12.0	30.00	31.00	1.03
12.5	30.00	26.00	.87
13.0	31.00	22.00	.71
13.5	30.00	20.00	.67
14.0	30.00	18.00	.60
14.5	30.00	15.00	.50
15.0	29.00	14.00	.48
16.0	27.00	13.00	.48
17.0	26.00	11.00	.42
18.0	26.00	8.50	.33
19.0	25.00	7.00	.28
20.0	24.00	6.00	.25
21.0	22.00	5.80	.26
22.0	20.00	6.30	.32
25.0	17.50	4.50	.26
30.0	13.00	3.60	.23
35.0	10.00	2.20	.22
40.0	7.60	2.00	.26

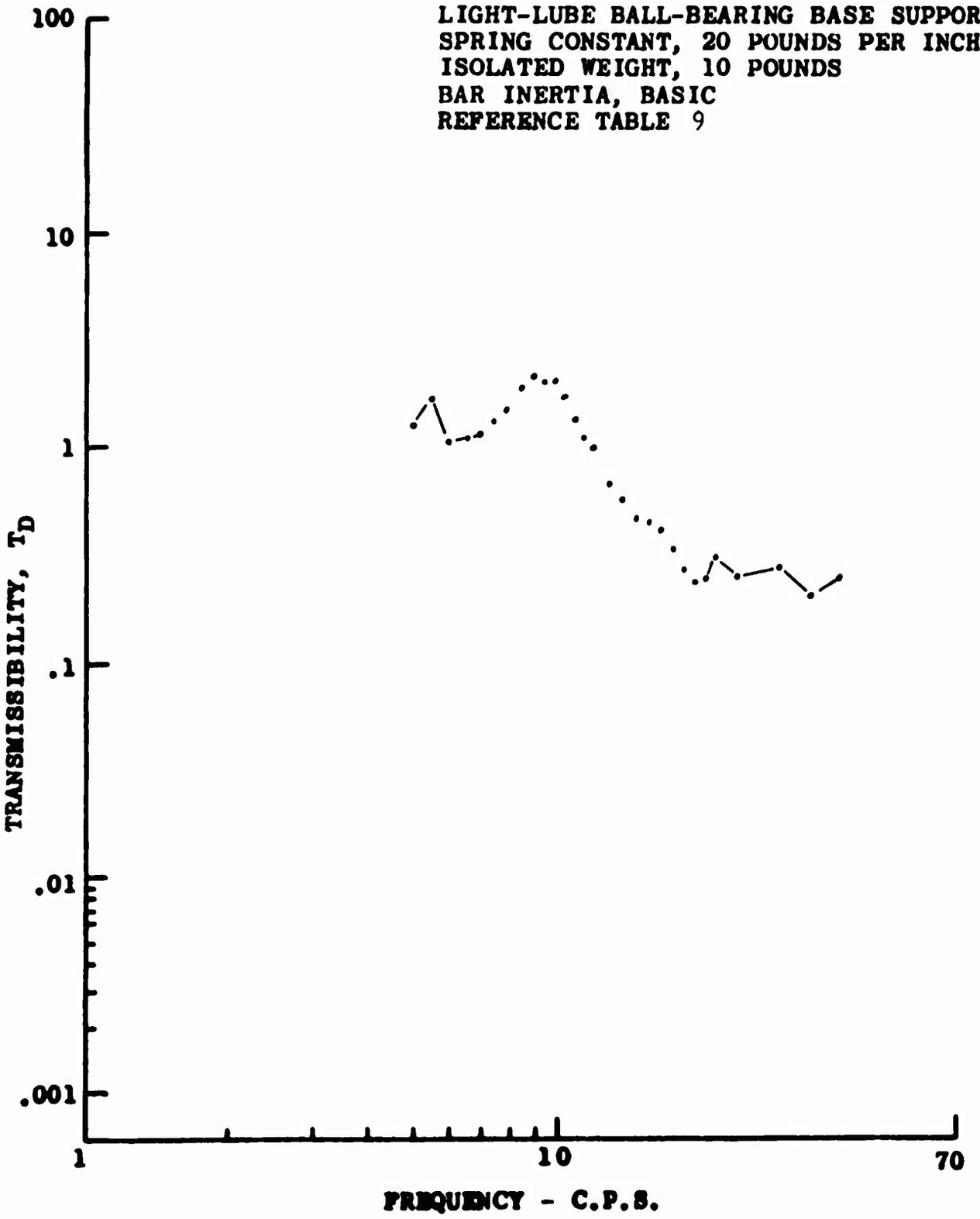

Figure 22. Sliding Pivot Configuration Response Curve

TABLE 10

DAVI TRANSMISSIBILITY TEST DATA
SLIDING PIVOT CONFIGURATION
BALL-BEARING BASE SUPPORT (LOOSE BOLT)
SPRING CONSTANT, 10 POUNDS PER INCH
ISOLATED WEIGHT, 10 POUNDS
BAR INERTIA, BASIC

Frequency (c.p.s.)	Input	Output	$\frac{\text{Output}}{\text{Input}}$
5.0	58.00	65.00	1.12
5.5	60.00	79.00	1.32
6.0	60.00	94.00	1.57
6.5	55.00	113.00	2.05
7.0	44.00	131.00	2.98
7.5	31.00	115.00	3.71
8.0	31.00	88.00	2.84
8.5	35.00	61.00	1.74
9.0	37.00	47.00	1.27
9.5	38.00	34.00	.90
10.0	39.00	26.00	.67
10.5	38.00	21.00	.55
11.0	39.00	18.00	.46
11.5	38.20	15.50	.41
12.0	38.00	13.00	.34
12.5	37.00	11.00	.30
13.0	36.00	10.50	.29
13.5	35.00	10.50	.30
14.0	33.50	10.50	.31
14.5	32.00	10.50	.33
15.0	31.00	10.00	.32
15.5	30.00	10.00	.33
16.0	29.00	9.50	.33
16.5	28.00	9.00	.32
17.0	28.00	8.00	.29
17.5	27.00	8.00	.30
18.0	26.00	8.00	.31
18.5	25.00	8.00	.32
19.0	24.00	8.00	.33
20.0	22.50	8.00	.37
25.0	15.50	7.00	.45
30.0	11.00	5.10	.46
35.0	7.60	4.20	.55
40.0	5.50	4.40	.80

TABLE 11

DAVI TRANSMISSIBILITY TEST DATA
SLIDING PIVOT CONFIGURATION
BALL-BEARING BASE SUPPORT (TIGHT BOLT)
SPRING CONSTANT, 10 POUNDS PER INCH
ISOLATED WEIGHT, 10 POUNDS
BAR INERTIA, BASIC

Frequency (c.p.s.)	Input	Output	$\frac{\text{Output}}{\text{Input}}$
5.0	59.00	61.00	1.03
5.5	61.00	65.00	1.07
6.0	61.00	69.00	1.13
6.5	59.00	73.00	1.24
7.0	53.00	82.00	1.55
7.5	48.00	79.00	1.65
8.0	42.00	70.00	1.67
8.5	39.00	60.00	1.54
9.0	37.00	49.00	1.32
9.5	36.00	40.00	1.11
10.0	35.00	33.00	.94
10.5	35.00	29.00	.83
11.0	34.00	25.00	.74
11.5	36.00	23.00	.64
12.0	35.00	20.00	.57
12.5	35.00	17.00	.49
13.0	33.00	16.00	.49
13.5	33.00	15.00	.45
14.0	32.00	12.00	.38
14.5	31.50	11.50	.37
15.0	30.00	11.00	.37
15.5	29.50	10.00	.34
16.0	29.00	10.00	.35
16.5	28.00	9.50	.34
17.0	27.00	9.00	.33
17.5	26.00	9.00	.35
18.0	25.00	9.00	.36
18.5	24.00	9.00	.38
19.0	23.00	8.50	.37
20.0	21.50	8.00	.37
25.0	15.50	6.00	.39
30.0	13.00	4.60	.36
35.0	8.70	3.50	.40
40.0	6.90	2.60	.38

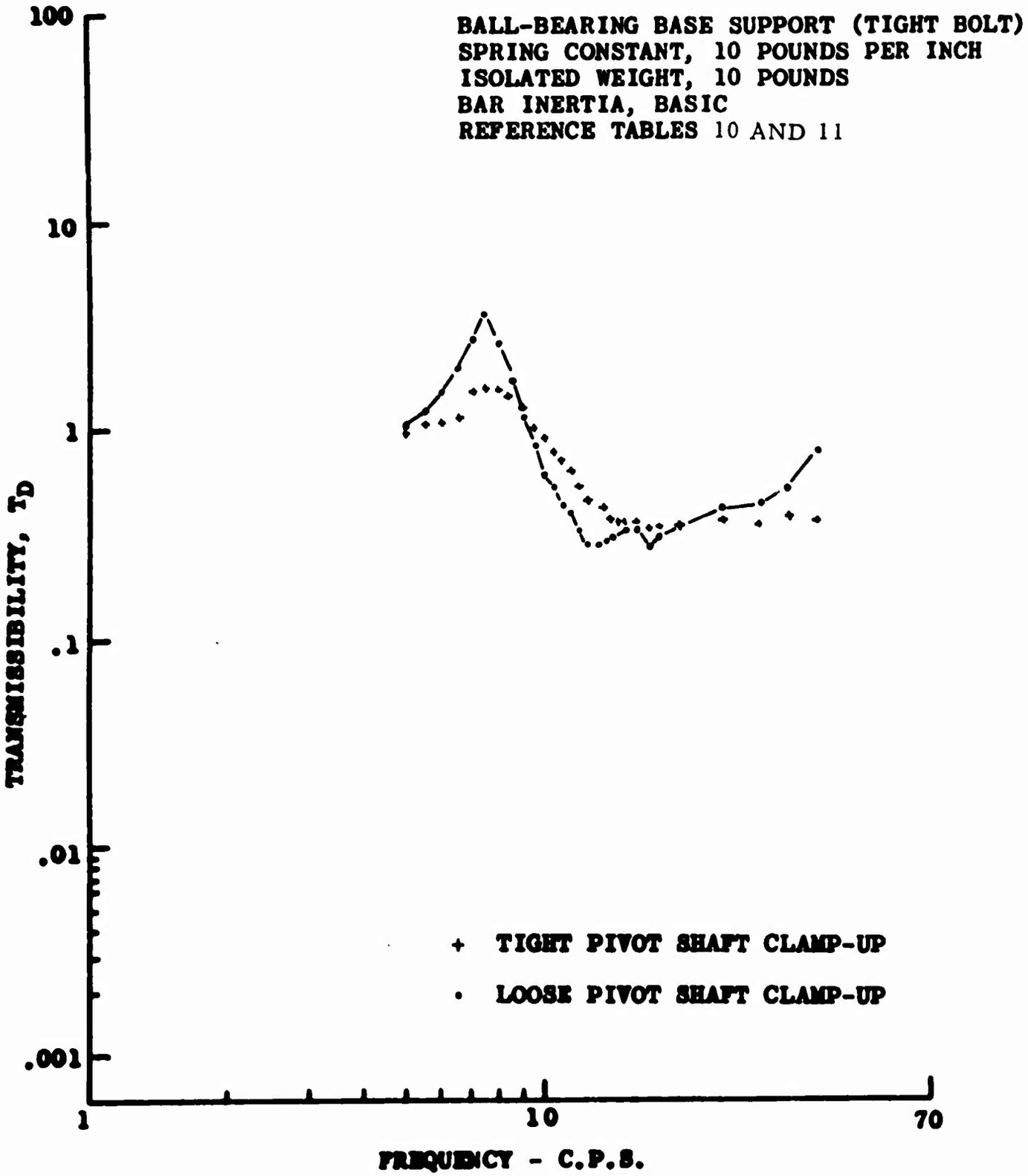

Figure 23. Sliding Pivot Configuration Response Curve

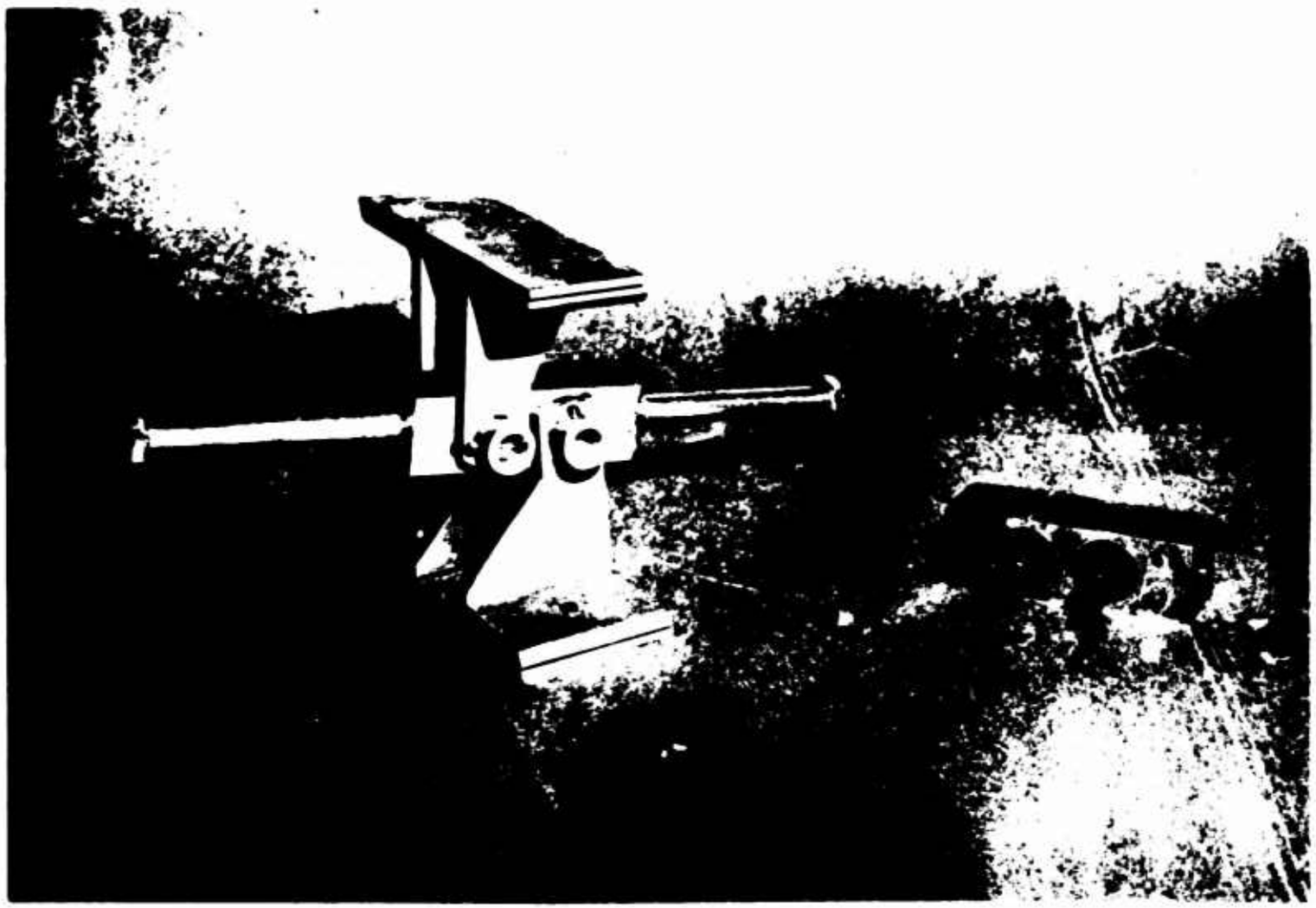

Figure 24. Rubber Pivoted DAVI Model

TABLE 12

DAVI TRANSMISSIBILITY TEST DATA
RUBBER PIVOT CONFIGURATION
40-DUROMETER NEOPRENE (0.25 ID x 0.625 OD x 0.9 LONG)
HORIZONTAL EXCITATION

Frequency (c.p.s.)	Input	Output	Output / Input
5.0	59.00	78.00	1.32
5.5	46.00	69.00	1.50
6.0	28.00	46.00	1.65
6.5	19.50	34.00	1.74
7.0	18.50	45.00	2.43
7.5	12.50	45.00	3.60
8.0	8.50	40.50	4.76
8.5	14.00	33.50	2.39
9.0	18.50	30.00	1.63
9.5	25.00	24.00	.96
10.0	28.00	16.00	.57
10.5	28.00	10.00	.36
11.0	26.00	17.00	.65
11.5	24.00	5.20	.22
12.0	23.50	4.70	.20
12.8	20.00	4.40	.22
13.0	20.00	4.30	.22
13.5	18.00	4.30	.24
14.0	15.40	4.10	.27
14.5	12.80	4.80	.38
15.0	12.80	4.60	.36
16.0	10.70	4.50	.42
17.0	9.50	4.40	.46
18.0	9.20	4.00	.43
19.0	7.60	3.80	.50
20.0	7.00	3.75	.54
22.0	6.40	3.80	.59
24.0	5.00	3.50	.70
26.0	4.25	3.00	.71
28.0	3.60	2.40	.67
30.0	2.40	2.40	1.00
32.0	2.10	2.10	1.00
34.0	3.60	1.90	.53
36.0	3.40	2.00	.59
38.0	2.90	1.20	.41
40.0	4.40	2.00	.46
45.0	3.70	0.20	.54
50.0	2.10	0.70	.33

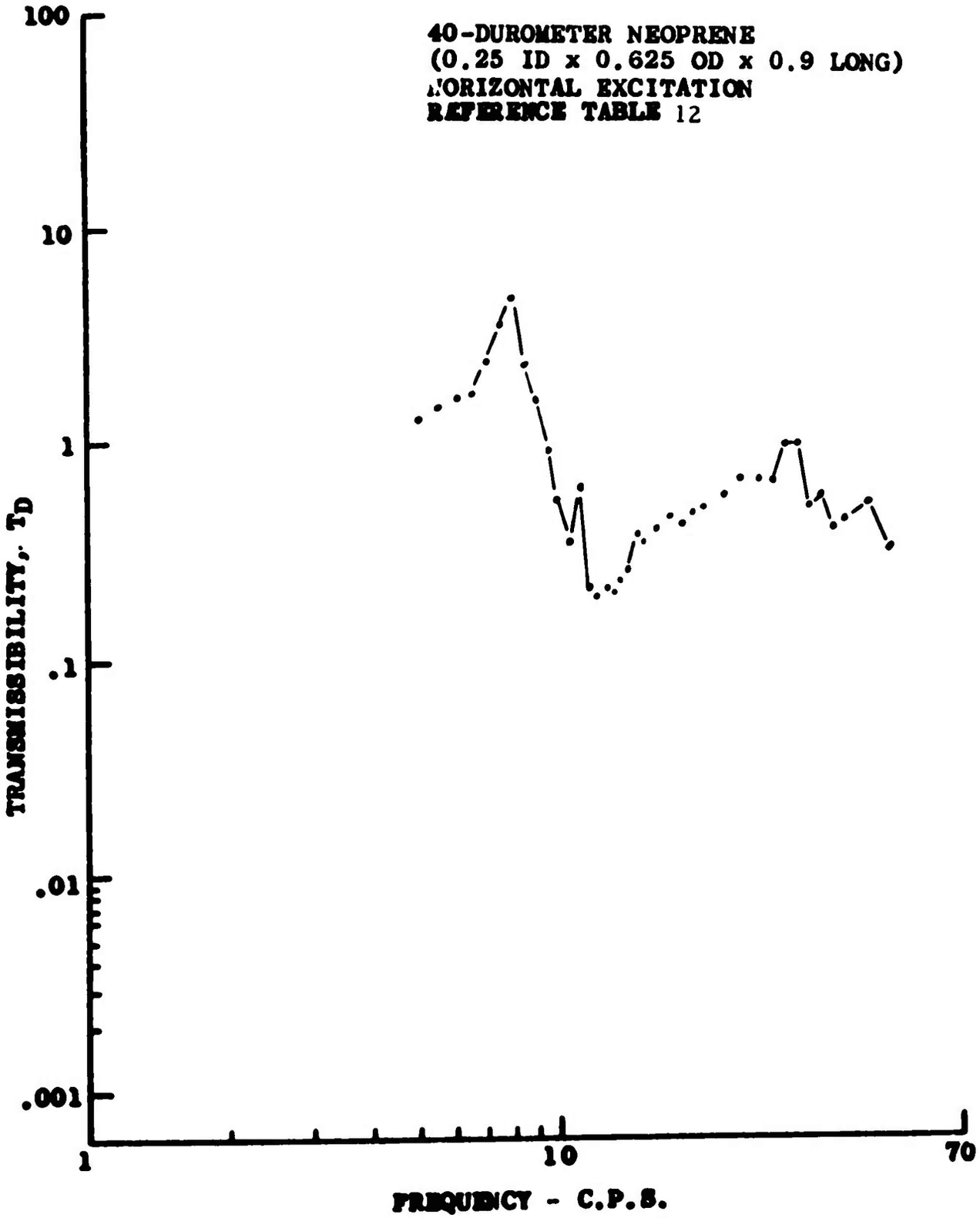

Figure 25. Rubber Pivot Response Curve

TABLE 13

DAVI TRANSMISSIBILITY TEST DATA
RUBBER PIVOT CONFIGURATION
40-DUROMETER NEOPRENE (0.25 ID x 0.625 OD x 0.9 LONG)
ISOLATED WEIGHT, 5 POUNDS

Frequency (c.p.s.)	Input	Output	Output / Input
4.0	60.00	72.00	1.20
4.5	58.00	76.00	1.31
5.0	48.00	71.00	1.85
5.5	31.00	60.00	1.94
6.0	25.00	55.00	2.20
6.5	15.00	47.00	3.13
7.0	11.50	38.00	3.30
7.5	13.50	30.00	2.22
8.0	20.50	21.70	1.06
8.5	26.10	15.20	.58
9.0	31.00	9.80	.32
9.5	34.00	5.10	.15
10.0	33.50	4.72	.14
10.5	32.00	4.90	.15
11.0	31.00	5.00	.16
11.5	31.00	4.00	.13
12.0	29.00	4.50	.16
12.5	28.00	5.00	.18
13.0	25.00	5.20	.21
14.0	21.50	5.30	.25
15.0	18.00	5.00	.22
16.0	15.80	5.00	.32
17.0	14.50	4.85	.33
18.0	13.10	4.70	.36
19.0	12.00	4.30	.36
20.0	11.00	4.00	.36
21.0	11.10	4.20	.38
22.0	10.00	3.80	.38
23.0	9.00	3.33	.37
24.0	8.10	3.40	.42
25.0	7.40	3.10	.42
27.0	6.00	2.80	.47
30.0	4.90	1.90	.39
32.0	4.40	1.60	.36

TABLE 13 (Contined)

Frequency (c.p.s.)	Input	Output	Output / Input
35.0	2.00	2.00	1.00
37.0	1.10	1.80	1.64
40.0	2.10	1.05	.50
45.0	3.00	.70	.23
50.0	3.80	1.00	.26
55.0	.30	.80	2.33
60.0	.25	.55	2.20

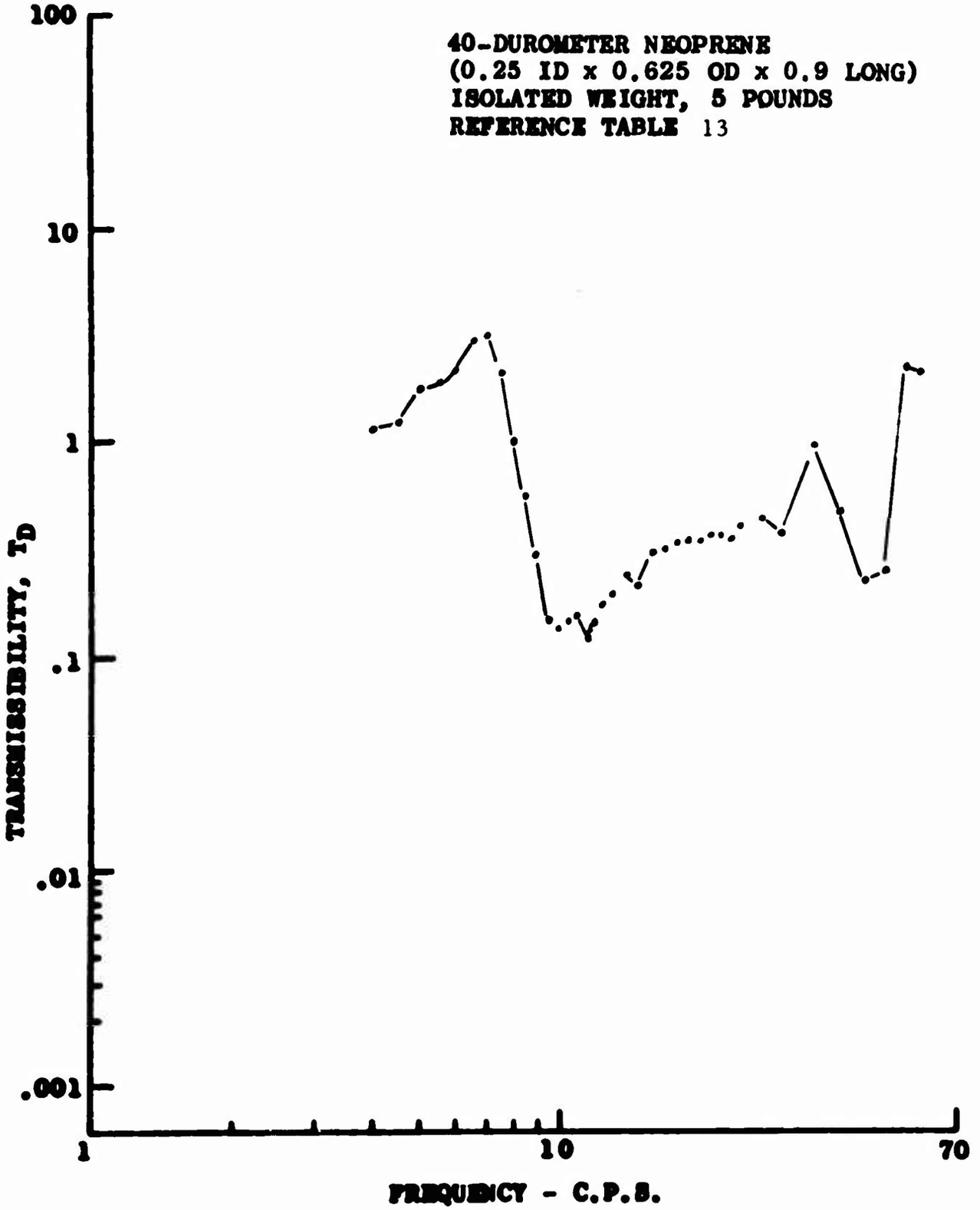

Figure 26. Rubber Pivot Response Curve

TABLE 14

DAVI TRANSMISSIBILITY TEST DATA
RUBBER PIVOT CONFIGURATION
40-DUROMETER NEOPRENE (0.25 ID x 0.625 OD x 0.9 LONG)
ISOLATED WEIGHT, 7 POUNDS

Frequency (c.p.s.)	Input	Output	Output / Input
4.0	54.00	62.00	1.15
4.5	55.00	69.00	1.26
5.0	48.00	66.00	1.38
5.5	37.00	60.00	1.62
6.0	26.00	51.00	1.96
6.5	15.70	44.00	2.80
7.0	8.80	37.20	4.24
7.5	8.30	30.50	3.78
8.0	12.50	25.00	2.00
8.5	17.70	20.00	1.13
9.0	21.80	15.10	.69
9.5	23.50	11.00	.47
10.0	25.50	7.50	.29
10.5	23.20	6.50	.28
11.0	21.80	6.90	.32
11.5	23.00	4.80	.21
12.0	23.10	3.00	.13
12.5	22.50	2.00	.09
13.0	21.50	1.80	.08
13.5	21.20	1.90	.09
14.0	20.00	2.00	.10
15.0	18.00	2.30	.13
16.0	15.80	2.40	.15
17.0	14.40	2.60	.18
18.0	13.30	2.60	.20
19.0	12.40	2.55	.21
20.0	11.20	2.50	.22
21.0	11.10	2.50	.23
22.0	10.00	2.40	.24
23.0	9.00	2.00	.22
24.0	8.10	1.75	.22
25.0	7.50	1.58	.21
26.0	6.90	1.45	.21
27.0	6.40	1.22	.19
28.0	6.00	1.00	.17

TABLE 14 **(Continued)**

Frequency (c.p.s.)	Input	Output	Output / Input
29.0	5.70	1.00	.18
30.0	4.30	1.80	.30
32.0	3.52	1.48	.42
34.0	3.10	1.30	.42
36.0	2.58	1.10	.43
38.0	2.80	2.20	.79
40.0	3.60	1.60	.44
42.0	6.60	1.70	.26
44.0	4.90	.55	.11
46.0	5.50	2.00	.36
48.0	2.00	1.85	.92
50.0	1.30	1.55	1.19

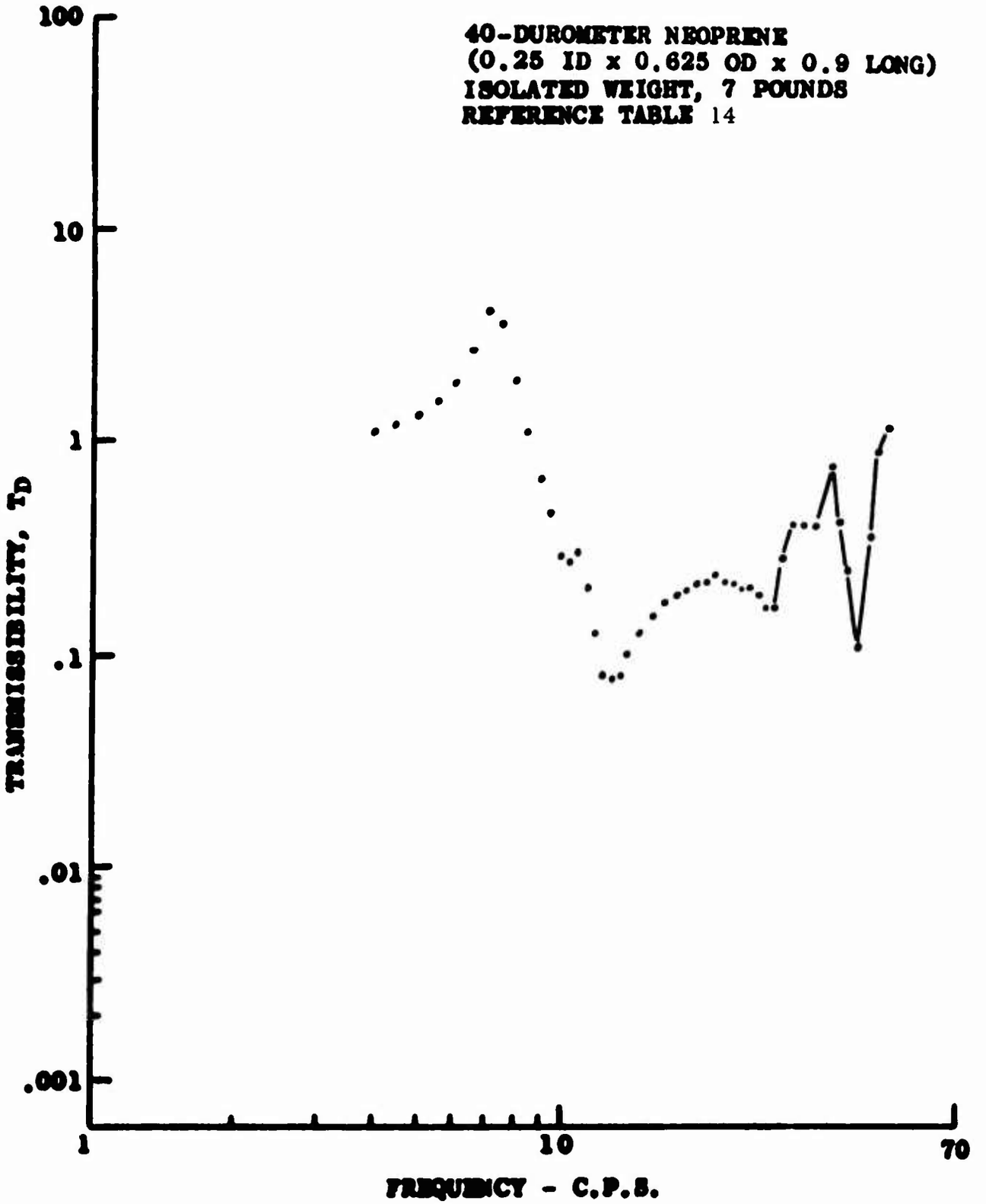

Figure 27. Rubber Pivot Response Curve

TABLE 15

DAVI TRANSMISSIBILITY TEST DATA
RUBBER PIVOT CONFIGURATION
40-DUROMETER NEOPRENE (0.375 ID x 0.75 OD x 0.9 LONG)
ISOLATED WEIGHT, 5 POUNDS

Frequency (c.p.s.)	Input	Output	Output / Input
4.0	67.00	71.00	1.05
4.5	69.00	75.00	1.09
5.0	67.00	75.00	1.12
5.5	52.00	62.00	1.19
6.0	56.00	70.00	1.25
6.5	49.00	63.00	1.28
7.0	41.00	56.00	1.37
7.5	35.00	50.00	1.43
8.0	29.00	44.00	1.52
8.5	24.00	39.00	1.63
9.0	19.00	35.00	1.84
9.5	15.00	32.00	2.13
10.0	7.40	19.00	2.56
10.5	8.00	26.00	3.25
11.0	5.00	23.00	4.60
11.5	4.00	21.00	5.25
12.0	6.00	18.00	3.00
12.5	9.00	17.00	1.88
13.0	14.00	15.50	1.11
13.5	18.00	13.50	.75
14.0	23.00	11.00	.47
15.0	32.00	6.00	.19
16.0	17.00	4.00	.24
17.0	20.00	2.50	.13
18.0	20.00	3.00	.15
19.0	19.00	3.40	.18
20.0	17.50	3.50	.20
22.0	15.50	4.00	.26
24.0	12.70	3.50	.28
26.0	11.40	3.00	.26
28.0	8.70	4.00	.46
30.0	5.00	3.00	.60
32.0	5.00	2.50	.50
34.0	5.00	2.00	.40

TABLE 15 (Continued)

Frequency (c.p.s.)	Input	Output	Output / Input
36.0	4.50	1.80	.40
38.0	2.70	1.80	.66
40.0	2.60	1.60	.62
42.0	2.40	1.30	.54
44.0	2.00	1.75	.88
46.0	1.70	1.50	.91
48.0	1.60	1.30	.81
50.0	1.50	1.10	.73

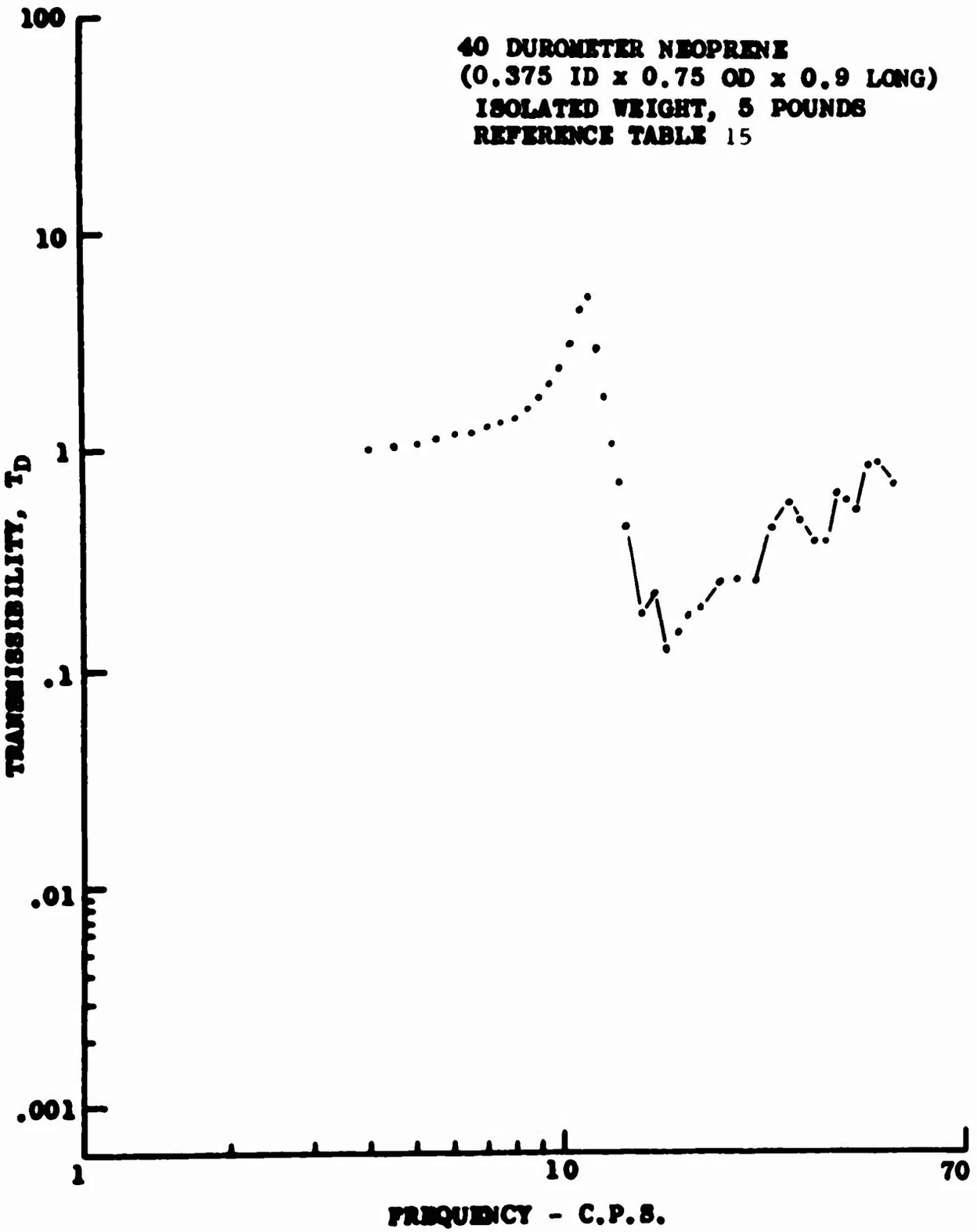

Figure 28. Rubber Pivot Response Curve

TABLE 16

DAVI TRANSMISSIBILITY TEST DATA
RUBBER PIVOT CONFIGURATION
40-DUROMETER NEOPRENE (0.375 ID x 0.75 OD x 0.9 LONG)
ISOLATED WEIGHT, 7 POUNDS

Frequency (c.p.s.)	Input	Output	Output / Input
4.0	67.00	71.00	1.06
4.5	69.00	74.00	1.07
5.0	65.00	73.00	1.12
5.5	59.00	69.00	1.17
6.0	52.00	63.00	1.21
6.5	45.00	56.00	1.24
7.0	39.00	50.00	1.29
7.5	34.00	46.00	1.35
8.0	29.00	41.00	1.41
8.5	24.00	37.00	1.54
9.0	19.50	33.00	1.69
9.5	16.00	30.00	1.88
10.0	12.00	27.00	2.25
10.5	9.00	25.00	2.78
11.0	6.00	22.50	3.75
11.5	4.50	20.50	4.56
12.0	5.50	18.50	3.36
12.5	8.50	16.50	1.94
13.0	12.20	15.00	1.23
13.5	16.50	13.00	.79
14.0	20.50	11.00	.54
14.5	25.00	9.00	.36
15.0	27.00	6.50	.24
15.5	29.00	4.30	.15
16.0	30.00	3.00	.10
16.5	29.00	2.40	.08
17.0	29.00	2.50	.09
17.5	29.00	2.60	.09
18.0	28.00	2.50	.09
18.5	18.00	2.40	.13
19.0	12.00	3.00	.25
19.5	12.60	3.30	.26
20.0	13.20	3.50	.27
22.0	14.50	4.00	.28
24.0	12.60	3.30	.26

TABLE 16 **(Continued)**

Frequency (c.p.s.)	Input	Output	Output / Input
26.0	12.10	2.50	.21
28.0	12.60	1.60	.13
30.0	6.00	3.00	.50
32.0	7.00	2.00	.29
34.0	7.50	1.60	.21
36.0	8.50	1.50	.18
38.0	6.80	2.00	.29
40.0	4.00	2.00	.50
42.0	2.90	2.00	.70
44.0	1.30	1.80	1.38
46.0	.40	1.40	3.50
48.0	.20	1.10	5.50
50.0	.30	1.00	3.33

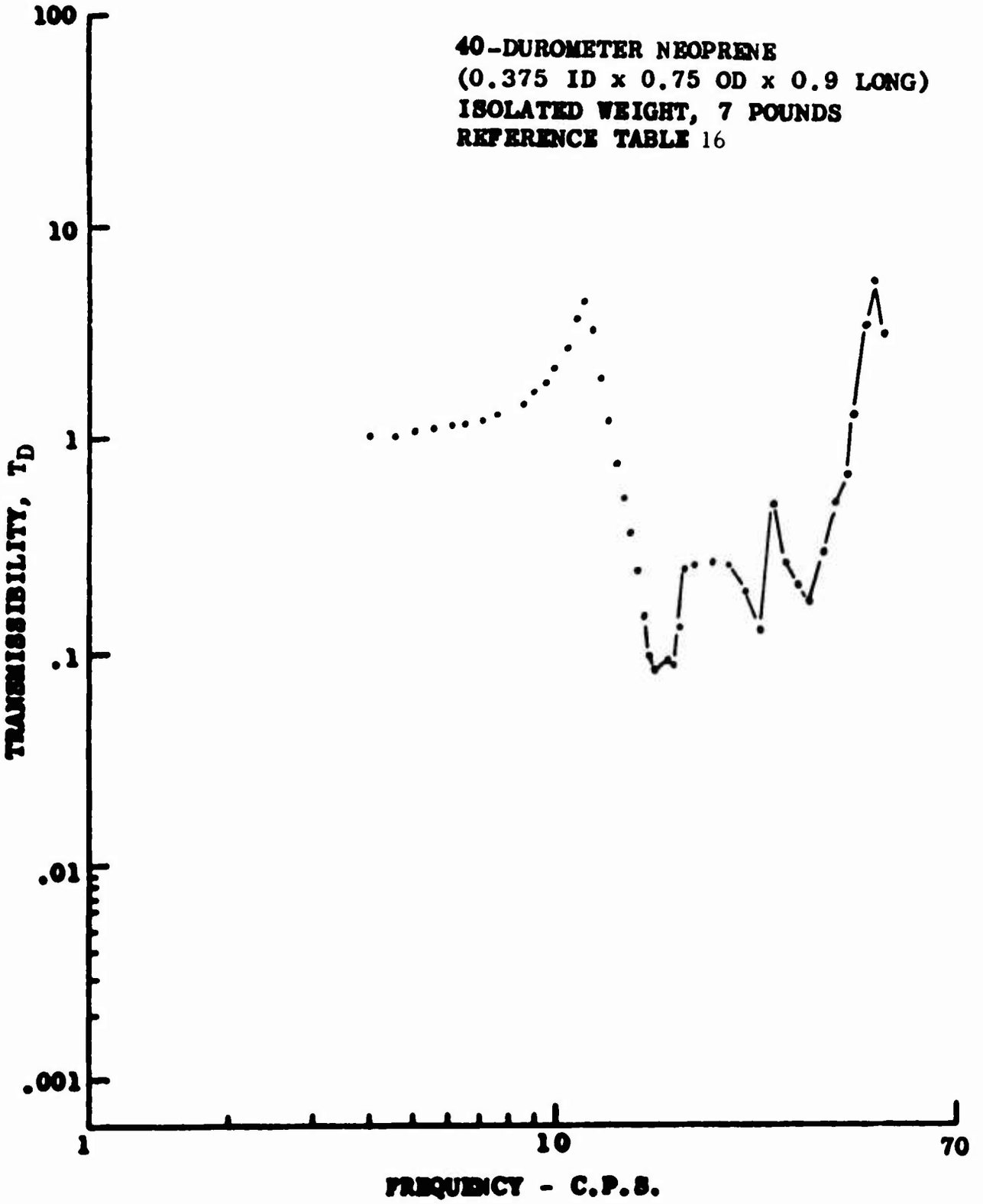

Figure 29. Rubber Pivot Response Curve

TABLE 17

DAVI TRANSMISSIBILITY TEST DATA
RUBBER PIVOT CONFIGURATION
40-DUROMETER NATURAL RUBBER (0.375 ID x 0.75 OD x 0.9 LONG)
ISOLATED WEIGHT, 5 POUNDS

Frequency (c.p.s.)	Input	Output	Output / Input
5.0	50.00	61.00	1.22
6.0	55.00	71.00	1.29
7.0	51.00	78.00	1.52
8.0	31.00	63.00	2.03
8.5	26.00	66.00	2.54
9.0	23.00	54.00	2.35
9.5	27.50	39.50	1.43
10.0	32.00	23.00	.72
10.5	34.50	14.00	.41
11.0	35.00	10.00	.29
11.3	35.00	10.00	.29
11.5	34.80	10.00	.29
12.0	34.20	11.20	.33
13.0	32.00	13.50	.42
14.0	29.50	14.20	.48
15.0	27.00	14.00	.51
17.0	23.00	13.00	.56
20.0	17.50	11.00	.63
25.0	12.40	8.60	.69
30.0	8.60	5.30	.62
35.0	5.90	4.00	.68
40.0	4.00	2.80	.70
50.0	2.90	2.40	.82
60.0	2.00	1.70	.85

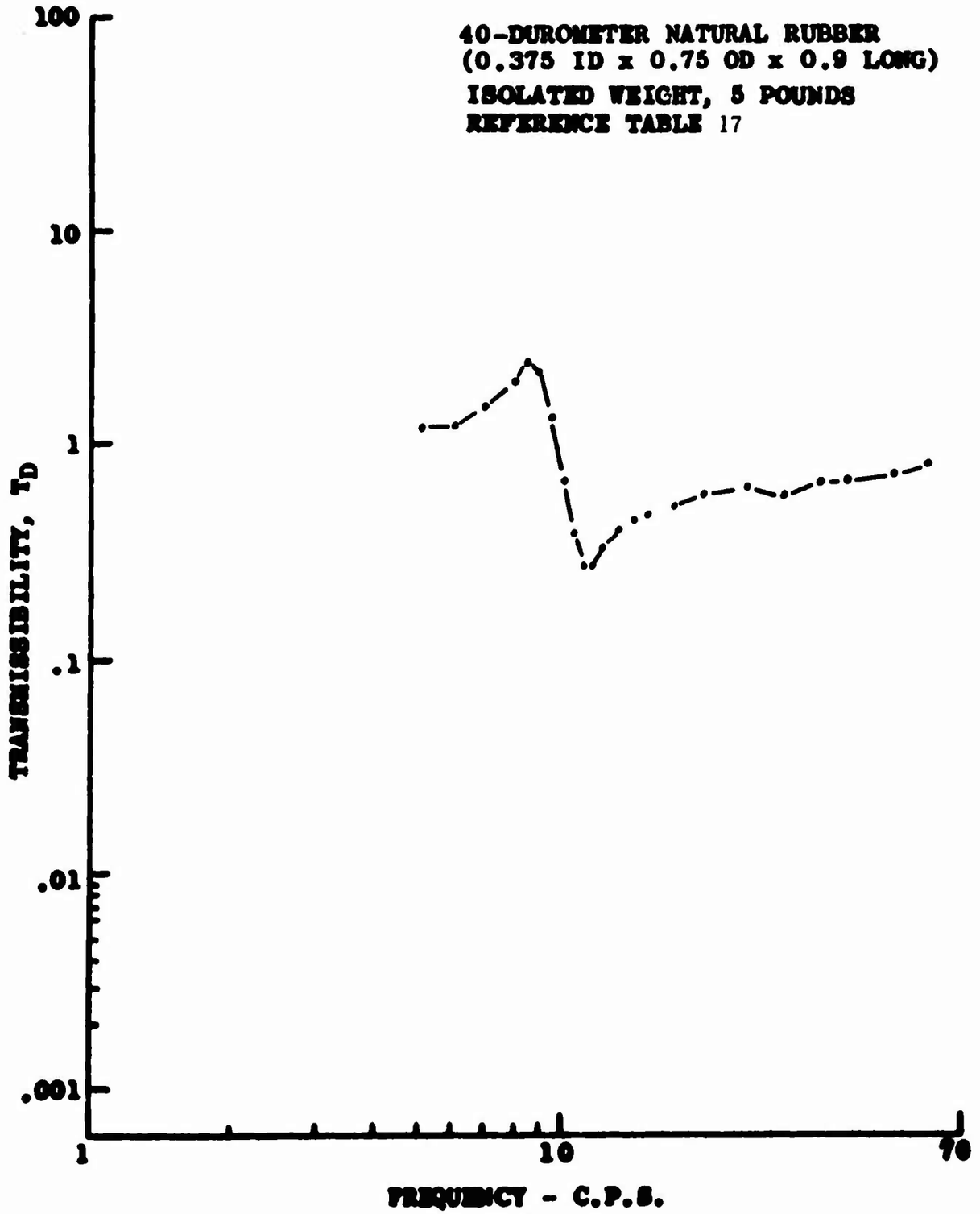

Figure 30. Rubber Pivot Response Curve

TABLE 18

DAVI TRANSMISSIBILITY TEST DATA
RUBBER PIVOT CONFIGURATION
65-DUROMETER NEOPRENE (0.375 ID x 0.75 OD x 0.9 LONG)
HORIZONTAL EXCITATION

Frequency (c.p.s.)	Input	Output	Output / Input
5.0	54.00	62.0	1.15
6.0	43.00	50.0	1.16
6.5	37.00	45.0	1.22
7.0	32.00	40.0	1.25
7.5	26.00	34.0	1.31
8.0	21.50	29.0	1.35
8.5	18.00	26.0	1.44
9.0	15.00	23.0	1.53
9.5	12.00	20.0	1.67
10.0	10.00	18.0	1.80
10.5	8.00	15.7	1.96
11.0	6.50	15.0	2.31
11.5	5.00	13.5	2.70
12.0	3.40	12.0	3.53
12.5	3.00	10.6	3.53
13.0	3.50	9.4	2.69
14.0	6.60	7.7	1.17
15.0	11.10	5.8	.52
16.0	15.50	3.5	.23
17.0	17.20	2.5	.15
17.2	36.00	5.0	.14
18.0	36.50	5.7	.16
19.0	32.00	7.1	.22
20.0	31.00	8.0	.26
22.0	25.50	9.1	.36
24.0	20.00	7.7	.39
26.0	15.00	6.3	.42
28.0	17.00	6.2	.95
30.0	14.80	5.1	.35
32.0	14.20	4.0	.28
34.0	15.10	2.5	.17
36.0	6.50	1.5	.23
38.0	2.30	2.0	.87
40.0	1.00	1.6	1.55
42.0	1.25	.9	.72
44.0	1.00	1.3	1.30
46.0	.80	1.1	1.38
48.0	1.15	1.0	.87
50.0	1.10	.9	.77

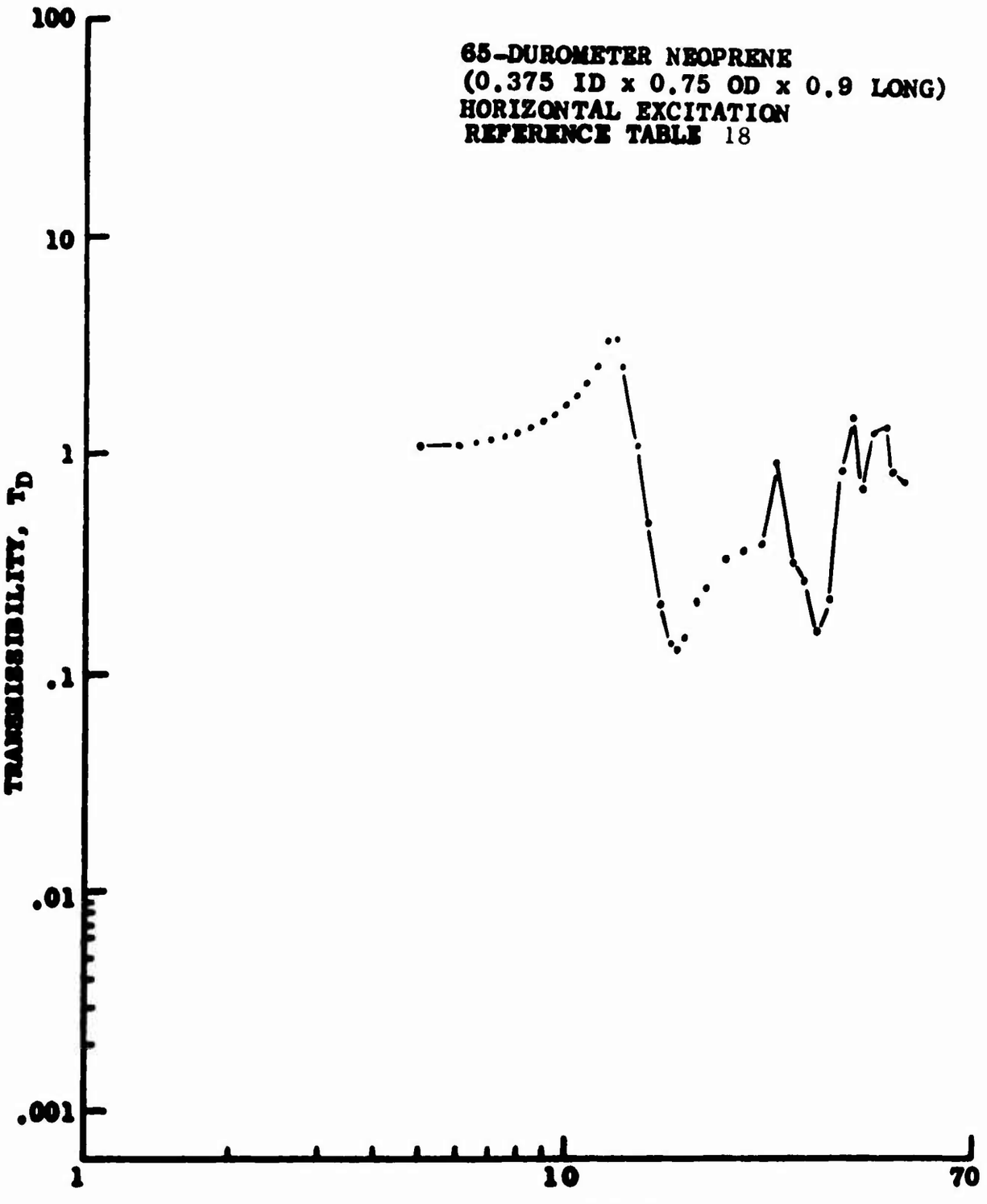

Figure 31. Rubber Pivot Response Curve

TABLE 19

DAVI TRANSMISSIBILITY TEST DATA
RUBBER PIVOT CONFIGURATION
65-DUROMETER NEOPRENE (0.375 ID x 0.75 OD x 0.9 LONG)
ISOLATED WEIGHT, 5 POUNDS

Frequency (c.p.s.)	Input	Output	Output / Input
5.0	50.00	55.00	1.10
5.5	45.00	50.00	1.11
6.0	41.00	47.00	1.15
6.5	37.00	44.00	1.19
7.0	34.00	40.00	1.18
7.5	30.00	36.00	1.20
8.0	27.00	32.00	1.18
8.5	24.00	29.00	1.21
9.0	21.00	27.00	1.29
9.5	18.00	24.00	1.33
10.0	17.00	23.00	1.35
10.5	15.00	20.00	1.33
11.0	13.00	19.00	1.46
11.5	11.00	17.00	1.54
12.0	9.60	15.00	1.56
12.5	9.00	14.50	1.61
13.0	7.60	13.20	1.73
13.5	6.60	12.20	1.85
14.0	5.60	11.20	2.00
14.5	4.60	10.30	2.23
15.0	3.60	9.20	2.56
16.0	1.80	7.60	4.22
17.0	.80	6.70	8.37
18.0	2.40	6.60	2.75
19.0	3.80	5.80	1.53
20.0	5.10	5.30	1.04
22.0	8.40	4.50	.54
24.0	11.90	2.10	.18
26.0	11.70	1.20	.10
28.0	7.00	1.55	.22
30.0	6.20	1.60	.29
32.0	5.60	1.50	.25
34.0	5.10	1.40	.27
36.0	4.70	1.20	.26
38.0	4.50	1.00	.22
40.0	3.40	1.05	.31

TABLE 19 (Continued)

Frequency (c.p.s.)	Input	Output	Output / Input
42.0	2.00	.95	.47
44.0	1.50	.90	.60
46.0	1.20	1.05	.87
48.0	1.15	1.00	.87
50.0	1.10	.85	.77

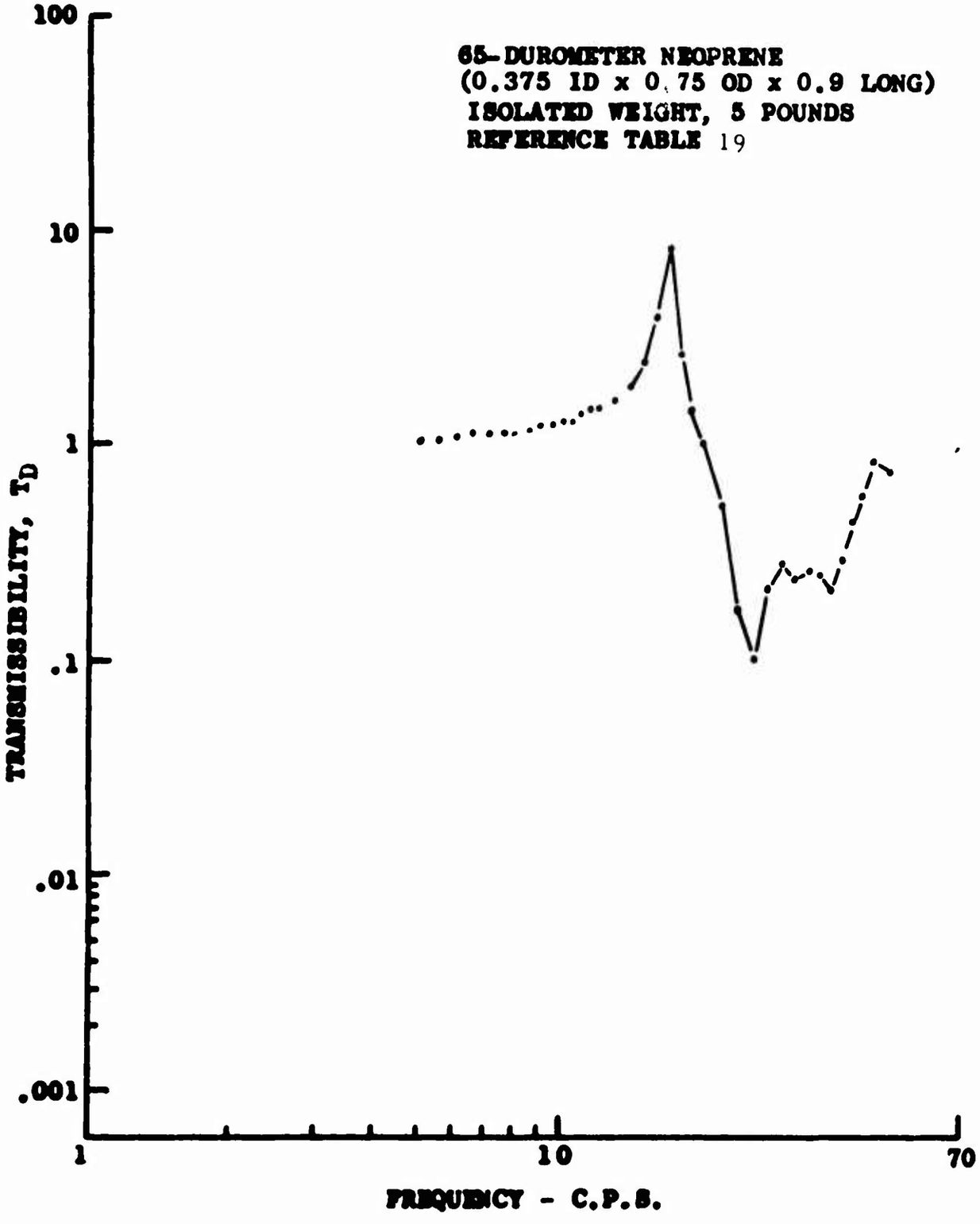

Figure 32. Rubber Pivot Response Curve

TABLE 20

DAVI TRANSMISSIBILITY TEST DATA
EFFECT OF ISOLATED WEIGHT ON RUBBER PIVOT CONFIGURATION
40-DUROMETER NEOPRENE (0.375 ID x 0.75 OD x 0.9 LONG)

	ISOLATED WEIGHT					
Frequency (c.p.s.)	5 Lb.	7 Lb.	9 Lb.	11 Lb.	13 Lb.	15 Lb.
5.0	1.10	1.14	1.18	1.24	1.41	1.37
6.0	1.19	1.32	1.43	1.70	2.09	2.28
7.0	1.20	1.39	1.71	2.00	3.56	4.67
7.4	-	-	-	-	-	5.13
7.5	-	-	-	-	4.07	-
7.7	-	-	-	5.54	-	-
8.0	1.44	2.08	-	5.08	2.00	2.07
8.5	-	-	4.36	-	-	-
8.8	-	4.00	-	-	-	-
9.0	2.35	3.33	2.00	0.95	0.57	0.61
9.4	3.00	-	-	-	-	-
10.0	1.06	0.54	0.53	0.23	0.16	0.23
10.8	-	-	-	0.11	0.08	-
11.0	0.25	0.16	0.13	0.10	0.09	0.06
11.1	0.24	-	-	-	-	-
11.2	-	-	-	-	-	0.06
11.5	-	-	0.11	-	-	-
12.0	0.37	0.26	0.12	-	0.14	0.09
13.0	0.49	0.37	-	0.25	0.22	-
14.0	0.57	0.43	0.26	0.30	0.25	0.20
16.0	0.72	0.54	0.37	0.40	0.32	0.22
18.0	0.66	0.59	0.50	0.40	0.34	0.23
20.0	0.75	0.62	0.56	0.42	0.41	0.23
25.0	0.86	0.71	0.68	0.48	0.75	0.58
30.0	0.94	0.85	-	0.89	0.87	0.77

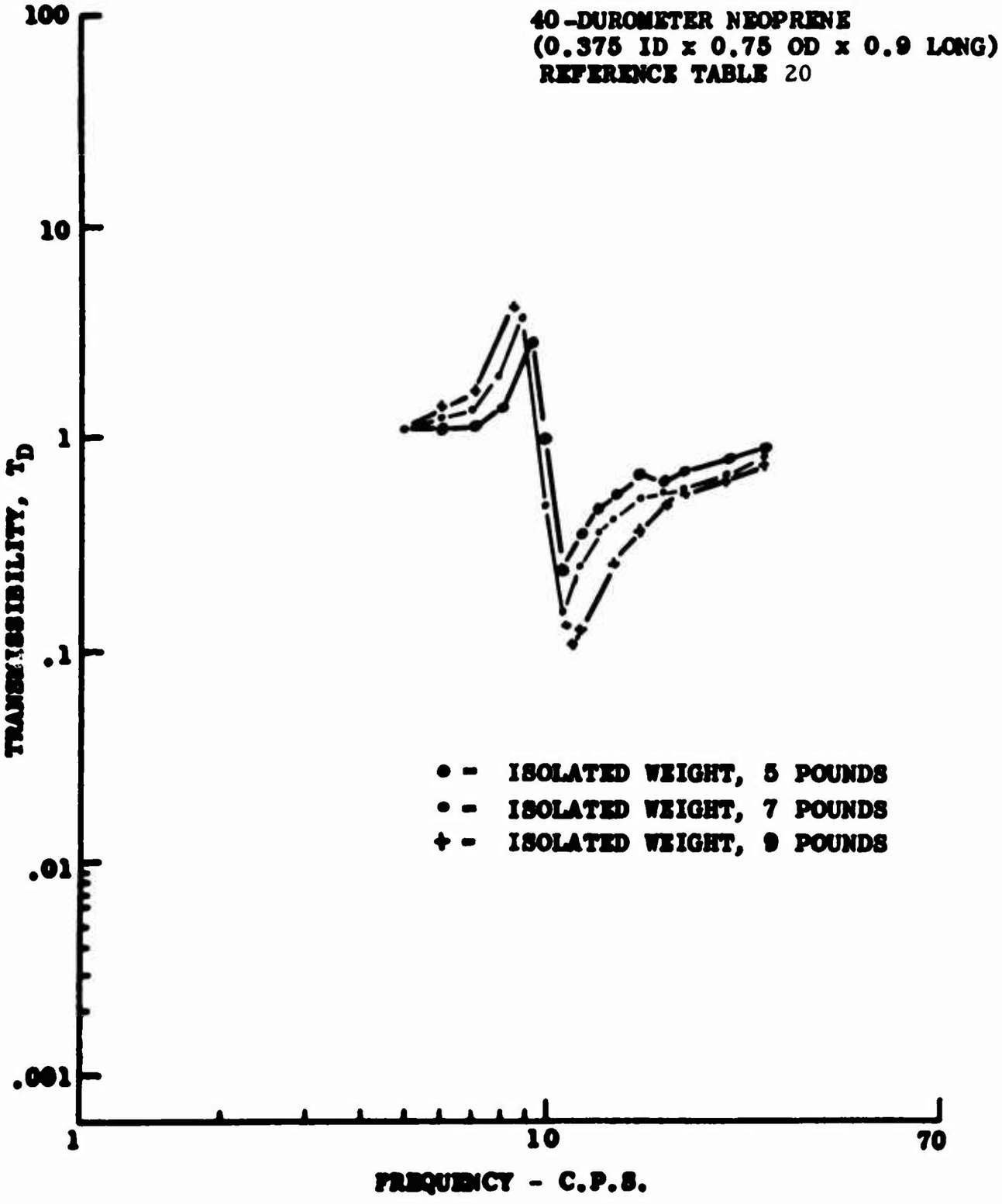

Figure 33a. Effect of Isolated Weight on Rubber Pivot Configuration

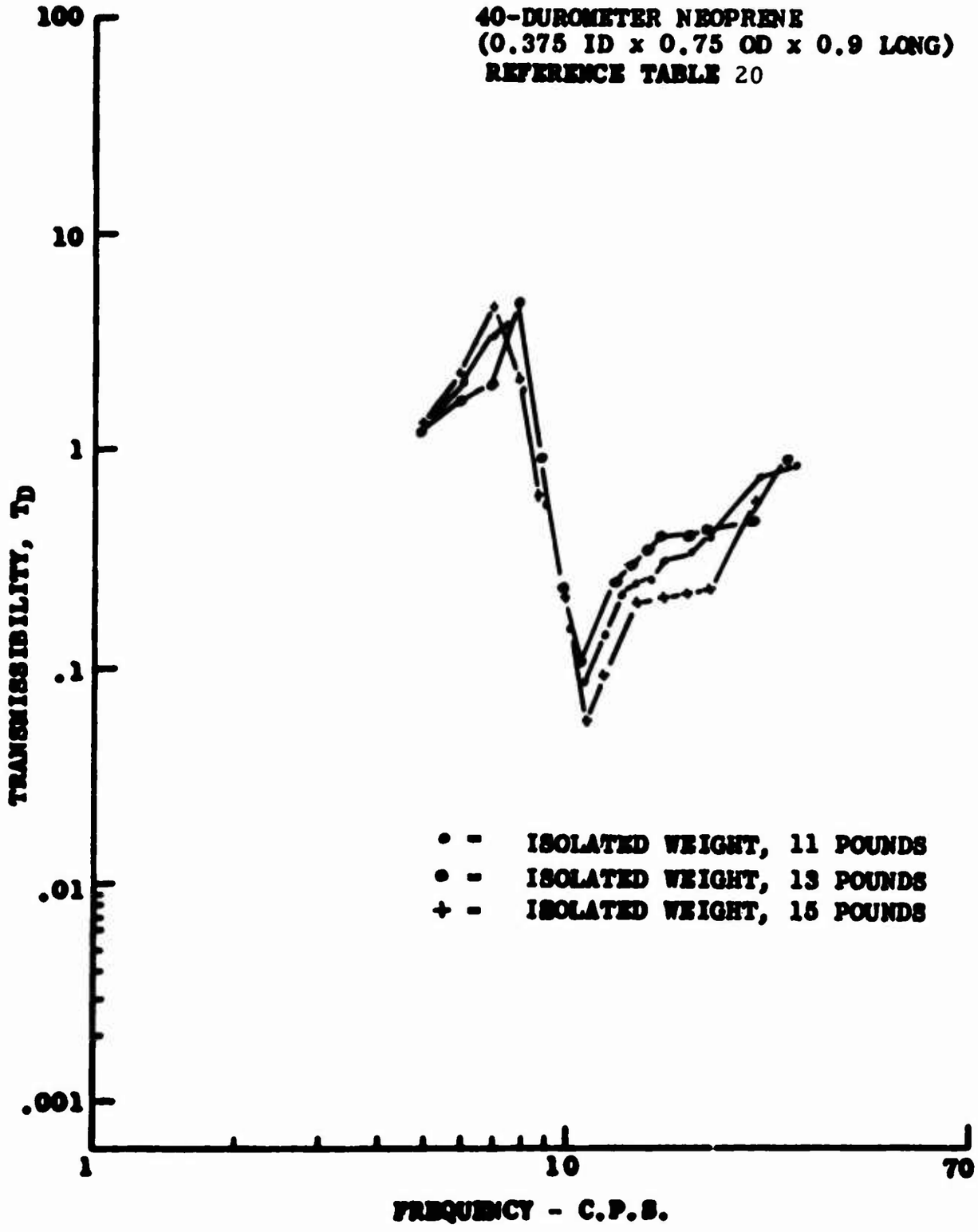

Figure 33b, Effect of Isolated Weight on Rubber Pivot Configuration

TABLE 21

EFFECT OF VARYING INERTIA AND ISOLATED WEIGHT
RUBBER PIVOT CONFIGURATION
40-DUROMETER NEOPRENE

Inertia (I)
Isolated Weight (W)
Resonant Frequency (ω_R)
Antiresonant Frequency (ω_A)
Transmissibility (T_D)

I (lb sec. in^2)	W (lb)	ω_R (cps)	ω_A (cps)	TD	Isolation (%)
.034	5	9.1	10.20	.333	66.7
	10	7.8	10.20	.124	87.6
	15	6.9	10.00	.081	91.9
.040	5	8.3	9.50	.385	61.5
	10	7.3	9.10	.158	84.2
	15	6.5	9.00	.105	89.5
.044	5	7.6	8.40	.452	54.8
	10	6.6	8.30	.179	82.1
	15	5.9	8.10	.097	90.3
.054	10	6.4	7.70	.231	76.9
	15	5.9	7.60	.151	84.9
	20	5.5	7.40	.091	90.9
.069	10	5.8	6.90	.273	72.7
	15	5.5	6.80	.195	80.5
	20	5.2	6.80	.148	85.2

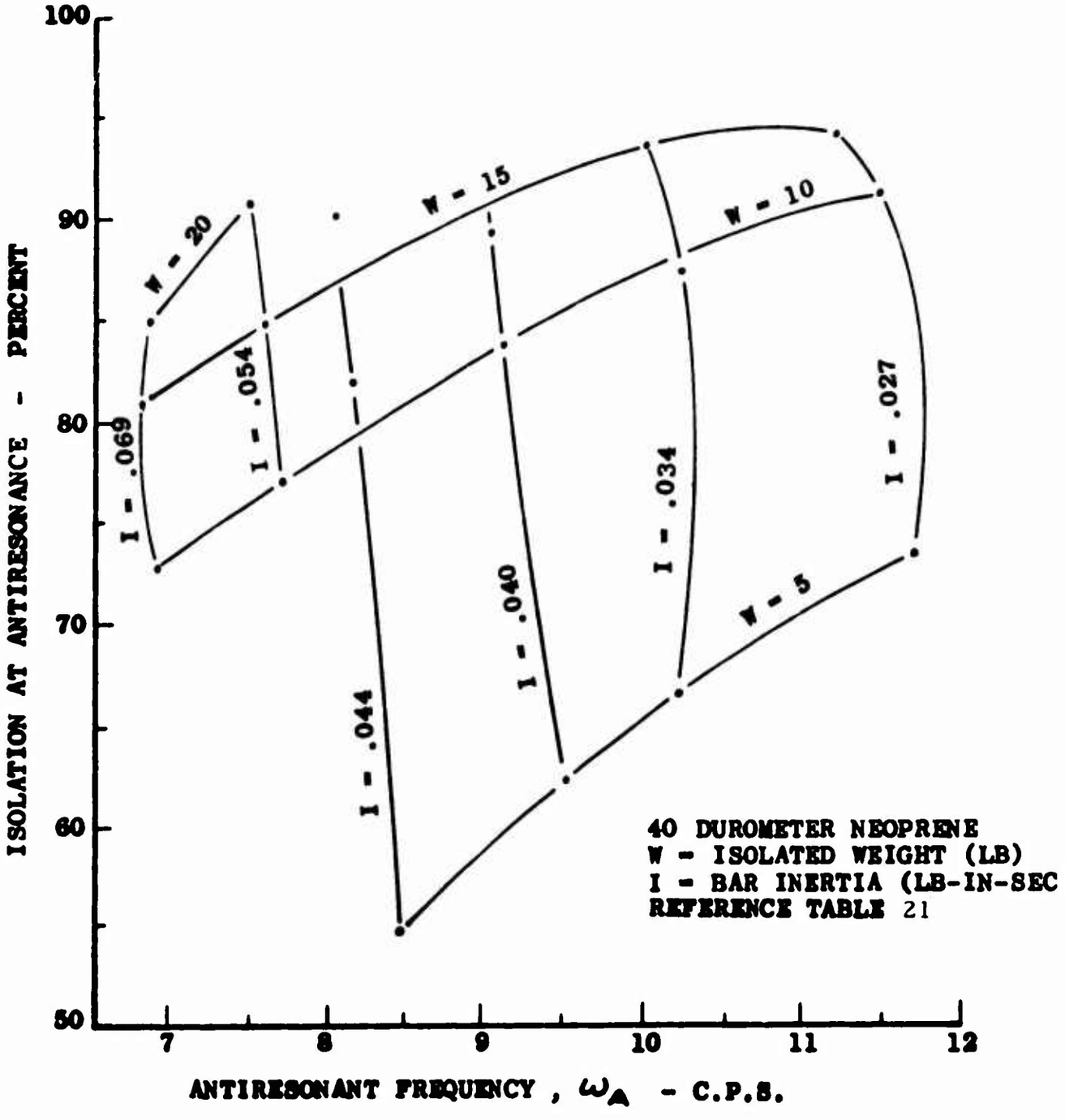

Figure 34. Variation of Antiresonant Frequency and Isolation With Bar Inertia and Isolated Weight

TABLE 22

EFFECT OF VARYING INERTIA AND ISOLATED WEIGHT
RUBBER PIVOT CONFIGURATION
65-DUROMETER NEOPRENE

Inertia (I)
Isolated Weight (W)
Resonant Frequency (ω_R)
Antiresonant Frequency (ω_A)
Transmissibility (T_D)

I (lb.sec.^{2}/in)	W (lb)	ω_R (cps)	ω_A (cps)	T_D	Isolation (%)
.027	10	11.40	16.30	.141	85.9
	15	10.00	15.30	.087	91.3
	20	8.50	13.80	.051	94.9
.034	10	10.60	13.90	.197	80.3
	15	9.30	13.40	.117	88.3
	20	8.10	12.60	.064	93.6
.040	10	9.90	12.60	.258	74.2
	15	8.80	12.00	.146	85.4
	20	7.90	11.70	.093	90.7
.044	10	9.40	11.60	.273	72.7
	15	8.50	11.20	.155	84.5
	20	7.20	11.00	.111	88.9
.054	10	8.80	10.60	.315	68.5
	15	8.10	10.40	.200	80.0
	20	7.10	10.10	.130	87.0
.069	10	8.10	9.50	.390	61.0
	15	7.40	9.20	.269	73.1
	20	6.80	8.60	.177	82.3

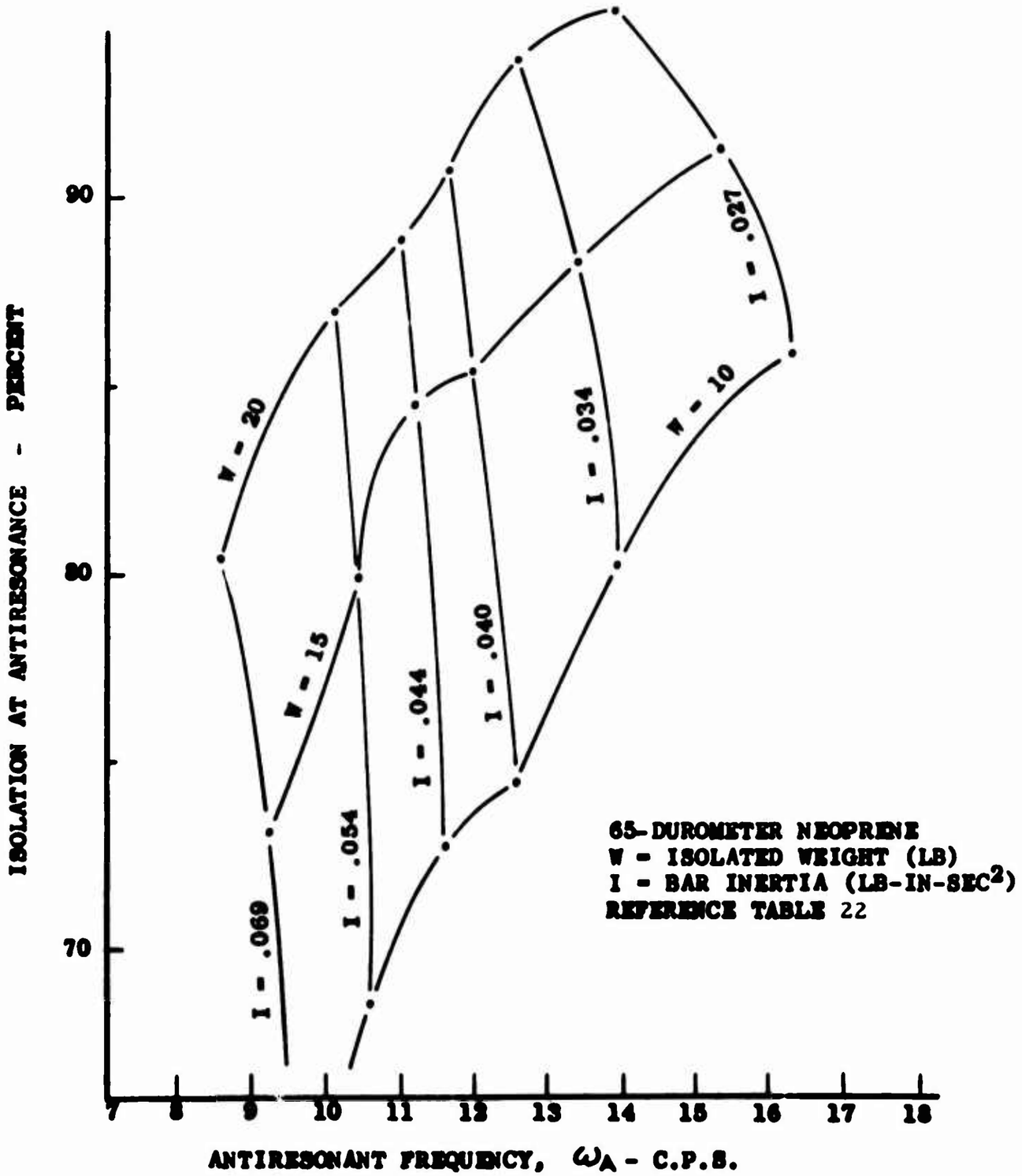

Figure 35. Variation of Antiresonant Frequency and Isolation With Bar Inertia and Isolated Weight

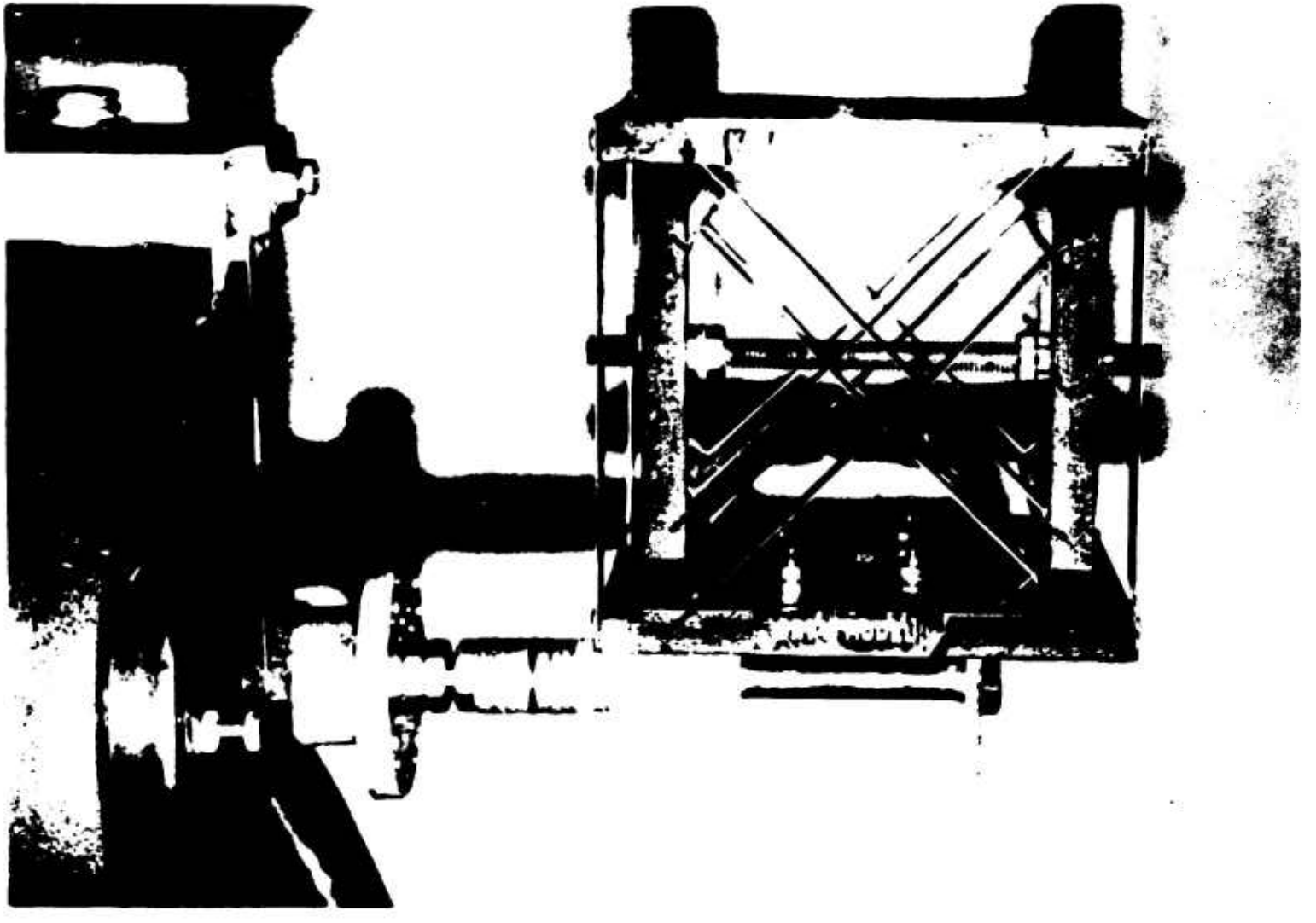

Figure 36. Kaman Flexural DAVI Model

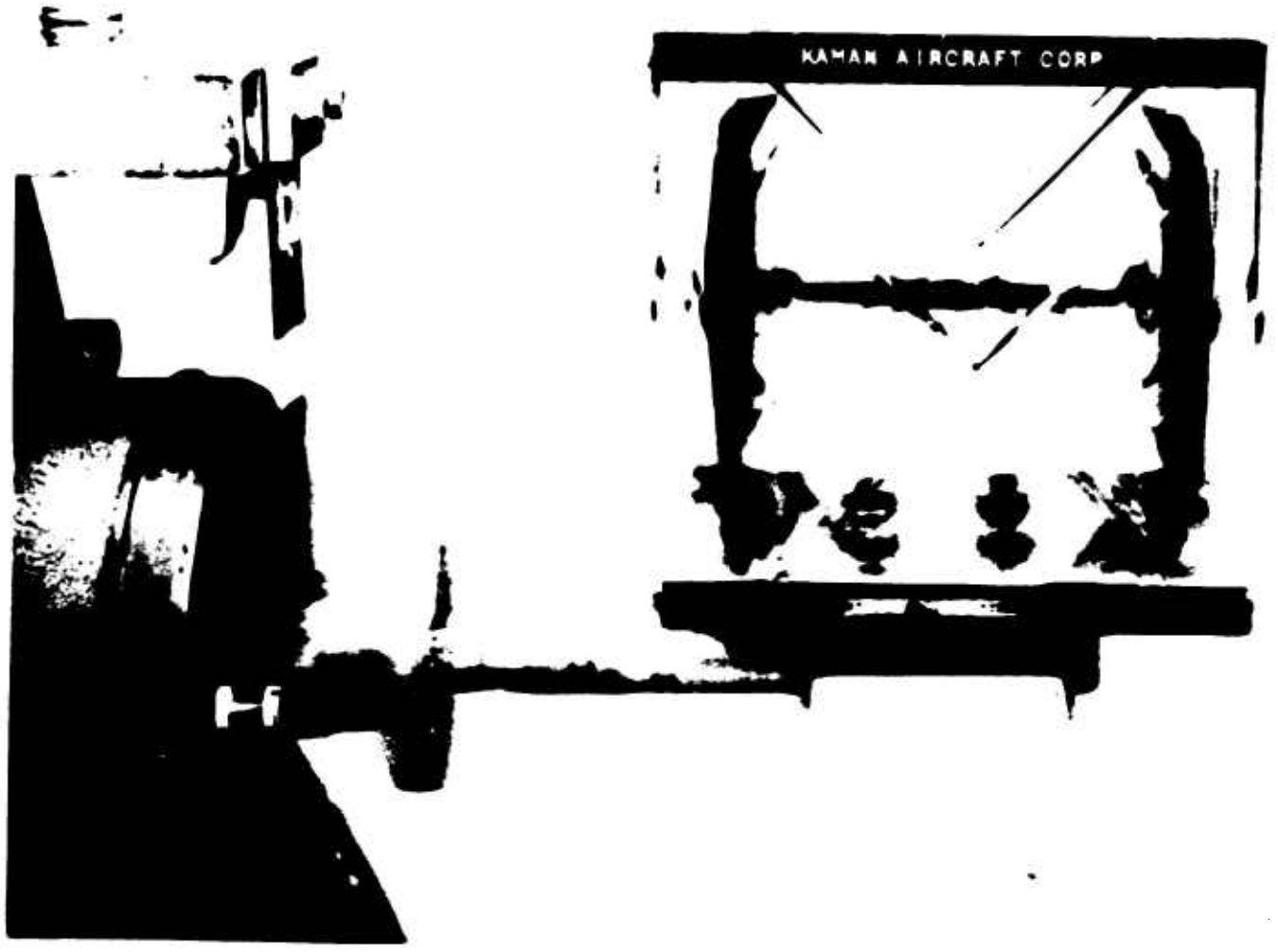

Figure 37. Flexural DAVI Model Isolating at 10 C.P.S.

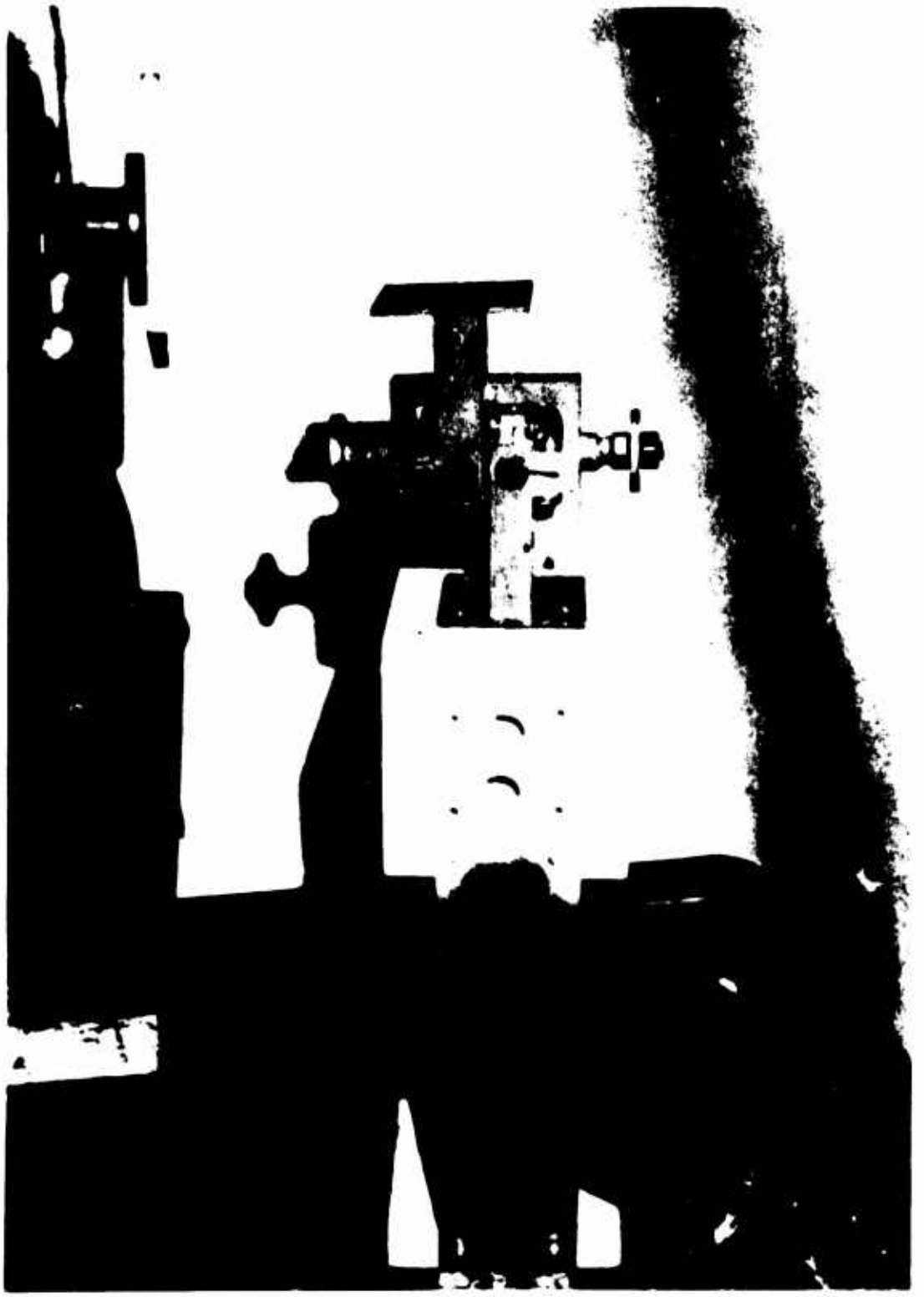

Figure 38. Two-Dimensional DAVI Model

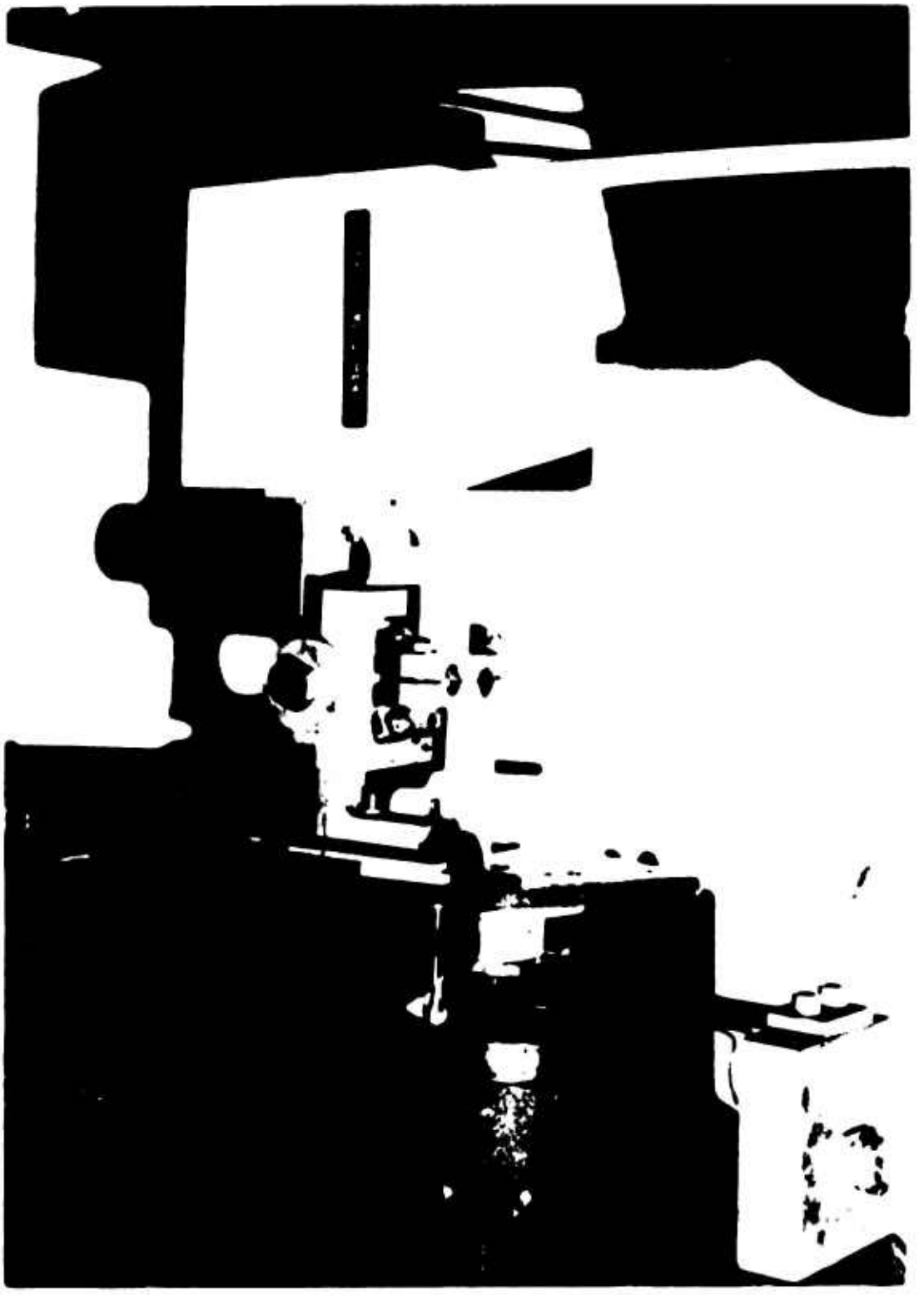

Figure 39. Two-Dimensional DAVI Model Mounted for Vertical Excitation

TABLE 23

TWO-DIMENSIONAL DAVI TRANSMISSIBILITY TEST DATA
15° FLEXURAL PIVOT
VERTICAL EXCITATION

Frequency (c.p.s.)	Output	Input	$\frac{\text{Output}}{\text{Input}}$
5.5	.64	.64	1.00
6.0	.79	.63	1.25
7.0	1.15	.53	2.17
7.5	1.01	.26	3.88
7.9	1.50	.09	16.70
8.0	1.55	.04	36.90
8.1	1.48	.14	10.60
8.5	1.00	.32	3.23
9.0	.54	.39	1.38
9.5	.27	.40	.66
10.0	.11	.39	.28
10.5	.02	.37	.07
10.7	.002	.36	.005
10.8	.002	.36	.005
11.0	.02	.35	.05
11.5	.07	.33	.20
12.0	.10	.32	.30
13.0	.12	.28	.43
14.0	.13	.25	.51
15.0	.12	.22	.56
20.0	.06	.13	.46
25.0	.05	.08	.55
30.0	.03	.05	.62
40.0	.02	.03	.68
60.0	.007	.008	.80

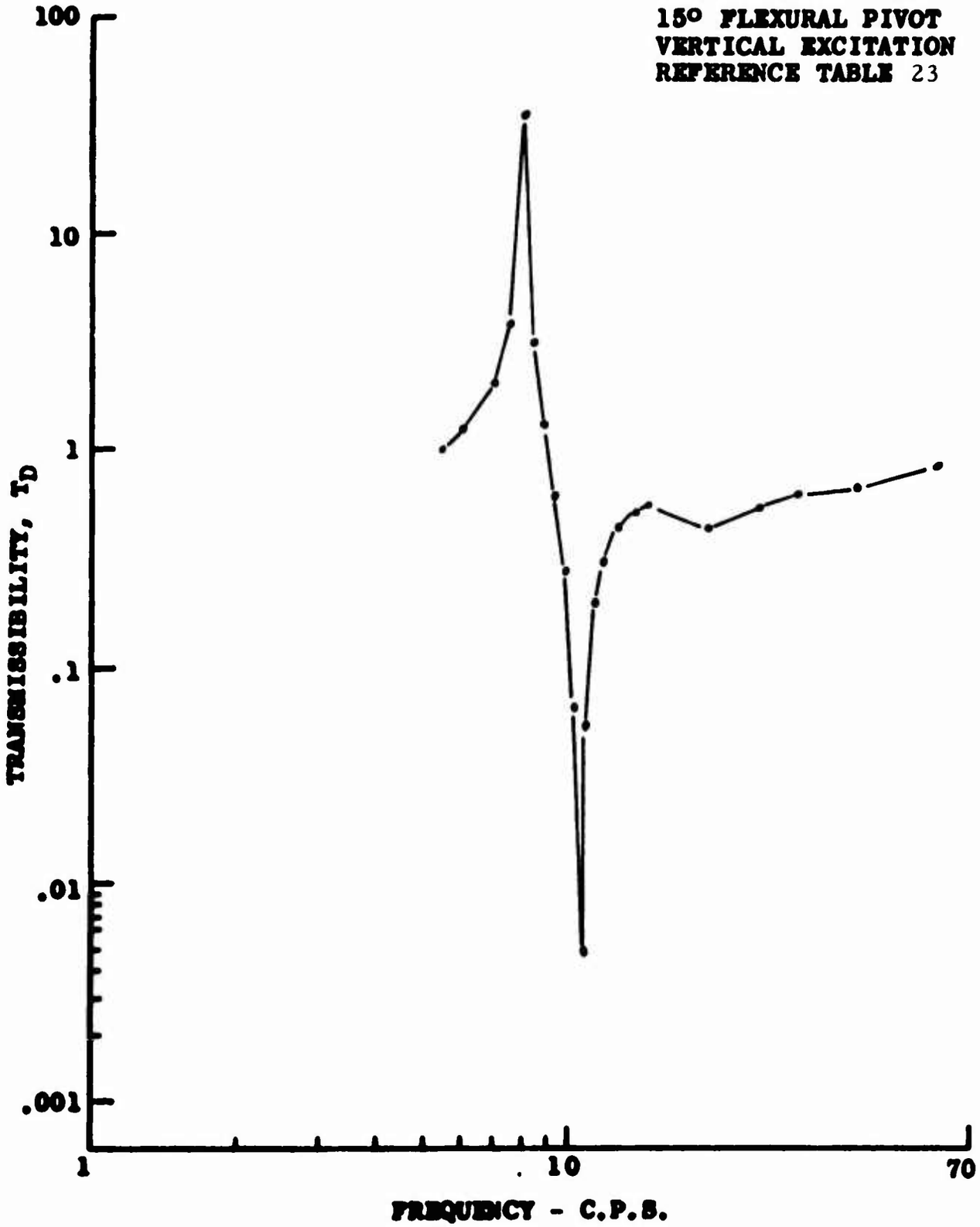

Figure 40. Response Curve for Two-Dimensional DAVI

TABLE 24

TWO-DIMENSIONAL DAVI TRANSMISSIBILITY TEST DATA
15° FLEXURAL PIVO
VERTICAL EXCITATION

Frequency (c.p.s.)	Output	Input	Output / Input
5.0	.60	.68	.88
6.0	.83	.65	1.28
6.5	1.10	.59	1.86
7.0	1.55	.49	3.16
7.5	1.50	.08	19.20
7.6	1.52	.02	72.40
7.7	1.55	.09	16.85
7.8	1.42	.18	7.98
8.0	1.12	.29	3.86
9.0	.28	.40	.70
9.5	.12	.40	.30
10.0	.03	.38	.07
10.2	.008	.38	.02
10.4	.001	.37	.003
10.5	.004	.36	.01
10.8	.02	.35	.06
11.0	.04	.34	.12
12.0	.10	.30	.33
14.0	.12	.23	.53
15.0	.12	.21	.58
20.0	.07	.12	.63
25.0	.05	.08	.59
30.0	.03	.05	.64
40.0	.02	.02	.76

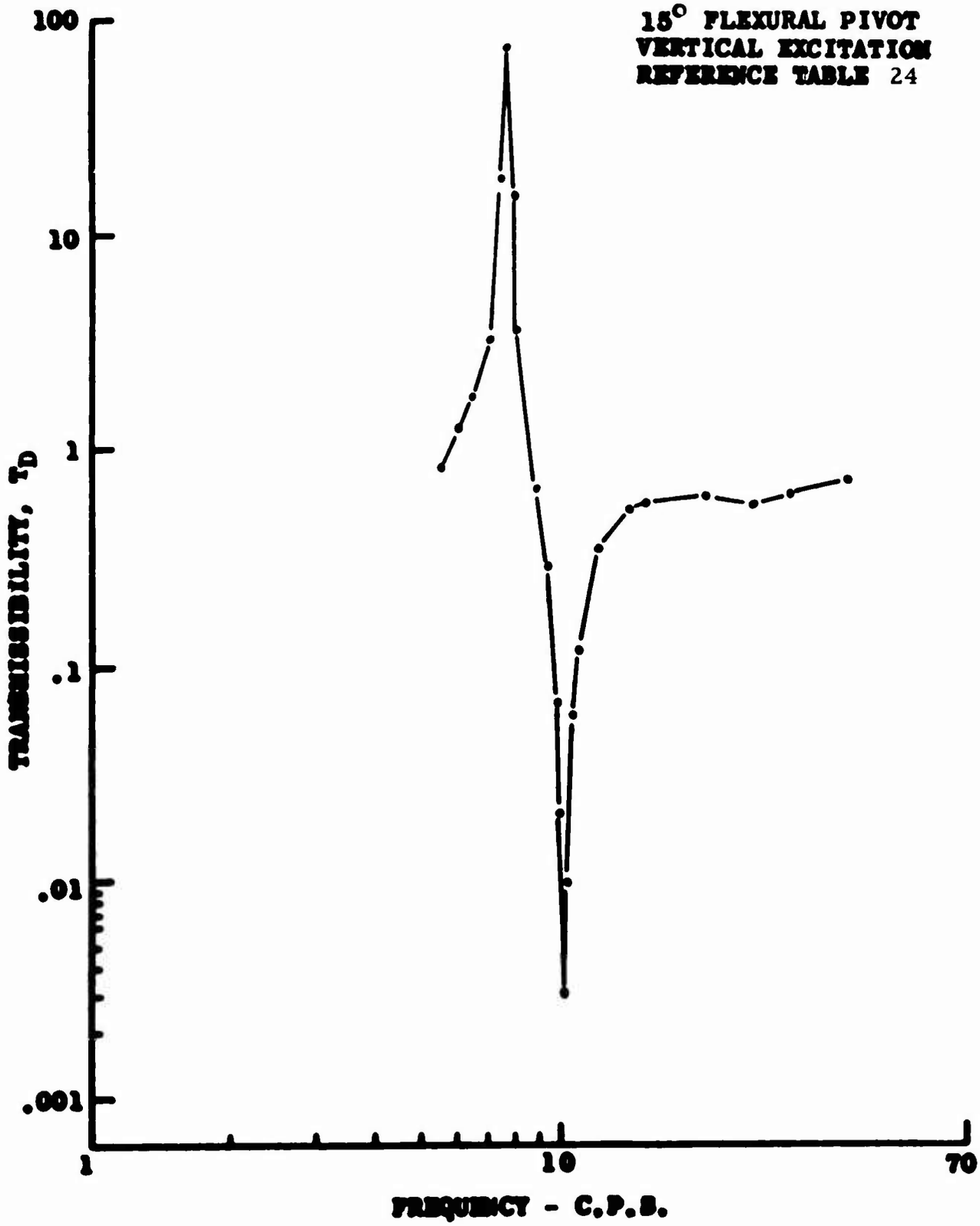

Figure 41. Response Curve for Two-Dimensional DAVI

TABLE 25

TWO-DIMENSIONAL DAVI TRANSMISSIBILITY TEST DATA
15° FLEXURAL PIVOT
VERTICAL EXCITATION

Frequency (c.p.s.)	Output	Input	Output / Input
5.5	1.93	1.86	1.04
6.0	2.28	1.88	1.21
6.5	2.60	1.77	1.47
7.0	1.78	1.02	1.74
7.2	1.90	1.01	1.88
7.5	2.28	.98	2.33
8.0	2.78	.73	3.81
8.4	2.85	.45	6.33
8.6	2.90	.40	7.25
9.0	2.05	.86	2.38
9.5	1.14	1.12	1.02
10.0	.66	1.14	.58
10.5	.36	1.10	.32
11.0	.17	1.05	.16
11.3	.10	1.01	.09
11.5	.04	.98	.04
11.6	.01	.96	.01
12.0	.09	.92	.09
13.0	.17	.80	.21
14.0	.21	.70	.29
15.0	.21	.63	.33
20.0	.16	.34	.46
25.0	.10	.20	.50
30.0	.07	.14	.55
40.0	.04	.07	.56

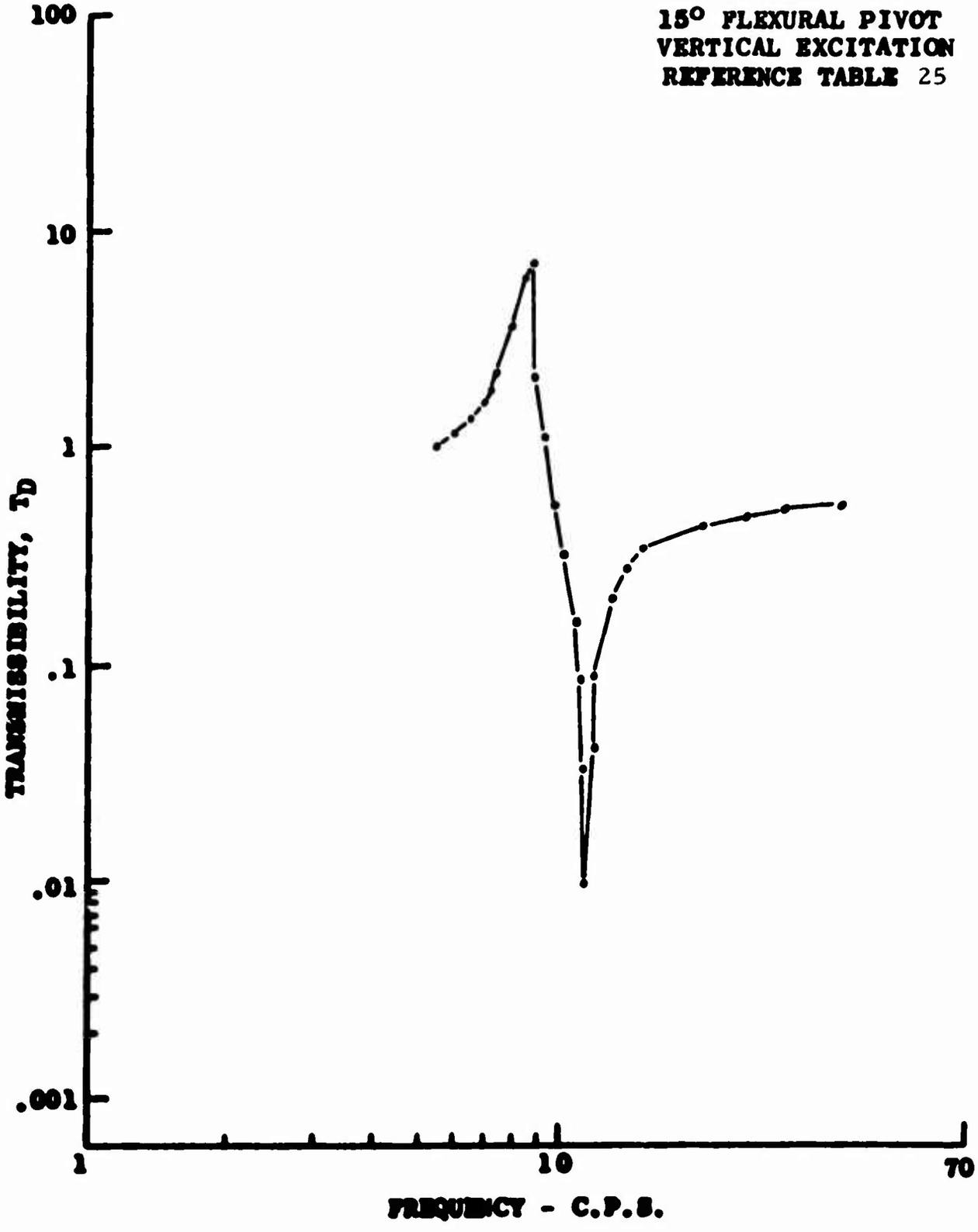

Figure 42. Response Curve for Two-Dimensional DAVI

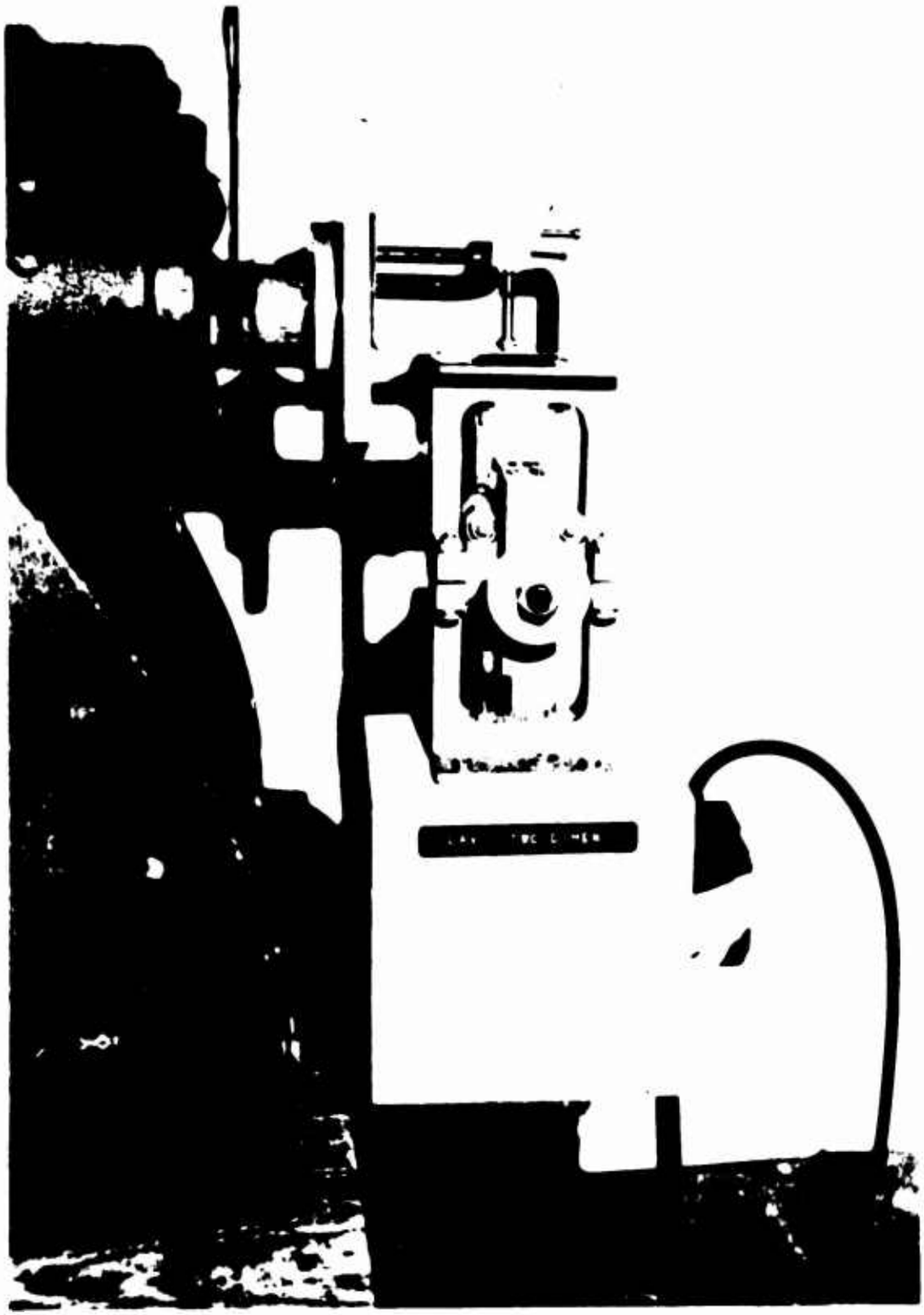

Figure 43. Two-Dimensional DAVI Model Mounted for Lateral Excitation

TABLE 26

TWO-DIMENSIONAL DAVI TRANSMISSIBILITY TEST DATA
15° FLEXURAL PIVOT
LATERAL EXCITATION

Frequency (c.p.s.)	Output	Input	Output / Input
5.5	.67	.86	.78
6.0	.90	.86	1.05
6.5	1.15	.78	1.47
6.8	1.00	.58	1.72
6.9	.95	.50	1.90
7.0	.96	.43	2.23
7.2	1.22	.40	3.05
7.5	1.65	.32	5.16
7.7	1.87	.21	9.00
7.8	1.96	.13	15.08
7.9	2.00	.06	33.33
8.0	1.95	.06	32.50
8.1	1.90	.21	9.13
8.5	1.42	.44	3.26
9.0	.88	.54	1.63
9.5	.52	.55	.95
10.0	.31	.52	.59
10.2	.24	.50	.48
10.4	.18	.48	.38
10.6	.13	.47	.28
10.8	.09	.46	.20
11.0	.06	.44	.13
11.4	.003	.42	.008
11.5	.002	.41	.005
11.6	.009	.40	.02
11.8	.03	.39	.09
12.0	.05	.38	.14
13.0	.12	.32	.38
14.0	.15	.26	.55
15.0	.16	.22	.71
20.0	.22	.06	3.96
25.0	.08	.06	1.32
30.0	.04	.05	.69
40.0	.02	.03	.49

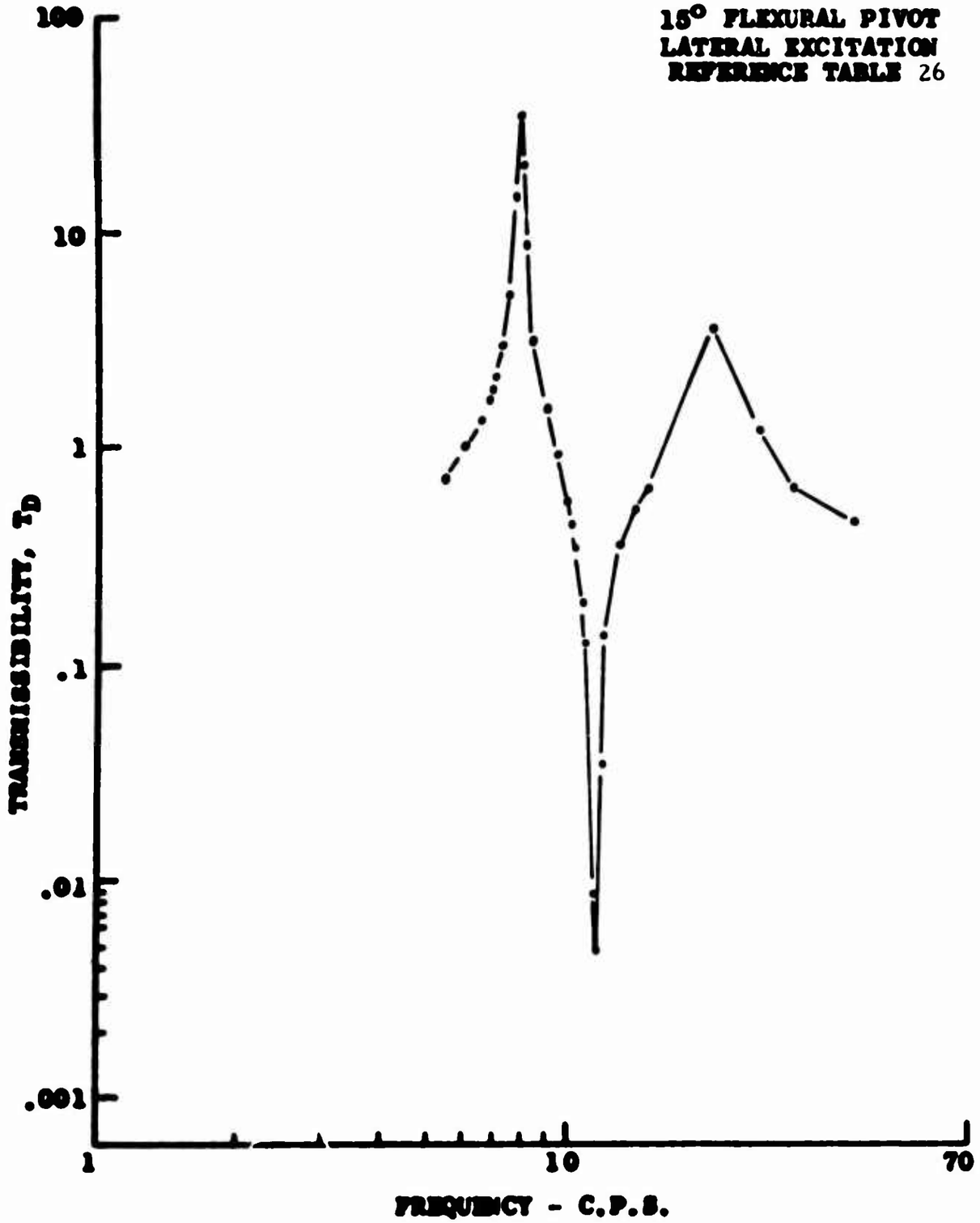

Figure 44. Response Curve for Two-Dimensional DAVI

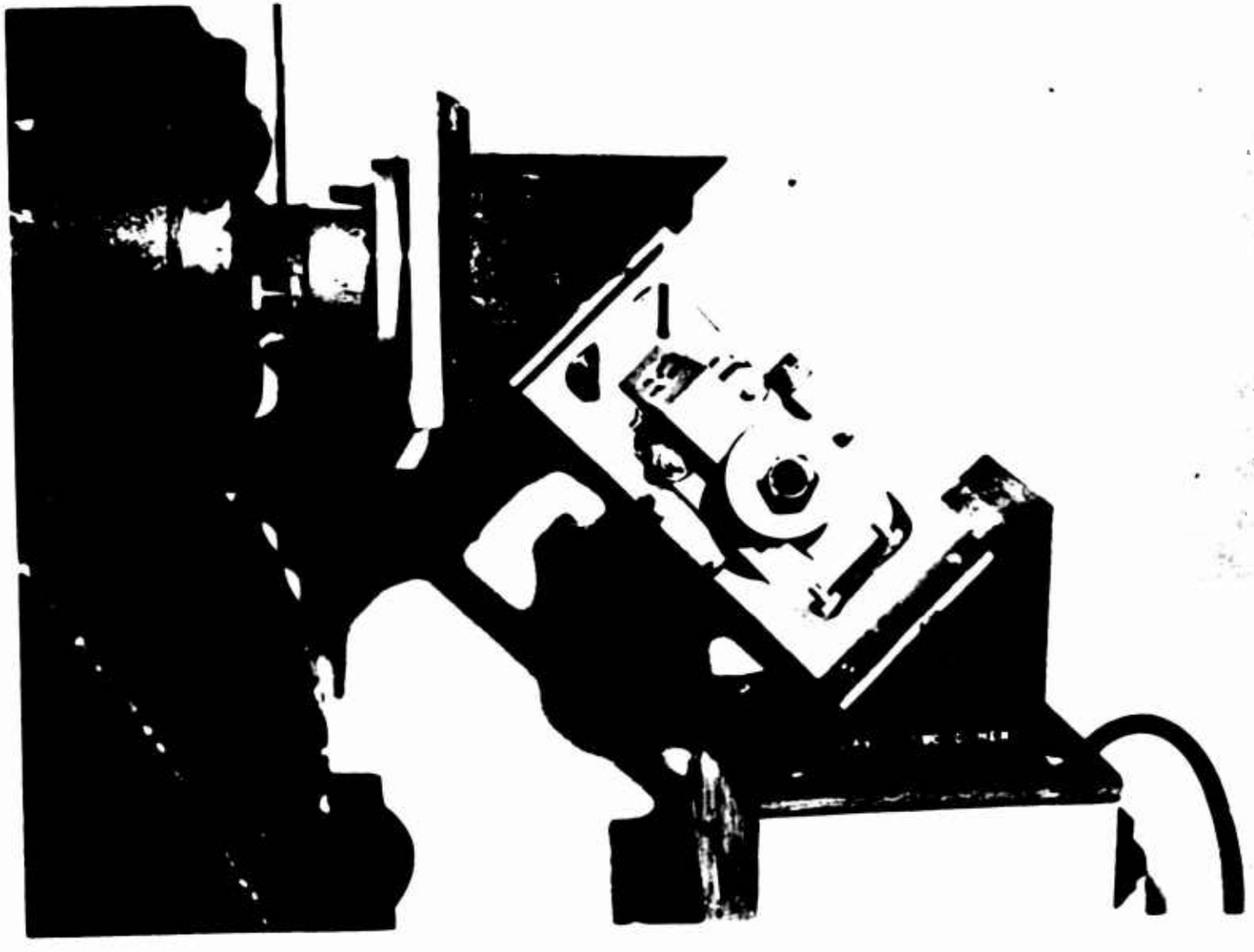

Figure 45. Two-Dimensional DAVI Model Mounted for Oblique Excitation

Figure 46. Two-Dimensional DAVI Model Mounted Showing Isolation in the Oblique Direction

TABLE 27

TWO-DIMENSIONAL DAVI TRANSMISSIBILITY TEST DATA
15° FLEXURAL PIVOT
OBLIQUE EXCITATION

Frequency (c.p.s.)	Output	Input	$\frac{\text{Output}}{\text{Input}}$
5.5	.64	.77	.83
6.0	.90	.75	1.20
6.5	1.23	.67	1.85
7.0	1.00	.34	2.99
7.4	1.57	.22	7.07
7.5	1.68	.15	10.98
7.6	1.77	.08	21.33
7.7	1.78	.02	80.91
7.8	1.75	.10	17.50
8.0	1.62	.25	6.40
8.5	1.05	.50	2.10
9.0	.64	.56	1.13
9.5	.37	.55	.67
10.0	.21	.52	.40
10.5	.10	.49	.20
11.0	.03	.46	.06
11.2	.006	.44	.01
11.3	.001	.43	.002
11.5	.006	.42	.01
11.7	.02	.41	.06
12.0	.04	.39	.11
13.0	.09	.34	.27
14.0	.10	.29	.36
15.0	.11	.25	.43
20.0	.09	.13	.71
25.0	.14	.05	2.93
30.0	.01	.07	.16
40.0	.02	.03	.77

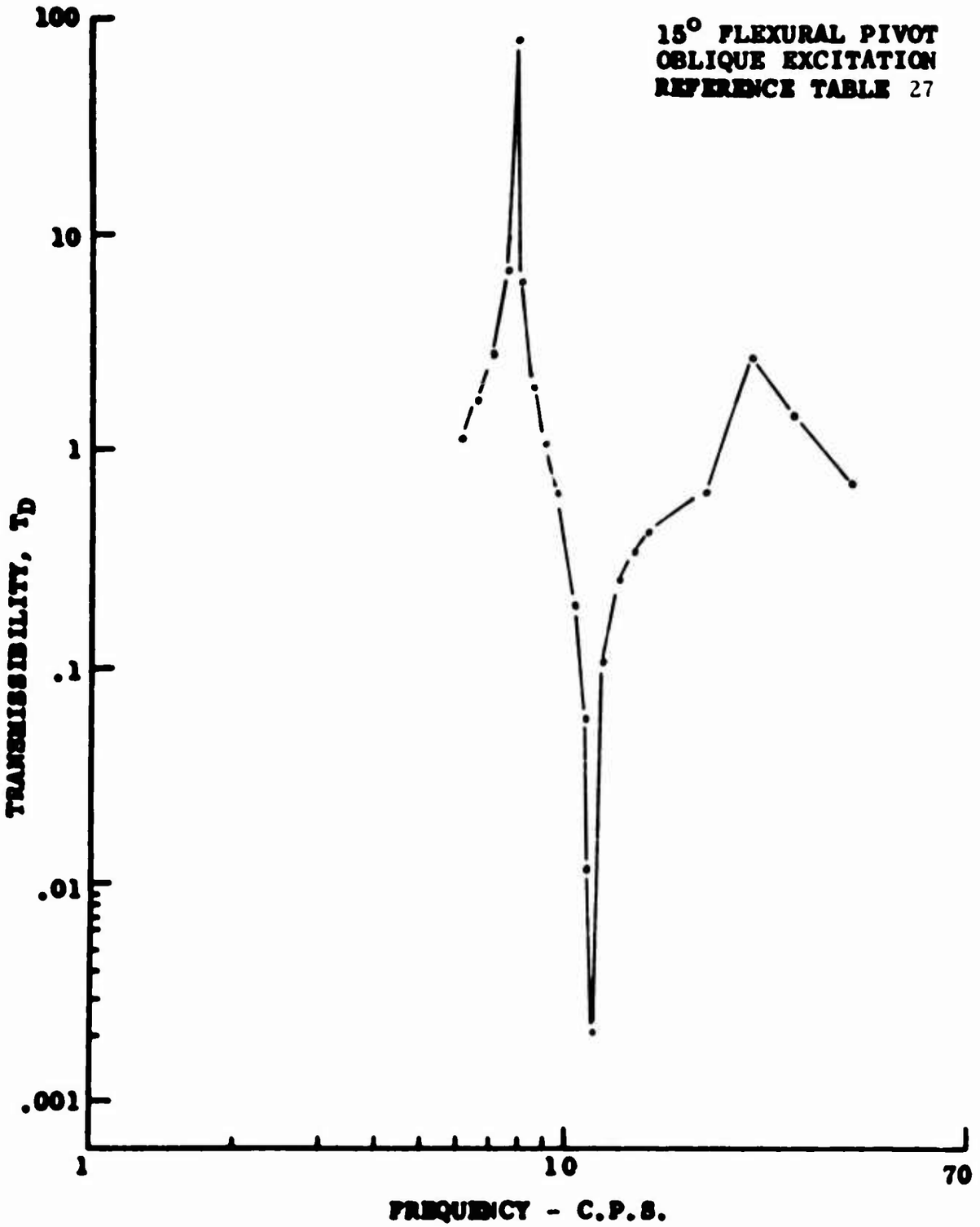

Figure 47. Response Curve for Two-Dimensional DAVI

TABLE 28

TWO-DIMENSIONAL DAVI TRANSMISSIBILITY TEST DATA
15° FLEXURAL PIVOTS
VERTICAL EXCITATION

Frequency (c.p.s.)	ISOLATED WEIGHT				
	5 LB.	10 LB.	15 LB.	20 LB.	30 LB.
5.0	1.02	1.09	1.13	1.18	1.50
6.0	1.04	1.15	1.25	1.48	2.20
7.0	1.09	1.25	1.54	2.06	4.46
8.0	1.13	1.50	2.50	3.45	1.61
8.2	-	-	-	3.80	1.72
8.4	-	-	-	7.00	1.97
8.5	1.28	2.05	4.40	-	1.61
8.6	-	-	-	5.00	1.03
8.8	-	-	-	2.54	.69
8.9	-	-	18.70	-	-
9.0	1.38	3.10	8.30	1.54	.47
9.2	-	-	-	.93	.35
9.4	-	16.10	-	.67	.21
9.5	1.65	7.68	1.21	-	-
9.6	-	-	-	.44	.14
9.8	11.03	-	-	.28	.10
10.0	-	-	.28	.15	.05
10.2	.05	-	-	.06	.02
10.4	-	-	-	.01	.02
10.5	-	.02	.02	-	.02
10.6	-	-	-	.06	.03
10.8	-	-	-	.10	.05
11.0	.60	.31	.21	.14	.06
12.0	.80	.54	.38	.24	.06
13.0	.85	.65	.49	.03	.11
14.0	.88	.71	.51	.26	.88
15.0	.89	.73	.54	.15	1.48
17.0	.88	.75	.53	1.02	.92
20.0	.93	.76	.63	.91	.85
25.0	.96	.81	1.02	.88	.80
30.0	.96	.85	.81	.82	.78
35.0	.95	.82	.78	.80	.73
40.0	.96	.87	.80	.78	.71

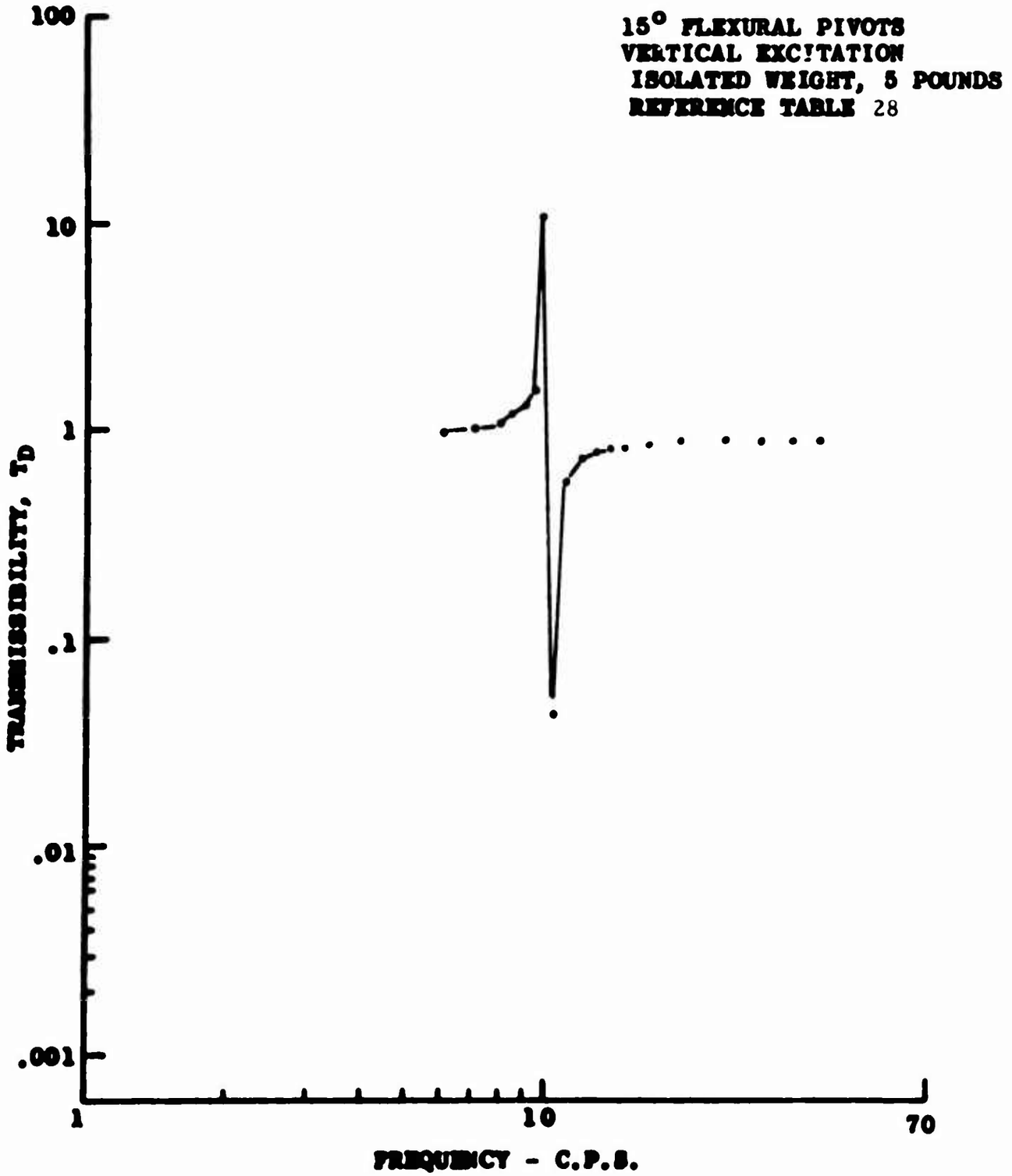

Figure 48. Response Curve for Two-Dimensional DAVI

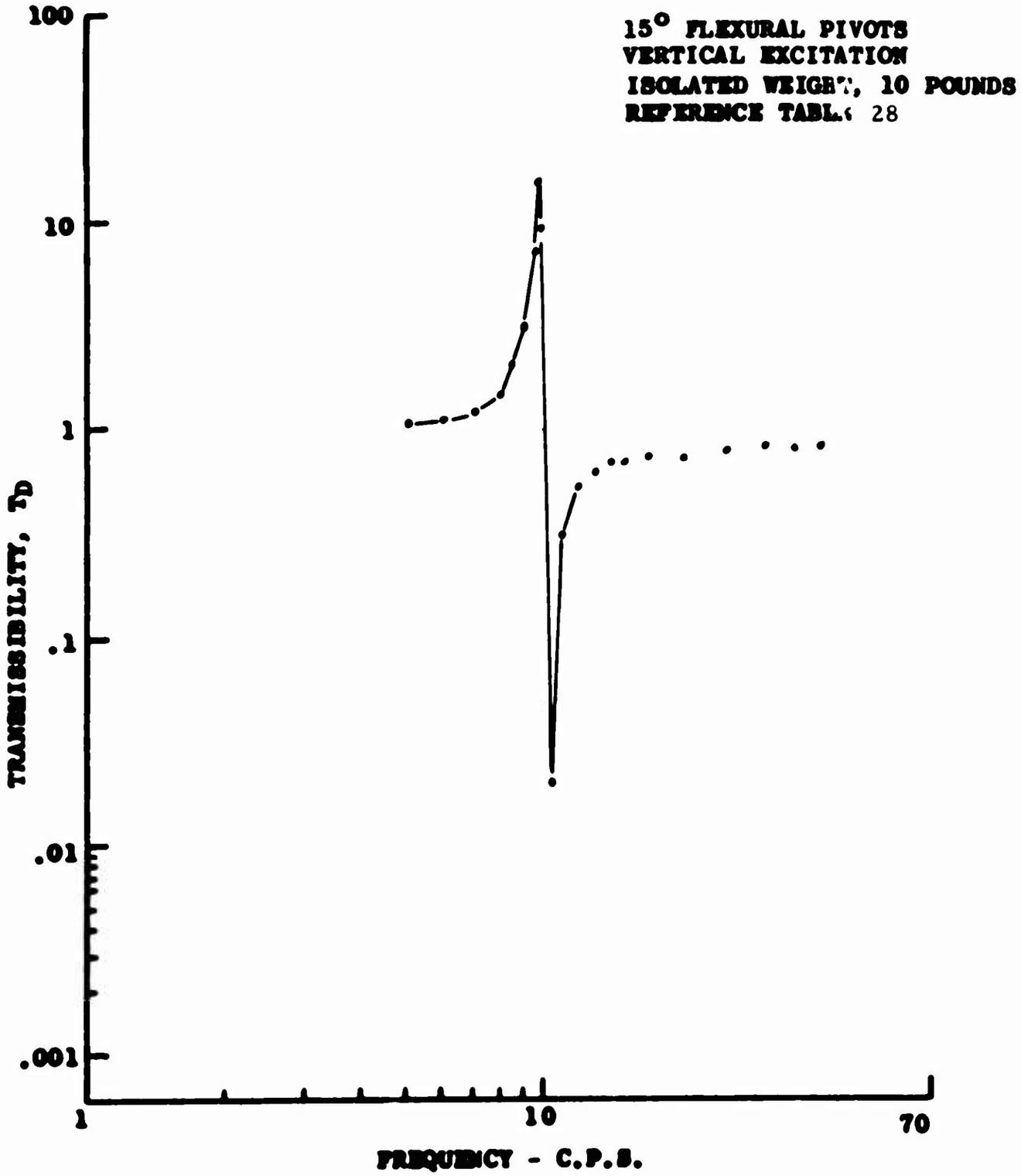

Figure 48. Response Curve for Two-Dimensional DAVI

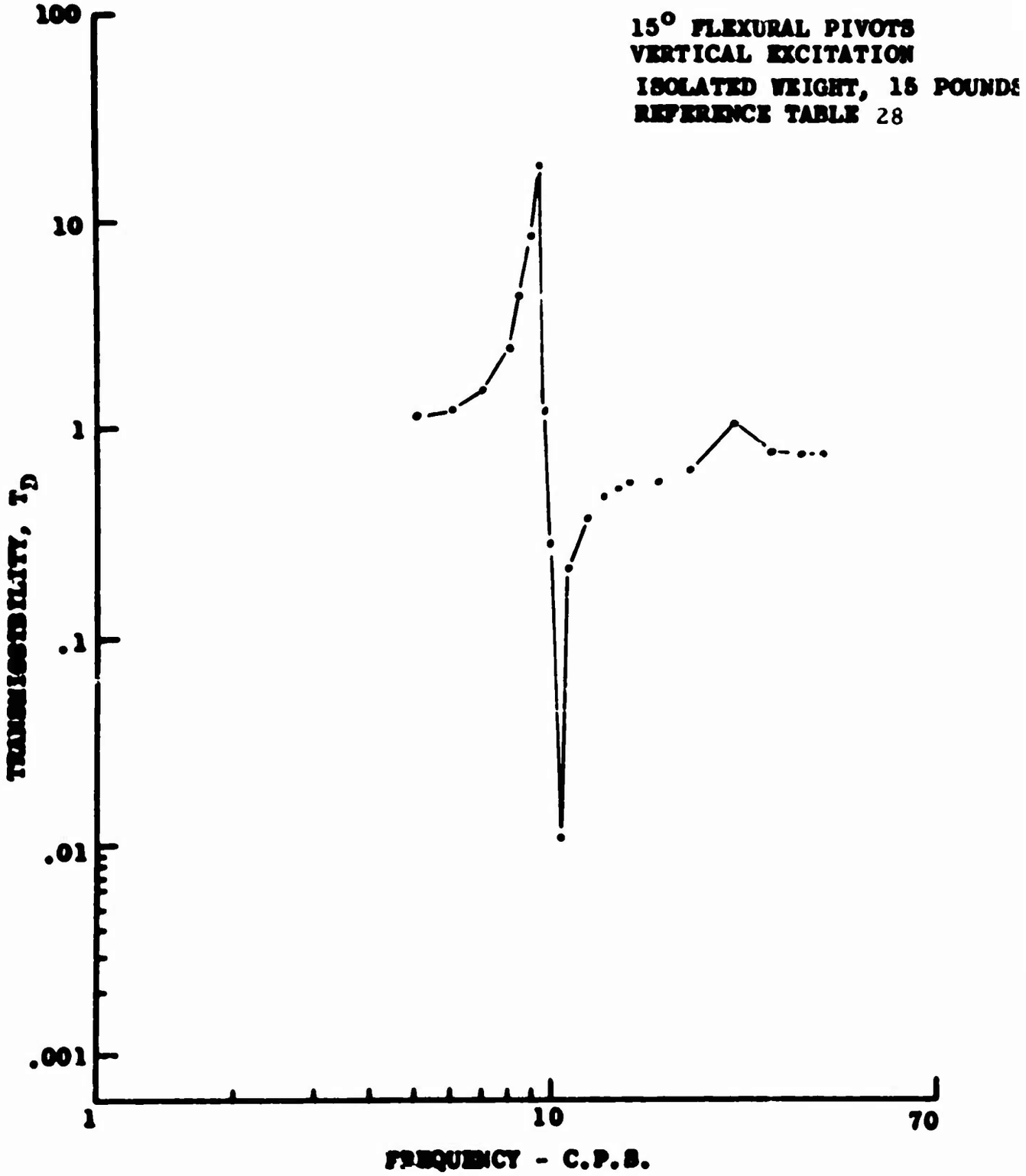

Figure 50. Response Curve for Two-Dimensional DAVI

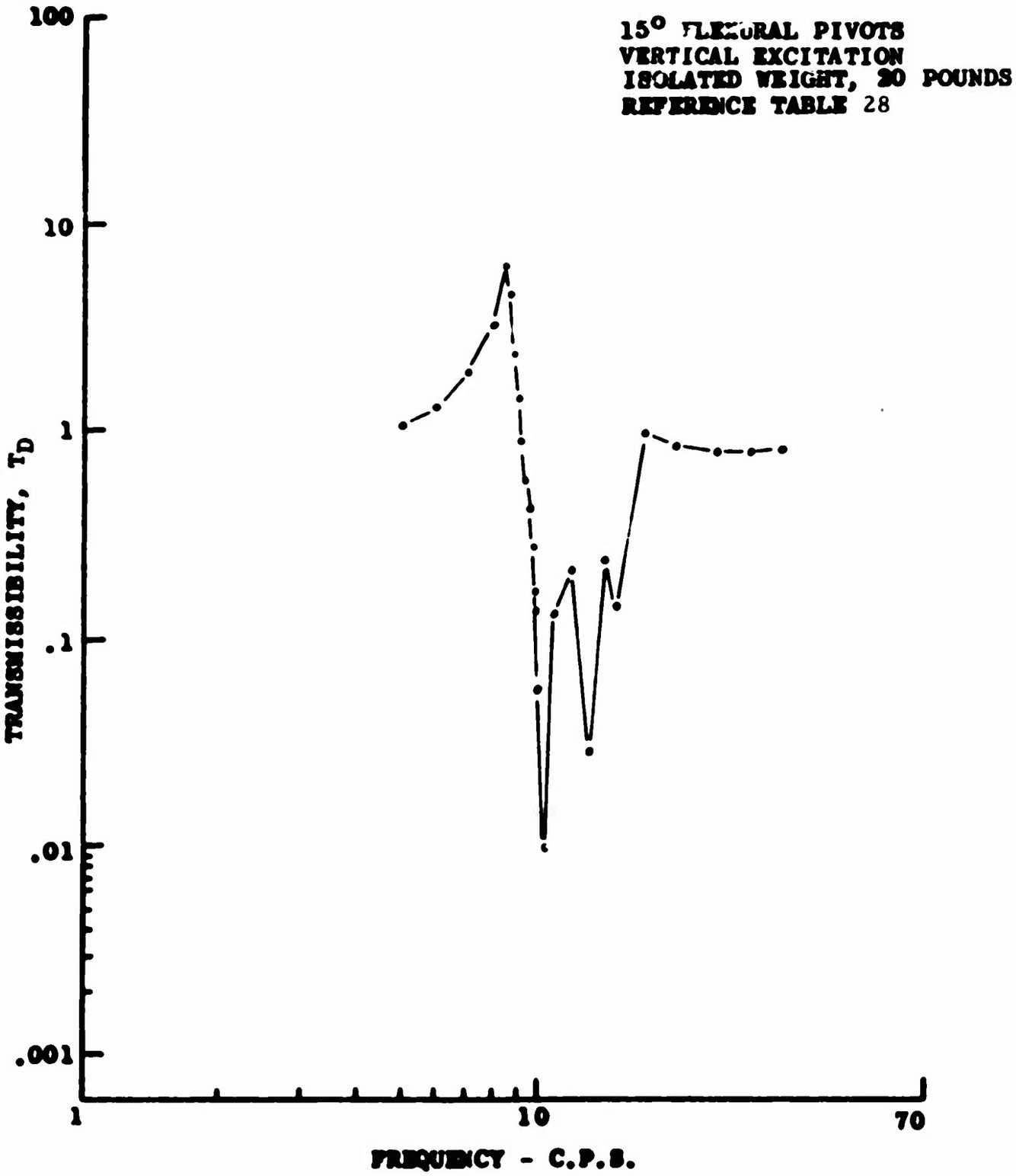

Figure 51. Response Curve for Two-Dimensional DAVI

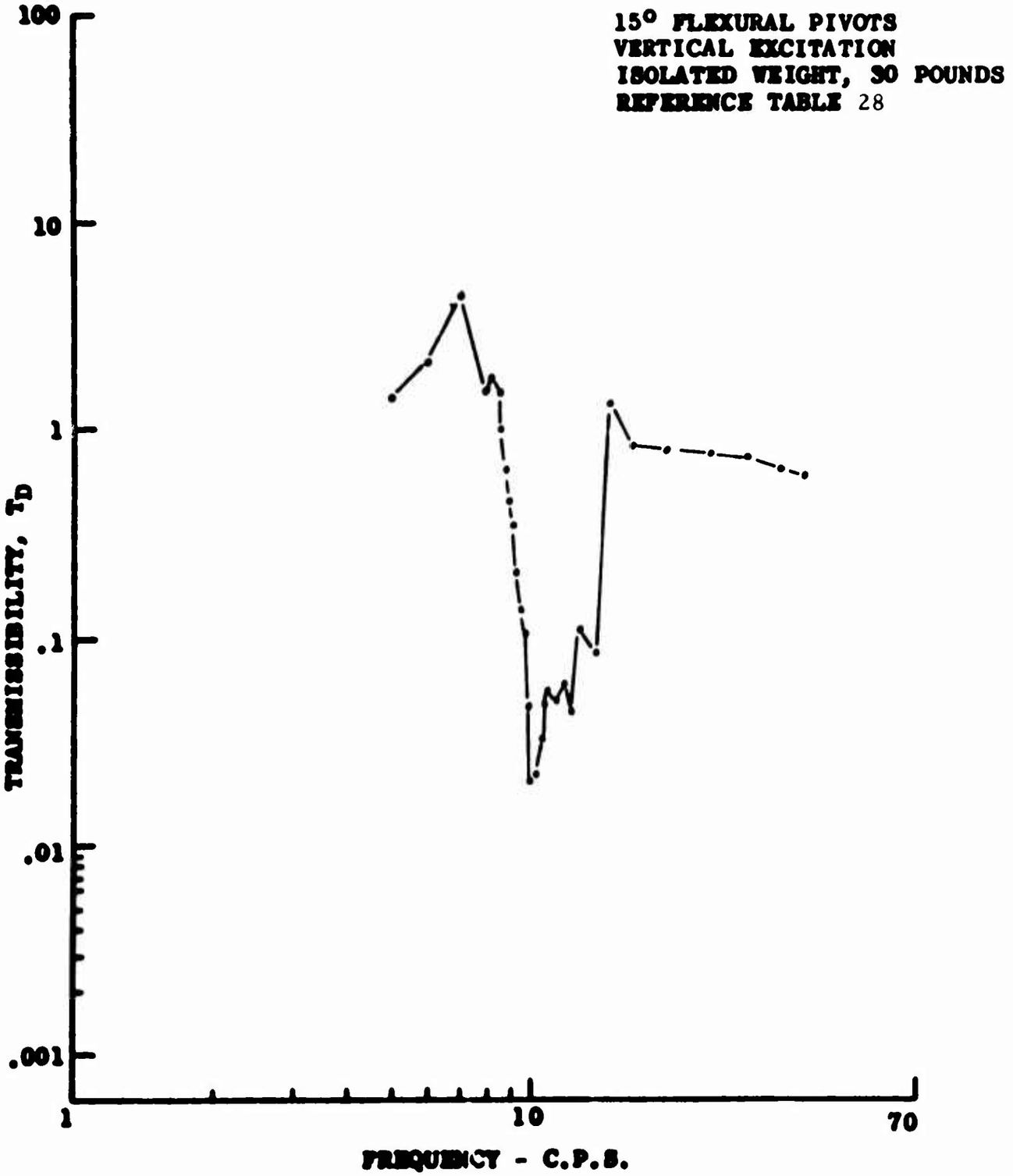

Figure 52. Response Curve for Two-Dimensional DAVI

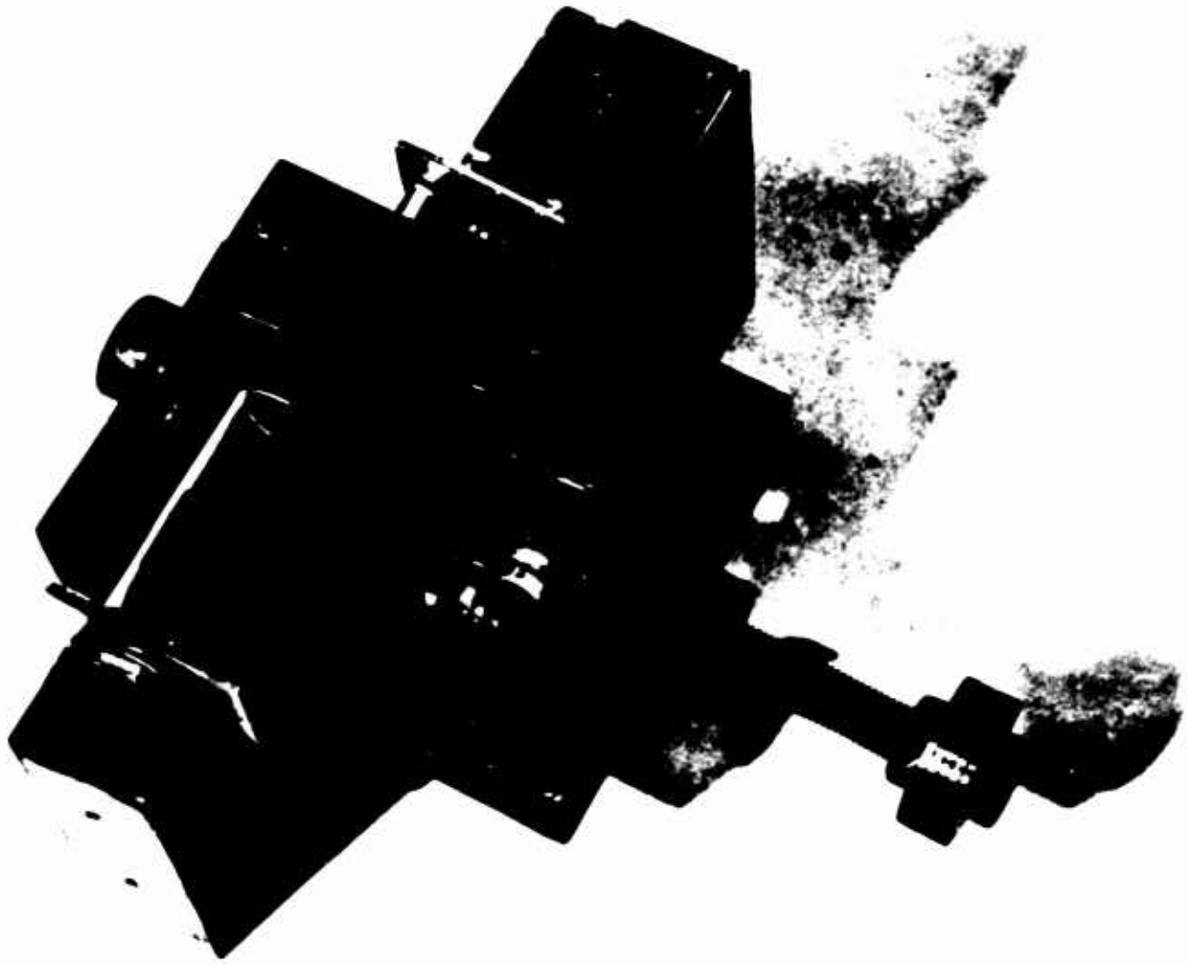

Figure 53. Two-Dimensional DAVI Model With Air Damper

TABLE 29

TWO-DIMENSIONAL DAVI TRANSMISSIBILITY TEST DATA
15° FLEXURAL PIVOTS
VERTICAL EXCITATION (AIR DAMPED)

Relative Damping Rate	Frequency (c.p.s.)	Output	Input	Output / Input
Zero	5.5	1.52	1.35	1.13
	6.0	1.80	1.33	1.35
	6.5	2.03	1.22	1.66
	7.0	1.87	.84	2.23
	7.2	2.18	.81	2.69
	7.5	2.67	.70	3.81
	7.7	2.97	.54	5.50
	8.0	3.22	.13	24.21
	8.1	3.20	.07	45.71
	8.3	2.56	.40	6.43
	8.5	2.10	.61	3.44
	9.0	1.22	.82	1.49
	9.5	.67	.87	.77
	10.0	.40	.85	.46
	10.5	.20	.81	.25
	11.0	.07	.77	.09
	11.3	.004	.74	.005
	11.5	.04	.71	.06
	12.0	.10	.67	.15
	13.0	.16	.59	.26
	14.0	.17	.51	.34
	15.0	.18	.45	.39
	17.0	.16	.35	.46
	20.0	.12	.25	.48
	22.0	.10	.21	.50
	25.0	.09	.16	.56
	30.0	.06	.10	.60
	35.0	.05	.07	.71
	40.0	.03	.06	.39
1	5.5	1.80	1.55	1.16
	6.0	2.06	1.52	1.36
	6.5	2.15	1.28	1.68
	7.0	2.12	.97	2.19
	7.5	2.90	.77	3.77

TABLE 29 (Continued)

Relative Damping Rate	Frequency (c.p.s.)	Output	Input	Output / Input
1	7.7	3.15	.57	5.53
	8.1	3.15	.17	19.10
	8.3	2.70	.42	6.43
	8.5	2.23	.63	3.57
	9.0	1.35	.90	1.50
	9.5	.80	.97	.82
	10.0	.45	.95	.47
	11.0	.09	.86	.10
	11.3	.02	.82	.02
	11.5	.04	.81	.05
	12.0	.11	.76	.14
	13.0	.17	.66	.26
	14.0	.19	.58	.33
	15.0	.20	.51	.38
	17.0	.18	.40	.45
	20.0	.13	.28	.48
	22.0	.12	.23	.50
	25.0	1.00	.18	.54
	30.0	.07	.11	.62
	35.0	.06	.07	.77
	40.0	.02	.07	.30
2	5.5	1.92	1.62	1.19
	6.0	2.20	1.58	1.39
	6.5	2.25	1.33	1.69
	7.0	2.22	1.03	2.16
	7.2	2.51	.97	2.59
	7.5	2.93	.80	3.66
	7.7	3.12	.63	4.99
	8.1	3.00	.26	11.45
	8.3	2.67	.40	6.68
	8.5	2.30	.60	3.83
	9.0	1.37	.90	1.53
	9.5	0.80	1.00	.80
	10.0	0.48	.98	.49
	10.5	0.25	.94	.26

TABLE 29 (Continued)

Relative Damping Rate	Frequency (c.p.s.)	Output	Input	Output / Input
2	11.0	.10	.89	.11
	11.4	.04	.84	.05
	11.7	.08	.80	.10
	12.0	.11	.78	.15
	13.0	.18	.67	.26
	14.0	.20	.61	.33
	15.0	.20	.54	.38
	17.0	.19	.42	.45
	20.0	.14	.30	.46
	22.0	.12	.24	.50
	25.0	.10	.18	.54
	30.0	.07	.12	.62
	35.0	.06	.08	.78
	40.0	.02	.08	.32
3	5.5	1.83	1.58	1.16
	6.0	2.07	1.55	1.34
	6.5	2.14	1.35	1.59
	7.0	1.96	1.02	1.92
	7.2	2.14	.97	2.21
	7.5	2.38	.86	2.77
	7.7	2.50	.74	3.38
	8.5	2.22	.38	5.81
	8.7	1.97	.52	3.83
	9.0	1.56	.68	2.29
	9.5	0.97	.87	1.12
	10.0	.62	.90	.69
	10.5	.38	.90	.42
	11.0	.19	.86	.22
	11.8	.07	.80	.09
	12.0	.08	.78	.11
	13.0	.15	.68	.15
	14.0	.18	.61	.30
	15.0	.19	.53	.36
	17.0	.18	.41	.44

TABLE 29 (Continued)

Relative Damping Rate	Frequency (c.p.s.)	Output	Input	Output / Input
3	20.0	.14	.28	.49
	22.0	.12	.24	.50
	25.0	.10	.18	.54
	30.0	.07	.12	.61
	35.0	.06	.07	.77
	40.0	.02	.07	.30
4	5.5	1.92	1.69	1.14
	6.0	2.13	1.63	1.31
	6.5	2.13	1.45	1.47
	7.0	2.00	1.13	1.76
	7.2	2.18	1.11	1.96
	7.5	2.45	1.03	2.38
	7.7	2.65	.93	2.86
	8.0	2.95	.71	4.16
	8.6	2.90	.21	14.15
	9.0	2.21	.59	3.78
	9.5	1.43	.90	1.59
	10.0	.86	.99	.87
	10.5	.50	.98	.51
	11.0	.29	.94	.31
	11.5	.12	.88	.13
	12.0	.03	.84	.04
	13.0	.13	.73	.18
	14.0	.18	.65	.28
	15.0	.19	.56	.33
	17.0	.18	.43	.44
	20.0	.15	.30	.49
	22.0	.13	.25	.49
	25.0	.10	.19	.54
	30.0	.08	.12	.62
	35.0	.06	.08	.77
	40.0	.02	.08	.31

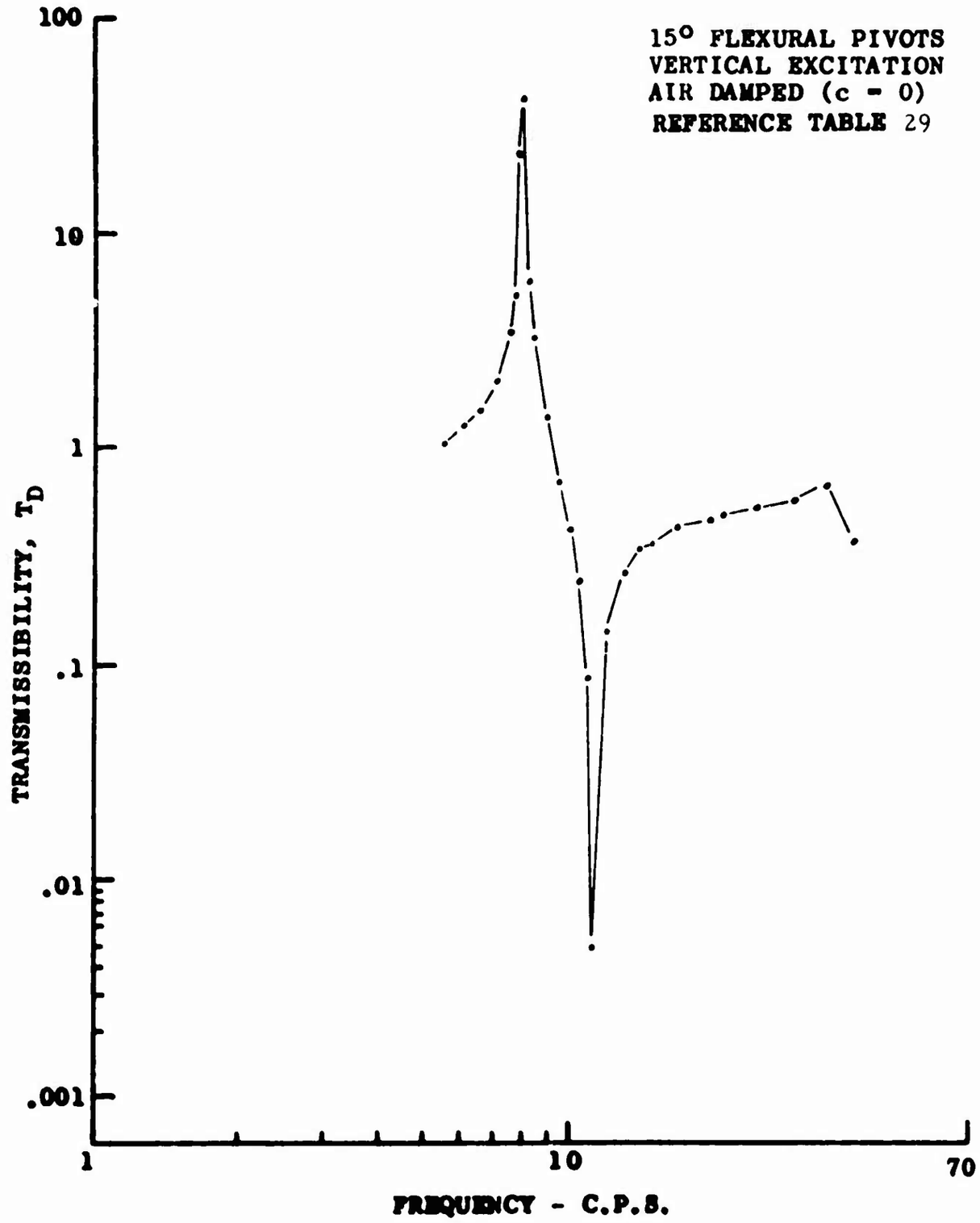

Figure 54. Response Curve for Two-Dimensional DAVI

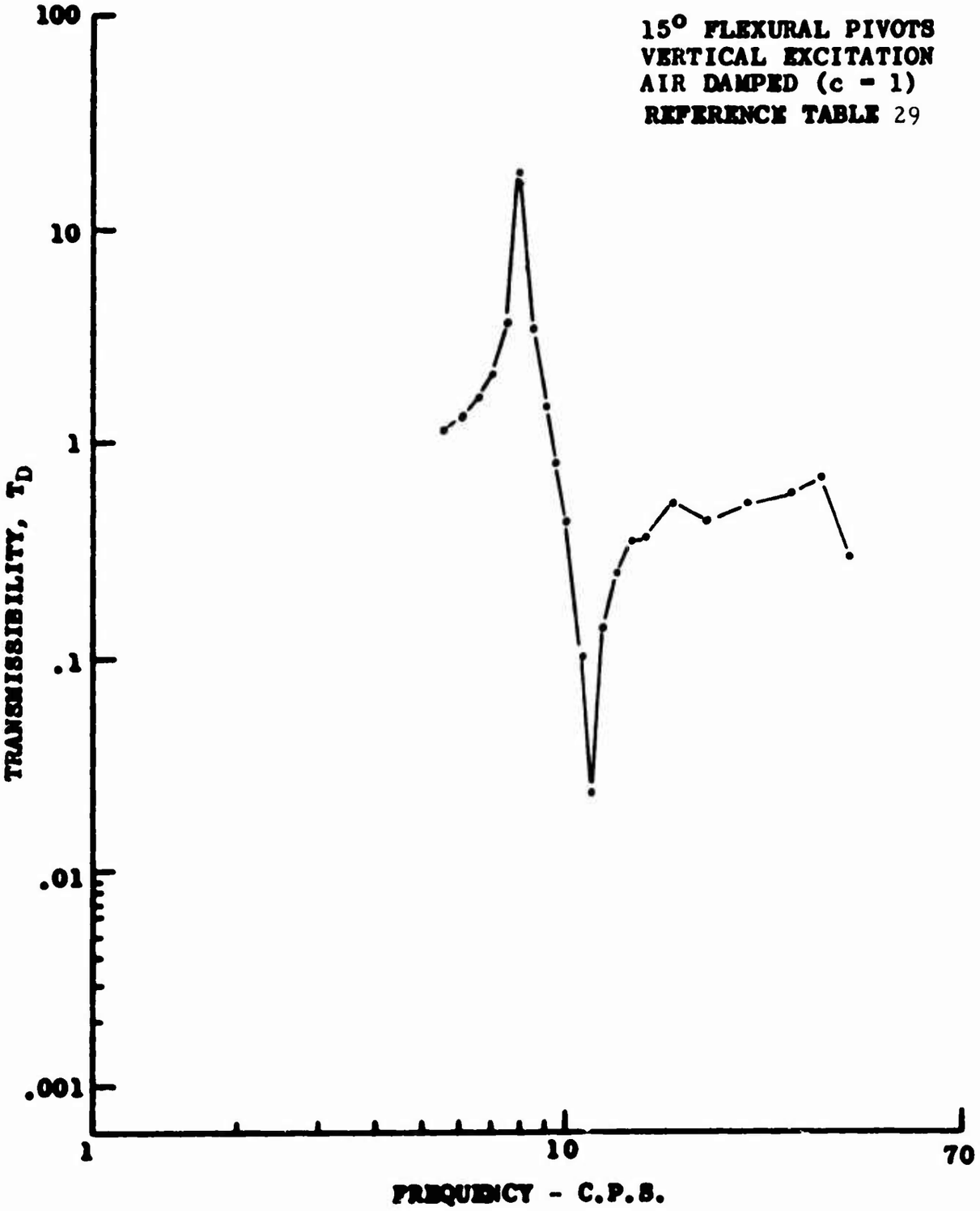

Figure 55. Response Curve for Two-Dimensional DAVI

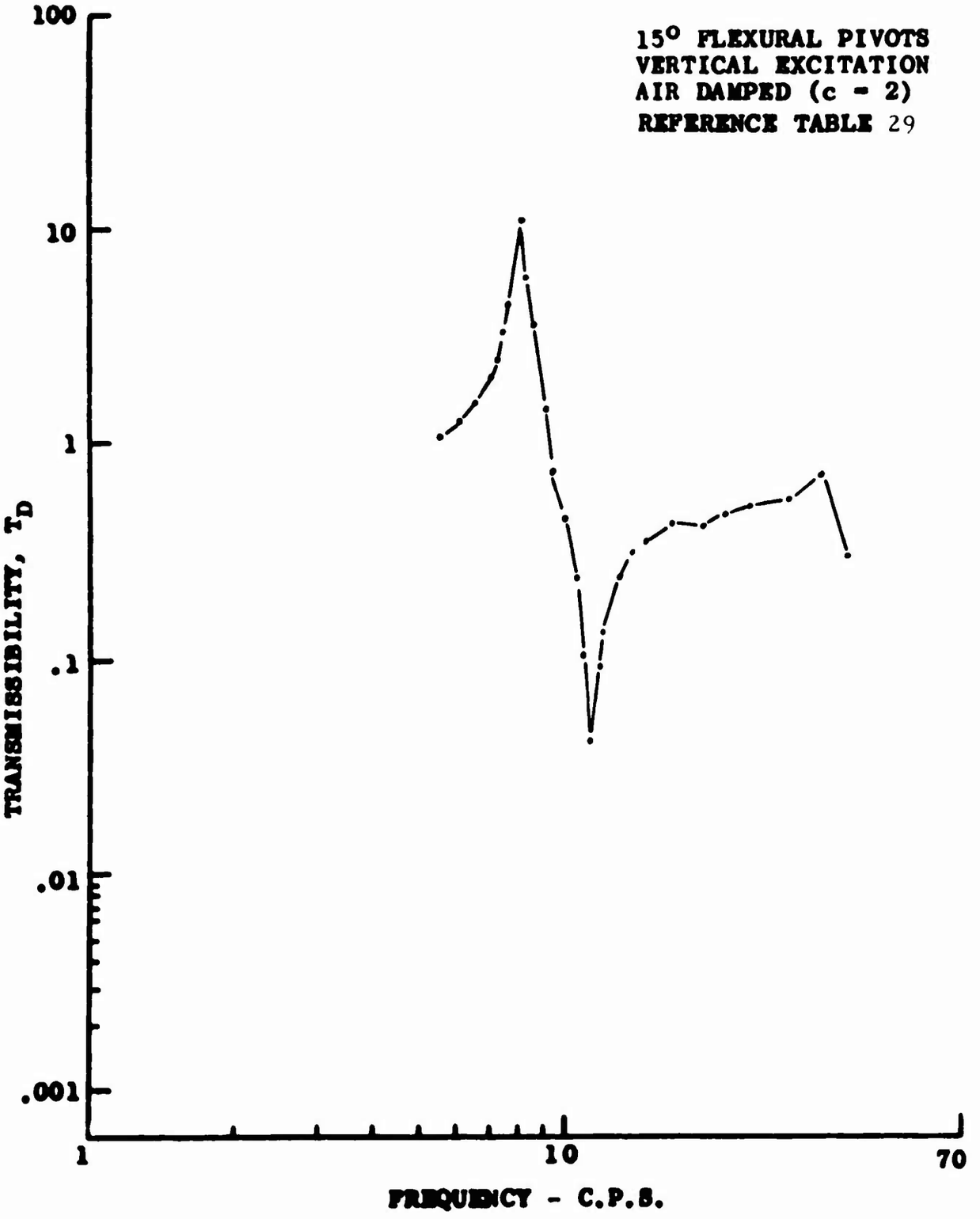

Figure 56. Response Curve for Two-Dimensional DAVI

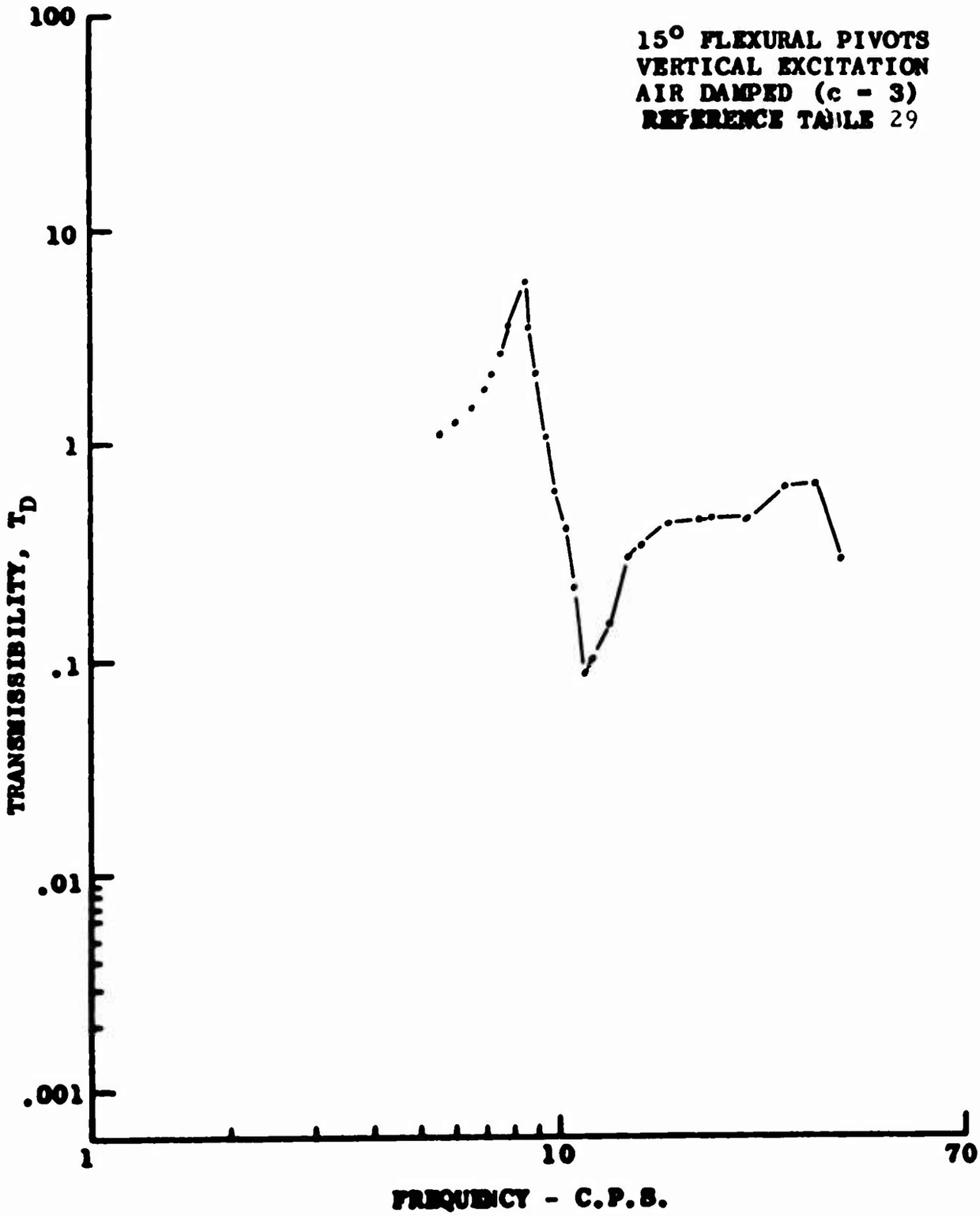

Figure 57. Response Curve for Two-Dimensional DAVI

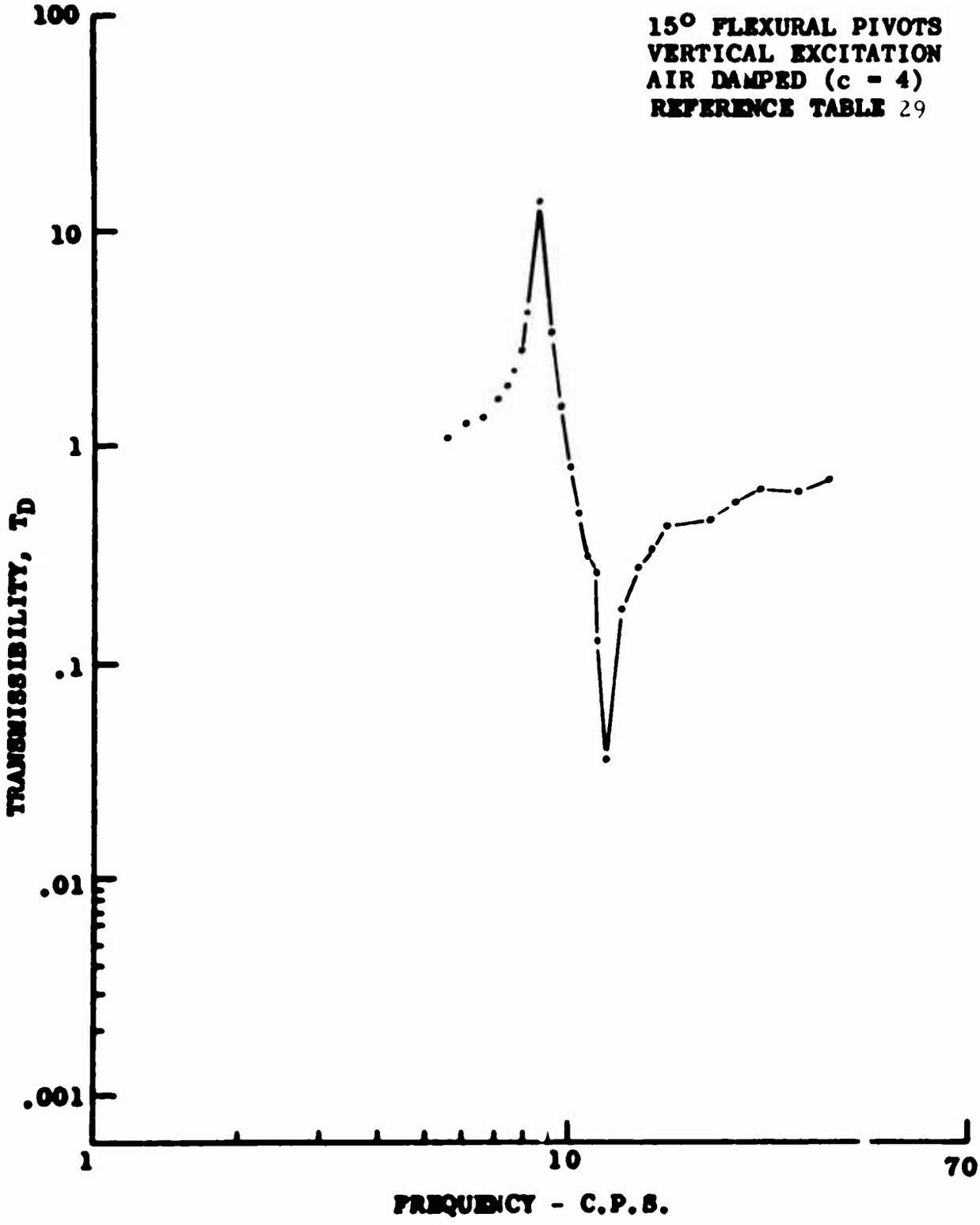

Figure 58. Response Curve for Two-Dimensional DAVI

TABLE 30

TWO-DIMENSIONAL DAVI TRANSMISSIBILITY TEST DATA
15° FLEXURAL PIVOTS
VERTICAL EXCITATION (LIQUID DAMPED)

Relative Damping Rate	Frequency (c.p.s.)	Input	Output	Output / Input
Zero	5.0	87.00	125.00	1.44
	5.5	86.00	140.00	1.63
	6.0	76.00	146.00	1.92
	6.2	64.00	159.00	2.48
	6.4	54.00	161.00	2.99
	6.6	43.00	161.00	3.75
	6.8	29.00	159.00	5.49
	7.0	15.80	146.00	9.25
	7.1	11.00	140.00	12.70
	7.2	12.40	138.00	11.10
	7.4	19.50	127.00	6.52
	7.6	29.00	113.00	3.89
	7.8	38.00	99.00	2.61
	8.0	44.60	84.00	1.88
	8.5	57.00	53.00	.93
	9.0	60.00	36.50	.61
	9.5	65.00	22.50	.35
	10.0	65.00	12.30	.19
	10.2	65.00	10.00	.15
	10.4	65.00	6.90	.11
	10.6	64.00	4.75	.07
	10.8	64.00	2.70	.04
	11.0	53.00	1.00	.02
	11.2	52.00	.40	.01
	11.4	51.00	1.55	.03
	11.6	51.00	2.60	.05
	11.8	53.00	3.70	.07
	12.0	51.00	4.60	.09
	14.0	44.00	8.20	.19
	16.0	39.00	9.60	.25
	20.0	27.80	9.20	.33
	30.0	12.80	4.90	.38
	40.0	6.10	4.45	.73

TABLE 30 (Continued)

Relative Damping Rate	Frequency (c.p.s.)	Input	Output	Output / Input
1	5.0	103.00	121.00	1.18
	5.2	103.00	123.00	1.29
	5.4	102.00	126.00	1.23
	5.6	101.00	127.00	1.26
	5.8	99.00	128.00	1.30
	6.0	96.00	129.00	1.35
	6.2	93.00	129.00	1.38
	6.4	89.00	129.00	1.45
	6.6	84.00	128.00	1.52
	6.8	79.00	128.00	1.62
	7.0	78.00	128.00	1.64
	7.2	71.00	126.00	1.78
	7.4	65.00	125.00	1.93
	7.6	57.00	123.00	2.16
	7.8	51.00	120.00	2.36
	8.0	44.00	117.00	2.66
	8.2	37.00	113.00	3.06
	8.4	30.00	109.00	3.64
	8.6	24.00	105.00	4.38
	8.8	20.00	100.00	5.00
	9.0	18.00	95.00	5.28
	9.5	25.00	81.00	3.24
	10.0	38.00	64.00	1.69
	10.2	41.00	60.00	1.46
	10.4	46.00	53.00	1.15
	10.6	49.00	49.00	1.00
	10.8	51.00	44.00	.86
	11.0	54.00	39.00	.72
	11.2	56.00	35.00	.63
	11.4	56.00	31.00	.55
	11.6	58.00	27.00	.47
	11.8	59.00	24.00	.41
	12.0	59.00	21.00	.36
	12.5	59.00	15.00	.25
	13.0	59.00	10.00	.17
	13.5	57.00	6.00	.11
	14.0	58.00	5.00	.09
	14.5	56.00	4.40	.08
	15.5	52.00	4.65	.09

TABLE 30 (Continued)

Relative Damping Rate	Frequency (c.p.s.)	Input	Output	Output / Input
1	16.0	50.00	5.10	.10
	16.5	46.00	5.00	.11
	17.0	36.00	4.90	.14
	20.0	32.00	6.70	.21
2	7.0	60.00	101.00	1.68
	7.5	48.00	96.00	2.29
	8.0	33.00	89.00	2.79
	8.2	30.00	87.00	2.90
	8.4	24.00	84.00	3.50
	8.6	20.00	81.00	4.05
	8.8	17.00	77.00	4.53
	9.0	15.00	72.00	4.80
	9.5	19.00	62.00	3.26
	10.0	28.00	50.00	1.79
	10.2	32.00	48.00	1.50
	10.4	36.00	44.00	1.22
	10.6	38.00	40.00	1.05
	10.8	41.00	37.00	.90
	11.0	43.00	33.00	.77
	11.2	44.00	30.00	.68
	11.4	45.00	27.00	.60
	11.6	46.00	24.00	.52
	11.8	47.00	21.00	.45
	12.0	48.00	18.00	.38
	12.5	48.00	13.00	.27
	13.0	48.00	9.00	.19
	13.5	47.00	6.00	.13
	14.0	46.00	4.50	.10
	14.5	45.00	3.70	.08
	15.0	43.00	3.60	.08
	15.5	42.00	3.60	.09
	16.0	40.00	4.00	.10
	16.5	39.00	4.40	.11
	17.0	32.00	4.30	.13
	20.0	27.00	5.00	.19

TABLE 30 (Continued)

Relative Damping Rate	Frequency (c.p.s.)	Input	Output	Output / Input
3	5.0	104.00	143.00	1.38
	5.5	94.00	167.00	1.77
	6.0	67.00	171.00	2.55
	6.5	37.00	160.00	4.33
	6.8	20.00	147.00	7.35
	6.9	17.00	144.00	8.47
	7.0	18.00	139.00	7.71
	7.2	26.50	125.00	4.73
	7.5	41.00	103.00	2.51
	8.0	58.00	62.00	1.07
	8.5	69.00	48.00	.70
	9.0	72.00	32.00	.44
	9.5	76.00	20.00	.26
	10.0	76.00	11.80	.16
	10.2	75.00	8.60	.12
	10.4	74.00	7.30	.10
	10.6	74.00	5.40	.07
	10.8	74.00	4.90	.07
	11.0	72.00	4.65	.06
	11.2	71.00	4.80	.07
	11.4	70.00	5.10	.07
	11.6	69.00	5.80	.08
	11.8	68.00	6.50	.09
	12.0	66.00	7.10	.11
	14.0	54.00	11.00	.20
	16.0	44.00	11.60	.26
	18.0	31.00	9.70	.31
	20.0	31.00	8.00	.25
	25.0	20.00	7.10	.36
	30.0	14.50	4.40	.30
	40.0	7.60	3.50	.46

TABLE 30 (Continued)

Relative Damping Rate	Frequency (c.p.s.)	Input	Output	Output / Input
4	5.0	41.00	64.00	1.56
	5.5	39.00	73.00	1.87
	6.0	28.50	75.00	2.63
	6.5	15.00	69.00	4.61
	6.9	8.10	58.00	7.16
	7.0	9.30	55.00	5.91
	7.2	12.00	49.00	4.08
	7.5	16.20	42.50	2.62
	8.0	24.00	30.00	1.25
	8.5	27.00	21.00	.78
	9.0	29.00	14.30	.49
	9.5	31.00	9.30	.30
	10.0	31.00	5.50	.18
	10.2	31.00	5.00	.16
	10.4	31.00	4.10	.13
	10.6	30.00	3.50	.12
	10.8	30.00	3.20	.11
	11.1	29.00	2.80	.10
	11.2	29.50	2.75	.09
	11.4	29.00	2.71	.09
	11.6	28.80	2.80	.10
	11.8	28.00	3.20	.11
	12.0	27.00	3.40	.13
	14.0	23.00	4.50	.20
	16.0	18.50	4.70	.25
	18.0	13.10	3.80	.29
	20.0	12.20	3.50	.29
	25.0	8.80	3.00	.34
	30.0	5.80	1.70	.29
	40.0	3.10	1.35	.44
5	5.0	39.00	50.00	1.13
	5.5	35.00	60.00	1.71
	6.0	26.00	58.00	2.23
	6.5	17.00	51.00	3.00

TABLE 30 (Continued)

Relative Damping Rate	Frequency (c.p.s.)	Input	Output	Output / Input
5	7.0	13.60	44.00	3.23
	7.2	13.50	41.00	3.03
	7.5	15.00	34.00	2.26
	8.0	19.00	24.50	1.36
	8.5	23.00	17.50	.76
	9.0	24.00	13.50	.56
	9.5	26.00	9.70	.37
	10.0	26.00	6.60	.25
	10.2	26.00	5.80	.23
	10.4	26.00	5.00	.19
	10.6	26.00	4.80	.19
	10.8	25.70	4.55	.18
	11.0	25.30	4.22	.17
	11.6	24.30	3.80	.16
	11.7	24.10	3.80	.16
	12.0	23.80	3.75	.16
	12.5	22.80	3.82	.17
	13.0	21.80	4.00	.18
	14.0	19.80	4.23	.21
	16.0	15.30	4.30	.28
	18.0	11.50	3.38	.29
	20.0	11.00	2.95	.27
	25.0	7.70	2.62	.34
	30.0	5.10	1.53	.30
	40.0	2.80	1.20	.43
6	5.0	91.00	92.00	1.00
	5.5	90.00	94.00	1.02
	6.0	86.00	92.00	1.07
	6.5	81.00	89.00	1.10
	7.0	74.00	84.00	1.14
	7.2	71.00	82.00	1.16
	7.4	66.00	80.00	1.21
	7.6	64.00	78.00	1.22

TABLE 30 (Continued)

Relative Damping Rate	Frequency (c.p.s.)	Input	Output	Output / Input
6	7.8	60.00	76.00	1.27
	8.0	57.00	74.00	1.30
	8.2	54.00	71.00	1.31
	8.4	51.00	70.00	1.40
	8.6	48.50	70.00	1.44
	8.8	47.00	67.50	1.44
	9.0	44.00	65.00	1.48
	9.2	41.00	64.00	1.56
	9.4	38.40	62.00	1.61
	9.6	35.20	60.00	1.70
	9.8	32.00	58.00	1.81
	10.0	29.80	56.00	1.88
	10.5	22.50	52.00	2.31
	11.0	19.10	49.50	2.59
	11.5	20.50	44.30	2.16
	12.0	26.80	38.00	1.42
	12.5	32.00	32.00	1.00
	13.0	38.00	25.80	.68
	14.0	44.00	14.80	.34
	15.0	45.20	8.10	.18
	16.0	43.20	4.85	.11
	16.5	42.00	4.40	.10
	17.0	38.00	4.60	.12
	17.5	29.00	3.45	.12
	18.0	32.00	4.40	.14
	18.5	31.50	4.70	.15
	19.0	29.50	5.00	.17
	20.0	28.00	5.00	.18
	25.0	18.00	5.10	.28
	30.0	13.00	3.25	.25
	40.0	6.50	2.85	.44
7	5.0	83.00	108.00	1.30
	5.5	76.00	109.00	1.43
	6.0	64.00	103.00	1.61
	6.5	53.00	91.00	1.72

TABLE 30 (Continued)

Relative Damping Rate	Frequency (c.p.s.)	Input	Output	Output / Input
7	7.0	45.50	81.00	1.78
	7.5	42.20	67.00	1.60
	8.0	41.50	55.00	1.32
	8.5	42.10	46.50	1.11
	9.0	43.90	39.00	.89
	9.5	45.00	32.00	.71
	10.0	46.00	26.00	.57
	10.5	46.10	21.70	.47
	11.0	46.10	18.00	.39
	11.2	46.00	17.00	.36
	11.4	46.00	15.90	.35
	11.6	46.00	14.80	.32
	11.8	45.50	14.70	.32
	12.0	45.20	14.10	.31
	12.5	45.00	12.60	.28
	13.0	44.00	11.50	.26
	13.5	42.70	10.50	.25
	14.0	41.20	10.00	.24
	14.5	40.00	9.50	.24
	15.0	38.50	9.10	.24
	16.0	35.80	8.50	.24
	17.0	29.00	7.20	.25
	18.0	25.60	6.80	.27
	20.0	24.50	6.00	.25
	25.0	16.00	5.30	.33
	30.0	11.80	3.40	.29
	40.0	6.20	2.70	.44
8	5.0	81.00	114.00	1.41
	5.5	78.00	114.00	1.46
	6.0	69.00	109.00	1.58
	6.2	65.00	104.00	1.60
	6.4	61.00	100.00	1.64

TABLE 30 (Continued)

Relative Damping Rate	Frequency (c.p.s.)	Input	Output	Output / Input
8	6.5	60.00	98.00	1.63
	6.6	58.00	95.00	1.64
	6.8	55.00	89.00	1.61
	7.0	52.00	85.00	1.63
	7.2	50.00	80.00	1.60
	7.4	47.30	78.00	1.65
	7.6	47.00	73.00	1.55
	7.8	46.00	69.00	1.50
	8.0	45.90	64.00	1.39
	8.2	45.80	59.00	1.29
	8.5	45.80	52.00	1.14
	9.0	46.00	43.00	.93
	9.5	43.10	33.80	.78
	10.0	43.00	28.50	.66
	10.2	43.00	26.70	.62
	10.4	43.00	25.10	.58
	10.6	43.30	23.50	.54
	10.8	43.30	22.30	.52
	11.0	43.40	21.10	.49
	11.2	43.40	20.00	.46
	11.4	43.10	19.00	.44
	11.6	42.90	18.00	.42
	11.8	42.80	17.00	.40
	12.0	42.40	16.10	.38
	12.5	42.10	14.60	.35
	13.0	42.00	13.50	.32
	13.5	41.00	12.50	.30
	14.0	39.90	11.75	.29
	14.5	38.70	11.10	.29
	15.0	37.50	10.60	.28
	15.5	36.30	10.20	.28
	16.0	35.20	9.90	.28
	16.5	34.00	9.70	.28
	17.0	32.50	9.60	.30
	17.5	31.00	9.10	.29
	18.0	31.70	7.50	.24

TABLE 30 (Continued)

Relative Damping Rate	Frequency (c.p.s.)	Input	Output	Output / Input
8	18.5	30.80	8.60	.28
	19.0	31.00	7.40	.24
	20.0	30.00	6.00	.20
	25.0	19.50	4.90	.25
	30.0	13.60	4.72	.34
	40.0	7.10	6.40	.90
9	5.0	79.00	116.00	1.47
	5.5	71.00	122.00	1.72
	6.0	58.00	120.00	2.07
	6.2	53.00	117.00	2.21
	6.4	45.70	113.00	2.47
	6.6	41.50	105.00	2.53
	6.8	38.00	98.00	2.57
	7.0	36.00	93.00	2.58
	7.2	36.80	84.00	2.28
	7.4	37.00	77.00	2.08
	7.6	38.20	67.50	1.77
	7.8	40.00	61.00	1.53
	8.0	42.00	56.00	1.33
	8.2	43.60	49.00	1.12
	8.4	46.00	44.00	.96
	8.6	47.00	39.70	.84
	9.0	49.00	31.80	.65
	9.5	51.00	23.50	.47
	10.0	46.50	16.90	.36
	10.2	46.50	15.50	.33
	10.4	47.00	13.90	.30
	10.6	47.50	12.70	.27
	10.8	47.50	11.90	.25
	11.0	47.30	11.10	.24
	11.2	47.00	10.70	.23
	11.4	47.00	9.90	.21
	11.6	46.30	9.40	.20
	11.8	46.00	9.10	.20

TABLE 30 (Continued)

Relative Damping Rate	Frequency (c.p.s.)	Input	Output	Output / Input
9	12.0	45.30	8.90	.20
	12.5	44.70	9.00	.20
	13.0	43.30	8.70	.20
	13.5	42.00	8.70	.21
	14.0	40.10	8.60	.21
	14.5	39.00	8.80	.18
	15.0	37.80	8.90	.24
	17.0	33.30	8.40	.25
	20.0	27.20	7.70	.28
	25.0	17.40	6.10	.35
	30.0	12.30	4.80	.39
	40.0	6.50	4.95	.76

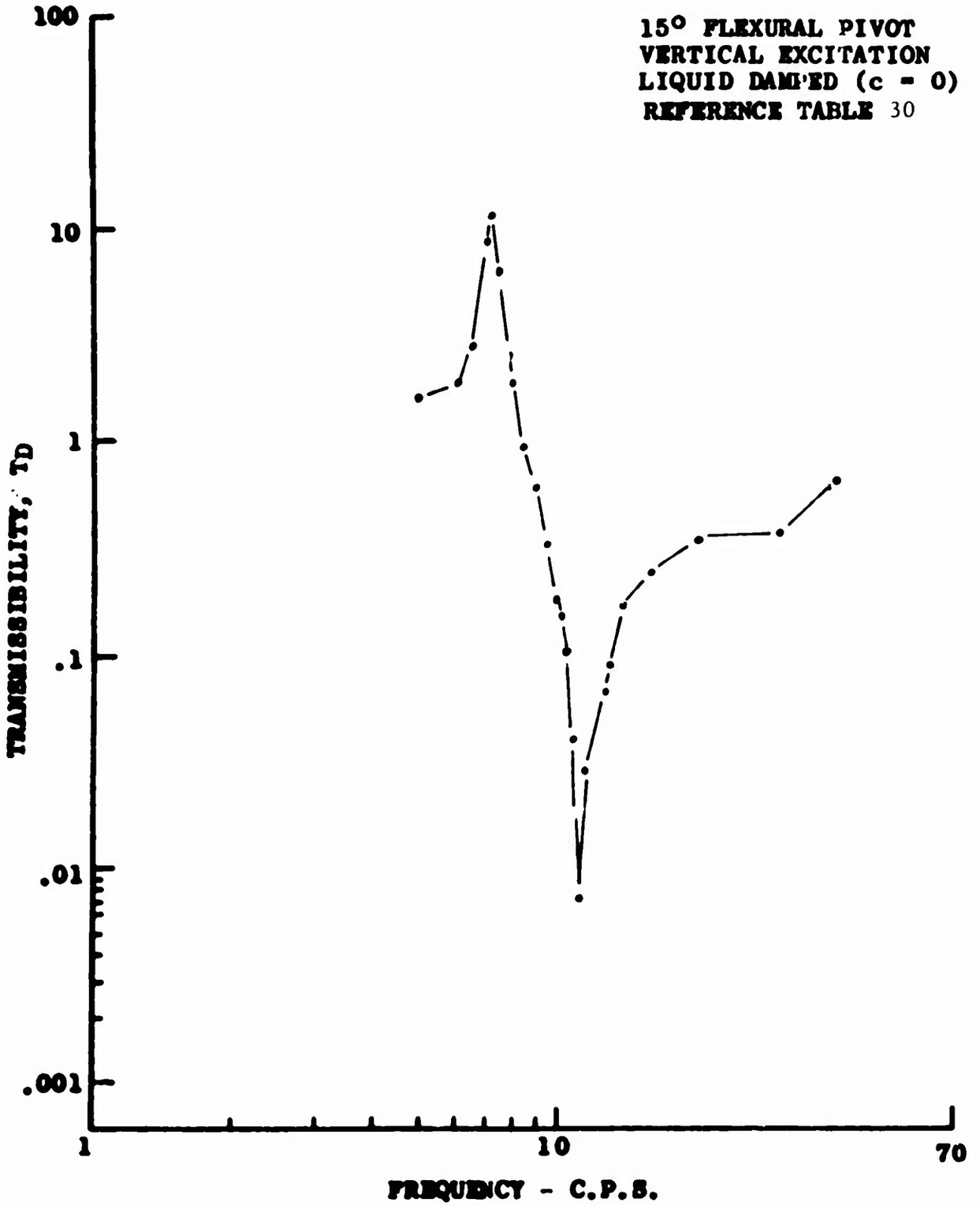

Figure 59. Response Curve for Two-Dimensional DAVI

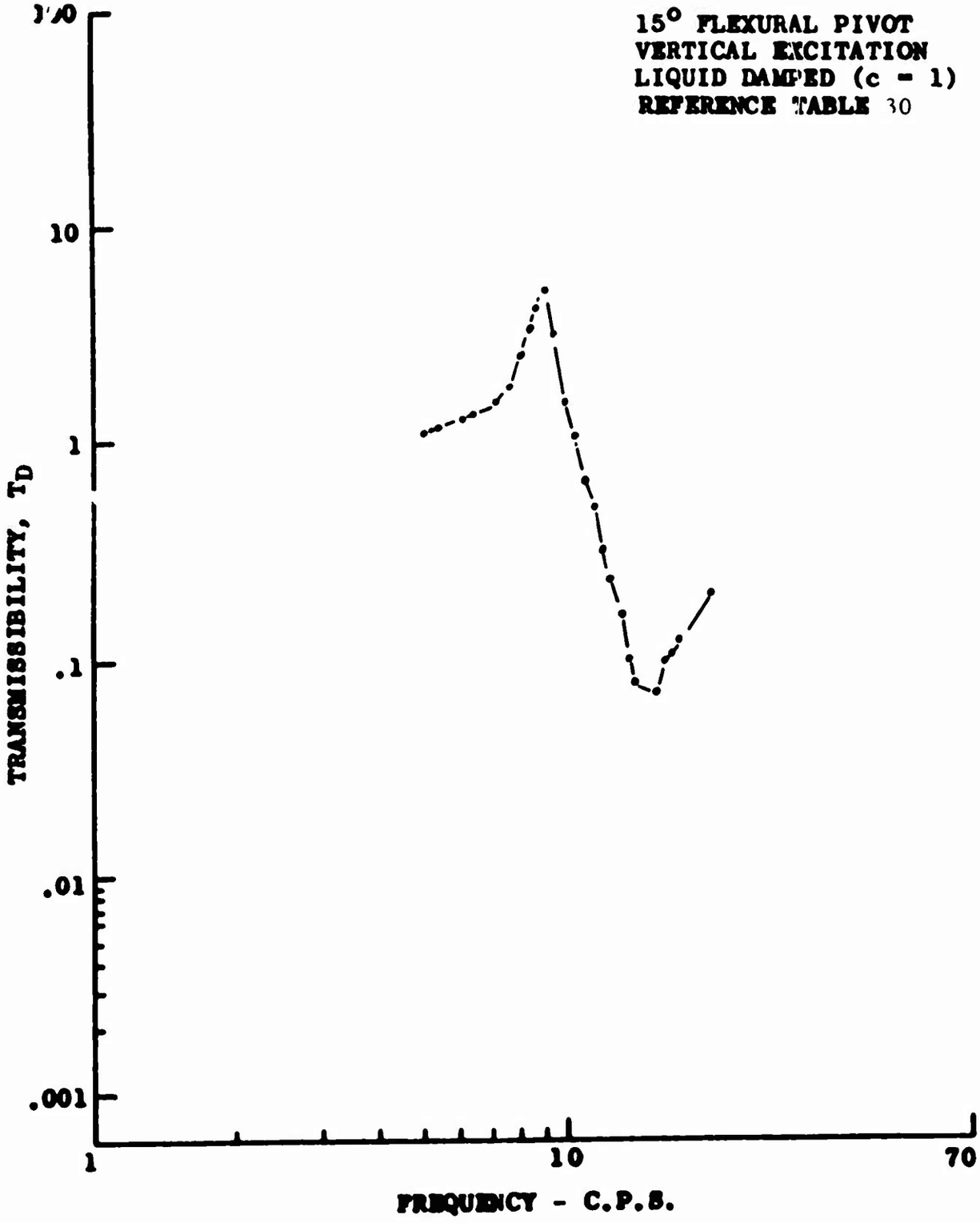

Figure 60. Response Curve for Two-Dimensional DAVI

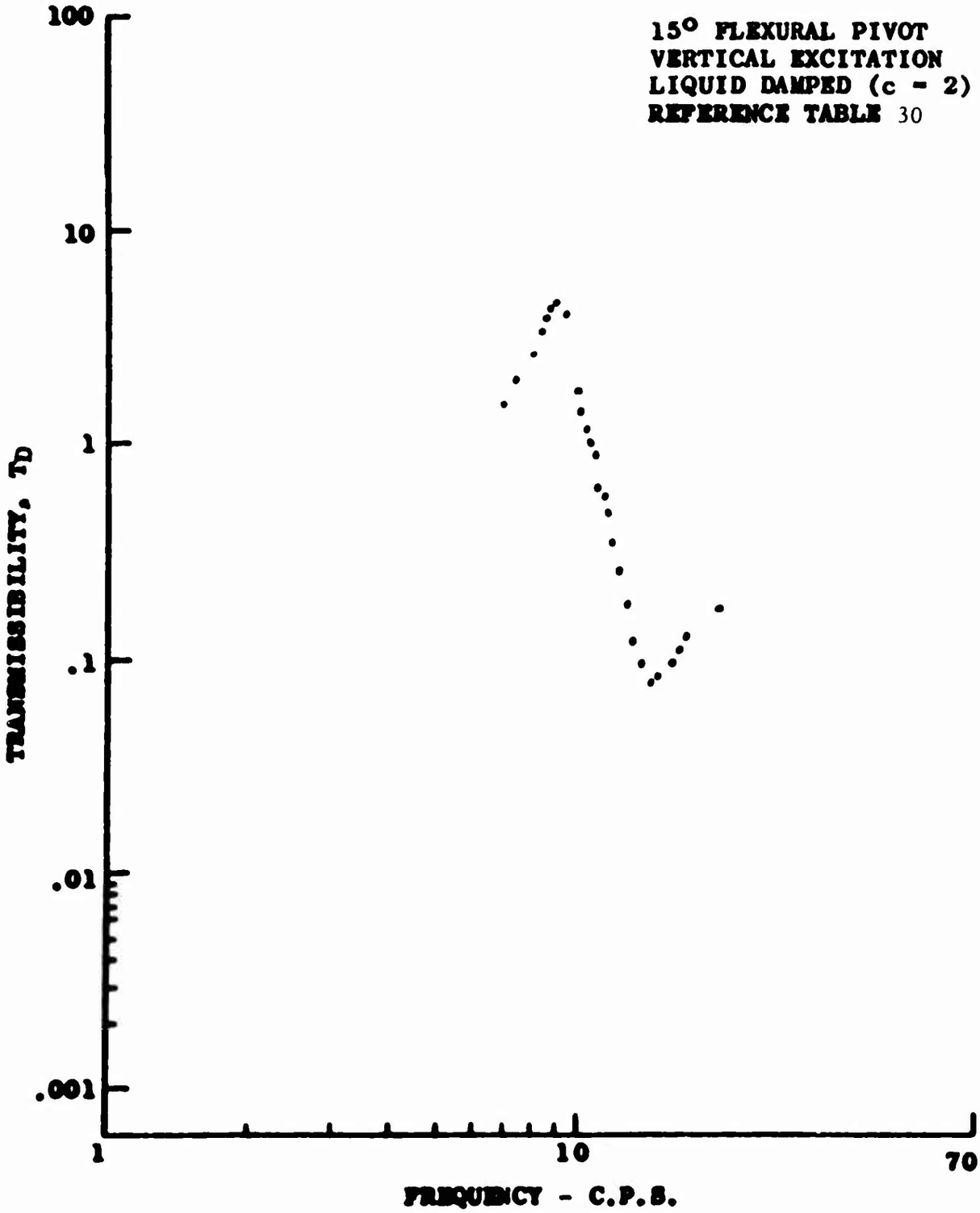

Figure 61. Response Curve for Two-Dimensional DAVI

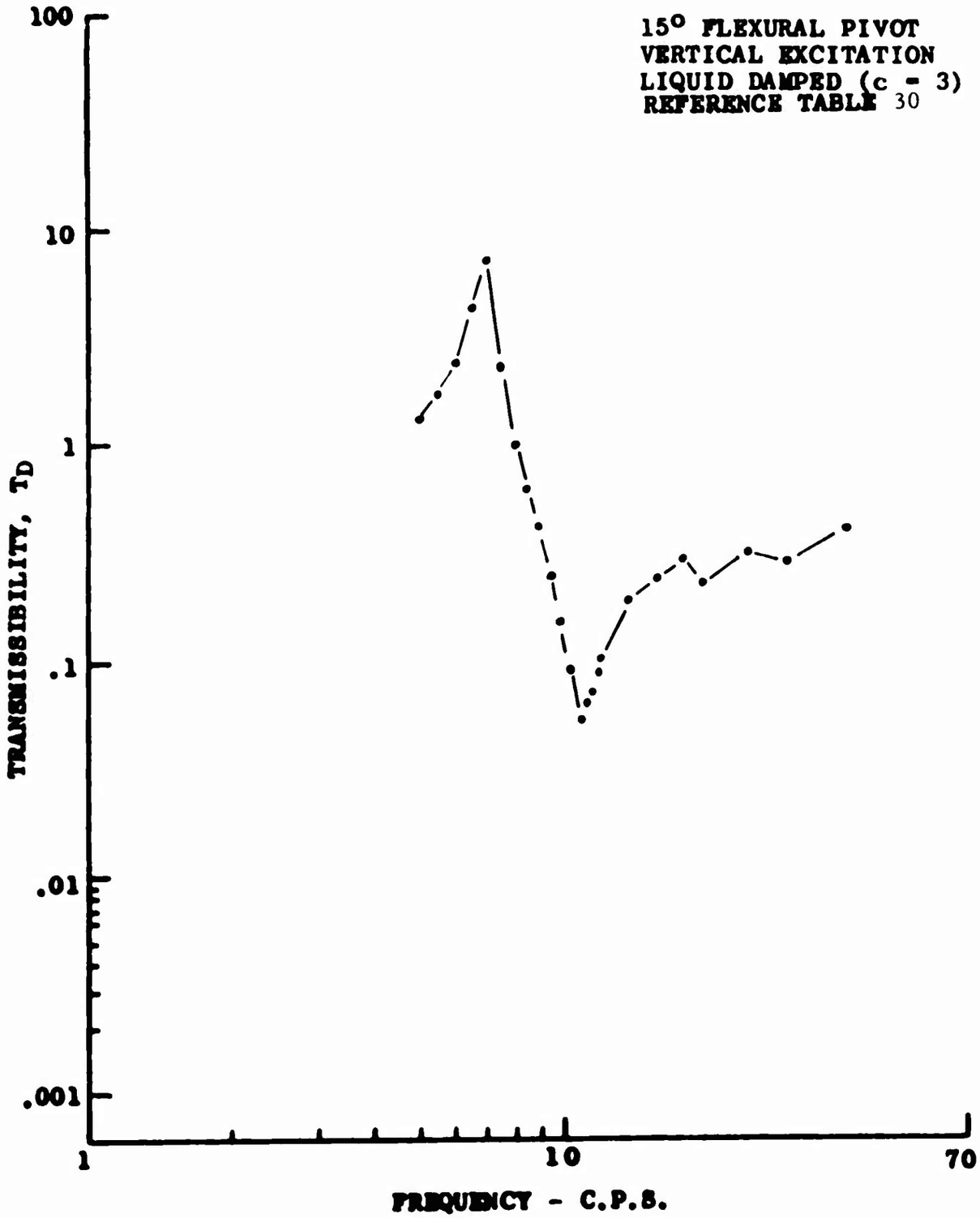

Figure 62. Response Curve for Two-Dimensional DAVI

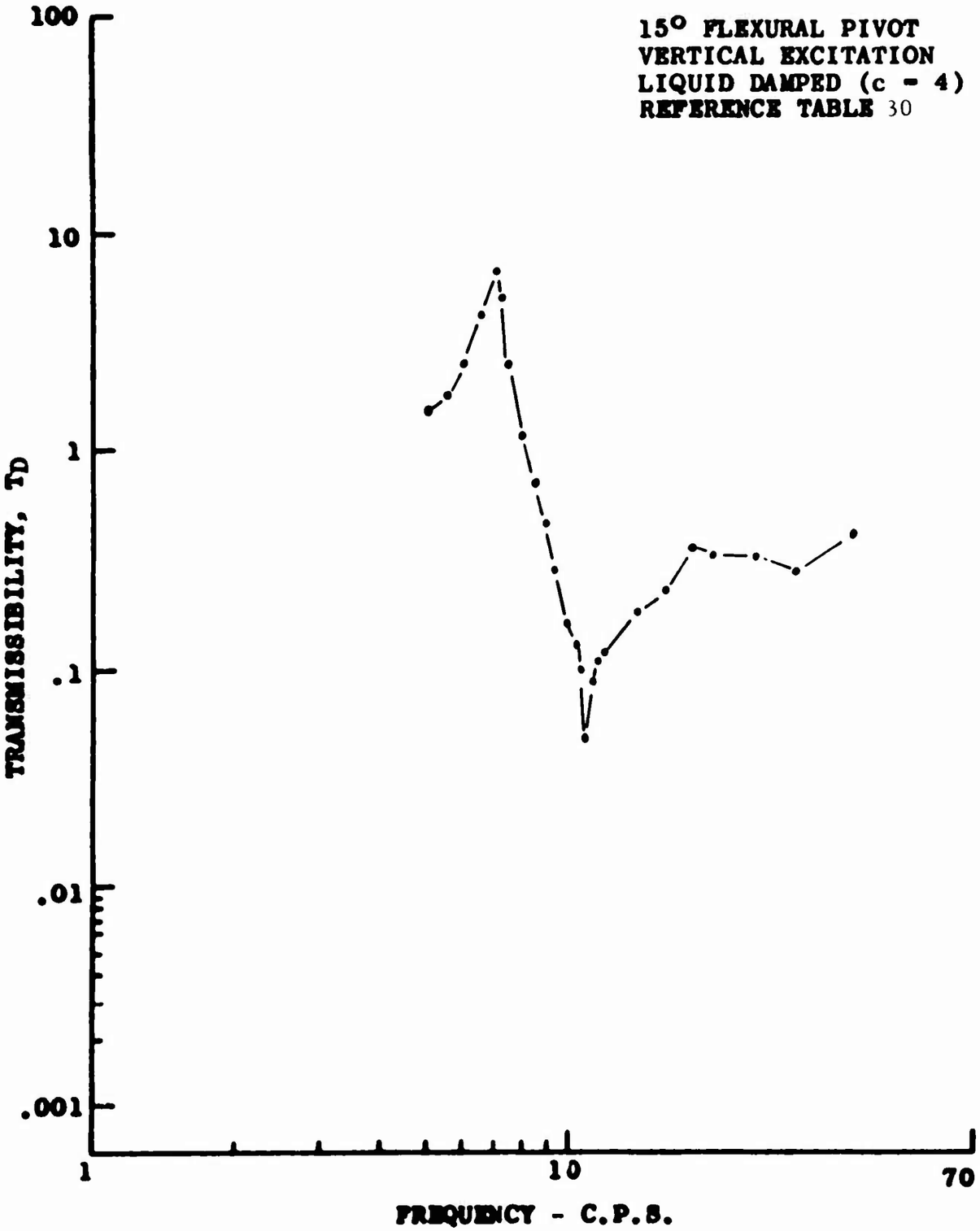

Figure 63. Response Curve for Two-Dimensional DAVI

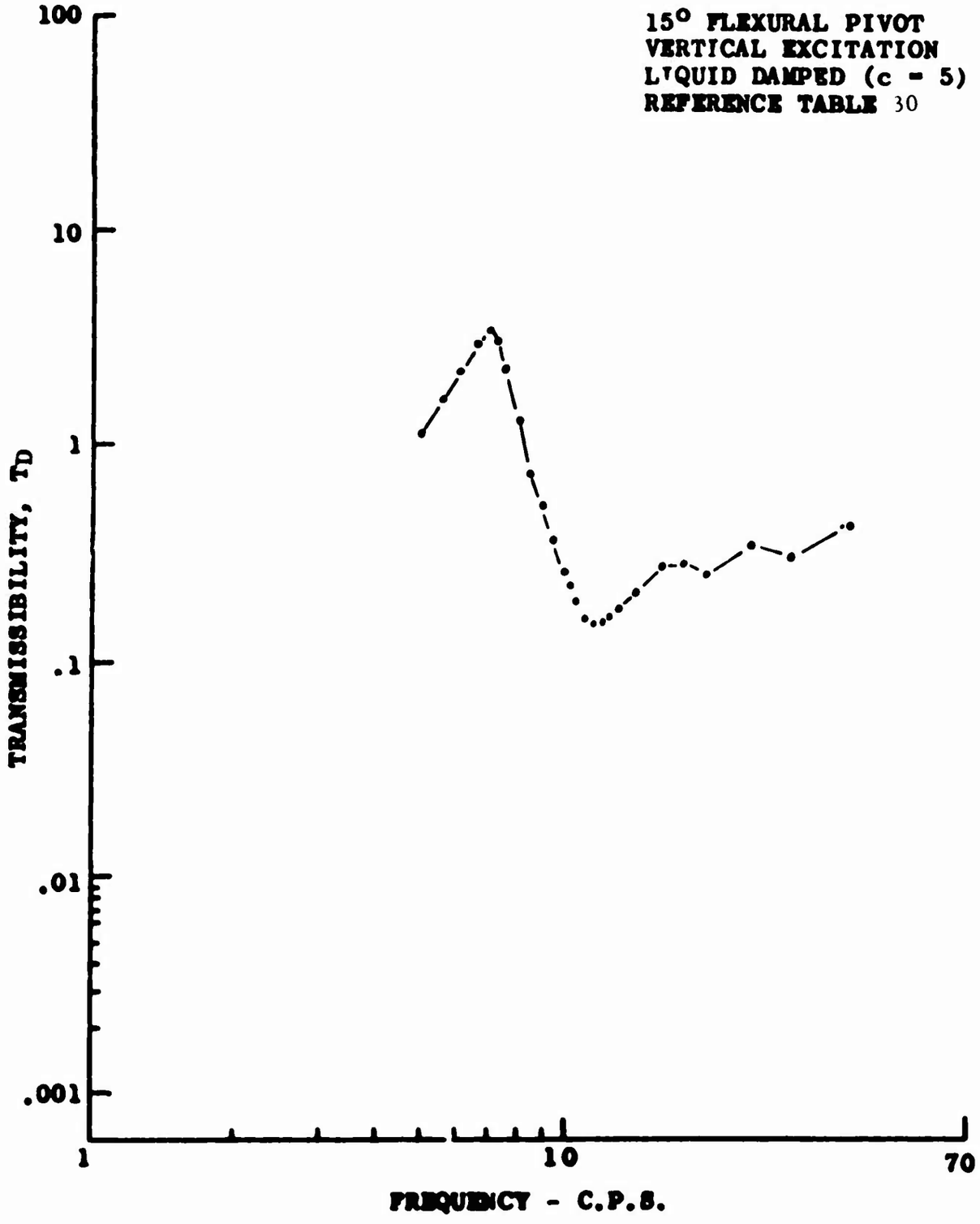

Figure 64. Response Curve for Two-Dimensional DAVI

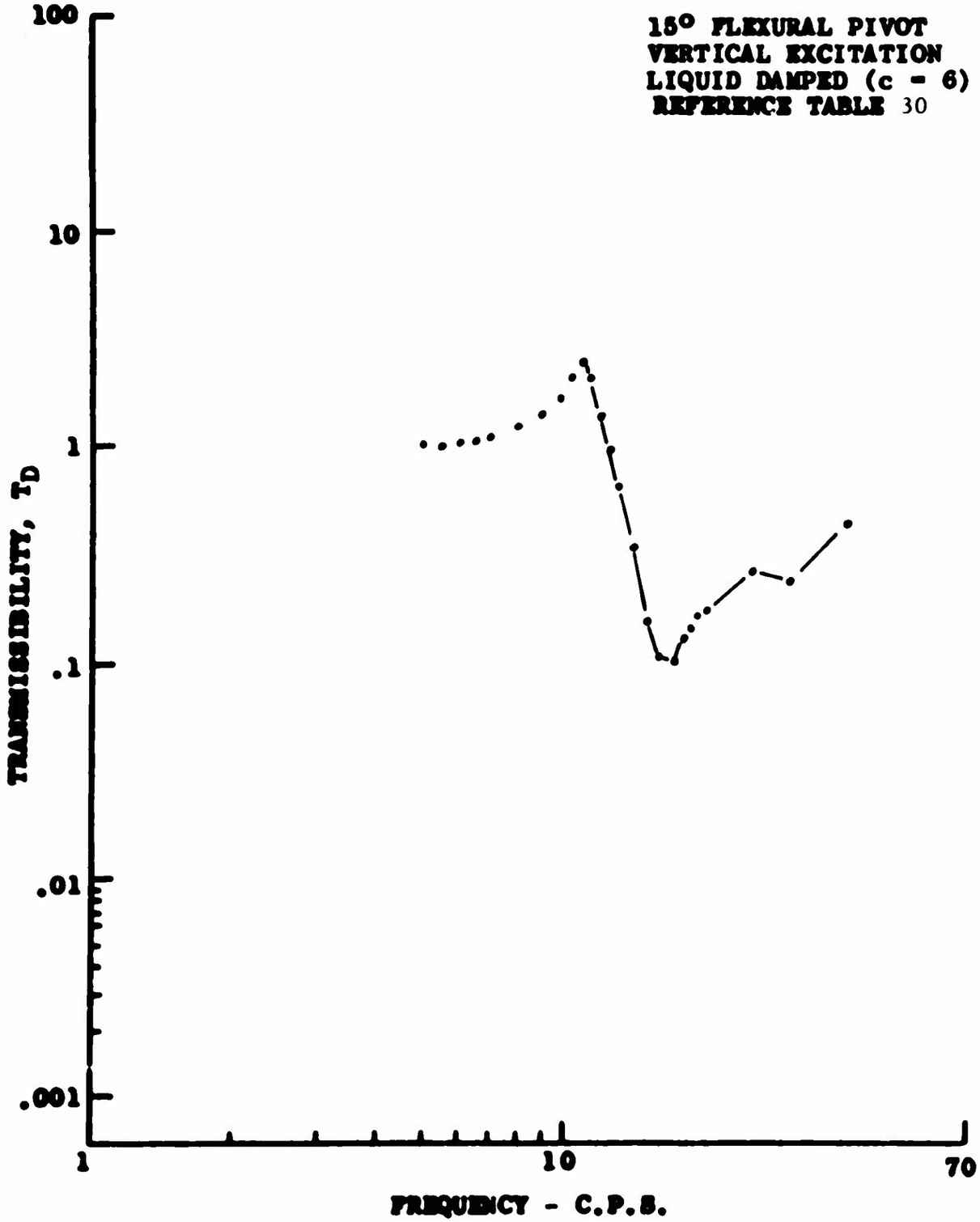

Figure 65. Response Curve for Two-Dimensional DAVI

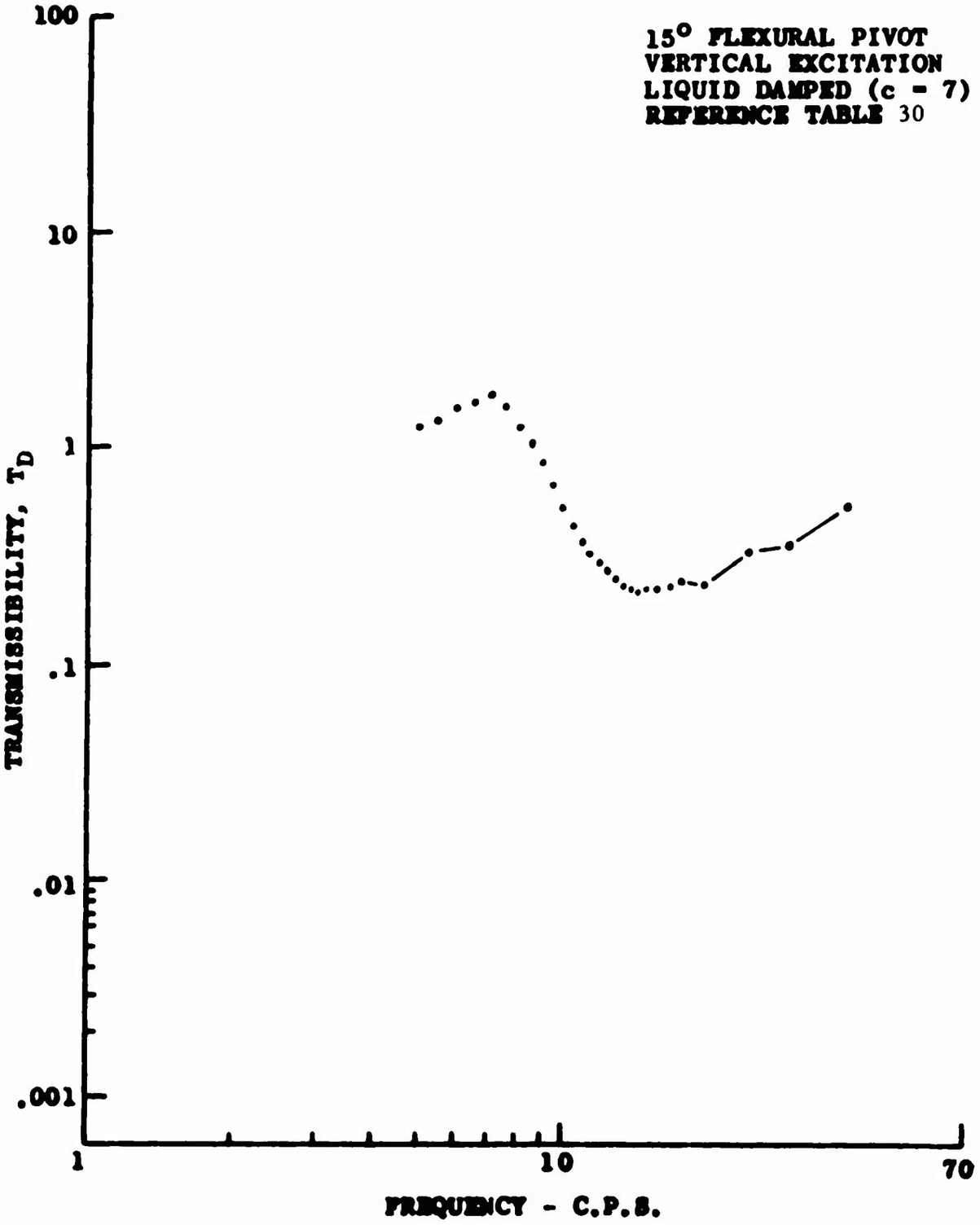

Figure 66. Response Curve for Two-Dimensional DAVI

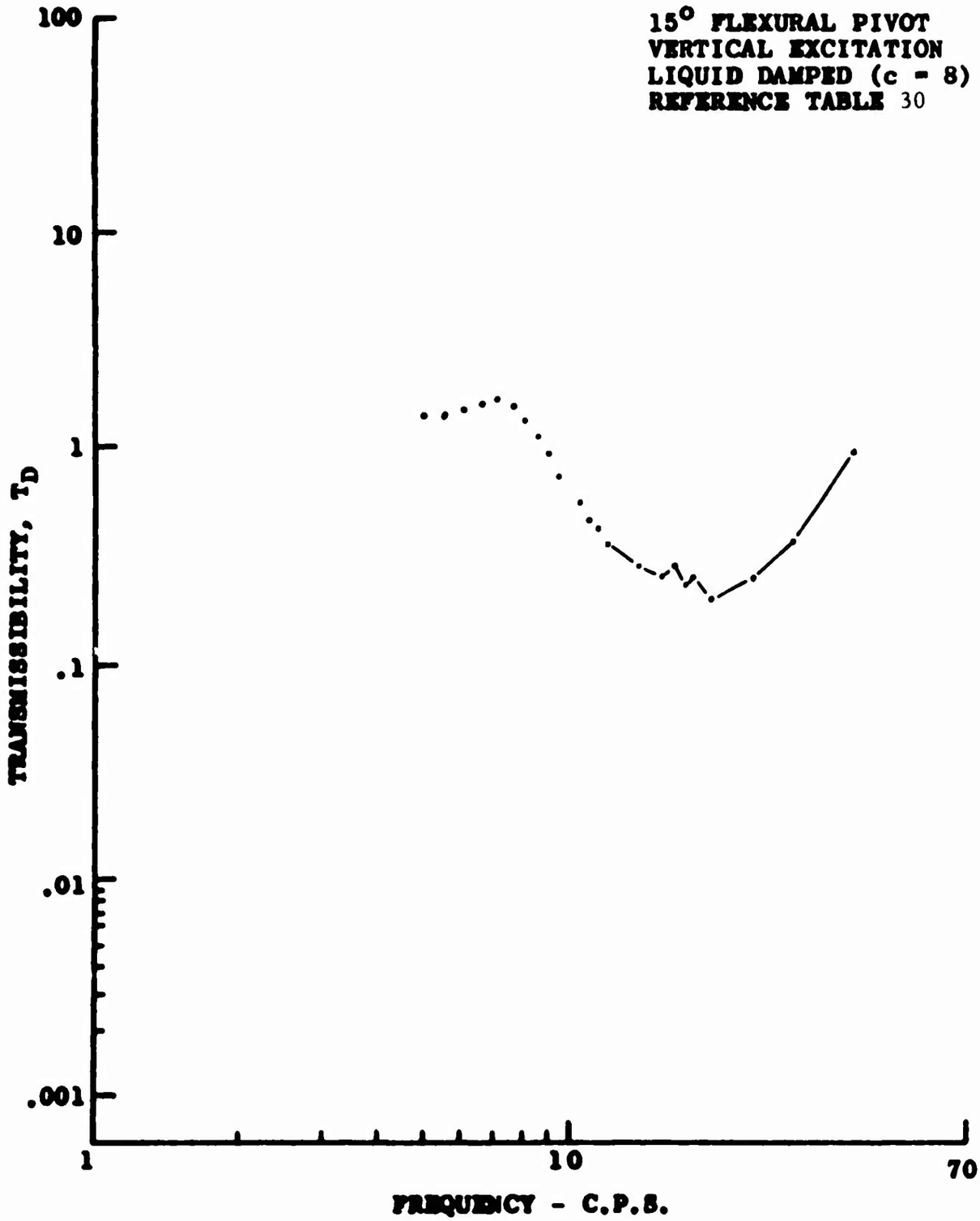

Figure 67. Response Curve for Two-Dimensional DAVI

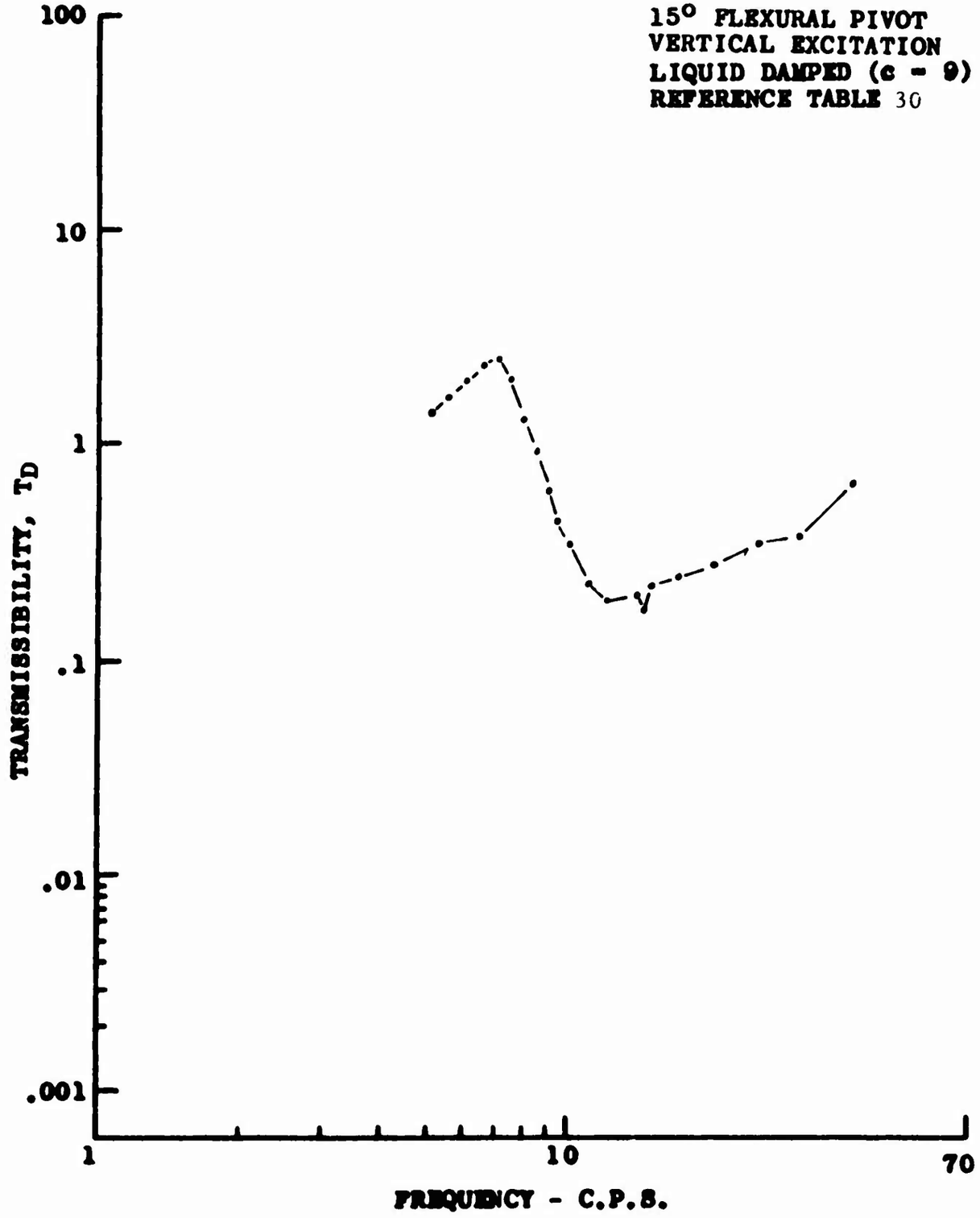

Figure 68. Response Curve for Two-Dimensional DAVI

TABLE 31

UNIDIRECTIONAL DAVI TRANSMISSIBILITY TEST DATA
15° FLEXURAL PIVOTS
VERTICAL EXCITATION

Frequency (c.p.s.)	Input	Output	Output / Input
5.0	51.00	45.00	.90
6.0	45.00	59.00	1.31
7.0	43.00	70.00	1.62
8.0	30.00	98.00	3.27
8.5	10.90	88.00	8.07
9.0	20.50	72.00	3.50
9.5	32.00	30.00	.94
10.0	34.00	10.00	.29
10.4	35.00	.35	.01
11.0	33.50	6.10	.18
11.5	33.00	8.50	.26
12.0	31.00	10.00	.32
13.0	29.00	11.20	.39
15.0	23.50	11.20	.47
17.0	20.00	10.20	.51
20.0	15.80	8.50	.54
25.0	10.50	6.20	.59
30.0	7.50	4.50	.60
35.0	5.40	3.20	.59
40.0	4.20	2.50	.60
45.0	3.40	2.10	.61
50.0	2.70	1.60	.59
60.0	1.70	1.10	.65

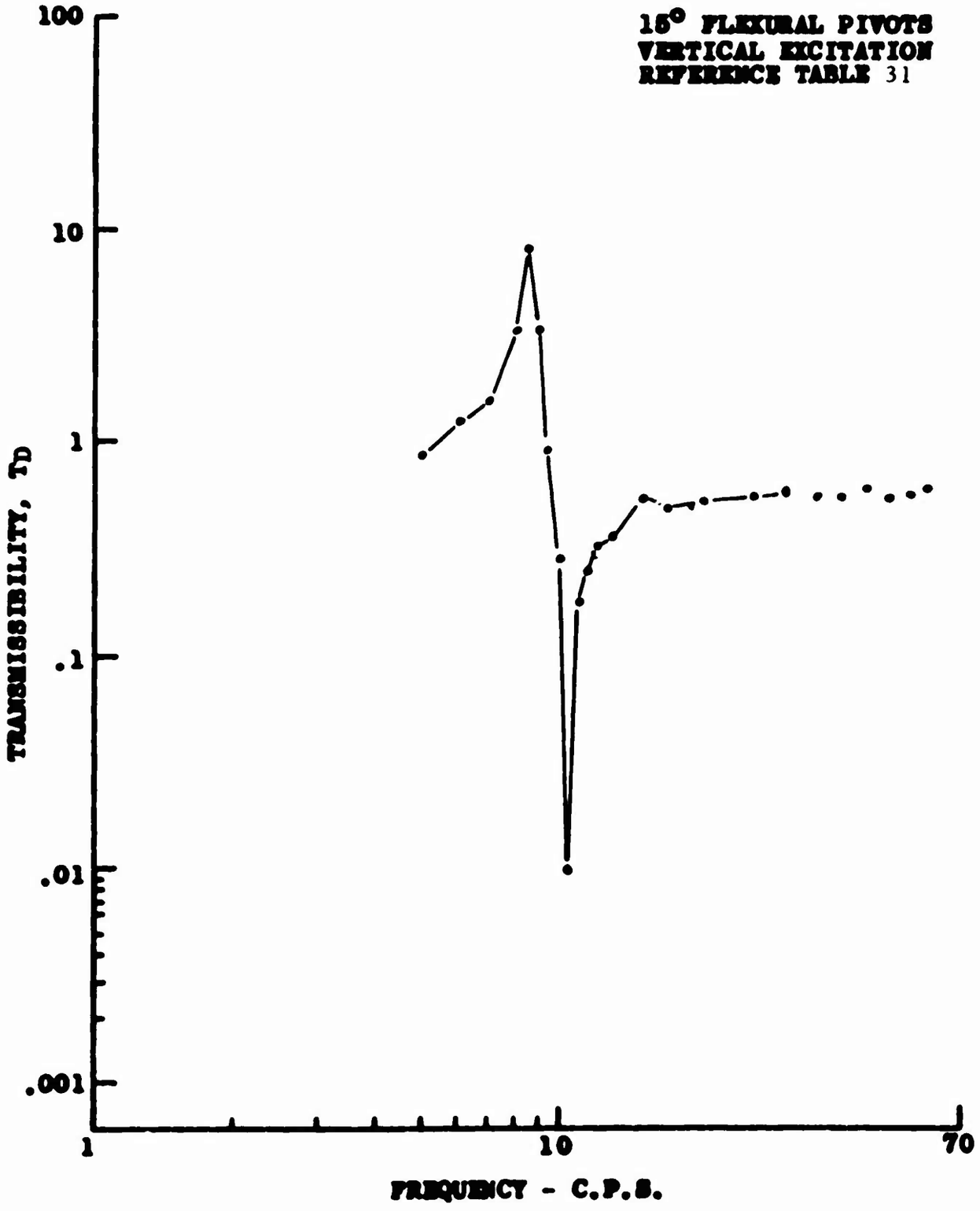

Figure 69. Response Curve for Single-Degree-of-Freedom DAVI

TABLE 32

UNIDIRECTIONAL DAVI TRANSMISSIBILITY TEST DATA
7-1/2° FLEXURAL PIVOTS
VERTICAL EXCITATION

Frequency (c.p.s.)	Input	Output	Output / Input
5.0	50.00	54.00	1.08
5.5	51.00	56.00	1.10
6.0	51.00	56.00	1.10
6.5	50.00	56.00	1.12
7.0	48.00	56.00	1.17
7.5	46.00	55.00	1.20
8.0	44.00	55.00	1.25
8.5	40.00	56.00	1.40
9.0	35.00	60.00	1.71
9.2	31.00	64.00	2.06
9.4	26.00	70.00	2.69
9.6	14.10	78.00	5.53
9.8	10.00	66.00	6.60
10.0	30.00	33.00	1.10
10.2	36.00	10.00	.28
10.3	36.50	.90	.02
10.4	36.50	5.10	.14
10.6	36.50	11.20	.31
10.8	35.00	15.00	.42
11.0	34.80	17.50	.50
11.5	32.00	20.00	.63
12.0	30.00	21.00	.70
13.0	26.00	20.00	.77
14.0	23.00	18.50	.80
15.0	21.00	17.00	.81
17.0	17.00	14.00	.82
19.0	14.20	12.20	.86
20.0	13.00	11.20	.86
25.0	8.90	7.60	.85
30.0	6.00	5.20	.86
35.0	4.30	3.85	.90
40.0	3.10	2.95	.95
50.0	2.20	1.10	.50
60.0	1.20	1.10	.91

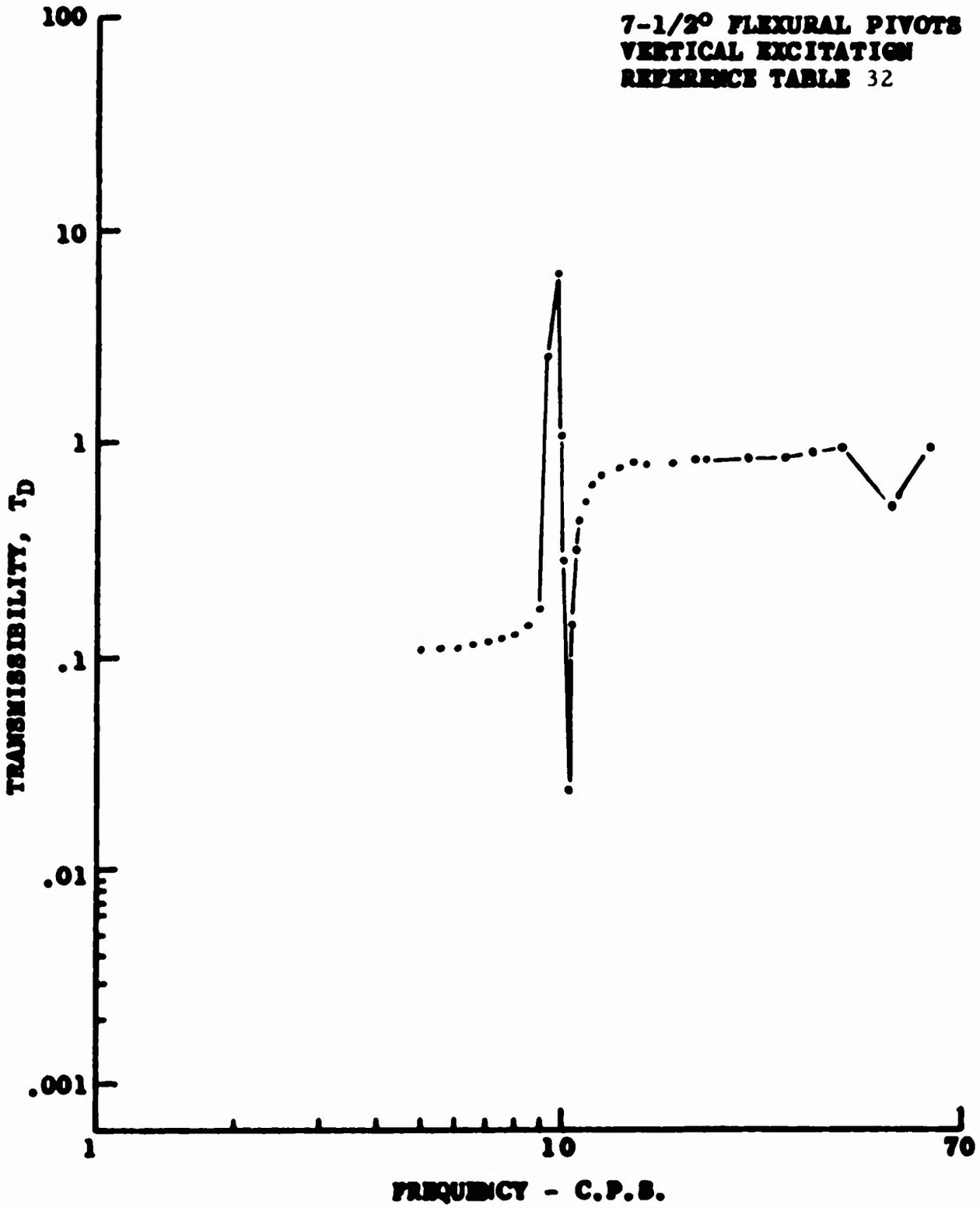

Figure 70 . Response Curve for Single-Degree-of-Freedom DAVI

MASS AND CENTER OF GRAVITY EFFECTS ON TRANSMISSIBILITY

DESIGN OF DAVI TEST PLATFORM

The Optimum DAVI

The optimum DAVI design from Task 4 is shown in Figure 71. It had performed well in tests, under Task 4, and had a 50-pound load-carrying capacity due to the use of a stiff flexural pivot which was doing double duty as the spring element and as a frictionless pivot. Thus, four new models of this type were constructed, leaving the existing test model from Task 4 as a spare.

The Unstiffened Platform

Preliminary investigation of the problem of constructing a working platform was kept simple. The four DAVI's were tuned to antiresonate at the same frequency (10.5 c.p.s.). They were then clamped underneath the four corners of a 36-inch-by-21-inch sheet of honeycomb aluminum sheeting and bolted by means of a 36-inch-by-21-inch sheet of 3/4-inch plywood to an electromagnetic shaker and tested for frequency response from 5 c.p.s. to 100 c.p.s.

It was found that this arrangement was satisfactory up to a load of approximately 50 pounds. But, with loads in excess of 50 pounds, the static deflection of the platform was significant. Also, under dynamic conditions, especially at the DAVI resonant frequency, because of the large vibratory deflection in the pivots, overloads could develop quite rapidly.

The large deflections also gave cause for concern that the flexural pivots were being subjected to an excessive amount of lateral torsion for which they were not designed.

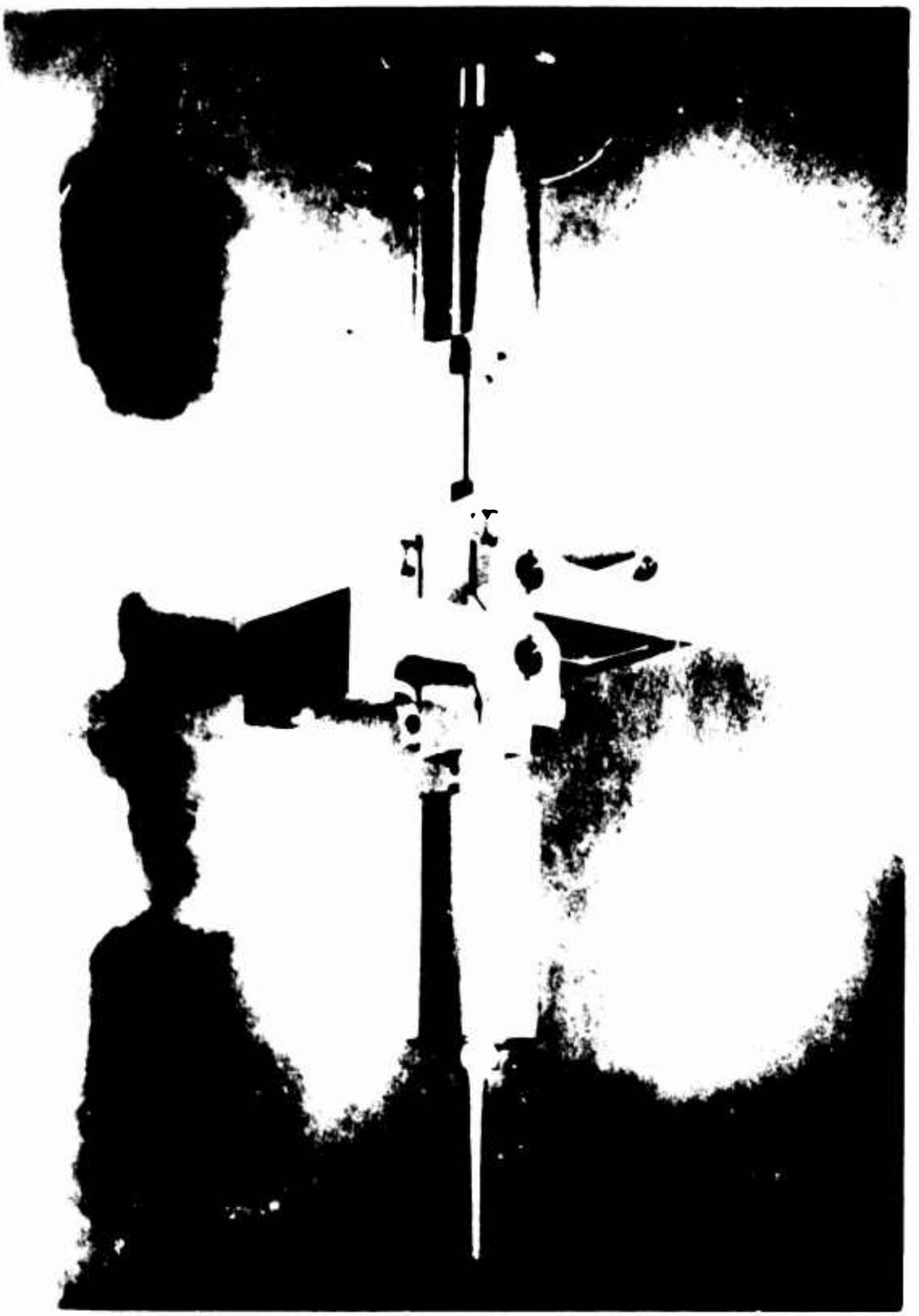

Figure 71. DAVI Model With Double Inertia Arm

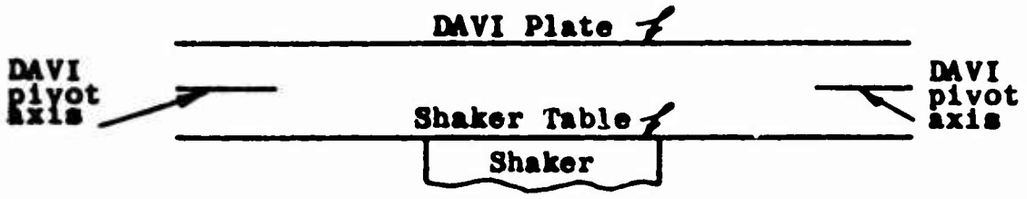

Figure 72a. DAVI Platform Schematic

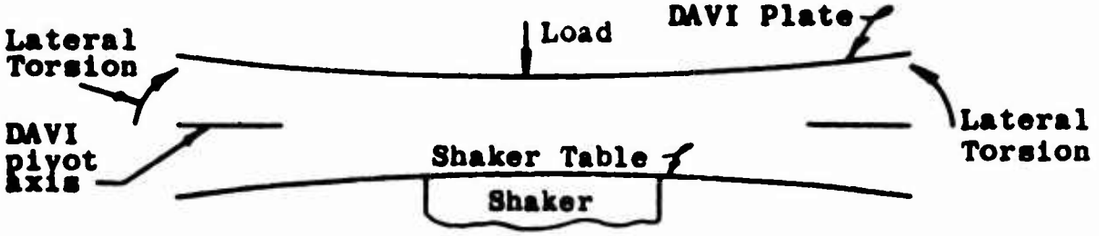

Figure 72b. DAVI Platform Schematic

Figure 72a is a typical cross section of the platform through the DAVI pivot axes with the platform unloaded. Figure 72b is an exaggerated view of the platform now loaded to large deflections. The relative positions of the DAVI axes and the edges of the platform and the supporting plates, before and after loading, clearly indicate that lateral torsional forces would tend to bend the flexural pivot perpendicular to its (designed) torsional axis. In extreme cases, this bending will have a significant effect on the torsional spring constant of the pivot.

The actual DAVI itself at this time was still a transitional configuration. The flexural pivots were doing double duty as the spring element and as the frictionless pivot. In the preliminary process of tuning a DAVI to a specific frequency, this configuration was found to be very sensitive to any misalignment in the surfaces to which the upper and lower plates of the DAVI were attached. This corroborated the observations of the previous paragraph.

Furthermore, under conditions of sinusoidal loading, unwanted low frequency resonant peaks, due to the flexibility of the platform, distorted the frequency response characteristic to such an extent that correlation with theoretical response curves was impossible.

All these considerations pointed to the necessity for stiffening the platform.

The Four-Bar Linkage

However, it was also feared that a stiffened platform would introduce new problems. The combination of a rigid platform, a rigid supporting structure, and two DAVI's in line constitutes a four-bar linkage (see Figure 73).

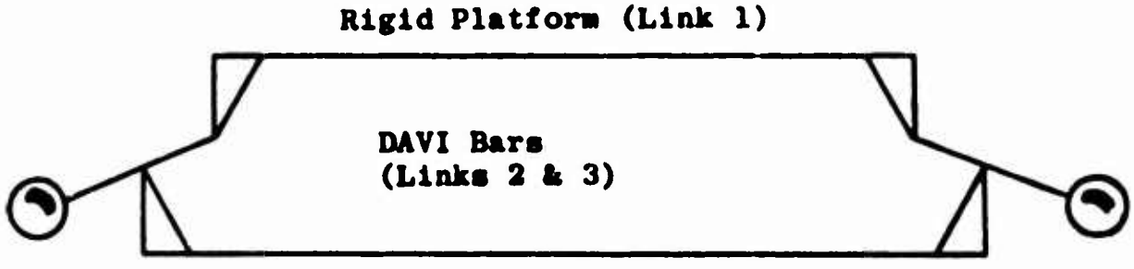

Figure 73. DAVI Platform Four-Bar Linkage

Elementary geometry dictates that for perfectly rigid links the motion of such a structure is severely limited. Yet, the present work required that the inertia bars of both DAVI's have complete independence of motion. Although, the angular motions of the DAVI inertia bars would be small, it was still thought that, even if the DAVI anti-resonant effect was not impaired, the fatigue life of the pivots would be drastically reduced.

Subsequent testing showed that most of the advantages hoped for, and none of the disadvantages feared, were forthcoming from the stiffened platform.

Thus, on the one hand, while stiffening greatly reduced the platform deflections and the lateral torsional torque on the flexural pivots and removed to higher frequencies the unwanted extraneous resonant peaks, the DAVI's were still quite sensitive to slight misalignment of mating faces. On the other hand, the four-bar rigid linkage effect was never in evidence, either in performance tests or in fatigue tests.

The Final DAVI Configuration

The last problems, that of stress in the flexural pivots and that of sensitivity in tuning of the DAVI to misalignment, were solved by changing the DAVI configuration. Whereas the flexural pivots had been required to act also as spring elements, they were now relieved of this duty by including a parallel spring to take the main load (see Figure 74). This was done mainly to solve the stress problem, which is discussed subsequently. However, it also served to make the DAVI's less sensitive in tuning to mating face misalignment, since the flexural pivot stiffness was greatly reduced. The reduction in sensitivity to misalignment is explained by the fact that a stiff flexural pivot, subjected to appreciable lateral torsion, experiences a percentage change in torsional spring constant; and, thus, the antiresonant frequency of the DAVI, which is directly proportional to this spring constant, will change by the same percentage. The new configuration, being sensitive to misalignment only insofar as the torsional spring constant of a much softer flexural pivot is involved, will thus alter the antiresonant frequency to a much smaller degree.

Shock Test

Since the platform was also to be tested under shock loading conditions, retaining clips were made to insure that the parallel helical spring would be able to withstand negative forces. These clips were subsequently required to be strengthened. The shock results are discussed elsewhere.

The Last Alteration

While considerations of weight economy were involved in solving the problem of constructing a working platform, this factor had not been allowed to play a dominant role. However, a good working platform was now in being. It was designed to support 200 pounds for a 1.0-g input at the tuned frequency and to give infinite life. The DAVI's also could be easily tuned to a specific frequency.

Consideration could now be given to weight savings within the DAVI configuration.

Hitherto, the criteria used in designing the DAVI was compactness and ease of calculation. Both of these were achieved by arranging the DAVI inertia bar to be balanced about the isolated mass pivot; that is, R/r = 1.

However, more efficient use is made of the DAVI mass, and, thus, some weight economy is achieved by arranging the mass center of gravity such that the mass terms in the equivalent DAVI inertia expression, $\frac{I}{r^2} + m_o \frac{R}{r}\left(\frac{R}{r} - 1\right)$, are significant.

By using this criterion, the actual weight of each DAVI was reduced approximately 50 percent by removing half of each inertia bar with further reduction possible if required. This is shown in Figure 77.

The final overall configuration of DAVI and the platform used in testing is shown in Figure 74. A close-up is shown in Figure 75. Loads up to 200 pounds were tested without difficulty.

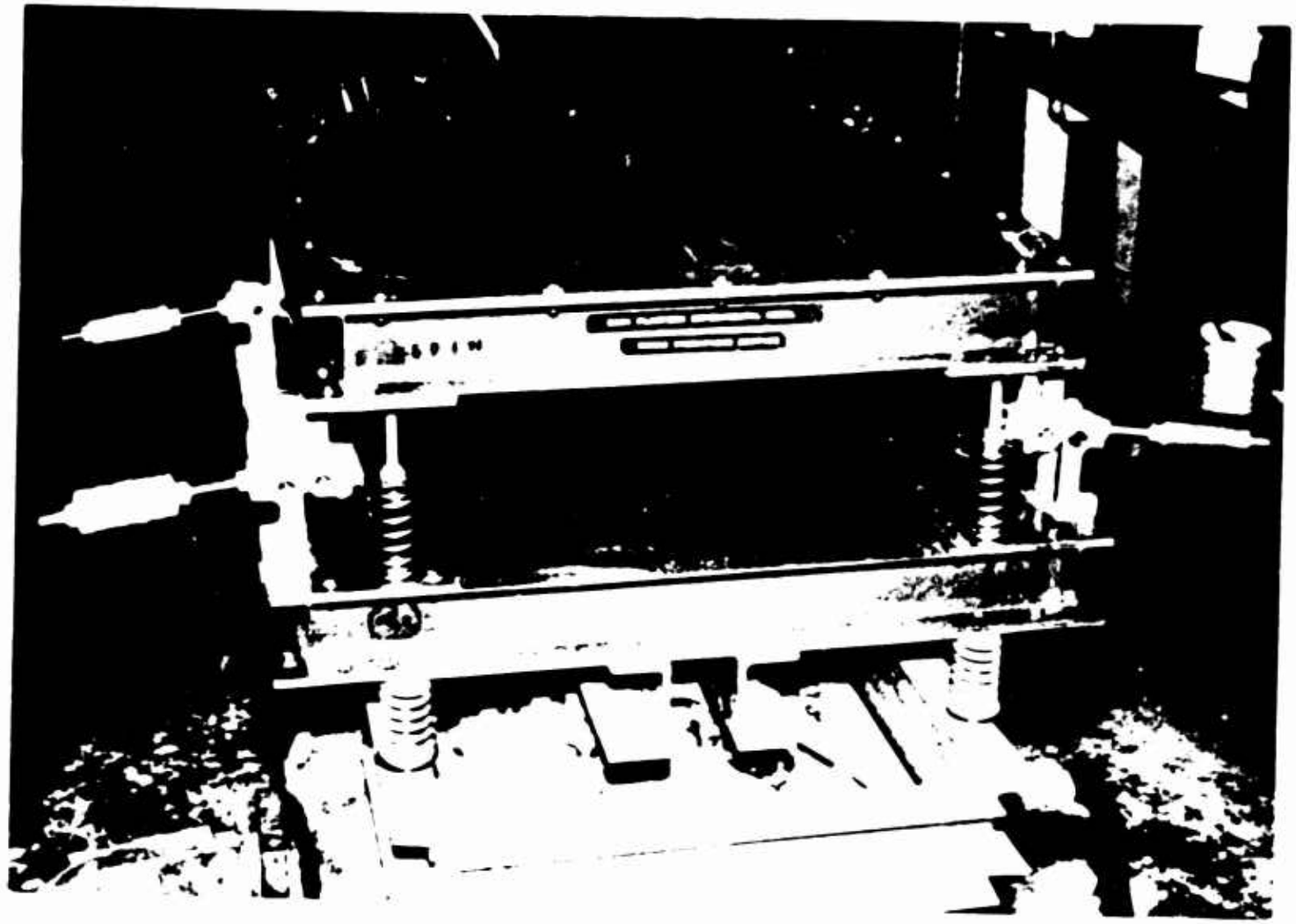

Figure 74. DAVI Platform Attachment to Shaker

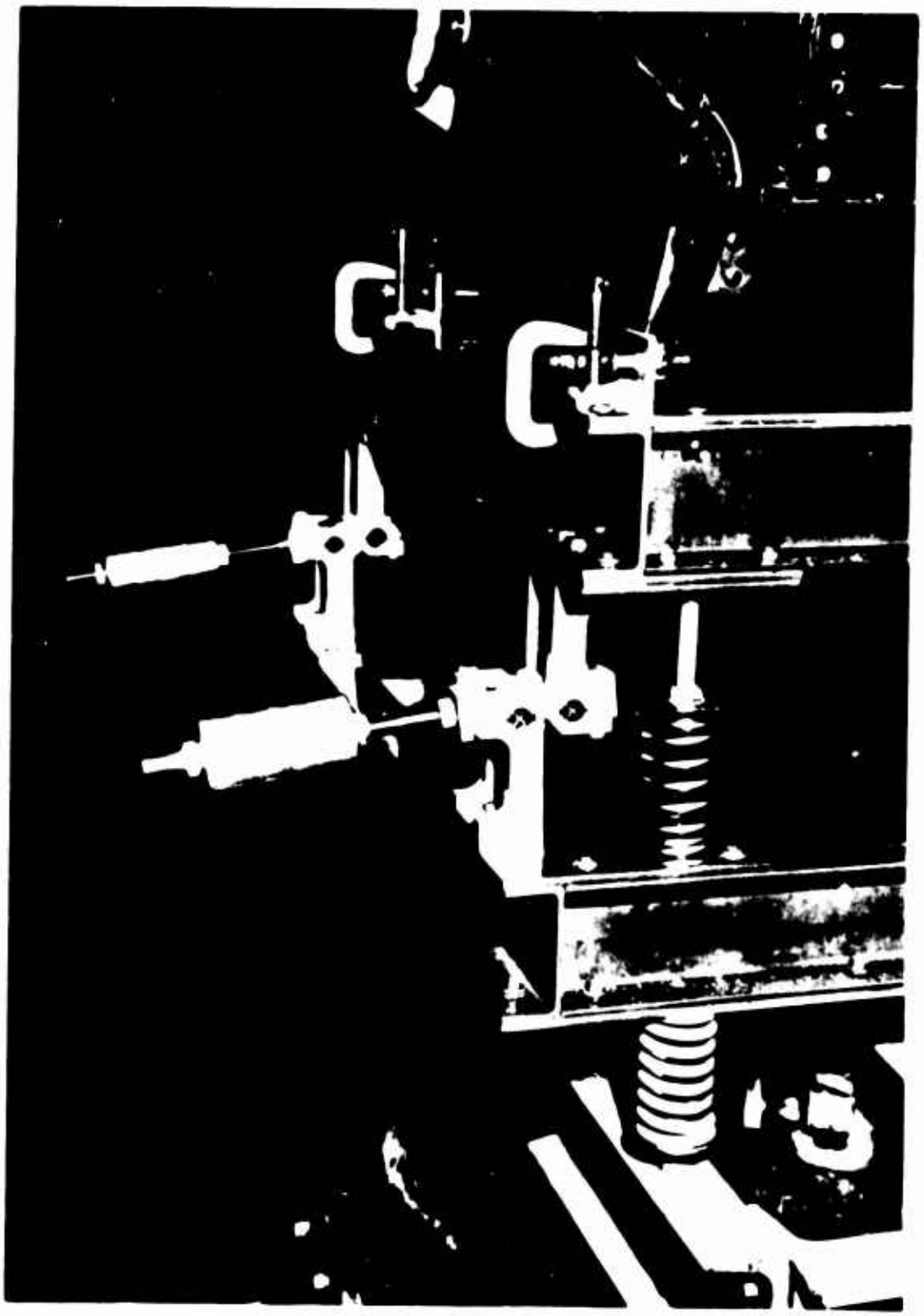

Figure 75. Close-up of DAVI Installed on Platform

SIX-DEGREE-OF-FREEDOM ANALYSIS

The Platform

The six-degree-of-freedom system analyzed here is drawn diagrammatically in Figure 76. It consists of a bottom platform called the DAVI-plate, supported at each corner by a DAVI, and a top platform called the top-plate, supported on the DAVI plate by a conventional isolator at each corner.

Assumptions

In the analysis, the corners of both top-plate and the DAVI plates are assumed to have vertical freedom of motion only. In terms of the overall system, this means that there are six degrees of freedom; that is, vertical translation, pitch, and roll in each plate.

Equations of motion are derived for general coupled motion by locating the center of gravity of each plate eccentric to the axes of symmetry.

The amplitude of input motions to the system are assumed to be such that angular motions of the DAVI bars remain in the small angle range. Thus, linearized simplifications are used throughout.

In order that the system have an antiresonance, it is necessary that the four DAVI's have an antiresonance at the same frequency. Thus, the analysis assumes that the four DAVI's have the same inertia, mass, and dimensional characteristics.

DAVI Configuration

In the practical testing, two configurations of the DAVI were used. In the early stages of testing, the DAVI bar was balanced around the mass pivot (see Figure 71). This allowed a simplification of the formula for the anti-resonant frequency and was a convenience in predicting performance. Later, significant weight savings were effected by altering the mass-inertia configuration of the DAVI bar. The new configuration is shown in Figure 77. However, the analysis includes both configurations. Figure 78 shows the final DAVI configuration with nomenclature.

THE ANALYSIS

In Figure 76, "Series-Damped DAVI ℵ Platform Schematic", it is indicated that the top-plate and the DAVI-plate both have freedom to pitch, roll, and translate vertically. The position direction assumed for each motion is indicated by the appropriate arrow.

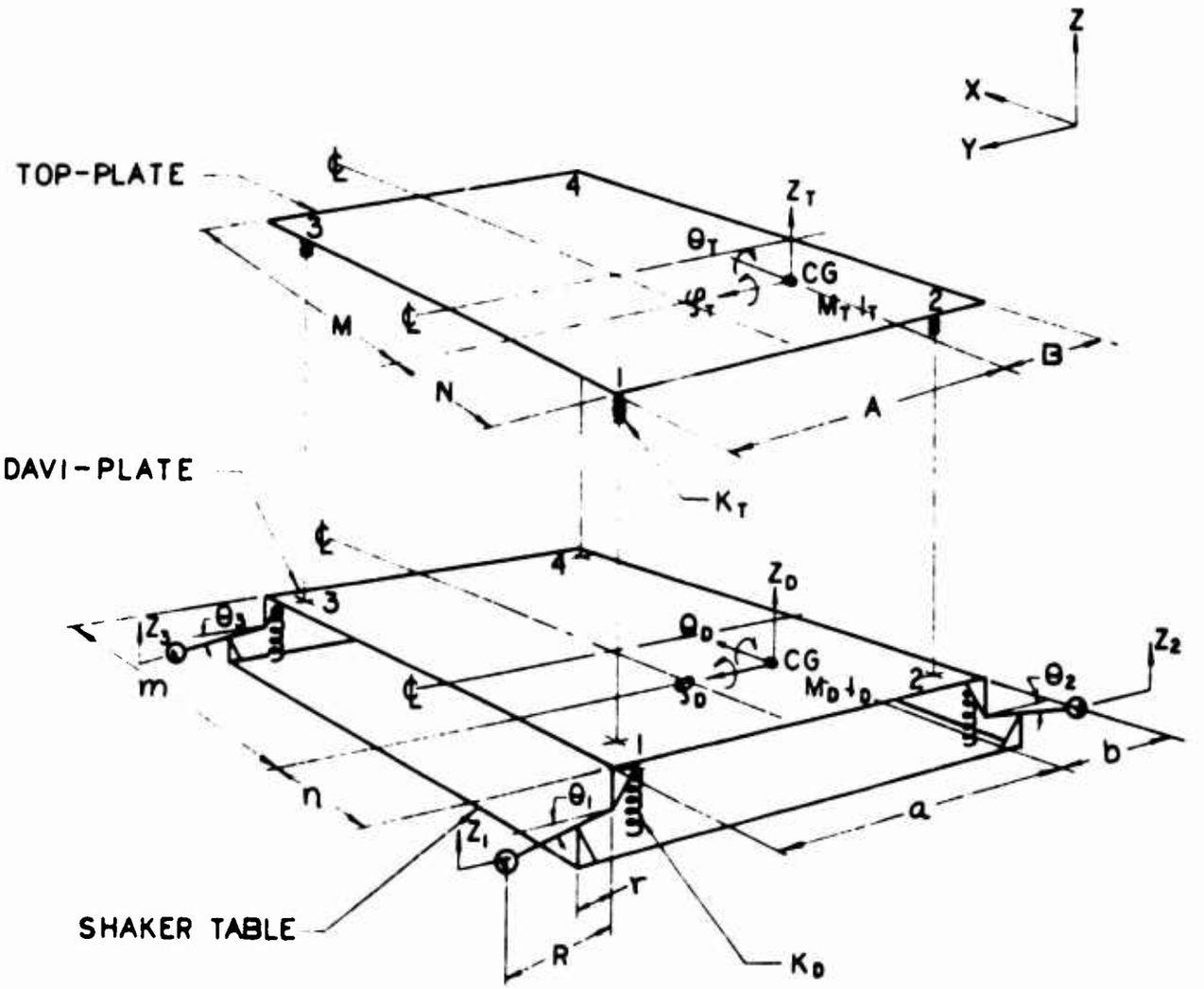

Figure 76. Series-Damped DAVI ℵ Platform Schematic

Figure 77. DAVI Model With Single Inertia Arm

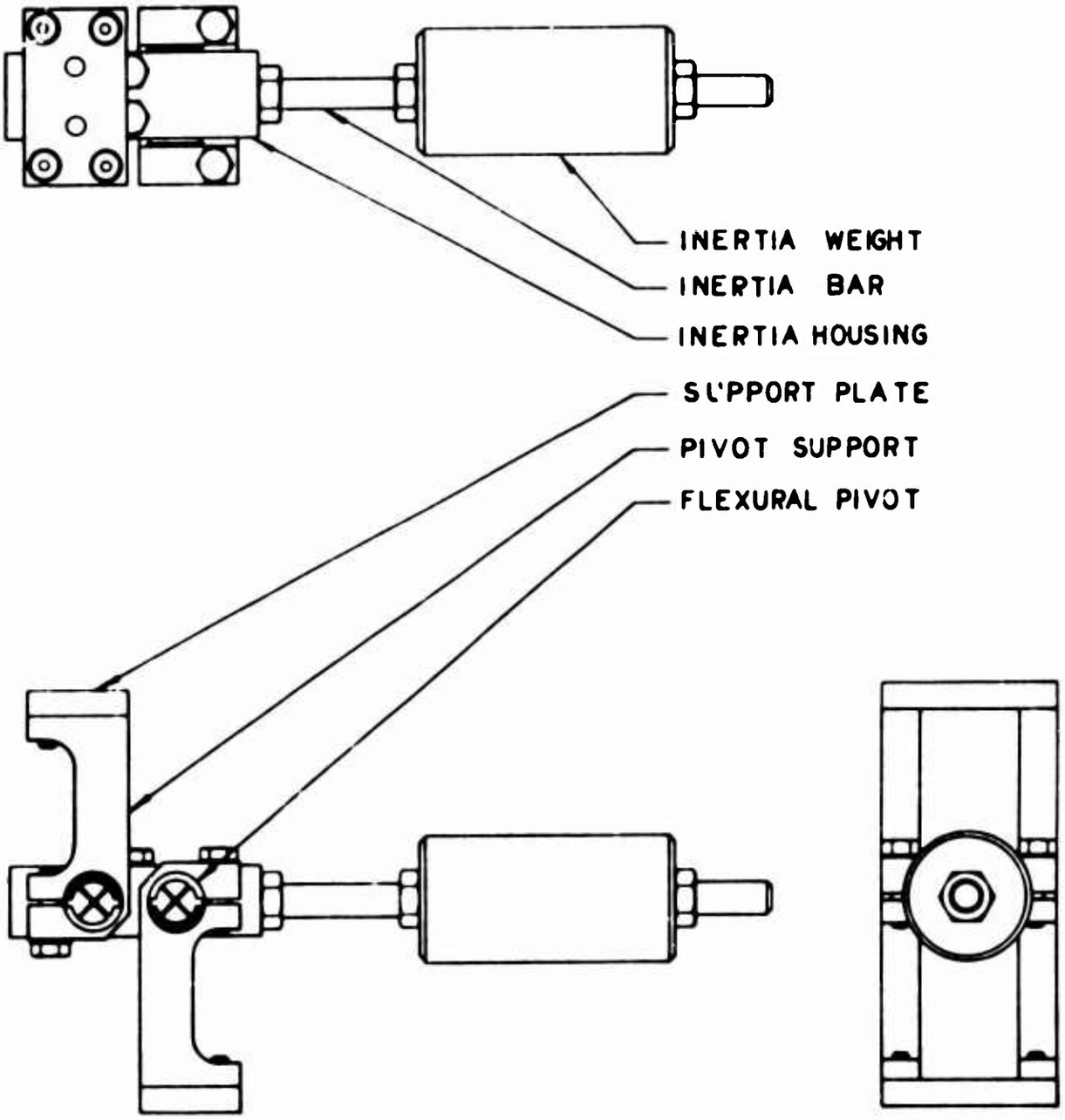

Figure 78. DAVI Assembly

Thus, vertical motion of each corner of each plate can be expressed as follows:

$$Z_{D_1} = Z_D + \theta_D a + \phi_D n \tag{54}$$

$$Z_{T_1} = Z_T + \theta_T A + \phi_T N \tag{55}$$

$$Z_{D_2} = Z_D - \theta_D b + \phi_D n \tag{56}$$

$$Z_{T_2} = Z_T - \theta_T B + \phi_T N \tag{57}$$

$$Z_{D_3} = Z_D + \theta_D a - \phi_D m \tag{58}$$

$$Z_{T_3} = Z_T + \theta_T A - \phi_T M \tag{59}$$

$$Z_{D_4} = Z_D - \theta_D b - \phi_D m \tag{60}$$

$$Z_{T_4} = Z_T - \theta_T B - \phi_T M \tag{61}$$

Next, the geometry of each DAVI bar rotating through angles θ_N (N = 1, 2, 3, 4) produces the following relations:

$$\theta_N = \frac{Z_{D_N} - Z_S}{r} = \frac{Z_{D_N} - Z_N}{R} \tag{62}$$

from which

$$Z_N = Z_{D_N}\left(1 - \frac{R}{r}\right) + \frac{R}{r} Z_S \tag{63}$$

where N = 1, 2, 3, 4 refers to conditions at each corner.

From (63) and (54):

$$z_1 = \left(1 - \frac{R}{r}\right)\left(z_D + \theta_D a + \phi_D n\right) + \frac{R}{r} z_S \quad (64)$$

From (63) and (56):

$$z_2 = \left(1 - \frac{R}{r}\right)\left(z_D - \theta_D b + \phi_D n\right) + \frac{R}{r} z_S \quad (65)$$

From (63) and (58):

$$z_3 = \left(1 - \frac{R}{r}\right)\left(z_D + \theta_D a - \phi_D m\right) + \frac{R}{r} z_S \quad (66)$$

From (63) and (60):

$$z_4 = \left(1 - \frac{R}{r}\right)\left(z_D - \theta_D b - \phi_D m\right) + \frac{R}{r} z_S$$

Next, from (62) and, in turn, (54), (56), (58), and (60):

$$\theta_1 = \frac{1}{r}\left(z_D + \theta_D a + \phi_D n\right) - \frac{1}{r} z_S \quad (67)$$

$$\theta_2 = \frac{1}{r}\left(z_D - \theta_D b + \phi_D n\right) - \frac{1}{r} z_S \quad (68)$$

$$\theta_3 = \frac{1}{r}\left(z_D - \theta_D a - \phi_D m\right) - \frac{1}{r} z_S \quad (69)$$

$$\theta_4 = \frac{1}{r}\left(z_D - \theta_D b - \phi_D m\right) - \frac{1}{r} z_S \quad (70)$$

The kinetic energy expression for the system can now be written:

$$T = \tfrac{1}{2} M_T \dot{z}_T^2 + \tfrac{1}{2} I_T \dot{\theta}_T^2 + \tfrac{1}{2} I_T \dot{\phi}_T^2 + \tfrac{1}{2} M_D \dot{z}_D^2 +$$

$$\tfrac{1}{2} I_D \dot{\theta}_D^2 + \tfrac{1}{2} I_D \dot{\phi}_D^2 +$$

$$\tfrac{1}{2} m_o \Big\{ \Big[(1 - \tfrac{R}{r})(\dot{z}_D + \dot{\theta}_D a + \dot{\phi}_D n) + \tfrac{R}{r} \dot{z}_S \Big]^2 +$$

$$\Big[(1 - \tfrac{R}{r})(\dot{z}_D - \dot{\theta}_D b + \dot{\phi}_D n + \tfrac{R}{r} \dot{z}_S \Big]^2 +$$

$$\Big[(1 - \tfrac{R}{r})(\dot{z}_D + \dot{\theta}_D a - \dot{\phi}_D m + \tfrac{R}{r} \dot{z}_S \Big]^2 +$$

$$\Big[(1 - \tfrac{R}{r})(\dot{z}_D - \dot{\theta}_D b - \dot{\phi}_D m) + \tfrac{R}{r} \dot{z}_S \Big]^2 \Big\} +$$

$$\tfrac{1}{2} \tfrac{I}{r^2} \Big[(\dot{z}_D - \dot{\theta}_D a + \dot{\phi}_D n - \dot{z}_S)^2 +$$

$$(\dot{z}_D - \dot{\theta}_D b + \dot{\phi}_D n - \dot{z}_S)^2 +$$

$$(\dot{z}_D + \dot{\theta}_D a - \dot{\phi}_D m - \dot{z}_S)^2 +$$

$$(\dot{z}_D - \dot{\theta}_D b - \dot{\phi}_D m - \dot{z}_S)^2 \Big] \quad (71)$$

The Potential Energy is:

$$V = \frac{1}{2} K_D \left[(z_D + \theta_D a + \phi_D n - z_S)^2 + \right.$$

$$z_D - \theta_D b + \phi_D n - z_S)^2 +$$

$$z_D + \theta_D a - \phi_D n - z_S)^2 +$$

$$\left. z_D - \theta_D b - \phi_D m - z_S)^2 \right] +$$

$$\frac{1}{2} K_T \left[(z_T + \theta_T A + \phi_T N - z_D - \theta_D a - \phi_D n)^2 + \right.$$

$$(z_T - \theta_T B + \phi_T N - z_D + \theta_D b - \phi_D n)^2 +$$

$$(z_T + \theta_T A - \phi_T M - z_D - \theta_D a + \phi_D m)^2 +$$

$$\left. (z_T - \theta_T B - \phi_T M - z_D + \theta_D b + \phi_D m)^2 \right] \quad (72)$$

Dissipation Function:

$$D = \tfrac{1}{2}C_{z_T}\dot{z}_T^2 + \tfrac{1}{2}C_{\theta_T}\dot{\theta}_T^2 + \tfrac{1}{2}C_{\phi_T}\dot{\phi}_T^2 + \tfrac{1}{2}C_{z_D}\dot{z}_D^2 + \tfrac{1}{2}C_{\phi_D}\dot{\phi}_D^2 +$$

$$\tfrac{1}{2}C_{\phi_D}{}^2\dot{\phi}_D^2 + \tfrac{1}{2}C_D\Big\{\Big[\Big(1-\tfrac{R}{r}\Big)\big(\dot{z}_D + \dot{\theta}_D a + \dot{\phi}_D n\big) + \tfrac{R}{r}\dot{z}_s\Big]^2 +$$

$$\Big[\Big(1-\tfrac{R}{r}\Big)\big(\dot{z}_D - \dot{\theta}_D b + \dot{\phi}_D n\big) + \tfrac{R}{r}\dot{z}_s\Big]^2 +$$

$$\Big[\Big(1-\tfrac{R}{r}\Big)\big(\dot{z}_D + \dot{\theta}_D a - \dot{\phi}_D m + \tfrac{R}{r}\dot{z}_s\Big]^2 +$$

$$\Big[\Big(1-\tfrac{R}{r}\Big)\big(\dot{z}_D - \dot{\theta}_D b - \dot{\phi}_D m + \tfrac{R}{r}\dot{z}_s\Big]^2\Big\} +$$

$$\tfrac{1}{2}C_\theta\Big[\big(\dot{z}_D + \dot{\theta}_D a + \dot{\phi}_D n - \dot{z}_s\big)^2 +$$

$$\big(\dot{z}_D - \dot{\theta}_D b + \dot{\phi}_D n - \dot{z}_s\big)^2 +$$

$$\big(\dot{z}_D + \dot{\theta}_D a - \dot{\phi}_D m - \dot{z}_s\big)^2 +$$

$$\big(\dot{z}_D - \dot{\theta}_D b - \dot{\phi}_D m - \dot{z}_s\big)^2\Big] \quad (73)$$

EQUATIONS OF MOTION

The equations of motion are derived by Lagrangian methods. After grouping terms they are:

Z_T equation

$$M_T \ddot{Z}_T + C_{Z_T} \dot{Z}_T + 4K_T Z_T + 2K_T (A-B)\Theta_T - 2K_T (M-N)\Phi_T - 4K_T Z_D - 2K_T (a-b)\Theta_D + 2K_T (m-n)\Phi_D = 0 \quad (74)$$

Θ_T equation

$$2K_T (A-B) Z_T + I_T \ddot{\Theta}_T + C_{\Theta_T} \dot{\Theta}_T + 2K_T (A^2+B^2)\Theta_T - K_T (A-B)(M-N)\Phi_T - 2K_T (A-B) Z_D - 2K_T (Aa+Bb)\Theta_D + K_T (A-B)(m-n)\Phi_D = 0 \quad (75)$$

Φ_T equation

$$-2K_T (M-N) Z_T - K_T (A-B)(M-N)\Theta_T + I_T \ddot{\Phi}_T + C_{\Phi_T} \dot{\Phi}_T + 2K_T (M^2+N^2)\Phi_T + 2K_T (M-N) Z_D + K_T (a-b)(M-N)\Theta_D - 2K_T (Mm+Nn)\Phi_D = 0 \quad (76)$$

Θ_D equation

$$2\left[m_o\left(1-\frac{R}{r}\right)^2+\frac{I}{r^2}\right](a-b)\ddot{z}_D+2\left[\left(1-\frac{R}{r}\right)^2 C_D+C_\Theta\right](a-b)\dot{z}_D +$$

$$2(K_D+K_T)(a-b)z_D +$$

$$\left\{I_D+2(a^2+b^2)\left[m_o\left(1-\frac{R}{r}\right)^2+\frac{I}{r^2}\right]\right\}\ddot{\Theta}_D +$$

$$\left\{C_{\Theta_D}+2(a^2+b^2)\left[\left(1-\frac{R}{r}\right)^2 C_D+C_\Theta\right]\right\}\dot{\Theta}_D +$$

$$2(a^2+b^2)(K_D+K_T)\Theta_D-(a-b)(m-n)\left[\left(1-\frac{R}{r}\right)^2 m_o+\frac{I}{r^2}\right]\ddot{\Phi}_D-$$

$$(a-b)(m-n)\left[\left(1-\frac{R}{r}\right)^2 C_D+C_\Theta\right]\dot{\Phi}_D-$$

$$(a-b)(m-n)(K_D+K_T)\Phi_D-2K_T(a-b)z_T -$$

$$-2(Aa+Bb)\Theta_T K_T+(M-N)(a-b)\Phi_T K_T$$

$$= 2(a-b)\left[-\frac{R}{r}\left(1-\frac{R}{r}\right)m_o+\frac{I}{r^2}\right]\ddot{z}_S +$$

$$2(a-b)\left[-\frac{R}{r}\left(1-\frac{R}{r}\right)C_D+C_\Theta\right]\dot{z}_S+2(a-b)K_D z_S \quad (77)$$

Φ_D equation

$$-2(m-n)\left[\left(1-\frac{R}{r}\right)^2 m_o + \frac{I}{r^2}\right]\ddot{z}_D + 2(n^2+m^2)(K_D+K_T)\phi_D -$$

$$2(m-n)\left[\left(1-\frac{R}{r}\right)^2 C_D + C_\theta\right]\dot{z}_D - 2(m-n)(K_D+K_T)z_D -$$

$$(m-n)(a-b)\left[\left(1-\frac{R}{r}\right)^2 m_o + \frac{I}{r^2}\right]\ddot{\theta}_D -$$

$$(m-n)(a-b)\left[\left(1-\frac{R}{r}\right)^2 C_D + C_\theta\right]\dot{\theta}_D -$$

$$(m-n)(a-b)(K_T+K_D)\theta_D +$$

$$\left\{I_D + 2(m^2+n^2)\left[\left(1-\frac{R}{r}\right)^2 m_o + \frac{I}{r^2}\right]\right\}\ddot{\Phi}_D +$$

$$\left\{C\phi_D + 2(m^2+n^2)\left[\left(1-\frac{R}{r}\right)^2 C_D + C_\theta\right]\right\}\dot{\Phi}_D + 2K_T(m-n)z_T +$$

$$(A-B)(m-n)K_T\theta_T - 2(Mm+Nn)\Phi_T K_T$$

$$= 2(m-n)\left[\frac{R}{r}\left(1-\frac{R}{r}\right)m_o - \frac{I}{r^2}\right]\ddot{z}_S +$$

$$2(m-n)\left[\frac{R}{r}\left(1-\frac{R}{r}\right)C_D - C_\theta\right]\dot{z}_S - 2K_D(m-n)z_S \quad (78)$$

Z_D equation

$$\left[M_D + 4m_o\left(1-\frac{R}{r}\right)^2 + 4\frac{I}{r^2}\right]\ddot{z}_D + \left[C_{ZD} + 4\left(1-\frac{R}{r}\right)^2 C_D + 4C_\Theta\right]\dot{z}_D +$$

$$4(K_D+K_T)z_D\, 2(a-b)\left[m_o\left(1-\frac{R}{r}\right)^2 + \frac{I}{r^2}\right]\ddot{\theta}_D +$$

$$2(a-b)\left[\left(1-\frac{R}{r}\right)^2 C_D + C_\Theta\right]\dot{\theta}_D + 2(a-b)(K_D+K_T)\theta_D +$$

$$2(m-n)\left[m_o\left(1-\frac{R}{r}\right)^2 + \frac{I}{r^2}\right]\ddot{\Phi}_D -$$

$$2(m-n)\left[\left(1-\frac{R}{r}\right)^2 C_D + C_\Theta\right]\dot{\Phi}_D +$$

$$2(m-n)(K_D+K_T)\Phi_D - 2K_T(A-B)\Theta_T +$$

$$2K_T(M-N)\Phi_T - 4K_T z_T$$

$$= 4\left[m_o\frac{R}{r}\left(1-\frac{R}{r}\right) - \frac{I}{r^2}\right]\ddot{z}_S -$$

$$4\left[\frac{R}{r}\left(1-\frac{R}{r}\right)C_D - C_\Theta\right]\dot{z}_S - 4K_D z_S \qquad (79)$$

$-M_T\omega^2+C_{z_T}i\omega+4K_T$	$2K_T(A-B)$	$-2K_T(M-N)$	$-4K_T$	
$2K_T(A-B)$	$-I_T\omega^2+C_{\theta T}i\omega$ $+2K_T(A^2+B^2)$	$-(A-B)(M-N)K_T$	$-2K_T(A-B)$	-2
$-2K_T(M-N)$	$-K_T(A-B)(M-N)$	$-I_T\omega^2+C_{\phi_T}i\omega$ $+2K_T(M^2+N^2)$	$2K_T(M-N)$	K_T
$-4K_T$	$-2K_T(A-B)$	$2K_T(M-N)$	$-\{M_D+4m_o(1-\frac{R}{r})^2+4\frac{I}{r^2}\}\omega^2$ $+\{C_{z_D}+4(1-\frac{R}{r})^2C_D+4C_\theta\}i\omega$ $+4(K_D+K_T)$	$-2(a$ $+2(a$ $+$
$-2(a-b)K_T$	$-2(Aa+Bb)K_T$	$(M-N)(a-b)K_T$	$-2(a-b)\{(1-\frac{R}{r})^2m_o+\frac{I}{r^2}\}\omega^2$ $+2(a-b)\{(1-\frac{R}{r})^2C_D+C_\theta\}i\omega$ $+2(a-b)(K_D+K_T)$	$-\{I_D+$ $+\{C_{\theta_D}+$ $+$
$2K_T(m-n)$	$(A-B)(m-n)K_T$	$-2(Mm+Nn)K_T$	$2(m-n)[\{(1-\frac{R}{r})^2m_o+\frac{I}{r^2}\}\omega^2$ $-\{(1-\frac{R}{r})^2C_D+C_\theta\}i\omega$ $-(K_D+K_T)]$	$(m-r$ $x[$ $-\{(1-$

Figure 79. Equations of Motion for the S

$$
\begin{bmatrix}
 & -2K_T(a-b) & 2K_T(m-n) & \\
 & -2K_T(Aa+Bb) & K_T(A-B)(m-n) & \\
 & K_T(a-b)(M-N) & -2K_T(Mm+Nn) & \\
\omega^2 & -2(a-b)\left\{\left(1-\frac{R}{r}\right)^2 m_o+\frac{I}{r^2}\right\}\omega^2 & +2(m-n)\left\{m_o\left(1-\frac{R}{r}\right)^2+\frac{I}{r^2}\right\}\omega^2 & \\
i\omega & +2(a-b)\left\{\left(1-\frac{R}{r}\right)^2 C_D+C_\bullet\right\}i\omega & -2(m-n)\left\{\left(1-\frac{R}{r}\right)^2 C_D+C_\bullet\right\}i\omega & \\
 & +2(a-b)(K_D+K_T) & +2(m-n)(K_D+K_T) & \\
 & -\{I_D+2(a^2+b^2)\}\left\{\left(1-\frac{R}{r}\right)^2 m_o+\frac{I}{r^2}\right\}\omega^2 & (a-b)(m-n)\left\{\left(1-\frac{R}{r}\right)^2 m_o+\frac{I}{r^2}\right\}\omega^2 & \\
i\omega & +\{C_{\theta_D}+2(a^2+b^2)\}\left(1-\frac{R}{r}\right)^2 C_D+C_\bullet\}i\omega & -(a-b)(m-n)\left\{\left(1-\frac{R}{r}\right)^2 C_D+C_\bullet\right\}i\omega & \\
 & +2(a^2+b^2)(K_D+K_T) & -(a-b)(m-n)(K_D+K_T) & \\
\omega^2 & (m-n)(a-b) & -[I_D+2(m^2+n^2)\left\{\left(1-\frac{R}{r}\right)^2 m_o+\frac{I}{r^2}\right]\omega^2 & \\
 & \times\left[\left\{\left(1-\frac{R}{r}\right)^2 m_o+\frac{I}{r^2}\right\}\omega^2\right. & +\left[C_{\phi_D}+2(m^2+n^2)\left\{\left(1-\frac{R}{r}\right)^2 C_D+C_\bullet\right\}i\omega\right. & \\
 & \left.-\left\{\left(1-\frac{R}{r}\right)^2 C_D+C_\bullet\right\}i\omega\right. & \left.+2(m^2+n^2)(K_D+K_T)\right. & \\
 & \left.-(K_D+K_T)\right] & &
\end{bmatrix}
\begin{bmatrix} Z_T \\ \theta_T \\ \phi_T \\ Z_D \\ \theta_D \\ \phi_D \end{bmatrix}
=
\begin{bmatrix}
\left\{\frac{R}{r}\left(1-\frac{R}{r}\right)m_o-\frac{I}{r^2}\right\}\omega^2 \\
+\left\{\frac{R}{r}\left(1-\frac{R}{r}\right)C_D-C_\bullet\right\}i\omega \\
-K_D
\end{bmatrix} Z_S
\begin{bmatrix} 0 \\ 0 \\ 0 \\ -4 \\ -2(a-b) \\ 2(m-n) \end{bmatrix}
$$

(80

r the Six-Degree-of-Freedom DAVI Platform

TEST RESULTS

DAVI α Isolated Platform

Tables 33 through 38 give the numerical results and Figures 80 through 85 show the graphical results of the tests conducted on the DAVI α Isolated Platform. These tests were conducted for isolated weights of 55, 150, and 200 pounds with a neutral center of gravity. Three-inch lateral and longitudinal offset center of gravity tests were conducted at 150 pounds, and a test with a 3-inch lateral offset center of gravity at 200 pounds was done also.

It is seen from these results that although the magnitude of the isolated mass did change the natural frequency of the system, it did not affect the antiresonant frequency and that over 98-percent isolation at this frequency was obtained in all cases.

Series-Damped DAVI γ Isolated Platform

Table 39 and Figure 86 give the numerical and graphical results of the Series-Damped DAVI γ Isolated Platform test. This platform was constructed as shown in Figure 76. Conventional rubber mounts were used between the intermediate or DAVI-plate and the isolated platform. No external damping was used, and only damping obtained from the conventional rubber isolators is reflected in the testing. It is seen from the test results that two modes of motion were obtained, and at the natural frequencies the transmissibilities were greater than 1.0. This was due to the minimum amount of damping in the system. It is also seen that the antiresonance was not affected by the introduction of the Series System and that 97-percent isolation was obtained. The high frequency isolation as obtained in the test approached zero as in a conventional isolator. Analysis has shown that, with proper damping, over 50-percent isolation could be obtained for the second mode of motion on the Series-Damped DAVI.

Tables 40 and 41 show the numerical results and Figures 87 and 88 give the graphical results of the vertical and lateral excitations on the Series-Damped DAVI γ Isolated Platform. It is seen from these results that the vertical isolation was not affected by the lateral input.

Single DAVI α

Table 42 and Figure 89 give the results of a test on a Single DAVI α. These results, when compared to the results of the DAVI α Isolated Platform, are essentially the same, and they give the same antiresonant frequency. It is seen, therefore, that the four DAVI's acting in parallel did not affect the tuned frequency.

Conventional Isolation System

Table 43 and Figure 90 give the results of a test made on a conventional isolation system. This conventional system was obtained by removing the DAVI's and leaving only the spring. This was done for a 158-pound isolated weight with a neutral center of gravity. Therefore, a direct comparison can be made between Figure 90 and Figure 81, the results of the same condition, but with DAVI isolation. It is seen with this comparison that the DAVI isolated platform had a natural frequency of 6.8 c.p.s. and the conventional system had a natural frequency of 9.0 c.p.s., even though the spring rates are identical. The DAVI isolated platform started to isolate at 8.0 c.p.s., below the resonance of the conventional system, whereas the conventional system started to isolate at 12.5 c.p.s. At the tuned frequency of the DAVI, 98-percent isolation was obtained, and at this frequency the conventional system had an amplification of 5.57. The frequency at which the isolation for both systems became identical is approximately 17.5 c.p.s.

Correlation

Correlation of the analytical and test results was made. The results of the calculations are shown on Figures 81, 83, 85, and 86 and compared directly to the test results. Although equations of motion for six degrees of freedom were derived, only the analysis of the single degree of freedom of the DAVI α was required to correlate the results given in Figures 81, 83, and 85. The two-degree-of-freedom Series-Damped DAVI γ equations were used to correlate the results of Figure 86. It is seen from these results that excellent correlation was obtained.

TABLE 33

DAVI ∝ ISOLATED PLATFORM TRANSMISSIBILITY TEST DATA
CENTRAL CENTER OF GRAVITY
ISOLATED WEIGHT, 55 POUNDS

Frequency (c.p.s.)	Input	Output	Output / Input
5.0	3.20	4.00	1.25
5.5	3.70	5.00	1.35
6.0	4.20	5.70	1.35
6.2	4.40	6.00	1.36
6.4	4.50	6.50	1.44
6.6	4.70	7.50	1.59
6.8	4.80	8.00	1.67
7.0	5.00	8.80	1.76
7.2	4.90	9.50	1.93
7.4	4.60	10.50	2.28
7.6	3.80	11.00	2.89
7.8	2.80	10.50	3.75
8.0	1.30	9.20	7.07
8.2	.15	7.00	46.70
8.4	1.00	5.20	5.20
8.6	1.70	4.00	5.41
8.8	2.10	3.00	1.42
9.0	2.50	2.20	.88
9.2	2.80	1.50	.53
9.4	2.90	1.05	.36
9.6	3.20	.65	.20
9.8	3.30	.30	.09
10.0	3.50	.04	.01
10.2	3.50	.25	.07
10.4	3.50	.45	.13
10.6	3.70	.60	.16
10.8	3.50	.70	.20
11.0	3.60	.85	.24
11.2	3.60	.95	.26
11.4	3.80	1.10	.29
11.6	3.50	1.15	.33
11.8	3.50	1.20	.34
12.0	3.60	1.30	.36
12.5	3.50	1.40	.40
13.0	3.30	1.40	.42
13.5	3.20	1.40	.44
14.0	2.80	1.30	.46

TABLE 33 **(Continued)**

Frequency (c.p.s.)	Input	Output	Output / Input
14.5	2.80	1.30	.46
15.0	2.60	1.30	.50
16.0	2.30	1.20	.52
17.0	2.00	1.10	.55
18.0	1.70	1.05	.62
19.0	1.50	.95	.63
20.0	1.40	.85	.61
22.0	1.05	.70	.66
24.0	.85	.60	.71
26.0	.65	.50	.77
28.0	.52	.42	.81
30.0	.45	.38	.84
32.0	.35	.33	.94
34.0	.29	.29	1.00
36.0	.24	.25	1.04
38.0	.19	.23	1.21
40.0	.16	.21	1.31
42.0	.12	.19	1.58
44.0	.12	.19	1.58
46.0	.10	.17	1.78
48.0	.06	.16	2.67
50.0	.06	.17	2.83
52.0	.06	.15	2.50
54.0	.02	.15	6.82
56.0	.03	.15	5.00
58.0	.08	.10	1.25
60.0	.04	.15	4.29
62.0	.05	.16	3.20
64.0	.10	.18	1.80
66.0	.15	.16	1.07
68.0	.10	.15	1.50
70.0	.19	.23	1.21
72.0	.33	.23	.69
74.0	.13	.08	.58
76.0	.13	.05	.35
78.0	.06	.10	1.67
80.0	.11	.16	1.52

TABLE 33 **(Continued)**

Frequency (c.p.s.)	Input	Output	$\frac{\text{Output}}{\text{Input}}$
82.0	.34	.38	1.11
84.0	.19	.08	.42
86.0	.11	.16	1.46
88.0	.28	.37	1.32
90.0	.20	.13	.65
92.0	.16	.15	.94
94.0	.10	.17	1.70
96.0	.02	.28	14.00
98.0	.05	.15	3.08
100.0	.07	.06	.89

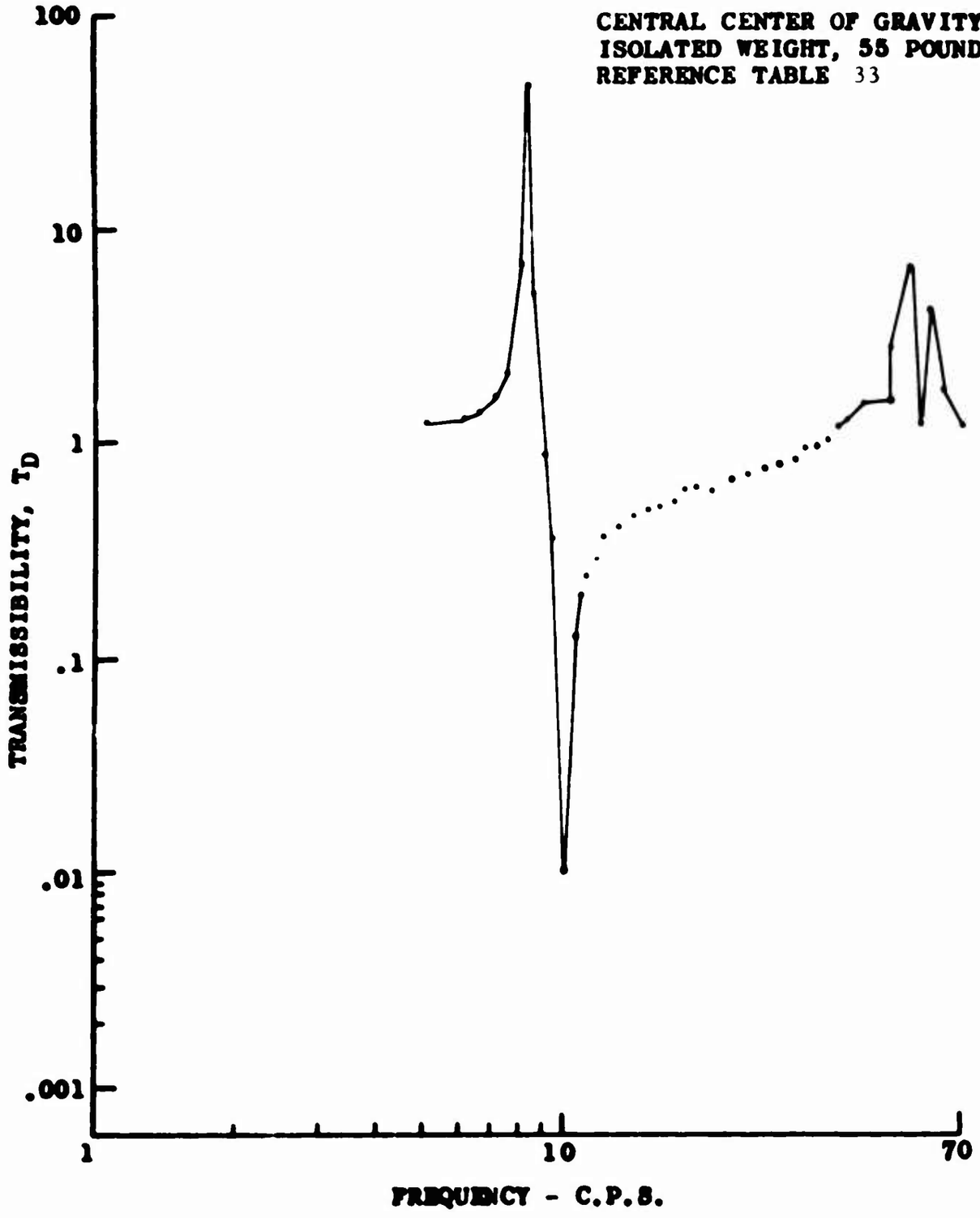

Figure 80. Response Curve for DAVI ∝ Isolated Platform

TABLE 34

DAVI OC ISOLATED PLATFORM TRANSMISSIBILITY TEST DATA
CENTRAL CENTER OF GRAVITY
ISOLATED WEIGHT, 150 POUNDS

Frequency (c.p.s.)	Input	Output	$\frac{\text{Output}}{\text{Input}}$
5.0	16.00	80.00	1.75
5.2	16.00	84.00	1.87
5.4	16.00	89.00	2.06
5.6	15.00	92.00	2.33
5.8	13.00	88.00	2.69
6.0	11.00	75.00	3.00
6.2	8.50	96.00	3.76
6.4	6.00	90.00	5.16
6.6	3.30	76.00	8.48
6.8	0.75	58.00	29.30
6.9	1.15	50.00	16.52
7.0	1.80	49.00	10.50
7.2	3.80	45.00	4.47
7.4	5.50	40.00	2.72
7.6	7.00	35.00	1.85
7.8	8.50	36.50	1.29
8.0	10.00	16.00	1.00
8.2	11.00	17.00	.81
8.4	12.50	15.00	.60
8.6	13.50	12.50	.48
8.8	15.00	10.50	.36
9.0	16.00	8.00	.28
9.2	17.00	6.00	.21
9.4	18.00	4.70	.15
9.6	18.00	3.10	.10
9.8	19.00	1.30	.06
10.0	20.00	.45	.02
10.2	21.00	1.50	.03
10.4	22.00	2.90	.06
10.6	22.00	4.10	.08
10.8	22.00	5.10	.11
11.0	23.00	6.10	.13
11.2	23.00	7.00	.15
11.4	23.00	8.30	.16
11.6	23.00	9.20	.19
11.8	24.00	10.10	.19
12.0	24.00	11.00	.21
12.5	23.50	17.50	.24

TABLE 34 **(Continued)**

Frequency (c.p.s.)	Input	Output	Output / Input
13.0	23.00	6.80	.25
13.5	23.00	9.10	.27
14.0	22.00	9.50	.29
15.0	20.00	10.00	.29
16.0	18.00	7.70	.34
17.0	16.00	8.40	.38
18.0	14.50	7.10	.40
19.0	13.50	6.60	.41
20.0	12.00	6.00	.43
22.0	10.00	5.10	.48
24.0	8.80	4.65	.50
26.0	7.20	4.35	.55
28.0	6.20	3.10	.59
30.0	5.20	2.80	.67
32.0	4.50	2.60	.73
34.0	3.70	2.30	.86
36.0	2.90	1.90	1.00
38.0	2.10	1.70	1.24
40.0	1.30	1.40	1.69
42.0	.90	1.40	2.11
44.0	.85	.50	1.88
46.0	1.05	.30	1.57
48.0	1.20	2.30	2.33
50.0	1.80	1.80	1.51
52.0	2.60	.50	1.11
54.0	3.80	1.60	.78
56.0	4.80	1.90	.64
58.0	5.80	1.50	.48
60.0	6.80	1.30	.44
62.0	9.00	2.00	.42
64.0	10.50	1.60	.36
66.0	11.00	1.10	.35
68.0	11.50	1.00	.29
70.0	12.00	.90	.25
72.0	11.50	.70	.28
74.0	7.00	.40	.30
76.0	3.50	.40	.49

TABLE 34 **(Continued)**

Frequency (c.p.s.)	Input	Output	$\frac{\text{Output}}{\text{Input}}$
78.0	6.00	1.05	.41
80.0	6.20	1.10	.89
82.0	4.00	.50	.68
84.0	2.80	.30	.50
86.0	3.00	.40	.57
88.0	3.90	.45	.51
90.0	5.00	.50	.50
92.0	5.00	.45	.38
94.0	3.30	.45	.64
96.0	4.20	.45	.50
98.0	5.50	.48	.36
100.0	7.50	.48	.29

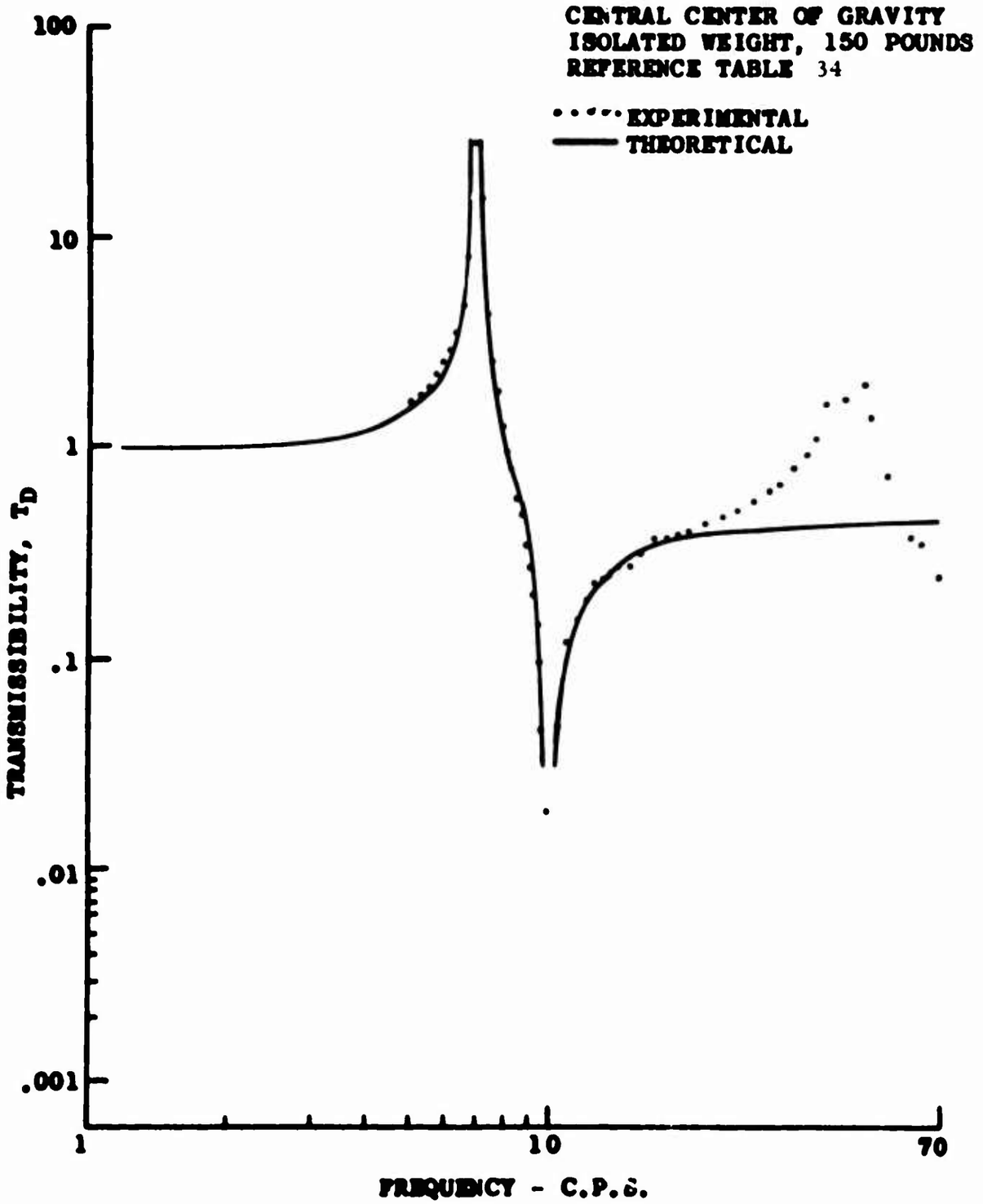

Figure 81. Response Curve for DAVI ∝ Isolated Platform

TABLE 35

DAVI α ISOLATED PLATFORM TRANSMISSIBILITY TEST DATA
CENTRAL CENTER OF GRAVITY
ISOLATED WEIGHT, 200 POUNDS

Frequency (c.p.s.)	Input	Output	Output / Input
5.0	6.70	14.00	2.08
5.2	6.00	15.00	2.50
5.4	4.80	13.50	2.81
5.6	4.20	14.00	3.33
5.8	3.00	13.00	4.33
6.0	2.00	12.50	6.25
6.2	1.05	12.50	11.90
6.4	.45	10.00	22.22
6.6	.95	7.00	7.37
6.8	1.60	6.00	3.75
7.0	2.20	5.80	2.64
7.2	2.90	4.80	1.66
7.4	3.30	4.50	1.36
7.6	3.80	3.40	.89
7.8	4.30	3.50	.81
8.0	4.80	3.30	.69
8.2	5.20	2.90	.56
8.4	5.80	2.50	.43
8.6	6.00	2.20	.37
8.8	6.50	1.80	.28
9.0	7.00	1.50	.21
9.2	7.30	1.20	.16
9.4	8.00	.98	.12
9.6	8.30	.70	.08
9.8	8.80	.45	.05
10.0	9.20	.28	.03
10.1	9.50	.23	.02
10.2	10.00	.25	.03
10.4	10.50	.44	.04
10.6	10.50	.65	.06
10.8	10.50	.88	.08
11.0	11.00	1.10	.10
11.2	11.00	1.30	.12
11.4	11.00	1.50	.14
11.6	11.00	1.75	.16
11.8	11.50	1.90	.17
12.0	12.00	2.20	.18

TABLE 35 (Continued)

Frequency (c.p.s.)	Input	Output	Output / Input
12.5	11.50	1.80	.16
13.0	11.50	2.30	.20
13.5	11.50	2.50	.22
14.0	11.00	2.60	.24
15.0	10.00	2.70	.27
16.0	9.20	2.80	.30
17.0	8.20	2.60	.32
18.0	7.80	2.50	.32
19.0	6.80	2.50	.37
20.0	6.20	2.40	.39
22.0	5.20	2.20	.42
24.0	4.50	2.00	.44
26.0	3.80	1.90	.50
28.0	3.20	1.80	.56
30.0	2.60	1.80	.69
32.0	2.20	1.70	.77
34.0	1.60	1.60	1.00
36.0	1.10	1.30	1.18
38.0	.88	1.30	1.48
40.0	.55	1.15	2.09
42.0	.45	1.10	2.44
44.0	.65	1.05	1.62
46.0	.75	1.10	1.47
48.0	1.05	1.50	1.43
50.0	1.40	1.50	1.07
52.0	2.30	1.80	.78
54.0	3.20	2.00	.62
56.0	3.70	2.40	.65
58.0	4.20	2.00	.48
60.0	4.50	2.20	.49
62.0	5.50	2.30	.42
64.0	3.40	2.10	.62
66.0	3.80	2.00	.53
68.0	4.40	1.80	.41
70.0	3.40	1.10	.32
72.0	2.10	1.30	.62
74.0	2.40	1.50	.63

TABLE 35 **(Continued)**

Frequency (c.p.s.)	Input	Output	Output / Input
76.0	3.30	1.75	.53
78.0	4.60	2.20	.48
80.0	4.50	2.40	.53
82.0	7.50	3.20	.43
84.0	1.30	1.70	1.31
86.0	2.50	2.30	.92
88.0	3.40	2.70	.79
90.0	4.40	2.70	.61
92.0	4.70	1.60	.34
94.0	2.40	.50	.21
96.0	3.10	.44	.14
98.0	4.80	.63	.13
100.0	7.00	.65	.09

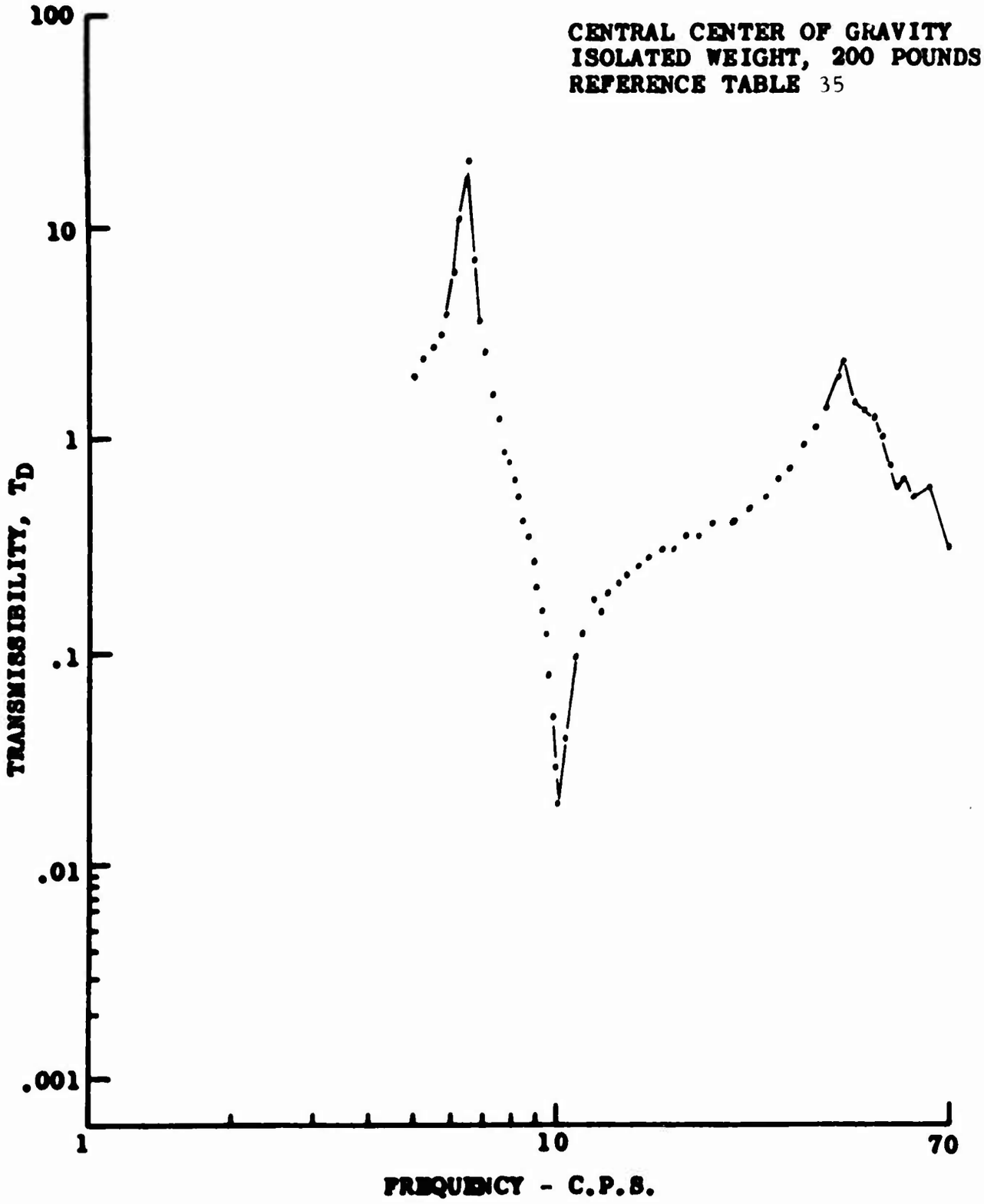

Figure 82. Response Curve for DAVI ∝ Isolated Platform

TABLE 36

DAVI α ISOLATED PLATFORM TRANSMISSIBILITY TEST DATA
3-INCH LATERAL OFFSET CENTER OF GRAVITY
ISOLATED WEIGHT, 150 POUNDS

Frequency (c.p.s.)	Input	Output	$\frac{\text{Output}}{\text{Input}}$
5.6	17.50	28.50	1.63
5.8	19.50	35.00	1.79
6.0	22.80	45.00	1.97
6.2	25.50	58.00	2.27
6.4	27.50	72.00	2.62
6.6	24.00	77.00	3.21
6.8	17.00	69.00	4.06
7.0	10.50	57.00	5.43
7.2	7.60	46.00	6.05
7.4	5.60	37.00	6.61
7.6	5.60	28.50	5.09
7.8	7.10	25.00	3.52
8.0	8.50	20.50	2.41
8.2	10.50	17.50	1.67
8.4	12.70	14.50	1.14
8.6	13.00	12.60	.97
8.8	14.00	11.50	.82
9.0	15.00	9.70	.65
9.2	16.50	8.00	.49
9.4	17.80	6.40	.36
9.6	18.80	5.50	.29
9.8	20.00	4.40	.22
10.0	21.50	3.20	.15
10.2	23.00	.46	.02
10.4	23.00	1.62	.07
10.6	25.00	1.75	.07
10.8	26.00	2.10	.08
11.0	28.00	2.80	.10
11.2	30.00	2.95	.10
11.4	29.00	3.90	.13
11.6	30.00	4.50	.15
11.8	31.00	5.20	.17
12.0	32.00	5.90	.18
12.5	34.00	7.50	.22
13.0	36.00	8.60	.24
13.5	35.00	10.70	.31
14.0	36.00	45.00	1.25

TABLE 36 **(Continued)**

Frequency (c.p.s.)	Input	Output	Output / Input
14.5	34.80	17.50	.50
15.0	31.50	16.40	.52
15.5	30.00	12.10	.40
16.0	29.00	11.60	.40
16.5	26.00	11.00	.42
17.0	24.50	10.50	.42
18.0	20.50	9.30	.45
19.0	17.50	8.20	.47
20.0	15.00	7.20	.48
22.0	12.70	7.50	.59
24.0	13.00	9.50	.73
26.0	9.60	6.70	.70
28.0	7.80	5.30	.68
30.0	6.50	4.70	.72
32.0	5.60	4.00	.71
34.0	4.40	3.50	.80
36.0	4.10	3.60	.88
38.0	4.20	3.90	.93
40.0	4.00	4.00	1.00
42.0	3.80	4.00	1.05
44.0	3.20	4.10	1.28
46.0	3.40	3.80	1.12
48.0	4.40	4.20	.95
50.0	3.50	3.50	1.00
52.0	4.40	4.40	1.00
54.0	6.50	10.50	1.62
56.0	9.80	11.00	1.12
58.0	9.00	10.90	1.21
60.0	5.50	6.30	1.15
62.0	7.20	4.90	.68
64.0	8.20	3.75	.46
66.0	10.60	3.15	.30
68.0	13.30	3.30	.25
70.0	13.50	4.50	.33
72.0	15.20	4.50	.30
74.0	27.00	5.80	.21
76.0	30.50	5.55	.18

TABLE 36 **(Continued)**

Frequency (c.p.s.)	Input	Output	$\frac{\text{Output}}{\text{Input}}$
78.0	32.00	4.78	.15
80.0	29.00	3.90	.13
82.0	32.00	3.90	.12
84.0	32.00	4.90	.15
86.0	36.00	5.90	.16
88.0	30.00	6.70	.22
90.0	42.00	9.50	.23

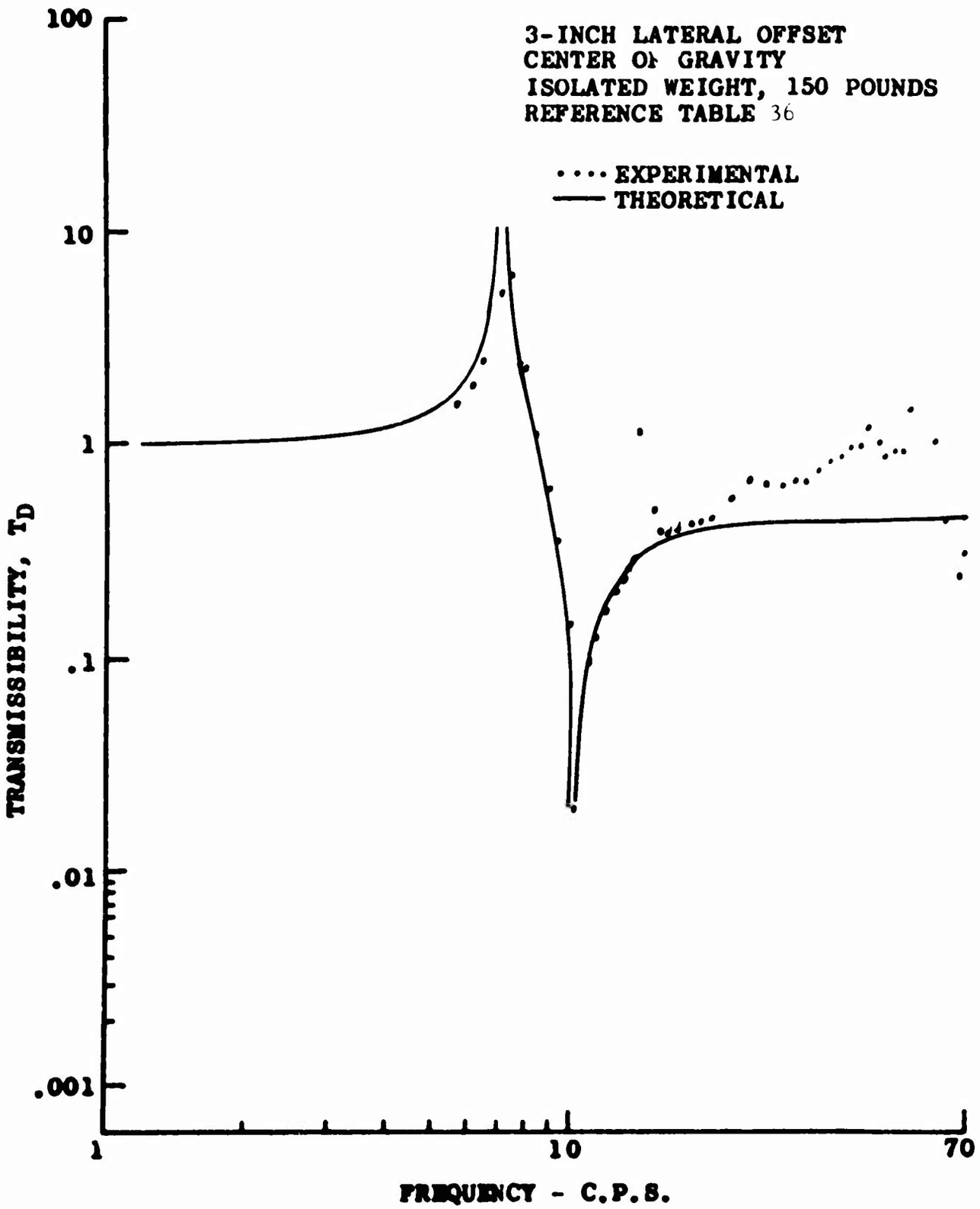

Figure 83. Response Curve for DAVI ∝ Isolated Platform

TABLE 37

DAVI α ISOLATED PLATFORM TRANSMISSIBILITY TEST DATA
3-INCH LONGITUDINAL OFFSET CENTER OF GRAVITY
ISOLATED WEIGHT, 150 POUNDS

Frequency (c.p.s.)	Input	Output	Output / Input
5.0	9.70	13.50	1.39
5.2	10.90	15.80	1.45
5.4	12.50	18.50	1.44
5.6	14.10	22.30	1.58
5.8	15.90	28.00	1.76
6.0	19.00	34.00	1.79
6.2	20.00	44.00	2.20
6.4	22.00	57.00	2.59
6.6	19.50	59.00	3.03
6.8	13.30	51.50	3.87
7.0	8.55	42.50	4.97
7.1	12.50	38.50	3.08
7.2	6.40	34.00	5.31
7.4	6.10	26.50	4.34
7.6	5.60	23.00	4.11
7.8	5.65	19.00	3.36
7.9	5.49	16.60	3.02
8.0	6.75	15.50	2.30
8.2	8.00	12.40	1.55
8.4	9.60	10.30	1.07
8.6	9.80	7.70	.79
8.8	12.60	11.40	.91
9.0	14.20	11.70	.82
9.2	16.00	12.00	.75
9.4	14.20	8.80	.62
9.6	15.50	6.80	.44
9.8	16.50	5.10	.31
10.0	17.50	3.85	.22
10.2	18.80	4.70	.03
10.4	31.00	1.00	.03
10.6	21.50	.95	.04
10.8	35.50	1.60	.05
11.0	37.00	2.40	.07
11.2	38.00	3.40	.09
11.4	38.00	4.40	.12
11.6	41.00	5.70	.14
11.8	43.00	6.80	.16

TABLE 37 (Continued)

Frequency (c.p.s.)	Input	Output	Output / Input
12.0	43.00	7.70	.18
12.5	45.00	9.70	.22
13.0	47.00	11.50	.25
13.5	34.00	8.70	.26
14.0	36.00	9.50	.26
14.5	35.50	10.10	.28
15.0	36.00	10.10	.28
15.5	34.00	9.80	.29
16.0	31.50	17.00	.19
16.5	33.00	17.50	.26
17.0	30.50	11.70	.38
18.0	26.50	9.50	.36
19.0	23.00	8.00	.35
20.0	20.00	6.90	.35
22.0	32.40	25.50	.79
24.0	15.80	10.70	.68
26.0	12.40	7.50	.61
28.0	5.40	5.50	1.02
30.0	9.10	4.35	.48
32.0	8.20	3.67	.45
34.0	7.20	3.18	.44
36.0	6.60	3.06	.46
38.0	6.10	2.75	.45
40.0	5.40	2.50	.46
42.0	5.10	2.25	.44
44.0	4.60	1.98	.43
46.0	4.10	1.75	.43
48.0	3.60	1.25	.35
50.0	3.10	1.10	.35
52.0	2.55	2.10	.82
54.0	10.70	14.70	1.47
56.0	6.90	9.20	1.34
58.0	4.85	5.80	1.19
60.0	4.20	4.50	1.07
62.0	3.70	3.90	1.05
64.0	3.70	4.20	1.14
66.0	3.80	3.70	.98

TABLE 37 (Continued)

Frequency (c.p.s.)	Input	Output	Output / Input
68.0	3.40	4.40	1.30
70.0	4.60	4.00	.87
72.0	3.20	3.40	1.06
74.0	4.20	5.20	1.24
76.0	5.10	5.00	1.00
78.0	6.20	5.40	.87
80.0	9.40	6.65	.71
82.0	12.80	7.50	.59
84.0	16.00	7.80	.50
86.0	18.00	5.80	.32
88.0	19.40	4.75	.25
90.0	4.40	4.10	.93

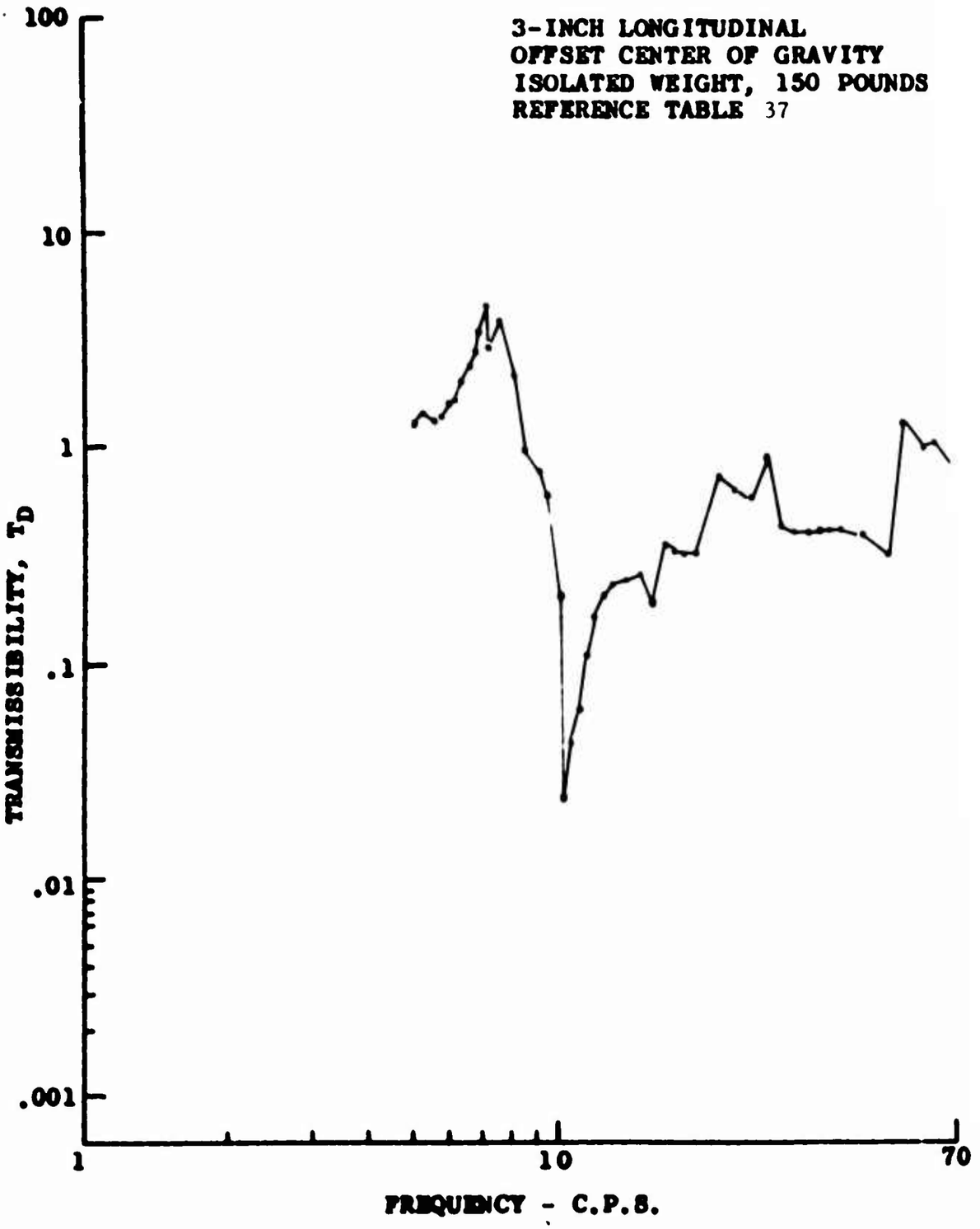

Figure 84. Response Curve for DAVI ∝ Isolated Platform

TABLE 38

DAVI ∝ ISOLATED PLATFORM TRANSMISSIBILITY TEST DATA
3-INCH LATERAL OFFSET CENTER OF GRAVITY
ISOLATED WEIGHT, 200 POUNDS

Frequency (c.p.s.)	Input	Output	Output / Input
5.0	1.60	3.30	2.06
5.2	2.20	5.20	2.36
5.4	2.30	6.50	2.83
5.6	1.20	4.50	3.75
5.8	.55	2.90	5.30
6.0	.21	2.10	10.00
6.2	.09	1.60	17.80
6.4	.18	1.30	7.20
6.6	.30	1.10	3.66
6.8	.42	.95	2.27
7.0	.51	.79	1.55
7.2	.62	.69	1.12
7.4	.71	.59	.75
7.6	.80	.59	.74
7.8	.90	.48	.53
8.0	.97	.48	.50
8.2	.95	.45	.47
8.4	1.10	.33	.30
8.6	1.10	.45	.41
8.8	1.10	.40	.36
9.0	1.30	.35	.27
9.2	1.40	.28	.20
9.4	1.60	.21	.13
9.6	1.70	.16	.09
9.8	1.80	.09	.05
10.0	2.00	.02	.01
10.05	2.00	.007	.002
10.2	2.10	.05	.02
10.4	2.30	.11	.05
10.6	2.50	.18	.07
10.8	2.60	.25	.10
11.0	2.80	.31	.11
11.2	3.00	.38	.13
11.4	3.20	.45	.14
11.6	3.30	.51	.16
11.8	3.50	.59	.17
12.0	3.50	.62	.18

TABLE 38 **(Continued)**

Frequency (c.p.s.)	Input	Output	$\frac{\text{Output}}{\text{Input}}$
12.5	3.50	.71	.20
13.0	3.30	.75	.23
13.5	2.80	.70	.25
14.0	2.30	.65	.28
14.5	2.20	.59	.27
15.0	2.10	.59	.28
16.0	1.60	.52	.33
17.0	1.20	.45	.38
18.0	1.00	.45	.45
19.0	1.20	.34	.28
20.0	1.20	.32	.27
22.0	.90	.28	.31
24.0	.72	.26	.36
25.0	.62	.24	.39
26.0	.59	.27	.46
28.0	.50	.30	.60
30.0	4.00	2.60	.65
32.0	3.20	2.48	.78
34.0	3.50	2.10	.60
36.0	3.40	2.05	.60
38.0	3.20	2.30	.72
40.0	3.00	2.50	.83
42.0	2.95	2.60	.88
44.0	2.25	2.60	1.16
46.0	2.70	2.60	.96
48.0	2.65	2.90	1.09
50.0	2.55	2.85	1.12
52.0	3.10	2.70	.87
54.0	3.40	4.30	1.26
56.0	2.90	3.10	1.07
58.0	3.10	2.40	.77
60.0	3.50	2.20	.63
62.0	4.50	2.70	.60
64.0	4.50	4.20	.93
66.0	4.90	3.70	.76
68.0	5.00	4.20	.84
70.0	4.60	4.70	1.02

TABLE 38 (Continued)

Frequency (c.p.s.)	Input	Output	$\frac{\text{Output}}{\text{Input}}$
72.0	7.80	4.30	.55
74.0	9.00	4.10	.46
76.0	10.50	4.50	.43
78.0	10.40	4.70	.45
80.0	10.80	5.20	.48
82.0	11.50	5.70	.50
84.0	11.00	5.90	.54
86.0	11.20	6.20	.55
88.0	9.20	6.70	.73
90.0	12.70	7.60	.60

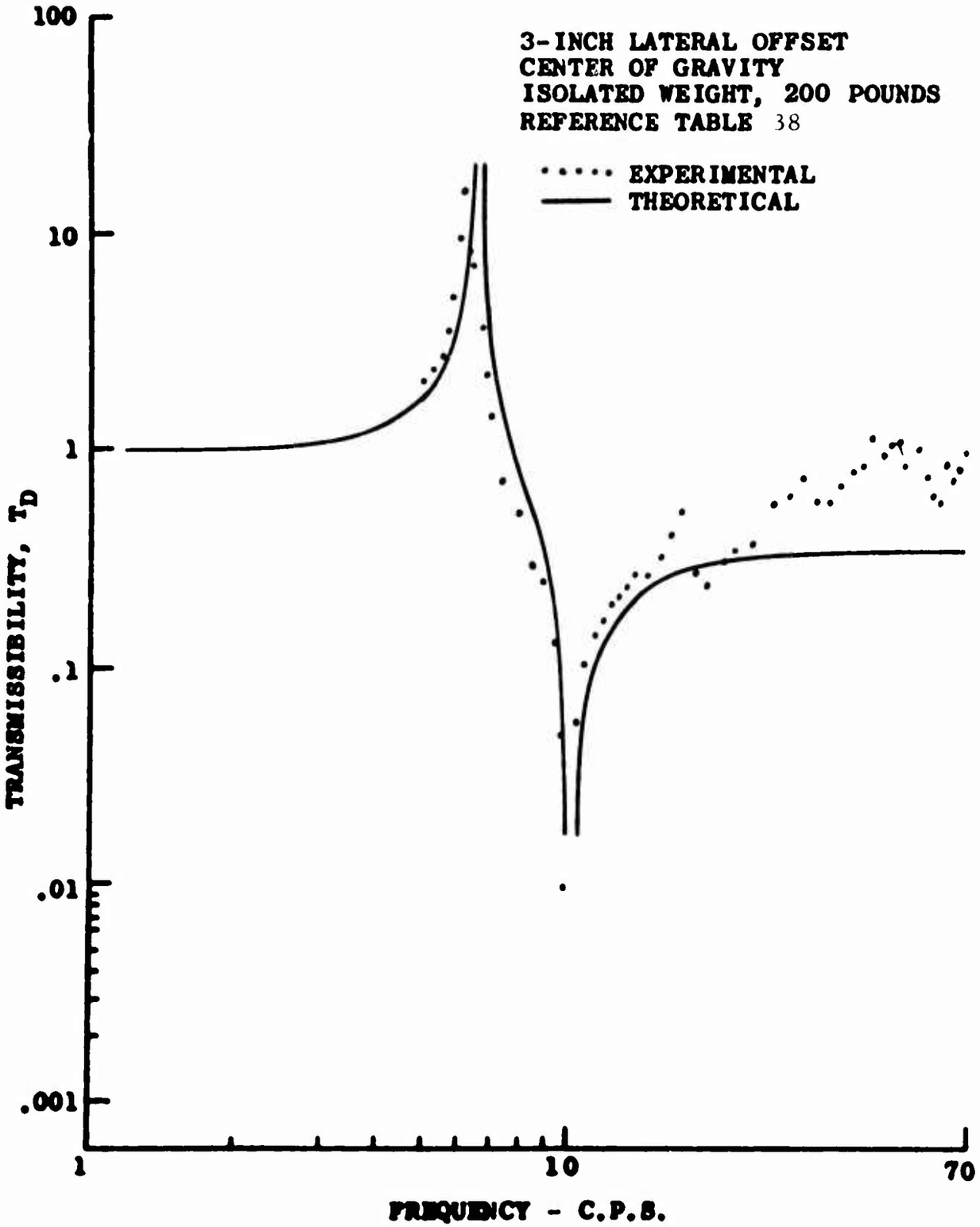

Figure 85. Response Curve for DAVI Ox Isolated Platform

TABLE 39

SERIES-DAMPED DAVI 7
ISOLATED PLATFORM TRANSMISSIBILITY TEST DATA
CENTRAL CENTER OF GRAVITY
ISOLATED WEIGHT, 150 POUNDS

Frequency (c.p.s.)	Input	Output	Output / Input
5.0	1.30	1.80	1.38
5.2	1.40	2.20	1.57
5.4	1.70	2.80	1.65
5.6	2.00	3.50	1.75
5.8	6.50	13.50	2.08
6.0	8.50	21.00	2.47
6.2	8.00	25.00	3.13
6.4	6.00	23.00	3.83
6.6	3.40	18.00	5.29
6.8	1.40	13.50	9.64
6.9	0.50	11.50	23.00
7.0	0.49	10.00	20.40
7.2	1.20	8.80	7.33
7.4	1.85	7.20	3.89
7.6	2.50	6.20	2.48
7.8	3.00	5.20	1.73
8.0	3.60	4.50	1.25
8.2	4.20	4.00	.95
8.4	5.00	3.40	.68
8.6	5.20	3.00	.58
8.8	4.40	2.60	.59
9.0	16.00	6.00	.38
9.2	17.00	5.00	.29
9.4	18.00	4.00	.22
9.6	20.00	3.00	.15
9.8	21.00	1.90	.09
10.0	22.00	1.00	.04
10.1	23.00	.65	.03
10.2	23.00	.60	.03
10.4	25.00	1.40	.06
10.6	25.00	2.20	.09
10.8	27.00	3.20	.12
11.0	28.00	4.00	.14
11.2	28.00	4.60	.16
11.4	28.00	5.50	.20
11.6	29.00	6.20	.21

TABLE 39 **(Continued)**

Frequency (c.p.s.)	Input	Output	$\frac{\text{Output}}{\text{Input}}$
11.8	30.00	7.00	.23
12.0	30.00	7.80	.26
12.5	32.00	10.00	.31
13.0	31.00	10.50	.34
13.5	30.00	11.00	.37
14.0	27.00	10.50	.39
14.5	25.00	11.00	.44
15.0	24.00	12.00	.50
15.5	21.00	11.00	.52
16.0	18.00	10.50	.58
16.5	16.50	9.80	.59
17.0	15.00	9.50	.63
17.5	14.00	9.00	.64
18.0	12.50	8.50	.68
18.5	12.00	8.20	.68
19.0	11.00	8.00	.73
19.5	10.00	7.80	.78
20.0	8.00	7.50	.94
22.0	5.00	6.80	1.36
24.0	3.30	6.20	1.88
26.0	1.70	6.20	3.65
28.0	3.00	6.00	2.00
30.0	2.70	6.00	2.22
32.0	4.40	6.20	1.41
34.0	6.80	6.50	.96
36.0	10.00	7.00	.70
38.0	13.00	7.80	.60
40.0	17.00	8.50	.50
42.0	19.50	8.50	.44
44.0	20.00	7.20	.36
46.0	18.00	5.80	.32
48.0	16.00	4.80	.30
50.0	14.00	3.70	.26
52.0	12.00	2.90	.24
54.0	11.00	2.50	.23
56.0	10.00	2.10	.21
58.0	8.80	1.85	.21

TABLE 39 **(Continued)**

Frequency (c.p.s.)	Input	Output	Output / Input
60.0	8.00	1.70	.21
62.0	7.50	1.20	.16
64.0	6.80	1.10	.16
66.0	6.50	1.00	.15
68.0	6.50	1.00	.15
70.0	6.00	.90	.15
72.0	4.50	.80	.18
74.0	5.50	.75	.14
76.0	4.70	.68	.15
78.0	4.00	.57	.14
80.0	3.40	.50	.15
82.0	11.50	.65	.06
84.0	9.50	.62	.07
86.0	8.50	.60	.07
88.0	8.00	.60	.08
90.0	7.00	.60	.03

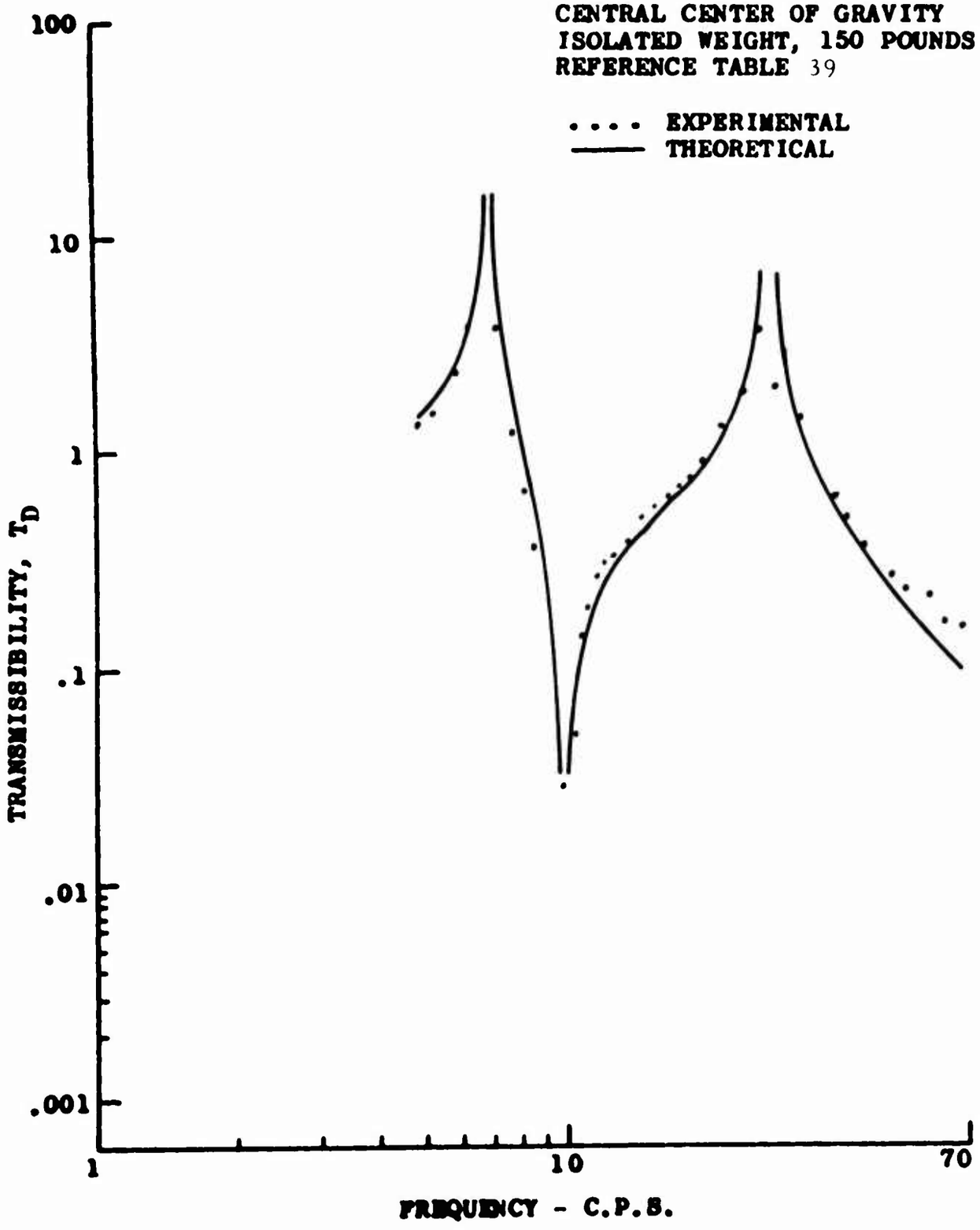

Figure 86. Response Curve for Series-Damped DAVI 7 Isolated Platform

TABLE 40

SERIES-DAMPED DAVI 7
ISOLATED PLATFORM TRANSMISSIBILITY TEST DATA
CONSTANT VERTICAL EXCITATION (10.4 C.P.S.)
VARIABLE LATERAL EXCITATION
CENTRAL CENTER OF GRAVITY
ISOLATED WEIGHT, 158 POUNDS

Frequency (c.p.s.)	Input	Output	$\frac{\text{Output}}{\text{Input}}$
5.0	22.00	.50	.02
5.2	20.00	.45	.02
5.4	22.00	.50	.02
5.6	21.00	.48	.02
5.8	21.00	.48	.02
6.0	21.00	.48	.02
6.2	21.00	.50	.02
6.4	20.00	.55	.03
6.6	20.00	.65	.03
6.8	22.00	.70	.03
7.0	22.00	.70	.03
7.2	22.00	.75	.03
7.4	22.00	.80	.04
7.6	21.00	.68	.03
7.8	22.00	.78	.04
8.0	22.00	.78	.04
8.2	22.00	.85	.04
8.4	22.00	.95	.04
8.6	25.00	1.00	.04
8.8	22.00	.70	.03
9.0	21.00	.58	.03
9.2	20.00	.58	.03
9.4	21.00	.60	.03
9.6	22.00	.60	.03
9.8	20.00	.70	.04
10.0	25.00	.70	.03
10.2	25.00	.70	.03
10.4	23.00	.55	.02
10.6	25.00	.65	.03
10.8	20.00	.55	.03
11.0	22.00	.70	.03
11.5	22.00	.68	.03
12.0	22.00	.70	.03
12.5	22.00	.60	.03
13.0	24.00	.95	.04
14.0	25.00	1.70	.07
15.0	22.00	1.30	.06

TABLE 40 (Continued)

Frequency (c.p.s.)	Input	Output	Output / Input
16.0	22.00	1.00	.05
17.0	22.00	.95	.04
18.0	22.00	1.00	.05
19.0	22.00	1.00	.05
20.0	22.00	.90	.04
22.0	22.00	.80	.04
24.0	21.00	.70	.03
26.0	20.00	.70	.04
28.0	21.00	.78	.04
30.0	25.00	.80	.03
32.0	23.00	.90	.04
34.0	21.00	.98	.05
36.0	21.00	1.50	.07
38.0	21.00	1.70	.08
40.0	22.00	1.50	.07
42.0	23.00	1.30	.06
44.0	22.00	.95	.04
46.0	22.00	.90	.04
48.0	22.00	.90	.04
50.0	22.00	.70	.03
52.0	22.00	.80	.04
54.0	24.00	.70	.03
56.0	31.00	.70	.02
58.0	40.00	.70	.02
60.0	45.00	.70	.02
62.0	55.00	3.60	.07
64.0	58.00	4.50	.08
66.0	30.00	.85	.03
68.0	29.00	.80	.03
70.0	31.00	.70	.02
72.0	33.00	.70	.02
74.0	36.00	.80	.02
76.0	38.00	.80	.02
78.0	42.00	.65	.02
80.0	47.00	.88	.02
82.0	50.00	1.00	.02
84.0	52.00	.75	.01
86.0	60.00	.85	.01
88.0	61.00	.95	.02
90.0	31.00	.75	.02

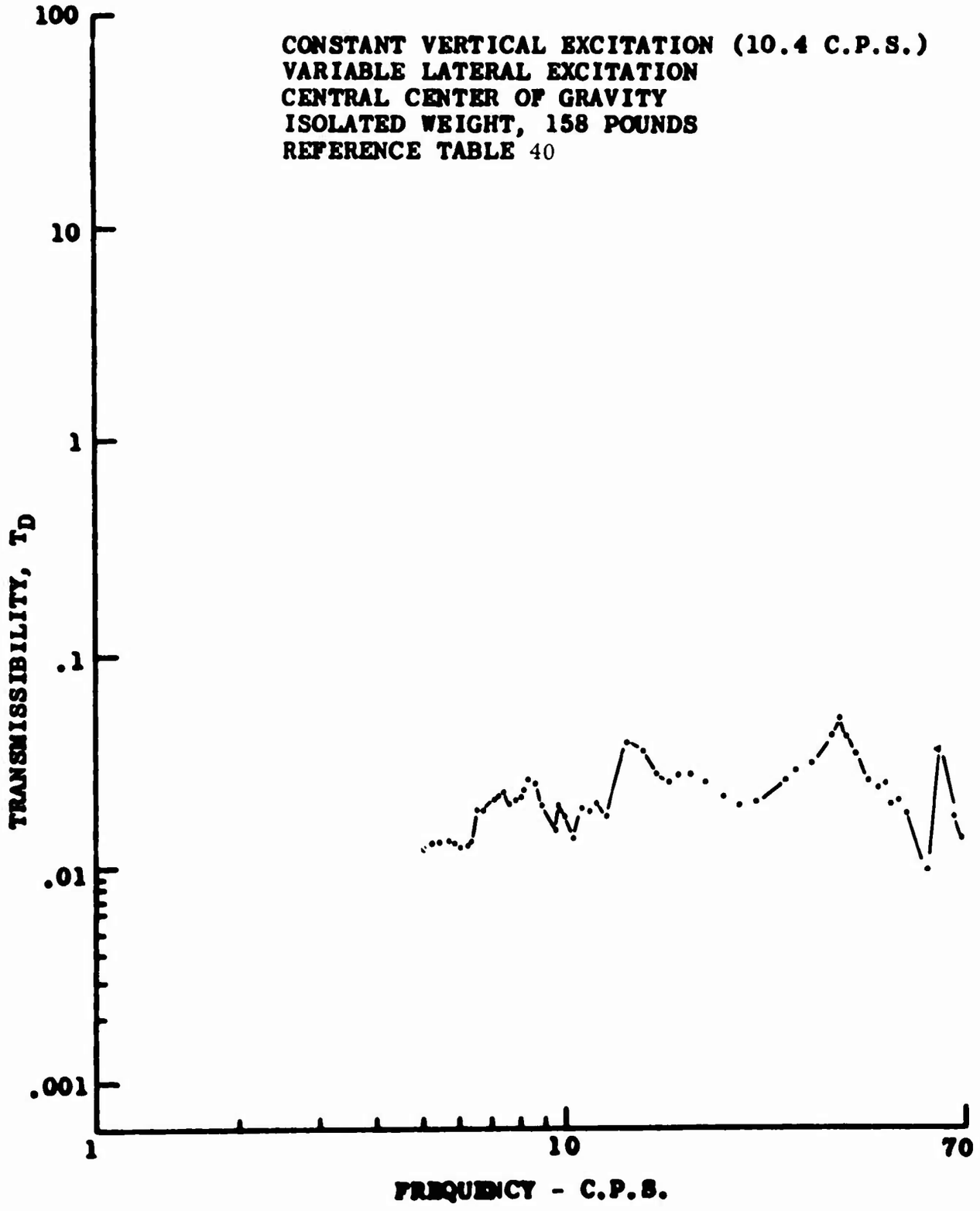

Figure 87. Response Curve for Series-Damped DAVI Isolated Platform

TABLE 41

SERIES-DAMPED DAVI 2
ISOLATED PLATFORM TRANSMISSIBILITY TEST DATA
SIMULTANEOUS VERTICAL AND LATERAL EXCITATION
CENTRAL CENTER OF GRAVITY
158-POUND ISOLATED WEIGHT

Frequency (c.p.s.)	Input	Output	Output / Input
5.0	3.30	.65	.20
5.2	3.00	.90	.30
5.4	3.00	1.15	.38
5.6	3.50	.55	.16
5.8	3.80	.75	.20
6.0	4.00	1.10	.28
6.2	4.00	1.30	.33
6.4	3.10	1.40	.45
6.6	5.00	1.30	.26
6.8	6.00	1.00	.17
7.0	7.80	1.00	.13
7.2	7.80	1.00	.13
7.4	7.00	1.00	.14
7.6	5.90	.85	.14
7.8	6.10	.80	.13
8.0	5.70	.78	.14
8.2	6.50	.85	.13
8.4	8.80	.70	.08
8.6	5.50	.42	.08
8.8	8.80	.70	.08
9.0	6.00	.45	.08
9.2	5.20	.42	.08
9.4	4.70	.40	.09
9.6	4.50	.42	.09
9.8	4.40	.42	.10
10.0	4.40	.39	.09
10.2	4.40	.35	.08
10.4	4.40	.34	.08
10.6	4.50	.40	.09
10.8	4.60	.34	.07
11.0	4.80	.35	.07
11.2	4.80	.35	.07
11.4	4.50	.35	.08
11.6	4.80	.36	.08
11.8	4.80	.40	.08
12.0	4.70	.48	.10
13.0	11.20	.95	.09

TABLE 41 (Continued)

Frequency (c.p.s.)	Input	Output	Output / Input
14.0	11.00	1.30	.12
14.5	11.00	1.40	.13
15.0	10.00	1.30	.13
16.0	8.50	1.05	.12
17.0	7.50	.88	.12
18.0	7.00	.88	.13
19.0	5.50	1.05	.19
20.0	4.50	.78	.17
24.0	4.20	.50	.12
28.0	6.00	.55	.09
32.0	11.50	1.50	.13
36.0	14.00	1.30	.09
40.0	10.00	1.30	.13
44.0	9.50	.70	.07
48.0	7.50	.60	.08
52.0	7.00	.50	.07
56.0	12.00	.35	.03
58.0	18.00	.36	.02
60.0	19.00	.50	.03
61.0	24.00	2.10	.09
62.0	25.00	2.40	.10
64.0	29.00	4.20	.14
66.0	40.00	2.50	.06
68.0	12.00	.80	.07
70.7	12.00	.85	.07
72.0	12.00	1.20	.10
74.0	13.00	1.10	.09
76.0	15.00	1.50	.10
78.0	17.00	1.40	.08
80.0	19.00	1.10	.06
82.0	19.00	1.00	.05
84.0	18.00	.80	.04
86.0	17.00	.60	.04
88.0	14.00	.50	.04
90.0	11.00	.42	.04

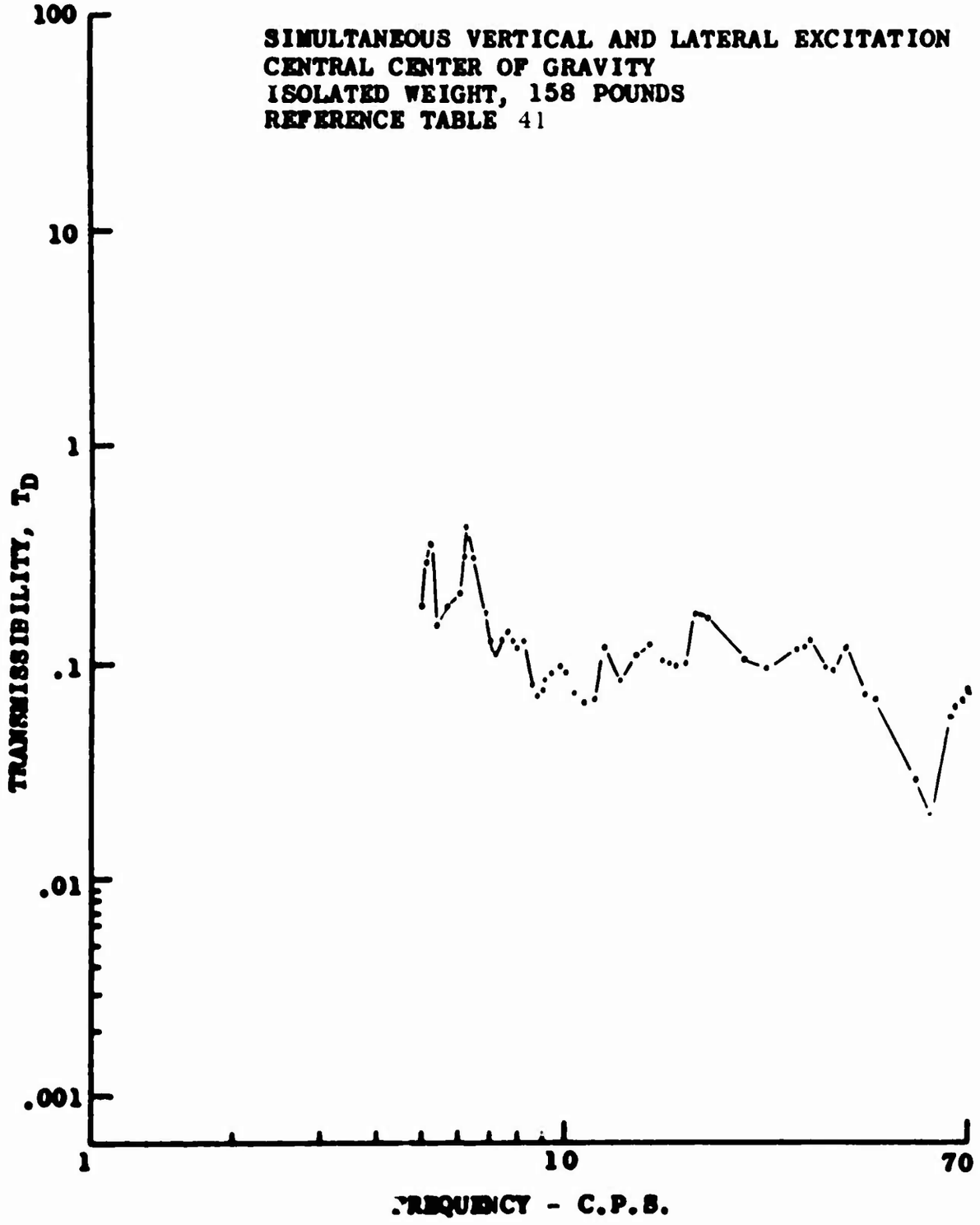

Figure 88. Response Curve for Series-Damped DAVI Isolated Platform

TABLE 42

SINGLE DAVI α TRANSMISSIBILITY TEST DATA
ISOLATED WEIGHT, 35 POUNDS

Frequency (c.p.s.)	Input	Output	$\frac{\text{Output}}{\text{Input}}$
6.0	1.30	3.00	2.31
6.2	1.40	3.50	2.50
6.4	1.50	4.00	2.67
6.6	1.60	4.90	3.06
6.8	1.60	6.50	4.06
7.0	.22	6.90	31.36
7.2	.33	5.90	17.88
7.4	.68	4.70	6.91
7.6	.90	3.70	4.11
7.8	1.10	3.00	2.73
8.0	1.20	2.40	2.00
8.2	1.35	1.90	1.41
8.4	1.50	1.50	1.00
8.6	1.60	1.20	.75
8.8	1.65	.90	.55
9.0	1.75	.69	.39
9.2	1.80	.50	.28
9.4	1.90	.37	.20
9.6	1.90	.22	.12
9.8	2.00	.11	.06
10.0	2.00	.01	.007
10.2	2.10	.09	.04
10.4	2.10	.16	.08
10.6	2.10	.23	.11
10.8	2.15	.29	.14
11.1	2.20	.35	.16
11.2	2.20	.40	.18
11.4	2.20	.44	.20
11.6	2.20	.48	.22
11.8	2.20	.50	.23
12.0	2.20	.55	.25
12.5	2.20	.61	.28
13.0	2.20	.68	.31
13.5	2.20	.70	.32
14.0	2.20	.72	.33
14.5	2.20	.75	.34
15.0	2.15	.78	.36

TABLE 42 (Continued)

Frequency (c.p.s.)	Input	Output	Output / Input
15.5	2.10	.78	.37
16.0	2.10	.79	.38
16.5	2.05	.78	.38
17.0	2.00	.79	.40
17.5	1.95	.75	.38
18.0	1.90	.75	.39
18.5	1.85	.75	.41
19.0	1.80	.75	.42
19.5	1.70	.75	.44
20.0	1.70	.72	.42
21.0	1.60	.70	.44
22.0	1.50	.69	.46
23.0	1.40	.65	.46
24.0	1.30	.62	.48
25.0	1.20	.60	.50
26.0	1.15	.59	.51
27.0	1.10	.57	.52
28.0	1.05	.55	.52
29.0	1.00	.55	.55
30.0	.95	.55	.58
35.0	.65	.42	.65
40.0	.68	.35	.52
41.0	.79	.35	.44
42.0	.95	.32	34
43.0	.60	.75	1.25
44.0	.70	.58	.83
45.0	1.20	.48	.40
46.0	1.55	.40	.26
47.0	2.00	.40	.20
48.0	2.30	.34	.15
49.0	2.80	.22	.08
50.0	2.70	.23	.09
51.0	2.20	.09	.04
52.0	2.10	.07	.03
53.0	1.60	.15	.09
54.0	1.50	.17	.11
55.0	1.30	.17	.13

TABLE 42 (Continued)

Frequency (c.p.s.)	Input	Output	Output / Input
57.0	1.00	.21	.21
60.0	.78	.23	.30
62.0	.62	.24	.39
64.0	.52	.27	.52
66.0	.50	.23	.46
68.0	.45	.17	.38
70.0	.34	.16	.47
72.0	.21	.16	.76
74.0	.12	.15	.13
76.0	.18	.25	1.39
78.0	.25	.35	1.40
80.0	.40	.38	.95
82.0	.70	.36	.51
84.0	1.10	.33	.30
86.0	1.25	.27	.22
88.0	1.15	.21	.18
90.0	1.00	.19	.19
92.0	.88	.18	.20
94.0	.78	.16	.21
96.0	.79	.16	.20
98.0	.95	.13	.14
100.0	1.05	.08	.08

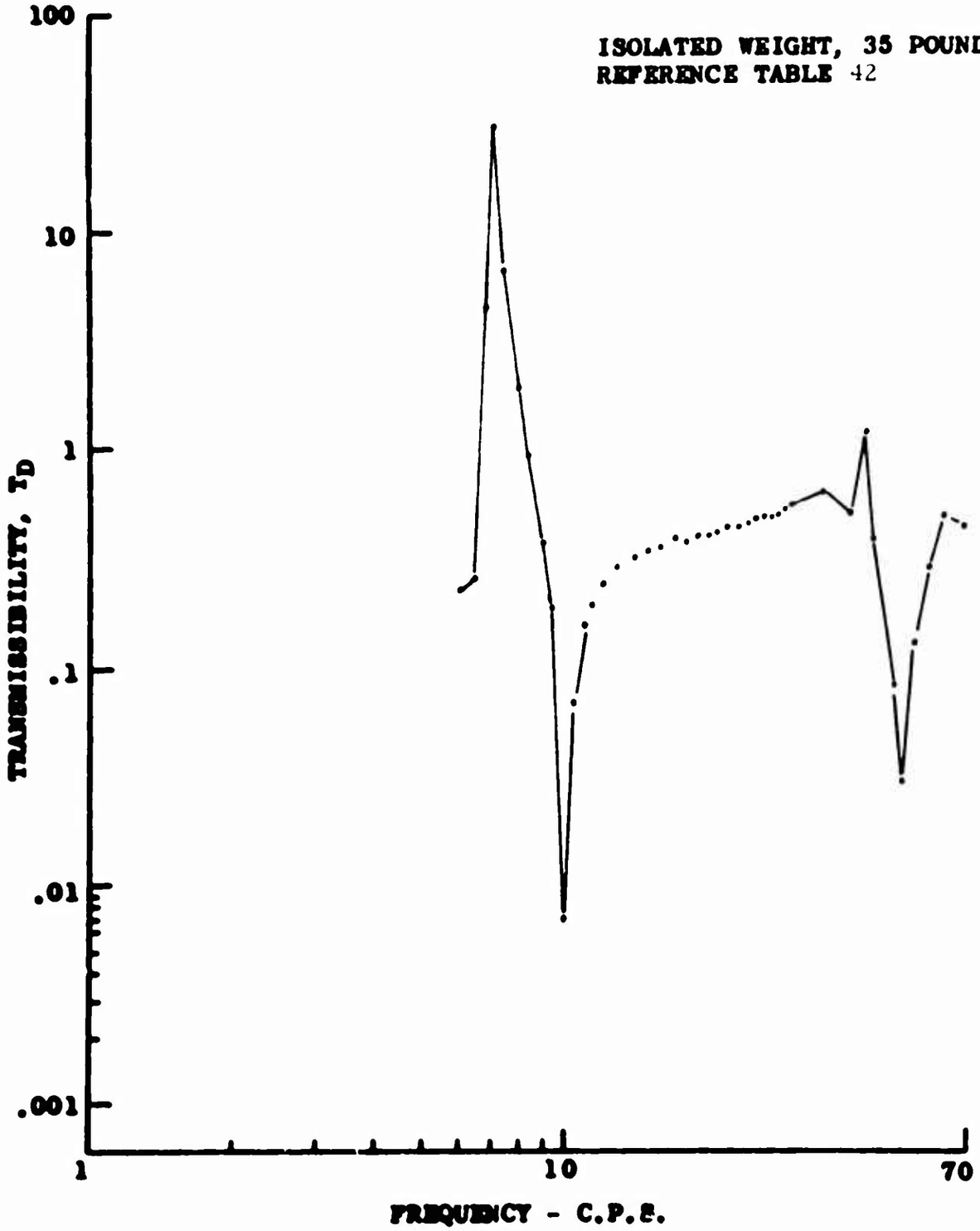

Figure 89. Response Curve for Single DAVIC

TABLE 43

CONVENTIONAL ISOLATOR TRANSMISSIBILITY TEST DATA
CENTRAL CENTER OF GRAVITY
ISOLATED WEIGHT, 158 POUNDS

Frequency (c.p.s.)	Input	Output	Output / Input
5.0	5.50	7.00	1.27
5.2	6.00	8.20	1.37
5.4	6.50	9.80	1.51
5.6	7.50	11.50	1.53
5.8	8.50	13.00	1.53
6.0	9.50	16.00	1.68
6.2	11.00	19.00	1.73
6.4	12.00	23.00	1.92
6.6	13.00	27.00	2.08
6.8	13.00	29.00	2.23
7.0	11.50	28.00	2.44
7.2	10.50	25.00	2.38
7.4	10.00	25.00	2.50
7.6	7.50	22.00	2.93
7.8	6.00	19.00	3.17
8.0	4.50	17.00	3.78
8.2	3.50	15.00	4.29
8.4	2.50	13.50	5.40
8.6	1.80	12.00	6.67
8.8	1.15	11.50	10.00
9.0	.70	10.50	15.00
9.1	.75	10.00	13.33
9.4	.85	9.20	10.82
9.6	.95	8.80	9.26
9.8	1.20	8.00	6.67
10.0	1.40	7.80	5.57
10.2	1.70	7.20	4.24
10.4	1.90	7.00	3.68
10.6	2.10	6.80	3.24
10.8	2.30	6.50	2.83
11.0	2.60	6.00	2.31
11.2	3.70	8.00	2.16
11.4	3.80	7.50	1.97
11.6	4.00	7.20	1.80
11.8	4.00	7.00	1.75
12.0	4.00	6.80	1.70
12.5	7.80	6.30	.81

TABLE 43 (Continued)

Frequency (c.p.s.)	Input	Output	Output / Input
13.0	7.50	6.00	.80
13.5	7.50	5.20	.69
14.0	7.50	5.00	.67
14.5	8.00	4.80	.60
15.0	8.00	4.50	.56
15.5	8.50	4.30	.51
16.0	9.00	4.00	.44
16.5	9.50	4.00	.42
17.0	9.80	3.60	.37
17.5	10.00	3.50	.35
18.0	10.50	3.30	.31
18.5	11.00	3.20	.29
19.0	11.50	3.20	.28
19.5	12.00	3.00	.25
20.0	12.00	2.90	.24
22.0	15.00	2.60	.17
24.0	17.00	2.30	.14
26.0	19.00	2.10	.11
28.0	21.00	1.70	.08
30.0	24.00	1.40	.06
32.0	30.00	1.20	.04
34.0	20.00	.80	.04
36.0	27.00	.48	.02
38.0	18.00	.85	.05
40.0	7.80	.75	.10
42.0	7.80	.75	.10
44.0	8.50	1.20	.14
46.0	8.00	.75	.09
48.0	7.80	.90	.15
50.0	7.20	1.20	.17
52.0	7.00	1.20	.17
54.0	7.00	1.15	.16
56.0	7.00	1.10	.16
58.0	7.00	.95	.14
60.0	6.80	.80	.12
62.0	6.50	.60	.09
64.0	6.00	.50	.08

TABLE 43 (Continued)

Frequency (c.p.s.)	Input	Output	Output / Input
66.0	5.60	.45	.08
68.0	5.50	.40	.07
70.0	5.00	.35	.07
72.0	4.80	.40	.08
74.0	4.50	.45	.10
76.0	3.80	.35	.09
78.0	3.00	.30	.10
80.0	7.50	.25	.03
82.0	10.00	.25	.03
84.0	9.50	.20	.02
86.0	8.00	.25	.03
88.0	7.00	.30	.04
90.0	6.50	.25	.04

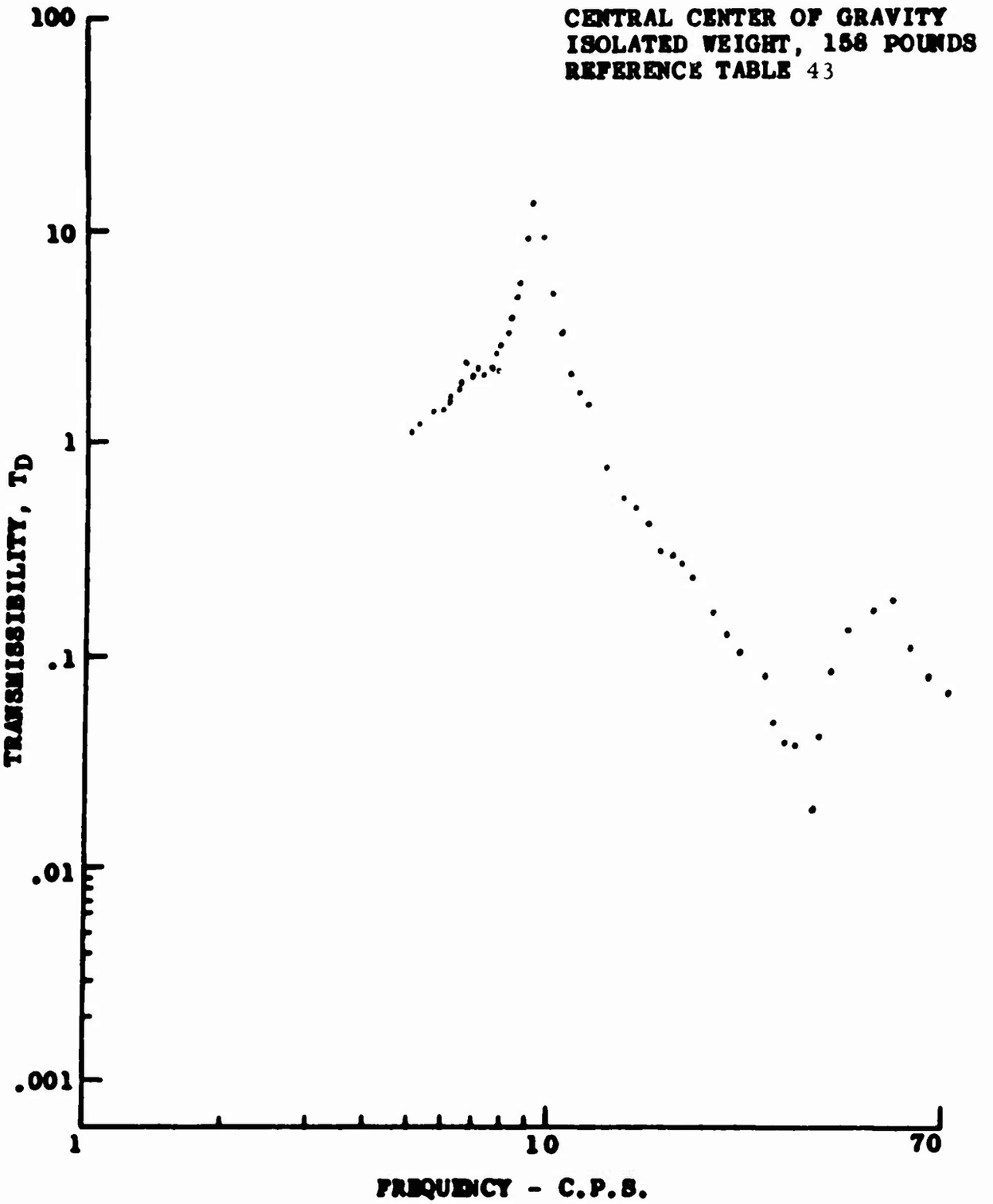

Figure 90. Response Curve for Conventional Isolator

DAVI Isolated Pilot Seat

Upon completion of the formal testing, instruments were mounted on the input and output side of the DAVI α isolated platform to visually obtain the effects on instrument isolation. Figures 91 and 92 show the results of a .5-g and 1.0-g input, respectively. It is seen from both figures that the instrument mounted on the output side of the DAVI platform is easily read with no noticeable evidence of vibratory input. The instrument located on the input side of the DAVI platform is starting to blur at .5-g and is noticeably blurred at 1.0-g input, making reading of the instrument very annoying. It should be noted that the instrument on the input side has much larger figures than that on the output side, making it easier to read. An instrument with smaller figures would make it virtually impossible to read accurately at these vibratory inputs.

A pilot seat was then mounted directly on top of the DAVI α isolated platform as illustrated in Figure 93. This was done for convenience rather than redesigning the system to incorporate a seat without the top platform. Figure 94 illustrates the ease at which the tuning of the DAVI could be accomplished for the purposes of this experimental testing. For a finalized design, the DAVI would be turned inward, thus reducing the envelope required.

Figure 95 shows a 150-pound man sitting in the DAVI α isolated seat being subjected to a 1.0-g input at 10.5 c.p.s. It is seen that there is no noticeable vibration on the occupant or on the seat, and over 98-percent isolation was obtained. Various individuals, ranging from a 105-pound secretary to a 220-pound test pilot were tested in the seat. The results were all the same as indicated in Figure 95. The tuned frequency was not affected by the variation in weight, and over 98-percent isolation was obtained.

Handwriting samples were also taken of the individuals seated on the DAVI isolated seat, while being subjected to a 1.0-g input. The handwriting, when compared to that taken with zero input, was essentially identical. However, handwriting done with a 1.0-g input and the DAVI's "shorted out" was unreadable.

The results of this testing show the feasibility of the DAVI configuration to isolate from low frequency excitation cargo pallets and pilot and passenger seats in which the weight varies.

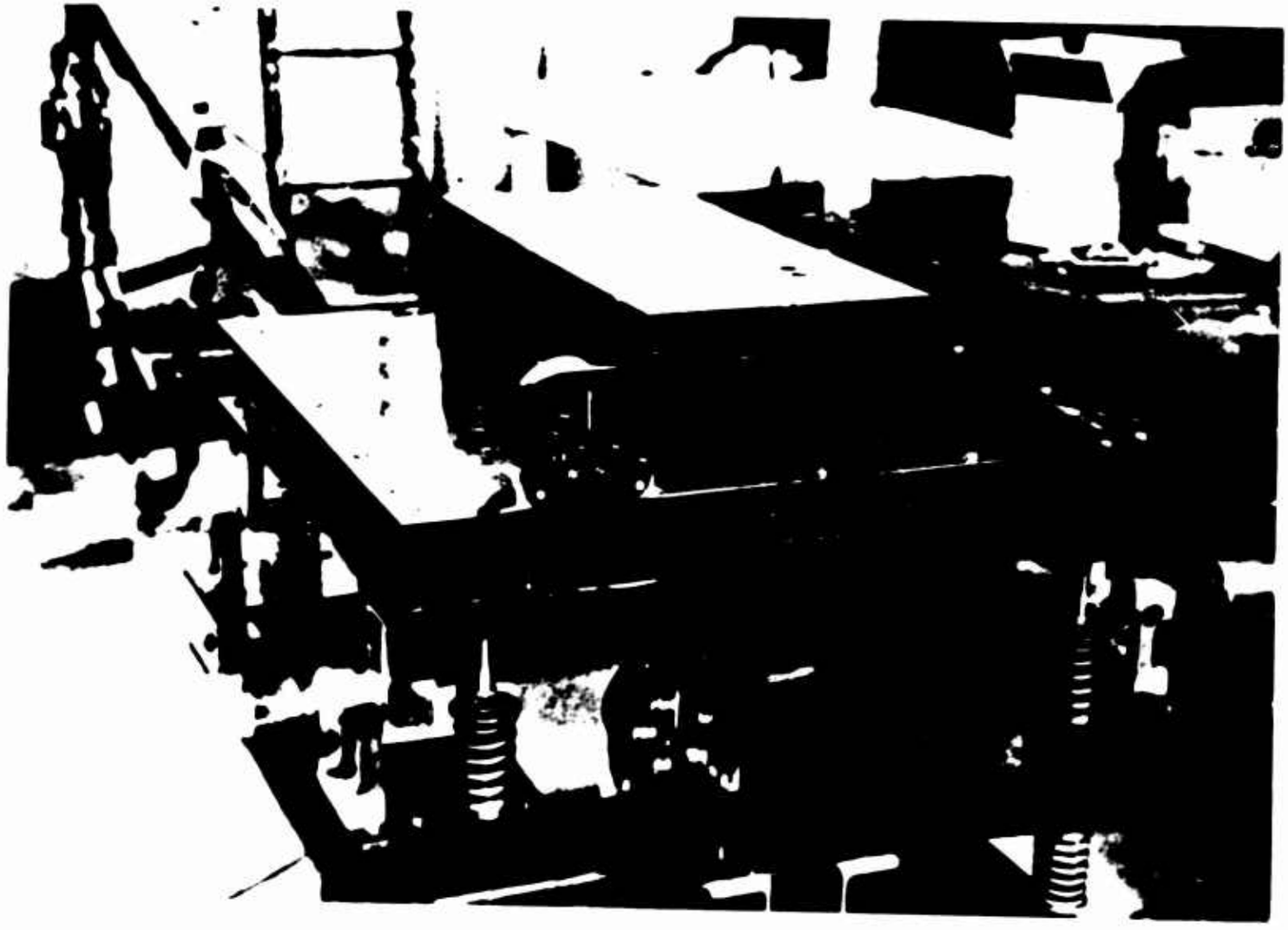

Figure 91. DAVI α Platform Isolation

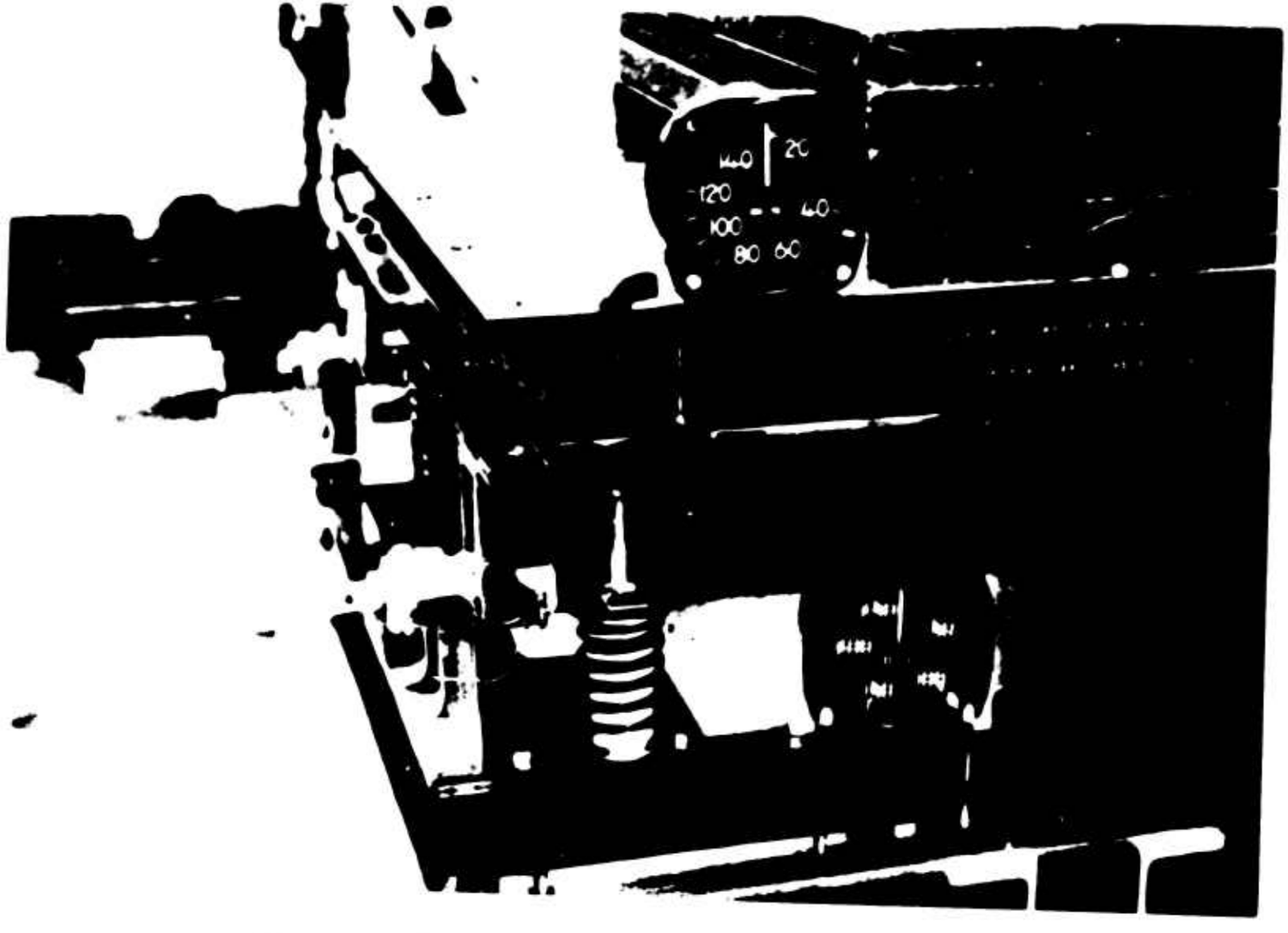

Figure 92. DAVI α Platform Isolation

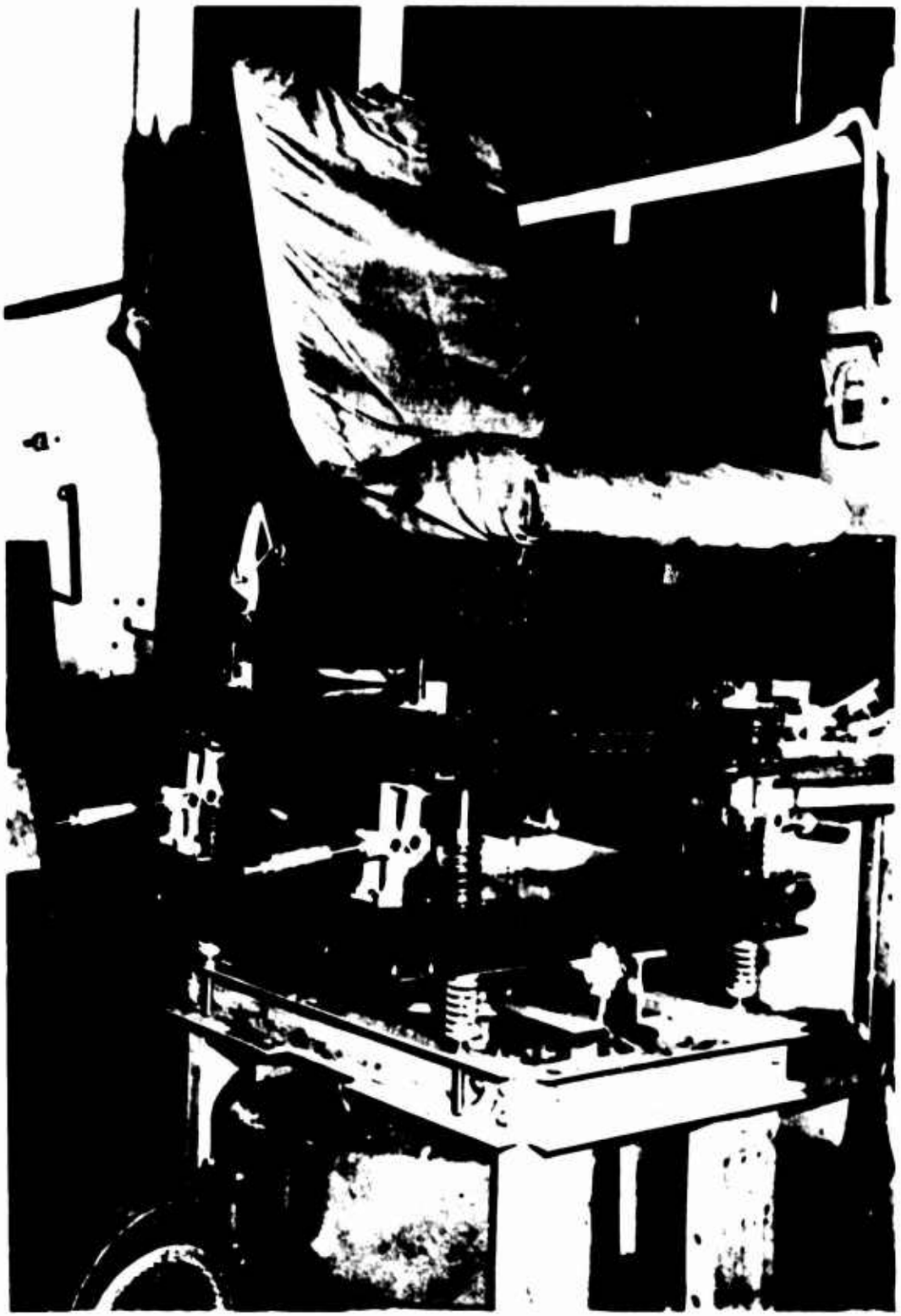

Figure 93. DAVI α Isolated Platform and Seat Installation

Figure 94. DAVI α Isolated Platform and Seat Installation

Figure 95. DAVI α Seat Isolation

DAVI PLATFORM SHOCK TESTING

Drop tests of the finalized DAVI α design were conducted on the same platform that was used in the transmissibility tests. A description of this platform is given in the preceding section. These drop tests were conducted on 12 and 13 April 1965, at Barry Controls, Watertown, Massachusetts, utilizing their drop test equipment and instrumentation.

The test equipment used was the VP-400 varipulse machine, which is a free-fall type of mechanical shock test machine in which peak "g" values are obtained by varying the height of the drop. For these drop test results, a half sine wave of twenty-millisecond duration was used as the input. Input peak "g" levels were varied from 5-g to 15-g.

Figure 96 shows an overall installation of the DAVI α isolated platform and the instrumentation used to record the results. Input and output accelerometers located on the base of the drop test machine and on top of the DAVI platform, respectively, were fed into a dual beam scope, the results being recorded on film. Figure 97 shows a close-up of the DAVI α isolated platform installation.

The purpose of these drop tests was to determine the shock transmissibility characteristics of the finalized DAVI α design. However, since the analysis given earlier in this report shows the DAVI, for a step velocity input, to have better shock characteristics than a conventional isolator with the same spring rate; drop tests of a conventional spring-mass system were done by removing the DAVI's to corroborate the theory. Figure 98 shows the installation of a conventional spring-mass system in the drop test machine.

Drop tests of the DAVI α isolated platform were made with 0, 40, 100, and 200 pounds on the platform. Drop tests were also done with a 200-pound isolated weight, having a 3-inch center of gravity offset. Figures 99 and 100 show the installation of the 100-pound and 200-pound neutral center of gravity, respectively. Figure 101 shows the installation of the 200-pound with a 3-inch offset.

Table 44 gives a complete tabulation of the 60 drop tests done. Figures 102 to 112, inclusive, show the results of the 200-pound drop tests. Only the 200-pound drop test results are shown, since this was the design weight of the DAVI α isolated platform and since this was the most critical. Figures 102 to 106 show the results for the DAVI α isolated platform with 200-pound neutral center of gravity for inputs from 5.5-g to 15-g. Figures 107 to 110 give the results of the 200-pound, 3-inch offset center of gravity on the DAVI α isolated platform for inputs ranging from 5.5-g to 11-g. Figures 111 and 112 show the results of the normal spring-mass system with 200-pound, 3-inch offset center of gravity for inputs of 12-g and 15-g respectively.

From the inspection of the results, it is seen that the DAVI α configuration gave shock isolation for all cases and that, although a pivot arrangement is used in the DAVI, there is no indication of a "short circuit"; that is, the inability of bar and pivot to react which would give a high amplitude, short-duration shock transmission. However, a further inspection of the results, when compared to the normal spring-mass system, shows the DAVI to have two modes of motion, a low frequency fundamental mode of approximately 8 to 10 c.p.s. and a high frequency mode of 60 to 70 c.p.s. The normal spring-mass system has only one mode of 14 to 15 c.p.s.

This low frequency mode on the DAVI is the normal mode expected for the DAVI α configuration. The high frequency mode, although not totally verified, appears to be a bending mode of the inertia bar.

The results of the drop test can be best summarized in a table in which the shock transmissibility is obtained by dividing output by input. Only the results from figures having the ordinate of 20 milliseconds/block are used so that both the low and high frequency mode of the DAVI can be obtained. This summary is shown in Table 45, where it is seen that excellent shock characteristics were obtained for the fundamental mode of the DAVI. The data in the table also confirmed the theoretical results, which showed the DAVI to be superior to the conventional spring-mass isolator in shock isolation performance. A short duration, higher amplitude shock was transmitted; however, this had a transmissibility which was always less than one. This appears to be associated with a flexural mode of the inertia bar. This was partially

verified in which an unrecorded shake test of the inertia bar as a cantilever was done. It had a natural frequency of 63 c.p.s. This is essentially the high frequency obtained in the drop tests.

In the experimental design for this program, no consideration was given to the flexural dynamics of the bar. It appears that this high mode could be eliminated by stiffer design of the inertia bar; however, further analytical and experimental tests would be required.

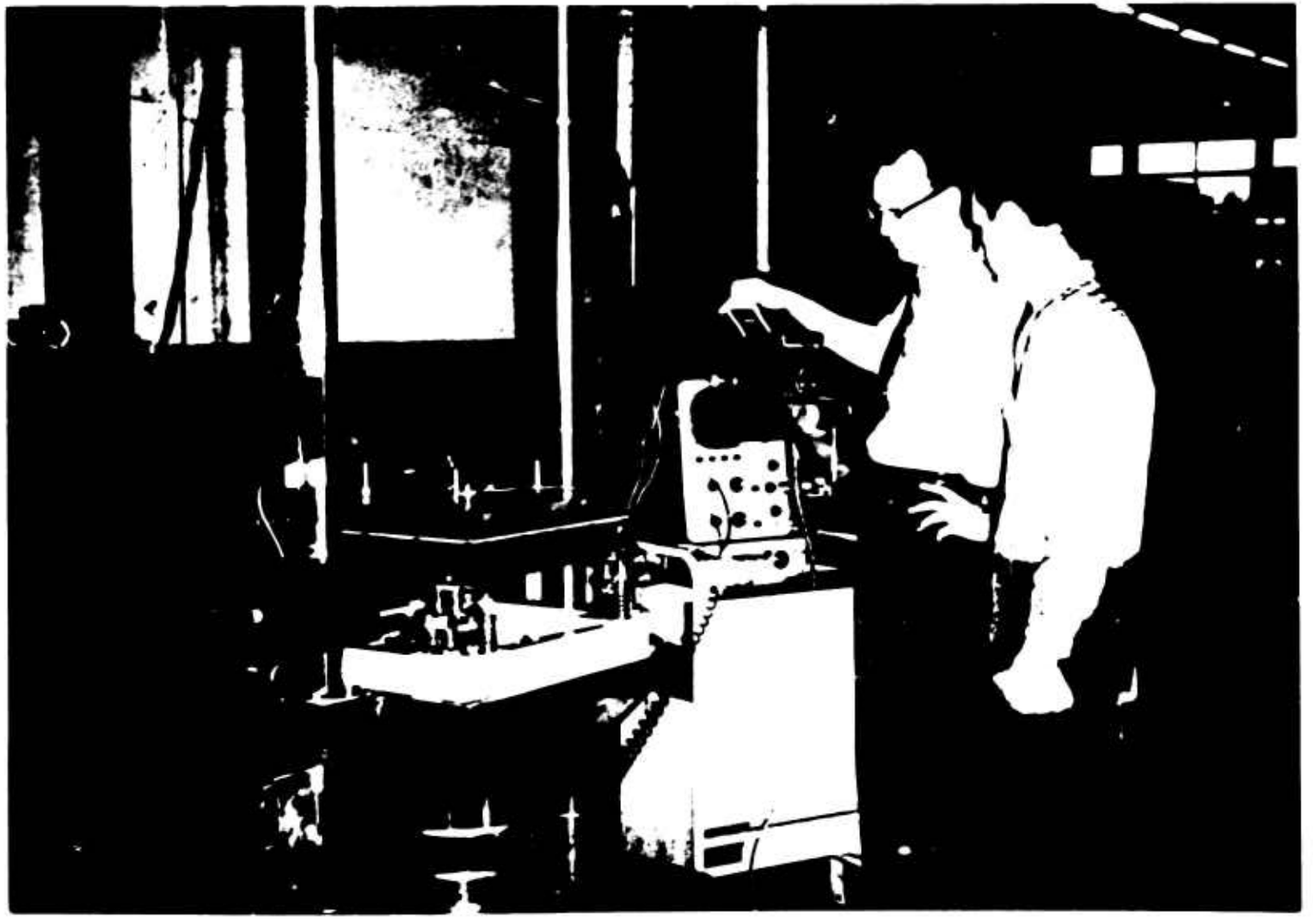

Figure 96. Drop Test Installation and Instrumentation - DAVI α Isolated Platform

Figure 97. Drop Test Installation - DAVI α Isolated Platform

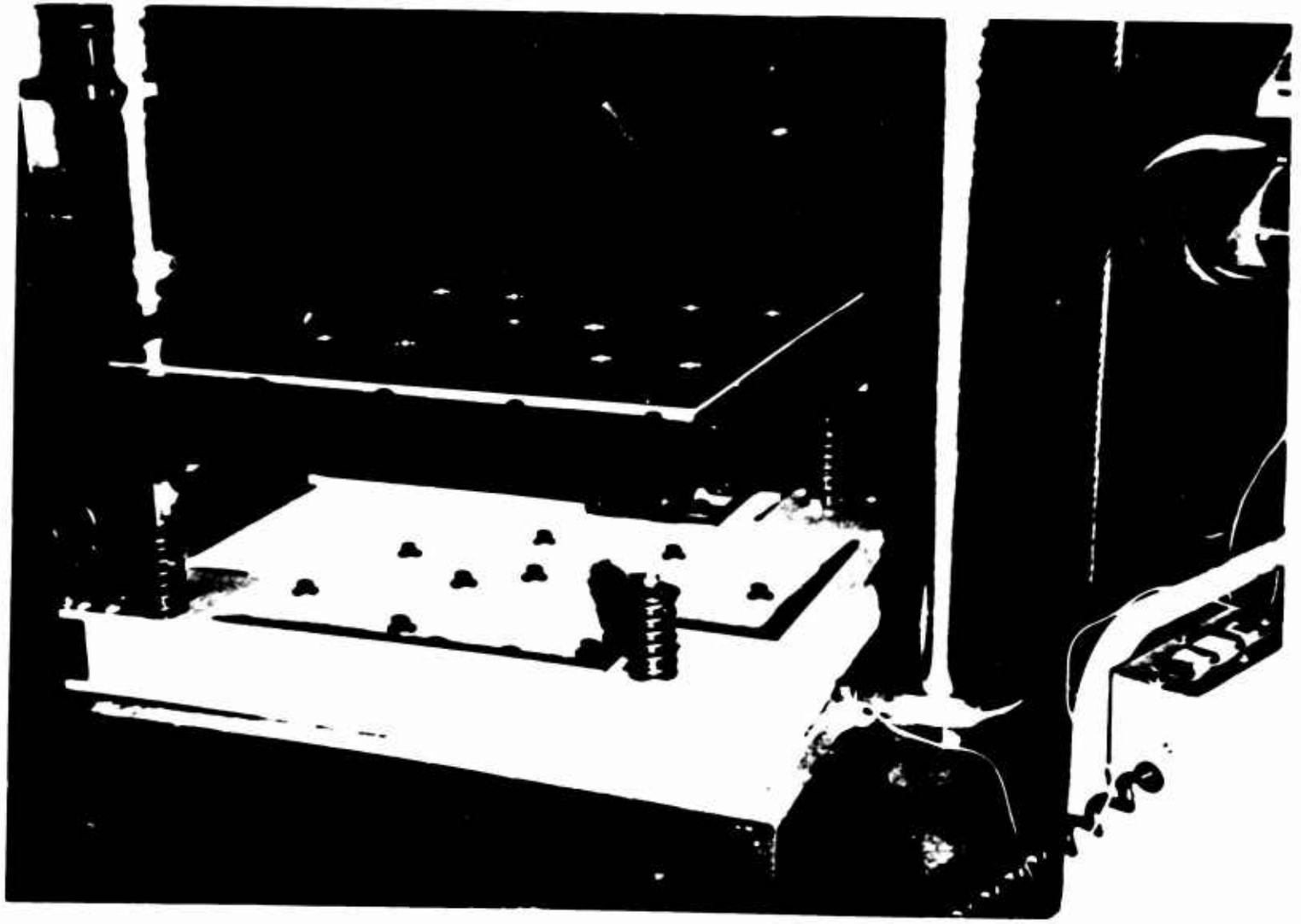

Figure 98. Drop Test Installation - Spring-Mass Isolated Platform

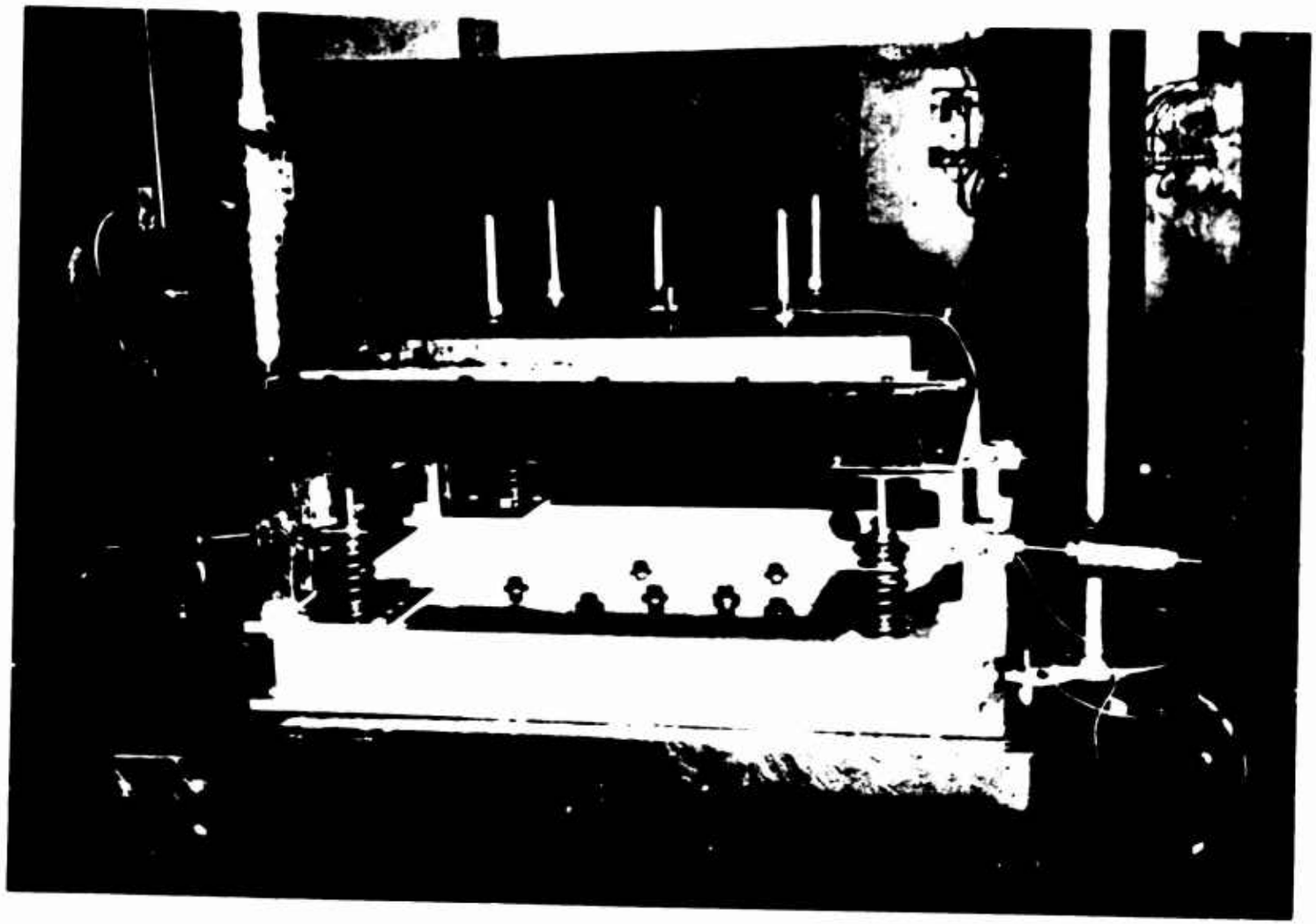

Figure 99. Drop Test Installation - 100-Pound Central Center of Gravity

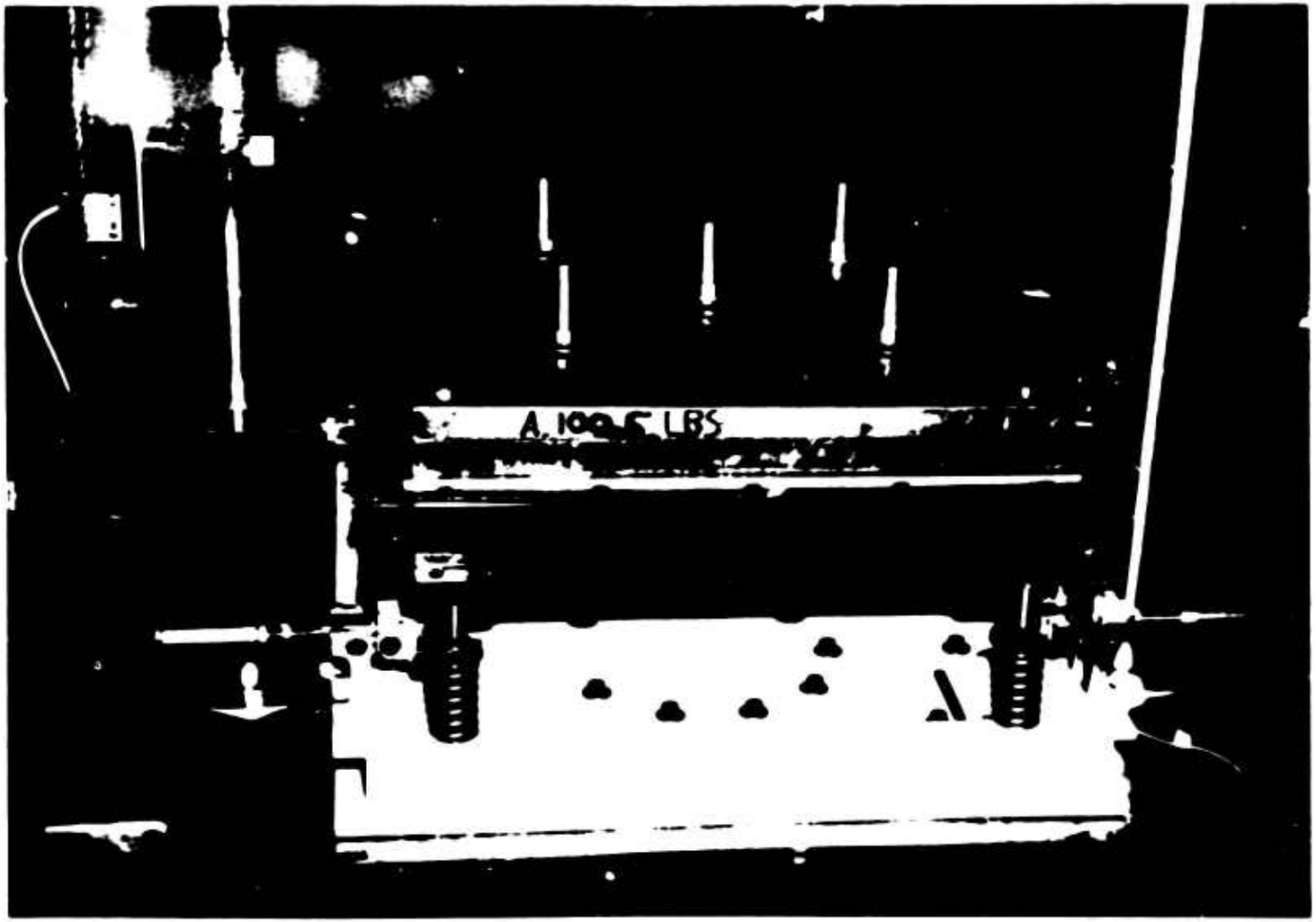

Figure 100. Drop Test Installation - 200-Pound Central Center of Gravity

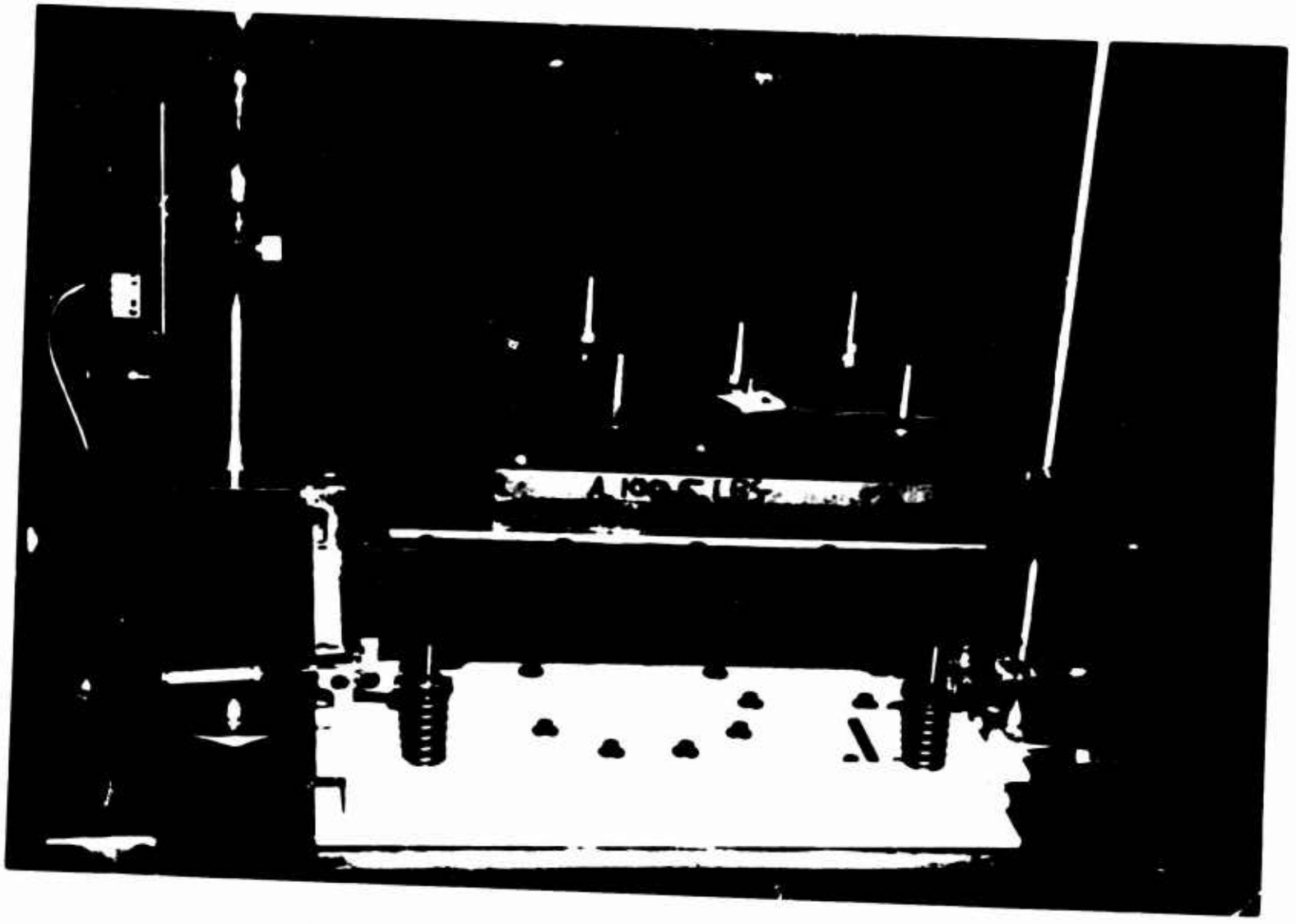

Figure 101. Drop Test Installation - 200-Pound Offset Center of Gravity

TABLE 44

ISOLATED PLATFORM SHOCK TEST DATA
VERTICAL CALIBRATION (G'S PER MAJOR DIVISION)
HORIZONTAL CALIBRATION (MILLISECONDS PER MAJOR DIVISION)

Record No.	Vert. Cal.	Horiz. Cal.	Load (Lb)	Platform Isolation Configuration
1	2	20	40	DAVI ∝
2	2	20	40	DAVI ∝
3	2	20	40	DAVI ∝
4	2	20	0	DAVI ∝
5	2	20	0	DAVI ∝
6	2	20	0	DAVI ∝
7	2	20	0	Spring-mass system
8	5	20	0	Bottom plate only
9	5	20	0	Bottom plate only
10	5	20	0	Spring-mass system
11	5	10	0	Spring-mass system
12	5	10	40	Spring-mass system
13	5	10	40	Spring-mass system
14	5	20	40	Spring-mass system
15	5	20	40	DAVI ∝
16	5	10	40	DAVI ∝
17	10	10	40	DAVI ∝
18	10	10	40	DAVI ∝
19	10	10	40	DAVI ∝
20	10	5	40	DAVI ∝
21	10	5	40	DAVI ∝
22	5	20	40	DAVI ∝
23	5	20	40	DAVI ∝
24	5	20	40	DAVI ∝
25	5	20	40	DAVI ∝
26	5	20	40	DAVI ∝
27	5	20	40	DAVI ∝
28	5	5	40	DAVI ∝
29	5	50	40	DAVI ∝
30	5	20	100	Both pick-ups on table
31	5	20	100	Spring-mass system
32	5	5	100	Spring-mass system
33	5	20	100	Spring-mass system
34	5	20	100	DAVI ∝
35	5	5	100	DAVI ∝
36	5	5	100	DAVI ∝
37	5	2	100	DAVI ∝
38	5	20	100	DAVI ∝
39	5	5	100	DAVI ∝

TABLE 44 (Continued)

Record No.	Vert. Cal.	Horiz. Cal.	Load (Lb)	Platform Isolation Configuration
40	5	20	100	DAVI∝ less inertia bar
41	5	5	100	DAVI∝ less inertia bar
42	5	20	100	DAVI∝ inertia wgt. inboard
43	5	5	100	DAVI∝ inertia wgt. inboard
44	5	20	200	DAVI∝
45	5	20	200	DAVI∝
46	5	5	200	DAVI∝
47	5	20	200	DAVI∝
48	5	5	200	DAVI∝
49	5	20	200	DAVI∝
50	2.5	5	200	DAVI∝
51	2.5	20	200	DAVI∝ , offset c.g.
52	5	20	200	DAVI∝ , offset c.g.
53	5	5	200	DAVI∝ , offset c.g.
54	5	5	200	DAVI∝ , offset c.g.
55	5	5	200	DAVI∝ , offset c.g.
56	5	5	200	DAVI∝ , offset c.g.
57	5	20	200	Spring-mass, offset c.g.
58	5	5	200	Spring-mass, offset c.g.
59	5	20	200	Spring-mass, offset c.g.
60	5	5	200	Spring-mass, offset c.g.

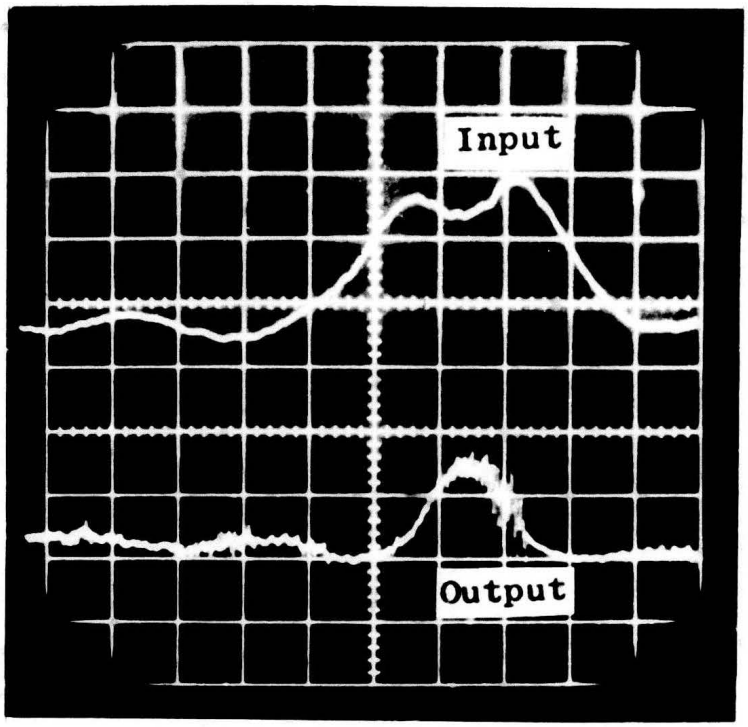

Figure 102. DAVI∝ Isolated Platform Drop Test 200-Pound Central Center of Gravity 5-1/2-g Input

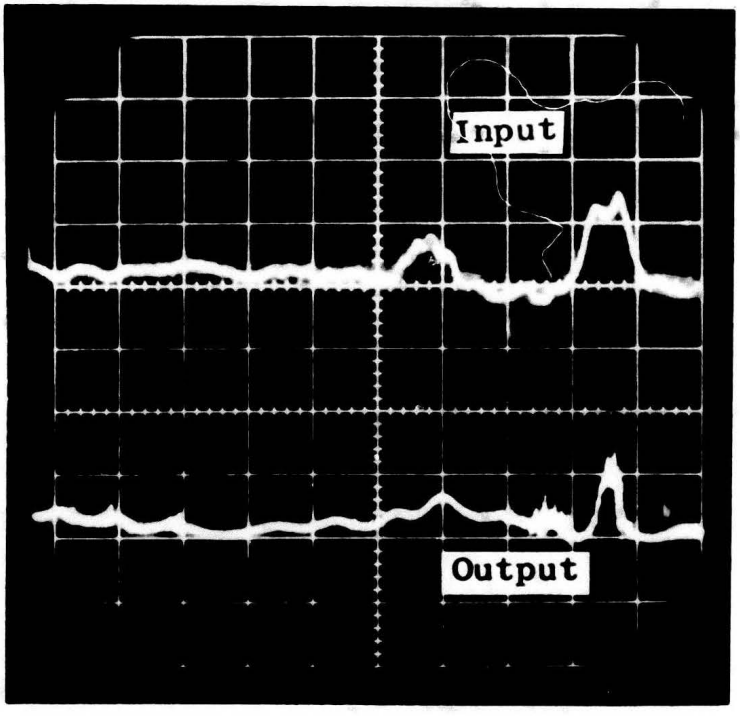

Figure 103. DAVI∝ Isolated Platform Drop Test 200-Pound Central Center of Gravity 7-g Input

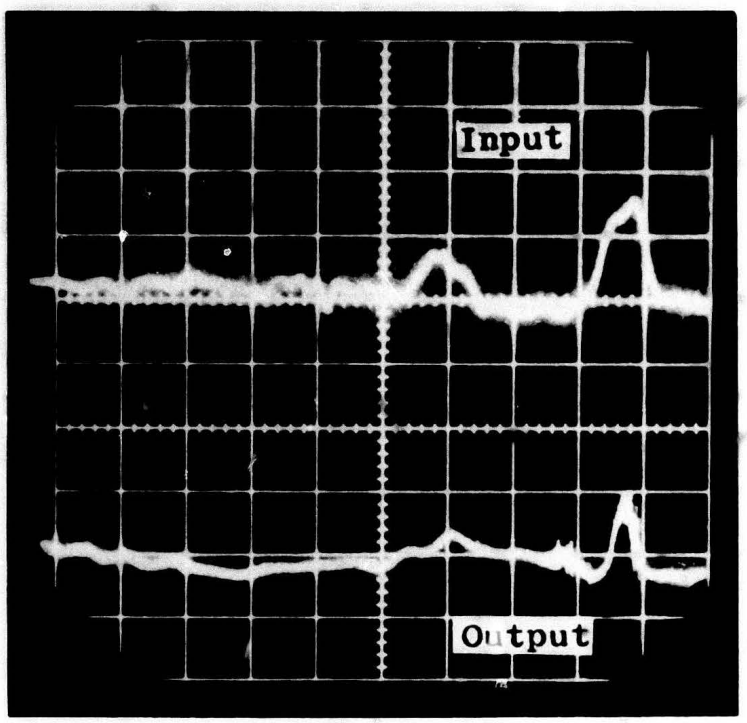

Figure 104. DAVI ∝ Isolated Platform Drop Test 200-Pound Central Center of Gravity 8-g Input

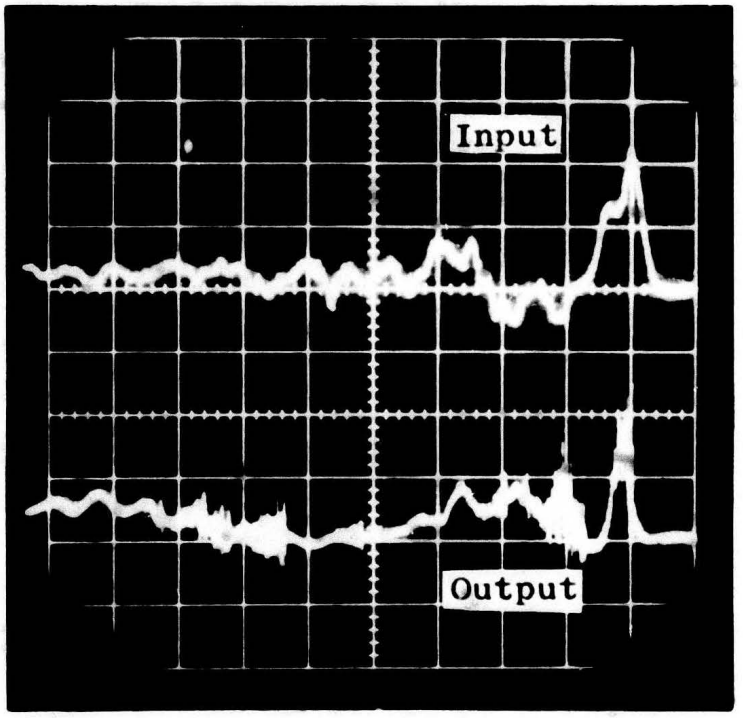

Figure 105. DAVI ∝ Isolated Platform Drop Test 200-Pound Central Center of Gravity 11-g Input

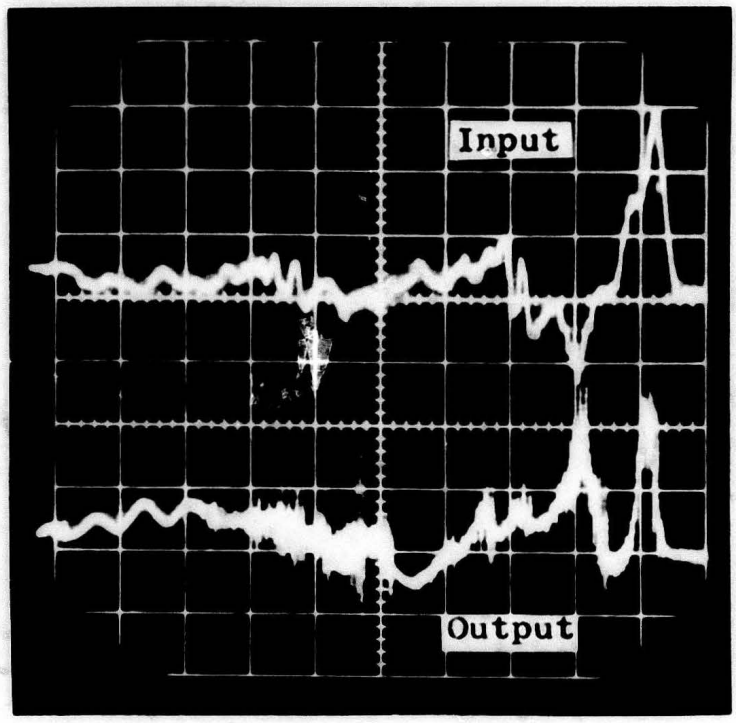

Figure 106. DAVI ∝ Isolated Platform Drop Test 200-Pound Central Center of Gravity 15-g Input

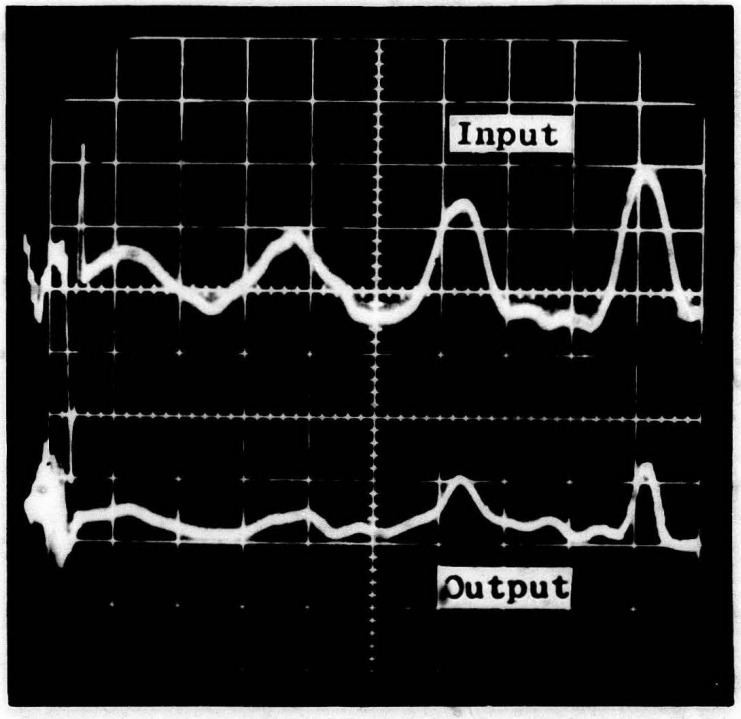

Figure 107. DAVI ∝ Isolated Platform Drop Test 200-Pound Offset Center of Gravity 5-1/2-g Input

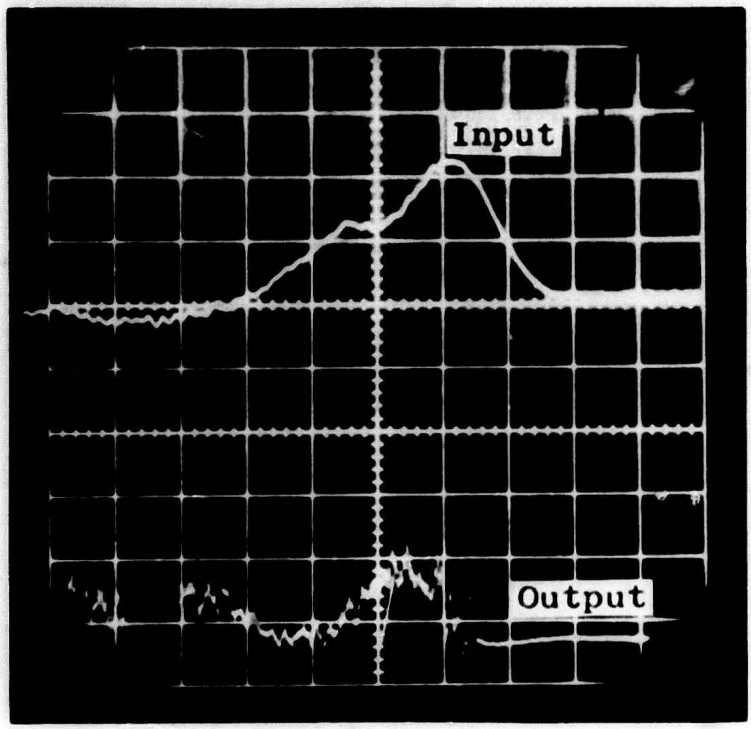

Figure 108. DAVI α Isolated Platform Drop Test 200-Pound Offset Center of Gravity 10-g Input

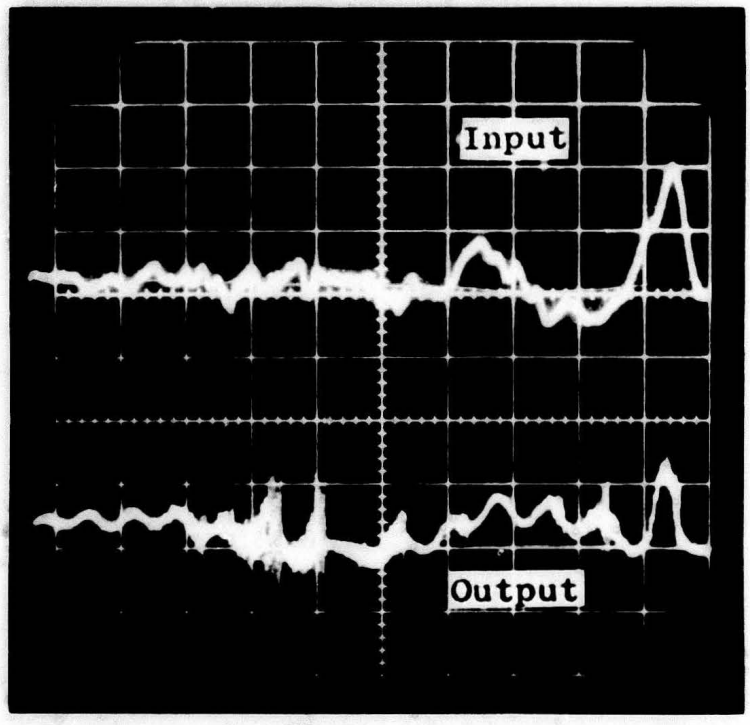

Figure 109. DAVI α Isolated Platform Drop Test 200-Pound Offset Center of Gravity 10-g Input

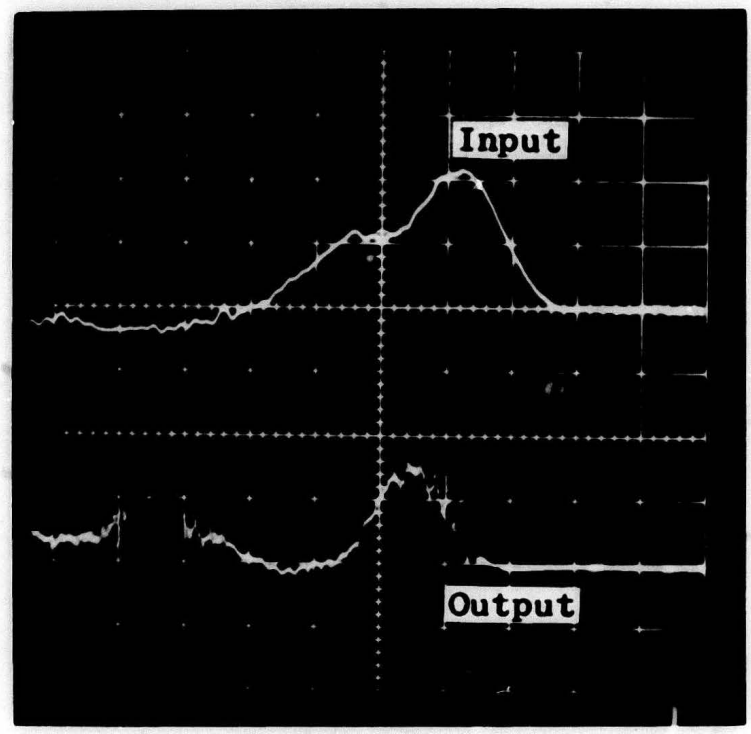

Figure 110. DAVI α Isolated Platform Drop Test 200-Pound Offset Center of Gravity 11-g Input

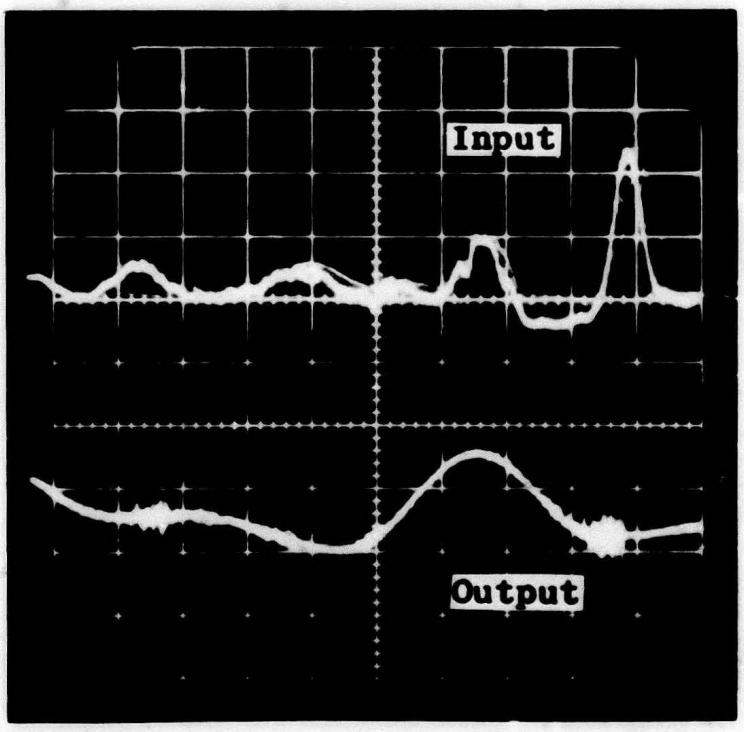

Figure 111. Spring-Mass Isolated Platform Drop Test 200-Pound Offset Center of Gravity 12-g Input

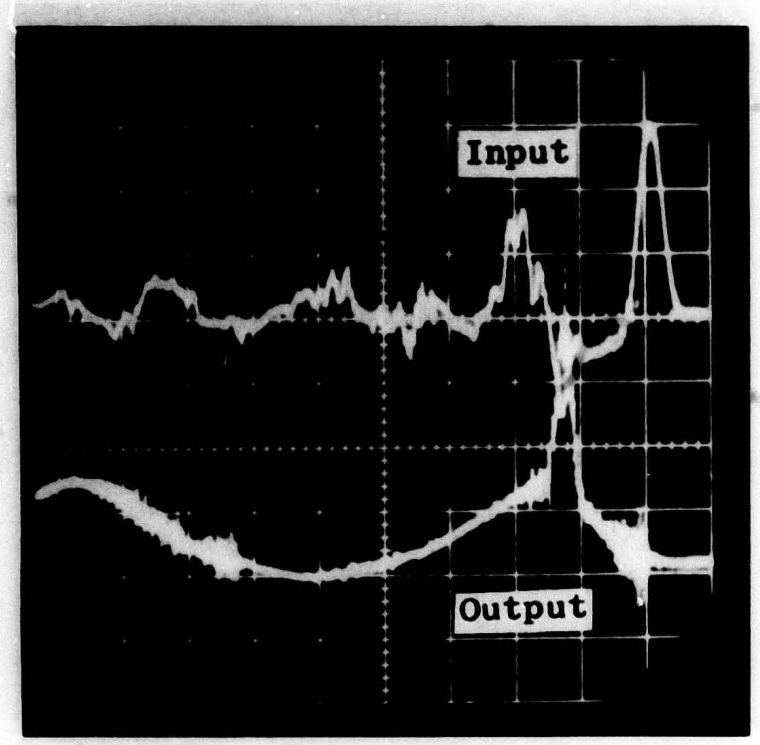

Figure 112. Spring-Mass Isolated Platform Drop Test
200-Pound Offset Center of Gravity
15-g Input

TABLE 45

SUMMARY OF TRANSMISSIBILITY TEST RESULTS

FIGURE	PLATFORM ISOLATION CONFIGURATION	C. G.	TRANSMISSIBILITY (OUTPUT/INPUT) LOW MODE	HIGH MODE
103	DAVI α	Neutral	.357	.715
104	DAVI α	Neutral	.312	.782
105	DAVI α	Neutral	.227	.820
106	DAVI α	Neutral	.268	.800
107	DAVI α	3" Offset	.228	.565
109	DAVI α	3" Offset	.250	.700
111	Spring-Mass	3" Offset	.455	----
112	Spring-Mass	3" Offset	.433	----

FATIGUE STRENGTH OF DAVI MODELS

The crucial items in the DAVI models are the flexural cross-spring pivots shown in Figure 115. Except for the coil springs, these pivots are the only components subjected to oscillatory flexure while under a steady load. The flexural pivots are utilized in such a manner that they will be the highest stressed components in the DAVI.

Largely because of the extensive empirical stress investigations and lengthy analyses that would be necessary if an entirely new flexural pivot design were to be used in the DAVI, it was decided to use commercial flexural pivots on which there was an existing body of qualifying fatigue data.

The Utica Division of the Bendix Corporation empirically obtained the curve shown in Figure 113 for the type of flexural pivot used in the DAVI. This pivot was decided upon after several lengthy discussions between Kaman engineers and Bendix stress engineers. The type of loading which resulted in the curve in Figure 113 is not precisely representative of the loading condition of the DAVI pivot, primarily in that the vertical radial loading is oscillatory in the DAVI while the curve is based on steady vertical radial loading. It was the opinion of Bendix engineers, based on previous experience, that the curve was sufficiently representative for the magnitudes of DAVI vertical loads. Independent testing at Kaman confirmed their expectations.

Because the "dead load" on the DAVI units is carried by the coil spring, the vertical radial load on the pivots is vibratory, and the magnitude of this load is a function of the vibratory angle and the DAVI spring rate. The line relating vibratory angle to vertical load is drawn on Figure 113, and it is seen that this line intersects the indefinite life curve (determined by Bendix) at slightly under six degrees.

To assure sufficient fatigue data, Kaman tested seven DAVI models, including twenty-eight pivots, in fatigue. The results of this testing, shown in S-N form in Figure 114, indicate that the Bendix curve is sufficiently accurate for this application.

The dashed line in Figure 114 shows the vibratory angle above which 99.87 percent of expected failures would occur. This line was calculated by subtracting three times the standard deviation of the vibratory angles of failed units from a mean line through the points. This line appears to asymptotically approach a vibratory angle of six degrees, which agrees quite well with the endurance limit of approximately six degrees as found using Figure 113.

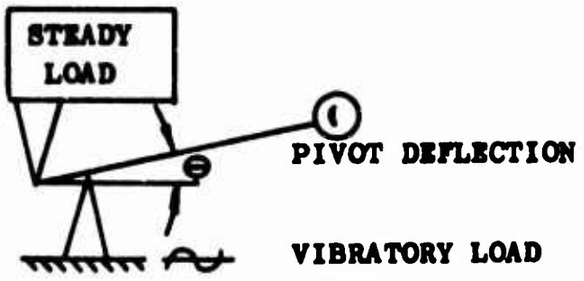

VERTICAL LOAD = STEADY LOAD + VIBRATORY LOAD

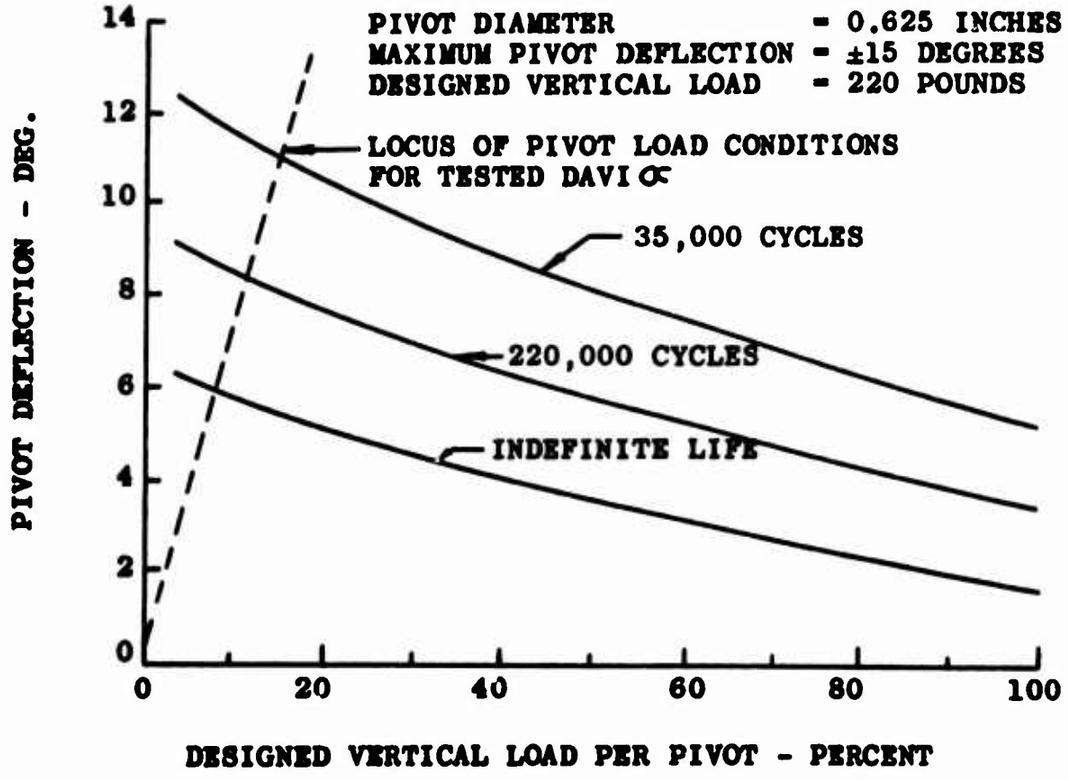

Figure 113. Fatigue Characteristics of DAVI Flexural Pivots

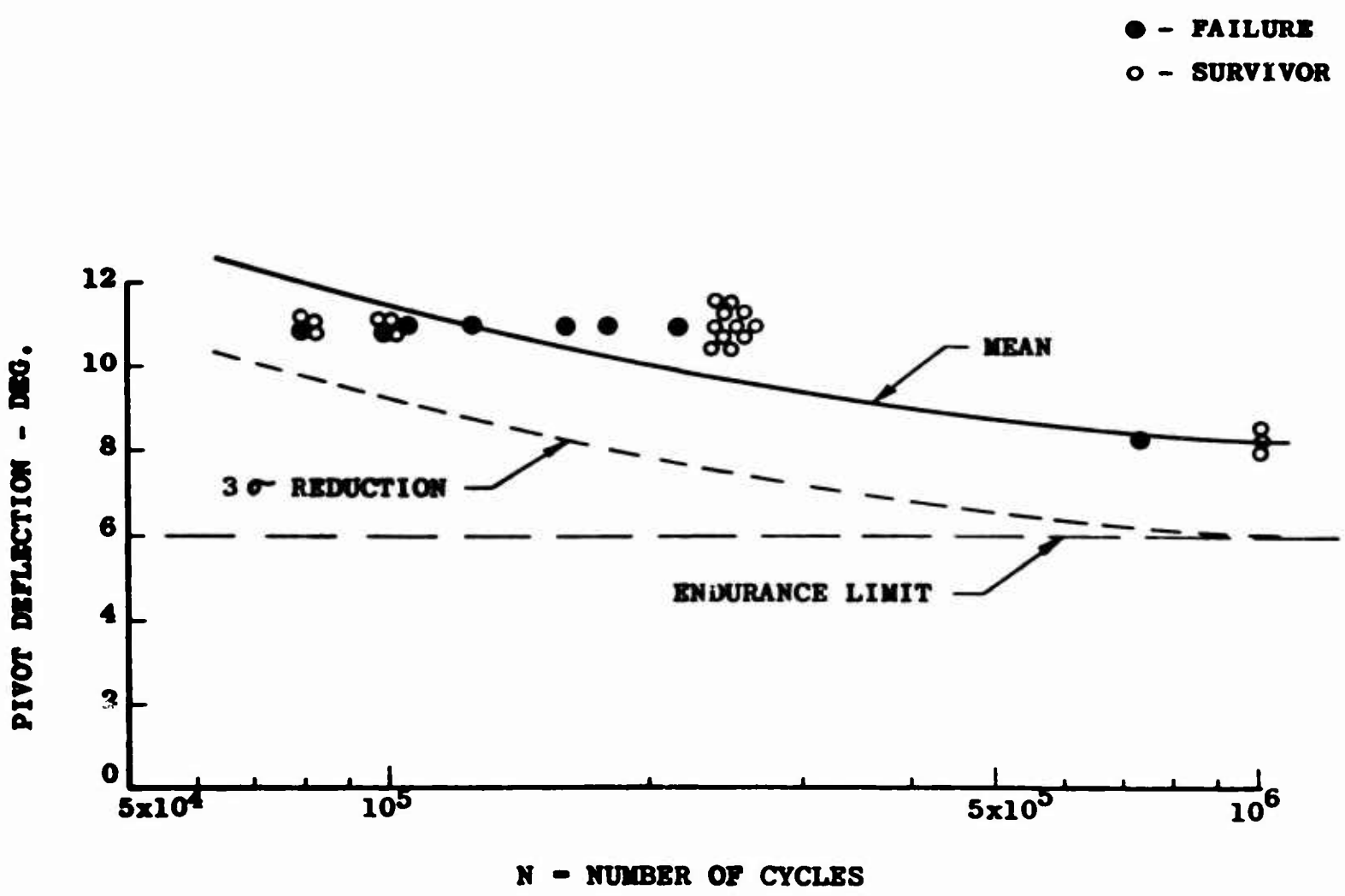

Figure 114. S-N Curve for DAVI Pivot From Kaman Tests

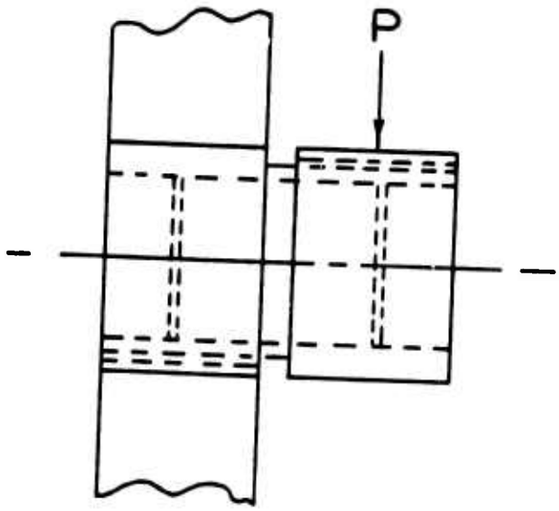

(a)

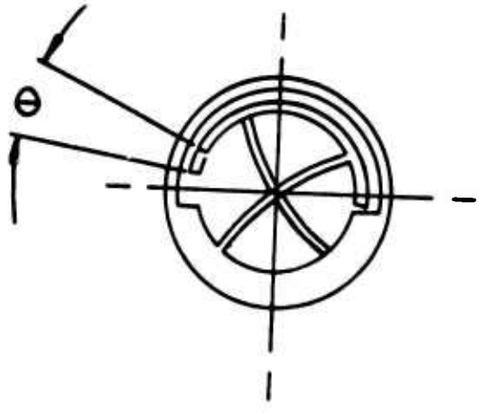

(b)

Figure 115. Flexural Pivot

TABLE 46

DAVI FATIGUE TEST DATA*

Test	Pivot Deflection (deg.)	Steady Load (lb.)	Vibratory Load (lb.)	Vertical Load (lb.)	Excitation Frequency (c.p.s.)	Cycles to Failure	Number of Survivors
Test No. 1	11.1	3.5	70.4	73.9	10.0	108,000	15
4-DAVI Platform						126,000	14
						161,000	13
						180,000	12
						216,000	11
					Test Ended At	252,000	11
Test No. 2	10.9	3.5	69.1	72.6	9.8	80,000	3
Single DAVI α Test Rig							
Test No. 3	10.9	3.5	69.1	72.6	9.95	100,000	3
Single DAVI α Test Rig							
Test No. 4	8.2	3.5	52.2	55.7	10.0	720,000	3
Single DAVI α Test Rig					Test Ended At	1,000,000	3

* Data is reduced to value per pivot

CONCLUSIONS

From the results of analysis and model testing, the following conclusions can be made:

1. Correlation of the analytical and test results was excellent.

2. The Dynamic Antiresonant Vibration Isolator configuration (DAVI α), analyzed and tested under this contract, is capable of over 98-percent isolation at its tuned frequency.

3. To obtain a 98-percent isolation at 10.5 c.p.s. on a conventional isolation system would require a static deflection of over 20 times that obtained on the DAVI α configuration.

4. The test results of a normal spring-mass system of essentially the same spring rate show an amplification of 10 at the same frequency that the DAVI α had 98-percent isolation.

5. The analysis and test results show that the amount of weight on the DAVI α platform or on the DAVI isolated seat did not change the tuned frequency or appreciably affect the amount of isolation, thus showing the capability of the DAVI as an isolation system for cargo pallets or pilot and passenger seats on which the isolated weight would vary.

6. Analysis and test showed that the DAVI α gave high frequency transmissibility approaching a finite value of less than 1.0 and can be designed to be less than 0.2.

7. In the process of testing, the weight of the DAVI α was reduced by approximately 50 percent by changing the ratio of R/r, thus showing the DAVI can be designed very efficiently to give a minimum weight penalty.

8. Analysis and test show that the Series-Damped DAVI (DAVI γ) is capable of 98-percent isolation at the tuned frequency of 10.5 c.p.s. and high frequency isolation approaching zero as in a conventional isolator.

9. Analysis and test show that the DAVI α has better shock transmissibility characteristics for its fundamental mode than a conventional isolator with the same spring rate.

10. Analysis and test on the effects of damping in the pivots show that minimum damping gives the best isolation.

RECOMMENDATIONS

Results of the studies made under the contract lead to several recommendations, from which improved DAVI characteristics may be derived.

1. A flight test program should be conducted on the DAVI platform and/or on a DAVI isolated copilot's seat installed in an Army CH-47 or UH-1 helicopter to determine its operation under an actual vibratory environment.

2. Further analyses and drop tests should be conducted to determine more precisely the source of the high frequency shock transmitted by the present DAVI configuration of this contract and to determine design means of eliminating this undesirable characteristic.

3. It is also recommended that both an analytical and model test parametric study be made on the present DAVI configuration (DAVI α) to determine the relationships among normalized frequency, high frequency transmissibility, bar mass and inertia, isolated mass, static deflection, and antiresonant frequency.

4. Both an analytical and a model test program should be conducted for a two-dimensional nonisotropic DAVI α configuration.

5. It is suggested that both an analytical and model test program be considered on three other arrangements of pivots in the DAVI configuration, designated the DAVI β, DAVI γ, and DAVI δ, which retains the desirable features of the DAVI α and obtains high frequency isolation approaching zero as in a conventional isolation system.

REFERENCES

1. Stabe, A., "Federgelenke im Messgerätebau", Zeitschrift des Vereines deutscher Ingenieur, Volume 83, 1939, pp. 1189 - 1196.

2. Eastman, F.S., "Flexure Pivots to Replace Knife-Edges and Ball Bearings", University of Washington Engineering Experimental Station, Bulletin No. 86, 1935.

3. Eastman, F.S., "Design of Flexure Pivots", Journal of the Aeronautical Sciences, 1937, pp. 16 - 21.

4. Young, W.E., "An Investigation of the Cross-Spring Pivot", Journal of Applied Mechanics A-114, June 1944.

5. Crede, C.E., Vibration and Shock Isolation, John Wiley and Sons, Inc., New York, New York, 1951.

6. Den Hartog, J.P., Mechanical Vibrations, Fourth Edition, McGraw-Hill Book Company, Inc., New York, New York, 1956.

7. Harris, C.M., and Crede, C.E., Shock and Vibration Handbook, Three Volumes, McGraw-Hill Book Company, New York, New York, 1961.

8. Flannelly, W.G., "Dynamic Antiresonant Vibration Isolator", Kaman Aircraft Corporation Report No. RN 63-1, November 1963.

9. Plunkett, R., "Machine Mounts for Vibration Isolation", General Electric Company, Report No. R53GL10, AD 33657, January 1953.

10. Rathbone, T. C., "Human Sensitivity to Product Vibration", Product Engineering, 5 August 1963.

UNCLASSIFIED

Security Classification

DOCUMENT CONTROL DATA · R&D

(Security classification of title, body of abstract and indexing annotation must be entered when the overall report is classified)

1 ORIGINATING ACTIVITY (Corporate author)	2a REPORT SECURITY CLASSIFICATION
Kaman Aircraft Corporation Bloomfield, Connecticut	Unclassified
	2b GROUP

3 REPORT TITLE

A Study of the Kaman Dynamic Antiresonant Vibration Isolator

4 DESCRIPTIVE NOTES (Type of report and inclusive dates)

Final Report

5 AUTHOR(S) (Last name, first name, initial)

Anderson, Roland C.
Smith, Michael F.

6 REPORT DATE	7a TOTAL NO OF PAGES	7b NO OF REFS
January 1966	256	10

8a CONTRACT OR GRANT NO	9a ORIGINATOR'S REPORT NUMBER(S)
DA 44-177-AMC-196(T)	USAAVLABS Technical Report 65-75
b PROJECT NO 1P125901A14229	
c	9b OTHER REPORT NO(S) (Any other numbers that may be assigned this report) Kaman Report No. R-574
d	

10 AVAILABILITY/LIMITATION NOTICES

Distribution of this document is unlimited.

11 SUPPLEMENTARY NOTES	12 SPONSORING MILITARY ACTIVITY
None	U. S. Army Aviation Materiel Laboratories Fort Eustis, Virginia

13 ABSTRACT

This report is the result of a research study conducted on the Dynamic Antiresonant Vibration Isolator (DAVI). Theoretical analysis and experimental model correlation show the DAVI to be capable of over 98 percent isolation at very low frequencies with low static deflections; and at a tuned frequency, the transmissibility is independent of the isolated mass. Analysis and drop tests show that the DAVI gives better shock transmissibility for its fundamental mode than a conventional isolation system with the same spring rate.

DD FORM 1 JAN 64 1473

UNCLASSIFIED

Security Classification

264-66

UNCLASSIFIED

Security Classification

14. KEY WORDS	LINK A		LINK B		LINK C	
	ROLE	WT	ROLE	WT	ROLE	WT
1. Vibration Isolation						
2. Antiresonant Isolator						
3. Low Frequency Isolation With Low Static Deflection						
4. Discrete Frequency Isolation Independent of Isolated Mass						
5. Isolation of High and Low Frequencies With Single Isolator						
6. Shock Attenuation						

INSTRUCTIONS

1. ORIGINATING ACTIVITY: Enter the name and address of the contractor, subcontractor, grantee, Department of Defense activity or other organization *(corporate author)* issuing the report.

2a. REPORT SECURITY CLASSIFICATION: Enter the overall security classification of the report. Indicate whether "Restricted Data" is included. Marking is to be in accordance with appropriate security regulations.

2b. GROUP: Automatic downgrading is specified in DoD Directive 5200.10 and Armed Forces Industrial Manual. Enter the group number. Also, when applicable, show that optional markings have been used for Group 3 and Group 4 as authorized.

3. REPORT TITLE: Enter the complete report title in all capital letters. Titles in all cases should be unclassified. If a meaningful title cannot be selected without classification, show title classification in all capitals in parenthesis immediately following the title.

4. DESCRIPTIVE NOTES: If appropriate, ente: the type of report, e.g., interim, progress, summary, annual, or final. Give the inclusive dates when a specific reporting period is covered.

5. AUTHOR(S): Enter the name(s) of author(s) as shown on or in the report. Enter last name, first name, middle initial. If military, show rank and branch of service. The name of the principal author is an absolute minimum requirement.

6. REPORT DATE: Enter the date of the report as day, month, year, or month, year. If more than one date appears on the report, use date of publication.

7a. TOTAL NUMBER OF PAGES: The total page count should follow normal pagination procedures, i.e., enter the number of pages containing information.

7b. NUMBER OF REFERENCES: Enter the total number of references cited in the report.

8a. CONTRACT OR GRANT NUMBER: If appropriate, enter the applicable number of the contract or grant under which the report was written.

8b, 8c, & 8d. PROJECT NUMBER: Enter the appropriate military department identification, such as project number, subproject number, system numbers, task number, etc.

9a. ORIGINATOR'S REPORT NUMBER(S): Enter the official report number by which the document will be identified and controlled by the originating activity. This number must be unique to this report.

9b. OTHER REPORT NUMBER(S): If the report has been assigned any other report numbers *(either by the originator or by the sponsor)*, also enter this number(s).

10. AVAILABILITY/LIMITATION NOTICES: Enter any limitations on further dissemination of the report, other than those imposed by security classification, using standard statements such as:

(1) "Qualified requesters may obtain copies of this report from DDC."

(2) "Foreign announcement and dissemination of this report by DDC is not authorized."

(3) "U. S. Government agencies may obtain copies of this report directly from DDC. Other qualified DDC users shall request through _____."

(4) "U. S. military agencies may obtain copies of this report directly from DDC. Other qualified users shall request through _____."

(5) "All distribution of this report is controlled. Qualified DDC users shall request through _____."

If the report has been furnished to the Office of Technical Services, Department of Commerce, for sale to the public, indicate this fact and enter the price, if known.

11. SUPPLEMENTARY NOTES: Use for additional explanatory notes.

12. SPONSORING MILITARY ACTIVITY: Enter the name of the departmental project office or laboratory sponsoring *(paying for)* the research and development. Include address.

13 ABSTRACT: Enter an abstract giving a brief and factual summary of the document indicative of the report, even though it may also appear elsewhere in the body of the technical report. If additional space is required, a continuation sheet shall be attached.

It is highly desirable that the abstract of classified reports be unclassified. Each paragraph of the abstract shall end with an indication of the military security classification of the information in the paragraph, represented as *(TS)*, *(S)*, *(C)*, or *(U)*.

There is no limitation on the length of the abstract. However, the suggested length is from 150 to 225 words.

14. KEY WORDS: Key words are technically meaningful terms or short phrases that characterize a report and may be used as index entries for cataloging the report. Key words must be selected so that no security classification is required. Identifiers, such as equipment model designation, trade name, military project code name, geographic location, may be used as key words but will be followed by an indication of technical context. The assignment of links, rules, and weights is optional.

UNCLASSIFIED

Security Classification